DOT-HS-807-159
DOT-TSC-NHTSA-86-5
Final Report

December 1987

Analysis of Head Response to Torso Acceleration
Vol. I - Development of Performance Requirements

C.H. Spenny

Transportation Systems Center
Cambridge, MA 02142
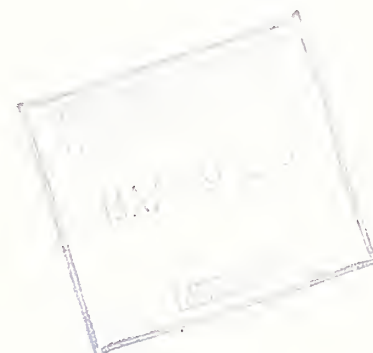
Prepared for

National Highway Traffic Safety Administration
Research and Development
Washington, DC 20590

1. Report No. DOT-HS-807-159	2. Government Accession No.	3. Recipient's Catalog No.
4. Title and Subtitle Analysis of Head Response to Torso Acceleration, Vol. I - Development of Performance Requirements		5. Report Date December 1987
		6. Performing Organization Code DTS-44
7. Author(s) C.H. Spenny*		8. Performing Organization Report No. DOT-TSC-NHTSA-86-5
9. Performing Organization Name and Address U.S. Department of Transportation Research and Special Programs Administration Transportation Systems Center Cambridge, MA 02142		10. Work Unit No. (TRAIS) HS476/R4434
		11. Contract or Grant No.
12. Sponsoring Agency Name and Address U.S. Department of Transportation National Highway Traffic Safety Administration Research and Development Washington, DC 20590		13. Type of Report and Period Covered Final Report December 1982 - July 1986
		14. Sponsoring Agency Code NRD-13

15. Supplementary Notes

*Department of Aeronautics & Astronautics
Air Force Institute of Technology
Wright-Patterson Air Force Base, Ohio 45433

16. Abstract

Performance requirements are developed which define the kinematic and kinetic response of the head for a seated subject exposed to frontal, lateral or oblique impact. Response is expressed in terms of variables which are readily measured in an anthropomorphic dummy and which are useful in injury prediction. The performance requirements are based on volunteer tests conducted by the U.S. Department of Navy, Naval Biodynamics Laboratory (NBDL) in which a four-point restraint system and a singular type of impact profile are employed. Other NBDL volunteer tests and volunteer and cadaver tests conducted by Wayne State University are used to evaluate the effects of variation in impact profile, type of restraint system and level of muscle activity.

17. Key Words Automotive Safety, Biomechanics, Human Impact Response, Anthropomorphic Dummies	18. Distribution Statement Document is available to the public through the National Technical Information Service, Springfield, VA 22161		
19. Security Classif. (of this report) Unclassified	20. Security Classif. (of this page) Unclassified	21. No. of Pages 186	22. Price

Form DOT F 1700.7 (8-72)   R production of completed page authorized

PREFACE

The head/neck analysis reported herein was performed under Project Plan Agreement HS-76 with the National Highway Traffic Safety Administration (NHTSA). Mr. Richard Morgan, the NHTSA project manager, provided crucial assistance in defining and guiding this activity. Dr. C. H. Spenny was the original TSC project leader and principal investigator. Support in data processing was provided by Messrs. Joe Burstein, Douglas A. Gordon, Tom Peters, and Richard Stevens of the Systems Development Corporation, an on-site contractor at TSC.

Analysis of the Wayne State University tests was performed while the principal investigator was on a one year research assignment at the University of Michigan Transportation Research Institute (UMTRI). Support in analysis was provided by N. Alem and B. Bowman of the UMTRI. The effort was completed as independent research by Dr. Spenny in his current faculty position at the U.S. Air Force Institute of Technology.

Load calculations made in this project for frontal and lateral tests were forwarded to the NHTSA Vehicle Research and Test Center (VRTC) under an informal agreement to jointly analyze head/neck response characteristics. The results of this effort have been published in the 27th and 28th Stapp Car Crash Conferences jointly with J. Wismans, Senior Research Scientist of the Research Institute for Road Vehicles, TNO, while he was a visiting project leader at the VRTC.

METRIC CONVERSION FACTORS

Approximate Conversions to Metric Measures

Symbol	When You Know	Multiply by	To Find	Symbol
		LENGTH		
in	inches	*2.5	centimeters	cm
ft	feet	30	centimeters	cm
yd	yards	0.9	meters	m
mi	miles	1.6	kilometers	km
		AREA		
in²	square inches	6.5	square centimeters	cm²
ft²	square feet	0.09	square meters	m²
yd²	square yards	0.8	square meters	m²
mi²	square miles	2.6	square kilometers	km²
	acres	0.4	hectares	ha
		MASS (weight)		
oz	ounces	28	grams	g
lb	pounds	0.45	kilograms	kg
	short tons (2000 lb)	0.9	tonnes	t
		VOLUME		
tsp	teaspoons	5	milliliters	ml
Tbsp	tablespoons	15	milliliters	ml
fl oz	fluid ounces	30	milliliters	ml
c	cups	0.24	liters	l
pt	pints	0.47	liters	l
qt	quarts	0.95	liters	l
gal	gallons	3.8	liters	l
ft³	cubic feet	0.03	cubic meters	m³
yd³	cubic yards	0.76	cubic meters	m³
		TEMPERATURE (exact)		
°F	Fahrenheit temperature	5/9 (after subtracting 32)	Celsius temperature	°C

*1 in. = 2.54 cm (exactly). For other exact conversions and more detail tables see NBS Misc. Publ. 286, Units of Weight and Measures. Price $2.25 SD Catalog No. C13 10 286.

Approximate Conversions from Metric Measures

Symbol	When You Know	Multiply by	To Find	Symbol
		LENGTH		
mm	millimeters	0.04	inches	in
cm	centimeters	0.4	inches	in
m	meters	3.3	feet	ft
m	meters	1.1	yards	yd
km	kilometers	0.6	miles	mi
		AREA		
cm²	square centimeters	0.16	square inches	in²
m²	square meters	1.2	square yards	yd²
km²	square kilometers	0.4	square miles	mi²
ha	hectares (10,000 m²)	2.5	acres	
		MASS (weight)		
g	grams	0.035	ounces	oz
kg	kilograms	2.2	pounds	lb
t	tonnes (1000 kg)	1.1	short tons	
		VOLUME		
ml	milliliters	0.03	fluid ounces	fl oz
l	liters	2.1	pints	pt
l	liters	1.06	quarts	qt
l	liters	0.26	gallons	gal
m³	cubic meters	36	cubic feet	ft³
m³	cubic meters	1.3	cubic yards	yd³
		TEMPERATURE (exact)		
°C	Celsius temperature	9/5 (then add 32)	Fahrenheit temperature	°F

iv

CONTENTS

CONTENTS (Cont'd)

CONTENTS (Cont'd)

LIST OF FIGURES

LIST OF FIGURES (Cont'd)

LIST OF TABLES

1. INTRODUCTION

1.1 BACKGROUND

When a seated human is rapidly accelerated in the horizontal plane with the torso restrained, large head excursions with respect to the torso occur. For automobile crash victims, injury can result if the excursions are large enough to permit head contact with the car interior. Noncontact acceleration levels may also be severe enough to produce lesions in the head or neck.

In an anthropomorphic test device (ATD) used to predict injury or to verify compliance with Federal Motor Vehicle Safety Standards, the trajectory and momentum characteristics of the head must be humanlike in order to establish the nature and extent of head contact with the vehicle interior. To predict injury, kinematic or load variables must be measurable in the dummy that can be correlated with human tolerance levels. The latter are more commonly used.

Performance requirements define, qualitatively and quantitatively, the degree of response fidelity required of a newly designed dummy. They can also be used in the field for calibration of an existing dummy. Performance requirements for neck response were developed by Mertz, Neathery and Culver [1] which are necessary conditions for achieving fidelity in flexion and extension (response to frontal and rear impact). These necessary conditions are referred to in this report as the Mertz performance requirement. They are functional relationships that apply during impact which relate torque at the occipital condyles to head orientation relative to the torso.

The Hybrid III dummy generally satisfies the Mertz flexion requirement [2]. In tests conducted at the NHTSA Vehicle Research and Test Center (VRTC) head orientation was observed to be more humanlike than was position of the head center-of-gravity [3]. This result is not surprising because the Mertz requirement is not a sufficient condition that assures complete fidelity. Since head contact with a car interior is critically dependent on head translation, as well as orientation, relative to the torso, additional performance requirements are needed for frontal response.

For lateral and oblique response no generally accepted performance requirements exist. <u>Because a dummy with omni-directional response capability is now being developed by NHTSA, performance requirements are needed for lateral and oblique response.</u>

1.2 OBJECTIVE

The objective of this study is: (1) to develop performance requirements which can be used to assure that all major head response observed in a set of volunteer tests is achieved in an omni-directional dummy and (2) to test the robustness of the performance requirement for variation in test conditions.

1.3 STUDY METHODOLOGY

Data for developing the performance requirements was obtained from a large number of tests of volunteers conducted by the Naval Biodynamics Laboratory (NBDL). Volunteer and cadaver tests conducted by Wayne State University (WSU), and additional volunteer tests conducted by the NBDL with other types of input acceleration profile are used to compare the response to variation in test conditions.

In all tests, the subject is restrained in a seated position and exposed to a rapid change in velocity in the horizontal direction. Linear and angular displacements of both the head and T1 vertebra, derived from film analysis, are used to describe head response relative to the torso. Accelerometer clusters mounted on the head in NBDL and WSU tests provided the accelerations (and angular velocities) required to calculate force and moment transfer between the head and neck. The head is assumed to be a rigid body for the purpose of calculating these loads.

<u>Development of Performance Requirements</u> - The following describes the manner in which the performance requirements were evolved:

A. <u>Characterization of Response</u> - The range of responses in the above tests were examined and those aspects of the response which were judged to be significant were identified.

B. Definition of Response Variables - A set of response variables was defined which describes all of the significant response, which would be readily measurable in a dummy, regardless of neck configuration and which would be useful in injury prediction. The response variables selected include four kinematic quantities:

1. Length of the neck chord line (i.e., the line joining the T1 vertebral point and the occipital condylar point).

2. Head angular position in the impact plane* with respect to the torso.

3. Neck chord line angular position in the impact plane with respect to the torso.

4. Head rotation about an inferior/superior (I/S) axis in the head.

and four kinetic (load) quantities:

1. Moment about a horizontal axis in the head that passes through the occipital condylar point and is perpendicular to the impact plane.

2. Moment about the head I/S axis.

3. Force parallel to the head I/S-axis that passes through the occipital condylar point.

4. Force resultant perpendicular to the head I/S axis that passes through the occipital condylar point.

The response variables are described in more detail in Section 4.

---

*The impact plane is defined by the sled thrust vector and a gravity vector passing through the track centerline.

C. Development of Response Corridors - The equations for transforming the human test data into response variables were programmed to operate in conjunction with a data retrieval and display system in order to produce graphical results. Cross plots of selected variables at selected sled impact levels were used to show that the response of all subjects is quite similar. Cross plots of the same variables by subject were used to show how response level varies with impact level. The variable pairs selected for cross-plotting are those which exhibit the most similar response when tests with varying peak impact levels are compared up to the peak response level of the less severe test. For the cross-plots of kinematic variables relatively narrow corridors describe the response of all subjects at all impact levels, corridor width being established primarily by variation in subject response and corridor length by the magnitude of response to the most severe impact. For load response variables, the same narrowness of corridor width could be established by superimposing only tests of comparable impact level. To characterize the load response for varying impact levels, multiple response corridors were created.

D. Definition of Input Profiles - The T1 vertebral point was selected as the point at which impact to the head/neck system would be specified for dummy tests. Since its acceleration, velocity and displacement were measured as a function of time in the human tests, it was possible to fully define major response of the head as a function of time by relating any one of the head response variables to any one of the kinematic characteristics of T1. Velocity of T1 in the direction of sled motion was selected because it also produced relatively narrow response corridors for tests of all subjects at all impact levels when cross-plotted with one of the response variables, namely, head angle.

E. Conversion of the Response Corridors into Performance Requirements - The mean response and statistical variation of the data which forms the response corridors was computed and professed as the performance requirements. The results are presented in both graphical and tabular form.

F. Evaluation of Performance Requirement Sensitivity to Test Condition Variations - The performance requirements are based on the volunteer tests which were conducted with healthy, young male subjects exposed to subinjury level impacts. Of more significance, 1) the subjects were rather tightly restrained by shoulder straps, a lap belt and an inverted-V pelvic strap tied to the lap belt and 2) the deviation in rise time of sled acceleration was less than ±25% for all tests. Cadaver tests of WSU and other volunteer tests of the NBDL and WSU were used to determine the effect of deviations from the test conditions of the baseline volunteers.

It should be noted that only one modelling assumption was made in developing the performance requirements. Specifically, kinetic variables were calculated based on the assumption that the head was a rigid body. The remainder of the development process is simply kinematic transformation of the test data into a form which is hopefully more useful in compliance testing and injury prediction.

1.4 APPLICATION OF THE STUDY RESULTS

The performance requirements for a given impact direction consist of a set of functional constraints between kinematic and kinetic variables which describe head response, and a prescribed input velocity profile for the T1 vertebra. A test of fidelity for the head/neck system of an ATD is performed by duplicating a prescribed velocity profile at T1 and measuring the appropriate head response variables. The response variables can be monitored remotely with high speed cameras and, load, accelerometer and displacement transducers imbedded in the dummy. When testing a fully assembled dummy, the prescribed input velocity at T1 is achieved by (1) duplicating the restraint system and one of the seat acceleration profiles used in the volunteer tests from which the performance requirement was formulated* or (2) rigidly fixing the spine to the seat up to the T1 vertebra and imparting to the seat the prescribed T1 velocity profile.

---

*Some adjustment of the seat acceleration profile and/or restraint resilience may be necessary if torso response is not sufficiently humanlike.

The primary purpose of the performance requirements is to establish a concise, well defined and easily applied standard for determining fidelity of an assembled head and neck system. They are also of use to the designer of an ATD in establishing excursion limits, but do not provide the spring and damping (and perhaps active element) characteristics he requires. Loads calculated from the human response tests do, however, provide a check of the dynamical stiffness of the dummy. The performance requirements are also of use in the conceptual stage of dummy development when decisions must be made on the degree of fidelity desired.

2. NBDL VOLUNTEER TEST DATA

2.1 TEST DATA DESCRIPTION

At the Naval Biodynamics Laboratory (NBDL) in New Orleans in the past years, an extensive research program has been conducted to determine the dynamic head-neck response of volunteers to impact acceleration. In these tests, the subjects are seated in an upright position on a sled driven by a $HYGE^{(R)}$ Accelerator and exposed to short duration accelerations simulating frontal, oblique or lateral impacts. The resulting three-dimensional motions of the volunteers head and first thoracic vertebral body (T_1) are monitored by anatomically mounted clusters of accelerometers and photographic targets. Figure 2-1 depicts typical instrumentation for a test. Multi-camera coverage of targets attached to the head and T1 vertebra permits the six components of displacement (three translational and three rotational) for these body parts to be derived. Accelerometer clusters attached to each of these body parts permit the six components of acceleration for the body parts to be derived. A detailed description of the instrumentation and test methodology is provided in references [4], [5] and [6].

Data processing by NBDL includes conversion of the target data (both photo and sensor) into kinematics of the head and T1 vertebral body as indicated in Table 2-1. The time histories of 92 variables are recorded on data tape for each test. Appendix A of Volume II identifies and defines the 92 variables.

One hundred and nineteen impact tests have been conducted for the NHTSA by the NBDL that involve nine subjects. In addition, the NBDL has provided the NHTSA with the results of 256 similar tests, conducted for other agencies, that involve sixteen additional subjects. Appendix A contains a complete list of these tests along with selected characteristics. Table 2-2 lists 312 of the tests for which the impact is defined by the NBDL to be "low rate-of-onset, long duration" (LOLD) [7].

HEAD CENTER
OF GRAVITY

HEAD ANATOMICAL
ORIGIN*

OCCIPITAL CONDYLES

SPINE PHOTO TARGET/
SENSOR PACKAGE

MOUTH PHOTO TARGET/
SENSOR PACKAGE

T1 ANATOMICAL ORIGIN LOCATED AT
FIRST THORACIC VERTEBRA
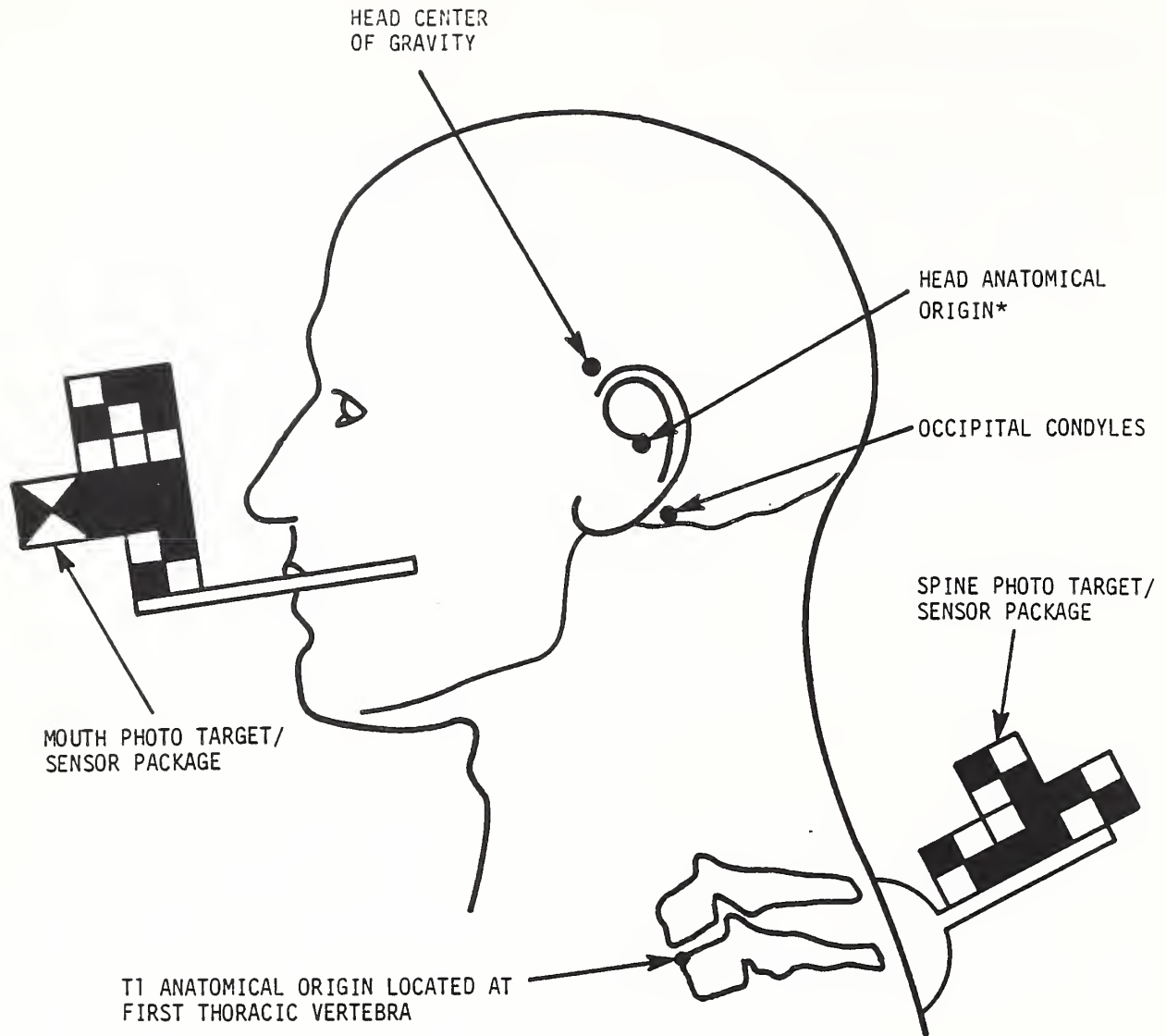
*Intersection of midsagittal plane and line connecting superior
 edges of auditory meati.

FIGURE 2-1.   LOCATION OF SENSORS AND PHOTOGRAPHIC TARGETS FOR NBDL
SIX-DEGREE-OF-FREEDOM MEASUREMENTS

TABLE 2-1. HEAD AND T1 VERTEBRAL BODY KINEMATICS AVAILABLE ON THE NBDL DATA TAPES

- Translations and linear velocities of the head and T1 anatomical origins with respect to the sled, derived from photographic as well as accelerometer data.

- Translations, linear velocities and linear accelerations of the head and T1 anatomical origins with respect to the laboratory derived from accelerometer data.

- Angular velocities of the head and T1 vertebra about their anatomical coordinate axes derived from photographic as well as accelerometer data.

- Angular accelerations of the head and T1 vertebra about their anatomical coordinate axes derived from accelerometer data.

- Rotations of the head and T1 vertebra expressed in Euler angles as well as quaternions with respect to the laboratory derived from photographic as well as accelerometer data.

- Acceleration, velocity and translation of the sled with respect to the laboratory.

TABLE 2-2. TABULATION OF LOW RATE-OF-ONSET, LONG DURATION TESTS BY SUBJECT, G-LEVEL AND IMPACT DIRECTION*

SUBJECT NUMBER

G-LEV	DIR	H 00044	H 00049	H 00060	H 00064	H 00065	H 00067	H 00083	H 00093	H 00096	H 00118	H 00119	H 00120	H 00127	H 00130	H 00131	H 00132	H 00133	H 00134	H 00135	H 00136	H 00138	H 00139	H 00140	H 00141	H 00142
3	FRT							3524	3525		3833/3796	3821/3797	3793	3794	3839/3803	3840/3804	3805	3841/3798	3807/3842	3808	3809					
	OBL							3053	3049																	
	LAT	1452	1470	1468	1449	1448	1453	1960							4050	4052	4053	4057	4054	4055	4058	4059	4069	4060	4068	4073
4	FRT												3814	3812	3815	3817	3818	3819	3822	3823	3824					
	OBL							3065	3061						4159	4161	4162	4163	4164	4166	4167	4168	4170	4234	4171	4172
	LAT	1458	1474	1475	1456	1454	1457	1998			3837				4070	4071	4155/4074	4075	4076	4078	4079	4080	4085	4081	4083	4084
5	FRT							3530	3531						4088	4089	4090	4093	4097	4095	4098	4092	4100	4089	4094	4104
	OBL							3077																		
	LAT				1471/1501	1487	1484	2013	2010/2294	2298																
6	FRT							3085/3100	3088/3106		3856/3875/3880		3851/3878	3893/3852	3854/3876	3857/3885	3858/3887	3869	3870	3871	3872					
	OBL														4107	4109	4110	4111	4112	4114	4142	4147	4118	4145	4119	4149
	LAT	1504			1507	1505	1503	2027	2032						4137	4138	4143	4151	4139	4140		4115	4144	4116	4148	4120
7	FRT							3536	3537						4235	4242	4244	4236	4237	4238	4247	4241	4243	4259	4248	4249
	OBL							3093/3102	3097																	
	LAT	1512			1513	1510	1509	2302	2282						4123	4124	4128	4125	4126	4131	4153	4129	4133	4130	4134	4135
8	FRT										3886		3882	3883	3889	3894	3900/3997	3895	3890	3898	3901					
	OBL							3133	3122																	
	LAT	1528			1524	1526	1525																			
9	FRT							3544	3548					3904												
	OBL							3145	3129						4206	4246	4261	4240	4264	4314	4263	4265	4313	4269	4270	4295
	LAT														4301					4266			4268	4302		4271
10	FRT								3550		3903/3985		3906/3995		3928/3991	3908/3999	3989/3909	3998/3913		3916/3994						
	OBL								3148						4286	4251	4287		4290	4316	3918	4284	4280	4293	4292	4288
	LAT														4276		4297		4298	4277		4296	4291	4281	4282	
11	FRT								3558						4309		4306		4307			4305	4303	4310		
	OBL																									
	LAT																									
12	FRT								3573		3920		3921	3924	3944	3926	3927	3939	3940		3942					
	OBL																									
	LAT																									
13	FRT								3578		3945		3946	3949			3850	3951	3961	3941	3953					
	OBL																									
	LAT																									
14	FRT								3583				3954			3948/3987		3963	3968	3955	3962					
	OBL																									
	LAT																									
15	FRT								3616		3958/3969		3972	3959		3990	3957/3982	3986	3983	3965/3970						
	OBL																									
	LAT																									

*THE PREFIX "LX" HAS BEEN OMITTED FROM THE TEST NUMBERS LISTED IN THE BODY OF THIS TABLE.

2-4

From this set of data, 131 tests, shown shaded in Table 2-2, were selected to characterize head and neck response. Frontal response of eight subjects is characterized at impact levels of 4, 8, 12 and 15 g's. Lateral response of twelve subjects is characterized at 3, 5 and 7 g's. Oblique response of the same twelve subjects is characterized at 4, 7 and 10 g's. Tests of subjects H00131 and H00132 are included even though they have been identified as having a "learned" response [10]. The response of subject H00134, who is judged to be typical, is presented at all impact levels for which he was tested.

Data for subject H00093 was not used due to a data processing error in the test data that has been noted by the NBDL [8]. Data for subjects H00044, --49, --60, --64, --67, and -83 was not used due to the inability of the analysis software to make meaningful comparison of the tests of these subjects with the remainder of the tests due to a variation in film digitization rates. Further, the sled deceleration profile was varied more for tests of these subjects, resulting in a more varied response. The response characteristics for some of the tests of the subjects not included here are contained in references [3] and [9].

Test LX2124, with an impact profile designation, "high rate-of-onset long duration" (HOLD) is used in the sensitivity study to illustrate the effect of variation in impact profile.

2.2 DATA PREPARATION FOR THIS STUDY

A data retrieval and display program was written for the NHTSA VAX computer which allows instantaneous access to the entire set of NBDL head-neck data from remote terminals. The user can retrieve any specified subset of data in numerical or graphical format, or he can ask for further processing including sums, differences, vector resultants and normalization based on maximum value. The program is useful for the development of performance corridors, since any pair of variables from any number of tests can be displayed on a single graph. Volume II describes the data retrieval and display program.

The database stored with the retrieval program is unaltered from that received from NBDL except as indicated in Sections 2.2.1, 2.2.2 and 2.2.3 which follow.

2.2.1   Database Compression

To minimize disk storage requirements and provide immediate access to the entire database, information is stored in binary format and only those "generic" variables are stored which cannot be constructed readily from others by integration. Integration routines are built into the retrieval program that reproduce the "nongeneric" NBDL variables to the fifth significant figure or better. This reconstruction process is transparent to the user.

2.2.2   Elimination of Data Gaps in the Photographic Data

There are occasional gaps in the data derived from the film, apparently as the result of loss of sight of a target by one or more cameras. For runs with data gaps within the first 300 milliseconds, the gaps were eliminated by inserting values based on accelerometer derived data as follows: Over the same time span the difference was computed between the accelerometer reading and the value obtained by straight line interpolation of the accelerometer data over the gap. This difference is added to the value obtained by straight line interpolation of the photo data over the gap. Figure 2-2 illustrates the technique. Gaps beyond 300 milliseconds (post peak excursion) were eliminated by straight line interpolation.

The gaps are identified by sudden drops in value of the variable to 0 (runs of subjects 44 to 67 of Appendix A) or to 2×10^6 (runs of subjects 83 to 142 of Appendix A). Photographic variables with data gaps could not be plotted using the retrieval and display program because automated axis scaling is present.

2.2.3   Correction of Measured Vertical and Angular Position of the T1 Vertebra

Neck length, calculated as described in Section 4.1.1 which follows, showed unexpected variation in initial length from test to test for a given subject. This variation was observed by Wismans [11] to be correlated with vertical height of the T1 vertebra in the sled fixed coordinates. With the expectation that initial neck length would be nearly constant in any one subject, and the acknowledged difficulty by the NBDL in placing the T1 sensor, the liberty was taken of altering the test data related to T1 vertical position by a technique that accounts for the observed correlation. The portion of the variation in T1 position that is not

$$x_{ip} = x_{1p} + \left\{ \frac{(x_{2p}-x_{1p})(t_2-t_i)}{(t_2-t_1)} + \left[x_{iA} - \frac{(x_{2A}-x_{1A})(t_2-t_i)}{(t_2-t_1)} \right] \right\}$$
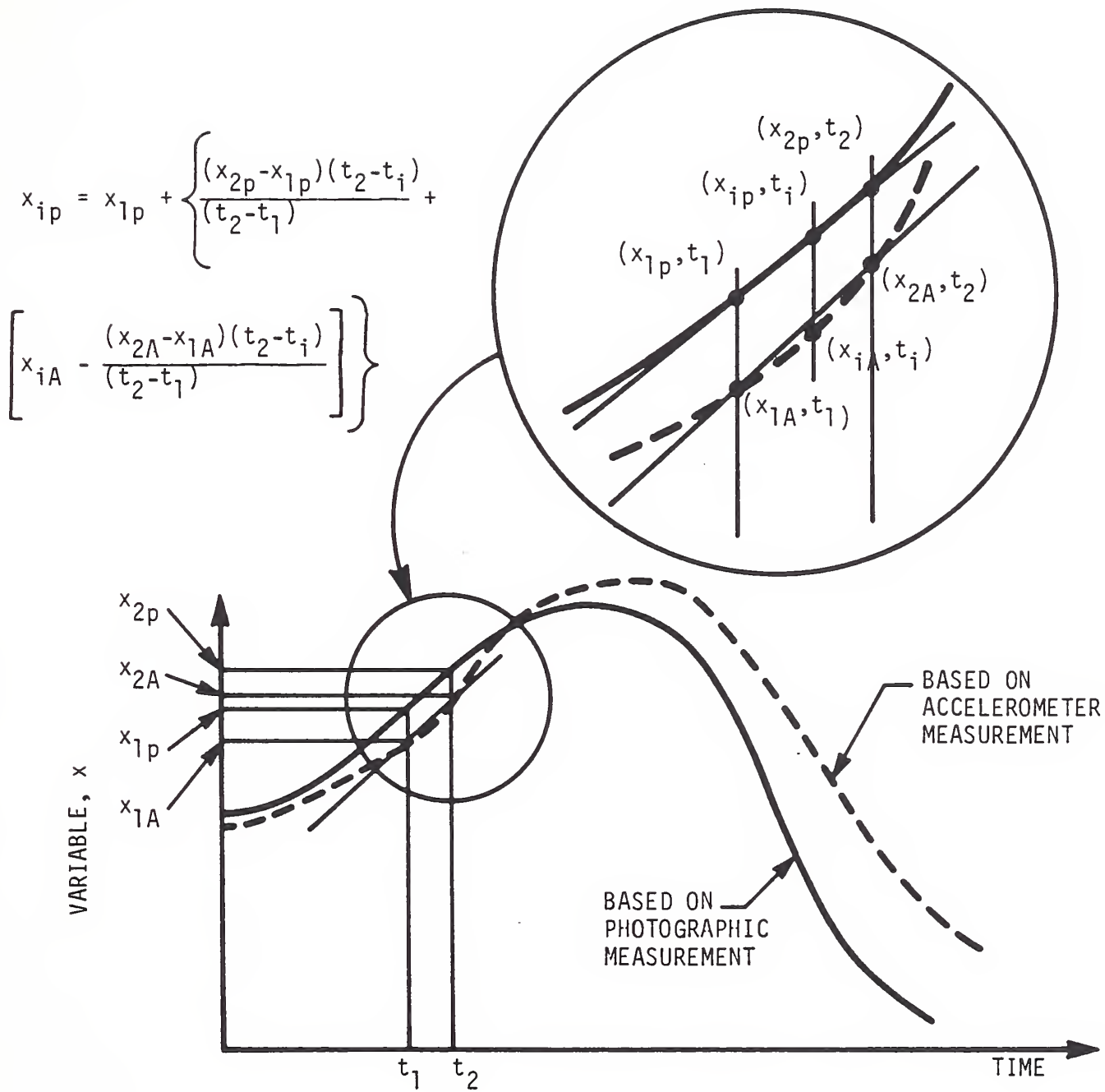
FIGURE 2-2. ILLUSTRATION OF THE PROCEDURE FOR ELIMINATION OF
PHOTOGRAPHIC DATA GAPS

correlated with initial neck length remains in the T1 variable as variation in seated position. The procedure for adjusting vertical position of T1 is described in Appendix B.

Initial angular orientation of the T1 vertebra of either subject from test-to-test also appears to vary more than expected. This could also result from variation in T1 sensor placement from test-to-test. With no obvious means for identifying the actual initial position, a new anatomical coordinate system was defined that is aligned with the sled fixed coordinate system at the start of each test. Thus, initial T1 orientation in this new T1 coordinate system is identical in all tests. The ability to evaluate the effect of variation in initial angular orientation of the T1 vertebra from test-to-test is forgone in order to gain greater consistency in measuring head and neck angular position with respect to the torso.

2.2.4   Selection of Photo and Accelerometer Derived Variables

There are two variables in the data base for each angular and linear displacement and velocity as indicated in Table 2-1. The duplication results from post test integration and differentiation of accelerometer and film records, respectively. Velocity and displacement obtained. by integrating accelerometer data is susceptible to drift if bias is present in the accelerometer while velocity obtained from digitized film data smooths high frequency response. A procedure has been developed by the NBDL to merge the photo and accelerometer based data into a single set [12] in order to improve the quality of the data. However, for purpose of this study, sufficient accuracy is achieved by using displacement results from the film record in conjunction with acceleration and velocity data from the accelerometers.

2.3   QUALITATIVE ANALYSIS OF THE DATA

In a frontal, or $-G_x$, test the head of the volunteer responds by nodding forward in flexion. In a lateral, or $+G_y$, test the head rotates about both vertical and horizontal axes such that the nose moves toward the right shoulder. In an oblique, or $-G_x+G_y$, test the response is similar to that of a lateral test except that the excursion limits are reduced.

A high degree of similarity exists in the response of the NBDL volunteers for tests in any of the three directions. Table 2-3 summarizes the noteworthy characteristics of the response for frontal, lateral or oblique impact. Equations are developed in Section 4 to permit quantification of these characteristics with response variables that are readily measured in an ATD. The characteristics of Table 2-3 are then quantitatively analyzed in Section 5 and a set of performance requirements is developed.

TABLE 2-3. NOTEWORTHY CHARACTERISTICS OF VOLUNTEER HEAD AND NECK RESPONSE

FRONTAL:

o There is a significant head rotation and CG translation in the impact plane.

o Translation of the T1 vertebra relative to the seat in the thrust vector direction varies between 4 and 8 cm. There is no other significant motion of T1.

o Neck chord length at peak excursion is reduced by 10%-30%.

LATERAL:

o There is significant head rotation and CG translation in the impact plane.

o The only significant head motion not in the impact plane is twist about a vertical axis in the head.

o Translation of the T1 vertebra along the thrust vector varies between 4 and 8 cm. There is no other significant motion of T1.

o Neck chord length at peak excursion is reduced by up to 20%.

OBLIQUE:

o (Similar to lateral response.)

3. OTHER VOLUNTEER AND CADAVER TEST DATA

3.1 TEST DATA DESCRIPTION

At Wayne State University, a series of sled tests were conducted on both volunteers and cadavers, using the Wayne State Accelerator Mechanism (WHAM III) [13][14]. All tests simulated frontal impact and in three of the cadaver tests a three-point torso harness was used in conjunction with upper and lower leg clamps. In the remainder of the tests, a lap belt was used in lieu of the three-point harness.

As in the case of the NBDL volunteers, the head and T1 vertebral body were instrumented with both accelerometers and photo targets so that three-dimensional translation and rotation of each could be monitored.

Table 3-1 lists the WSU tests which are used in this study. Peak sled g-level is used here to classify the test severity as in the NBDL tests. However, the "looser" restraint types employed in the WSU tests results in a highly attenuated head motion relative to the torso, making it meaningless to compare NBDL and WSU sled impact levels.

3.2 DATA PREPARATION FOR THIS STUDY

The WSU data was obtained from tests of spinal kinematics and kinetics conducted for the NHTSA. The response of the T1 vertebral body was analyzed as part of that study. However, head response data was not analyzed. For the current study the photographic data for the head and T1 vertebral body were digitized in order to compare the kinematic response with that of the NBDL volunteers.

3.2.1 Film Digitization

Film records for the runs listed in Table 3-1 were obtained from WSU and digitized using semi-automated digitization equipment and software available at

TABLE 3-1. SUMMARY OF WAYNE STATE UNIVERSITY
TESTS USED FOR THIS STUDY

RUN NO.	SUBJECT NO.	G-LEVEL	RESTRAINT TYPE
307	CAD 3788	5	3-Point
308	CAD 3788	5	3-Point
309	CAD 3788	4	Lap
310	CAD 3788	20	Lap
314	CAD 3814	25	Lap
331	CAD 3846	20	3-Point
332	CAD 3797	5	Lap
333	CAD 3797	30	Lap
343	CAD 3938*	20	Lap
345	CAD 3938*	10	Lap
453	VOL 0252	6	Lap
454	VOL 0252	6	Lap
455	VOL 0252	6	Lap

*Unembalmed

the University of Michigan's Transportation Research Institute.*   Figure 3-1 is a schematic which indicates the eight points digitized in each frame. The camera is fixed to the sled for the WSU tests. Hence, all target motion measured is relative to the sled. Point 8, a laboratory fixed point is used to establish sled motion.

3.2.2   Conversion to Volunteer Format

The eight sets of digitized camera coordinates were used to calculate seven NBDL defined variables as listed in Table 3-2. Out-of-impact plane motion was assumed to be small and was not calculated. The only three-point restrained cadaver tests used in this study were those that contained negligible out-of-plane response as observed by an overhead camera.

The equations used for calculating the NBDL variables of Table 3-2 are contained in Appendix C. A computer program written for the central computer at the University of Michigan was used to convert the digitized data into NBDL variables.   This data was then transferred to the NHTSA/VAX computer and compressed using the procedures described in Section 2.2.1, so that the WSU data could be analyzed in conjunction with that from the NBDL.

3.3   QUALITATIVE ANALYSIS OF THE DATA

Only frontal, or $-G_x$, tests were processed and analyzed. This limitation and the small number of tests (13) analyzed makes the observations and conclusions less substantial than for the NBDL volunteer tests. When analyzed in conjunction with the NBDL data, however, it is possible to identify similarities and differences in response that satisfy the intuition, thereby giving further credence to all of the results. Table 3-3 summarizes the noteworthy characteristics of the WSU tests as observed in the films. These results are quantified in Section 5.6 and compared to the characteristics of the NBDL volunteers.

---

*The hardware consists of a digitizer linked to a personal computer so that a hand held pointer can be used to digitize the location of up to 8000 points in each frame of a film and enter them into a computer file. Software for the system is documented in reference [15].
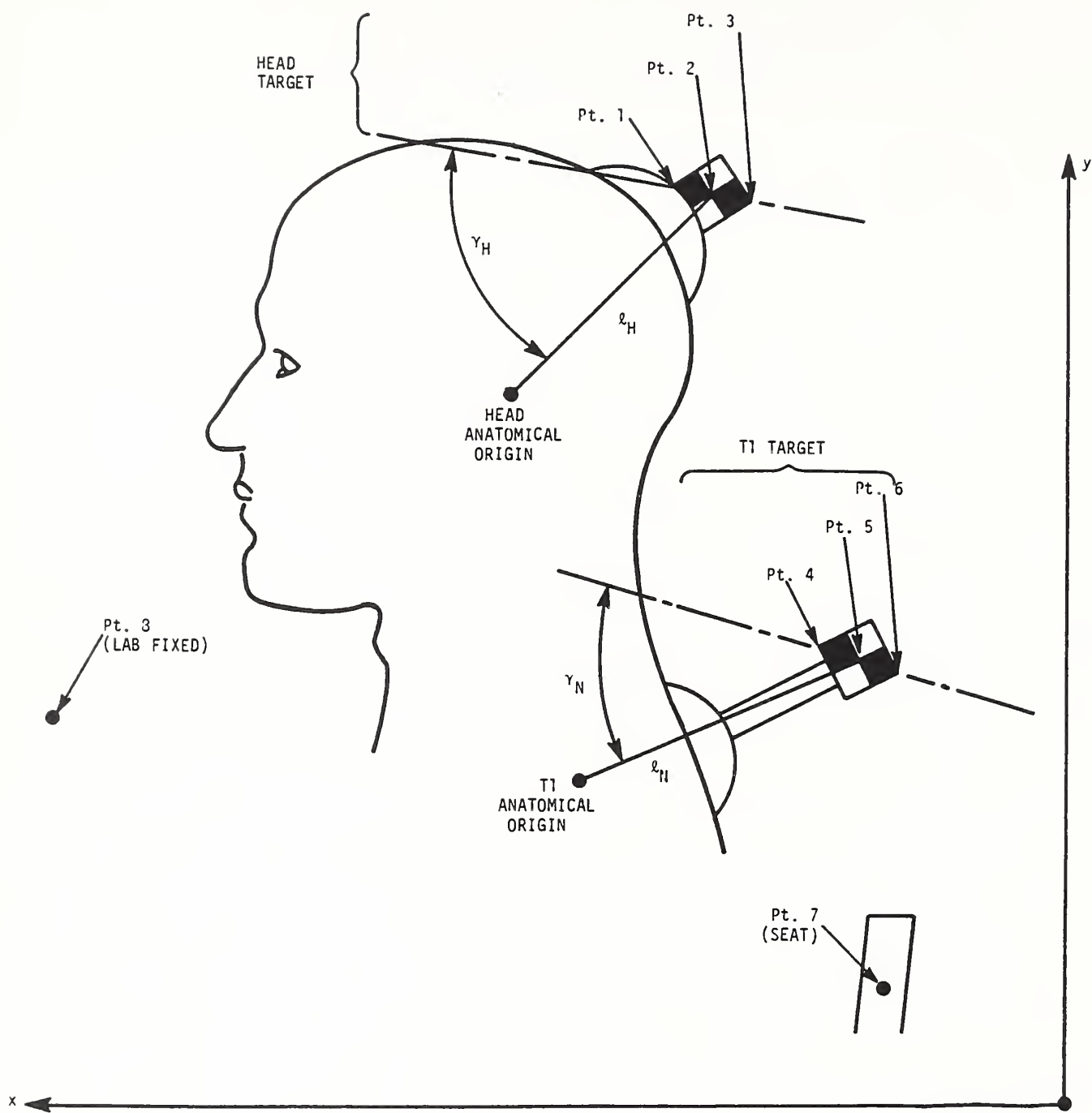
FIGURE 3-1. ILLUSTRATION OF THE POINTS DIGITIZED IN EACH FRAME OF FILM FOR THE WSU TESTS

TABLE 3-2. NBDL DEFINED VARIABLES CALCULATED
FOR THE WSU TESTS

Variable Symbol	Generalized Definitions(*)
DAXSOP DAZSOP	Translation of the head anatomical origin relative to the sled.
PHBO2P	Rotation of the head.
DNXSOP DNZSOP	Translation of the T1 anatomical origin relative to the sled.
PNBO2P	Rotation of the T1 vertebral body.
DCXSOP	Translation of the sled relative to the laboratory.

*The variables are fully defined in Appendix A of Volume II.

TABLE 3-3. NOTEWORTHY CHARACTERISTICS OF
THE WSU VOLUNTEER AND CADAVER
TESTS

VOLUNTEER FRONTAL TESTS:

o   There is significant rotation of both the head and torso
    in the impact plane.

o   Head forward rotation relative to the torso begins near
    the maximum torso rotation.

o   Translation of the T1 vertebra relative to the seat in the
    thrust vector direction varies between 18 and 20 cm.

o   There is no significant out-of-impact plane motion.

CADAVER FRONTAL TESTS (3-Point Restrained):

o   There is significant head forward rotation and
    translation in the impact plane.

o   Translation of the T1 vertebra relative to the seat in the
    thrust vector direction varies between 12 and 20 cm.
    There is no other significant motion of T1.

o   Neck chord length at peak excursion is lengthened up to
    25%.

CADAVER FRONTAL TEST (Lap Belt Restrained):

o   (Similar to WSU Volunteer Tests but with T1 translations
    of 30-50 cm.)

4. ANALYSIS PROCEDURES

In Section 4.1, a set of variables are defined which characterize the significant kinematic response observed in frontal, lateral and oblique tests. In Section 4.2, the equations are developed for establishing impact response loads at the occipital condylar and T1 vertebral points.

4.1   KINEMATIC ANALYSIS

4.1.1 Definition of Neck Chord Length

The position of the occipital condylar point with respect to the lab or sled can be determined from the position data for the head anatomical origin since these points are fixed relative to one another in any test subject. It is then possible to calculate the distance from the condylar point to the T1 vertebral point, herein referred to as the neck chord length at any instant from the test data.

Figure 4-1 shows the position vectors used to establish the neck chord vector, which is given by:

$$\bar{r}_{O/T} = \bar{r}_A + \bar{r}_{O/A} - \bar{r}_T \qquad (1)$$

Vectors $\bar{r}_A$ and $\bar{r}_T$ are obtained from the sled tests [16]. Vector $\bar{r}_{O/A}$ is subject dependent and can be estimated using x-rays.*

4.1.2 Coordinate System Definitions

Five coordinate systems are used to analyze three-dimensional head/neck motion in this study. Four have previously been defined by the NBDL [4] and these definitions are repeated here:

1.   The <u>laboratory reference coordinate system</u> (L) is fixed at the point occupied by the sled chair target center prior to the onset of acceleration. The +z-axis is opposite in direction to gravity and the +x-axis is opposite in direction to the sled acceleration stroke.

---

*For this work, averages were used. See Section 4.2.3.

G = Head center of gravity

A = Head anatomical origin

O = Occipital condylar point

T = T1 vertebral point

I = Inertial (Lab) fixed point
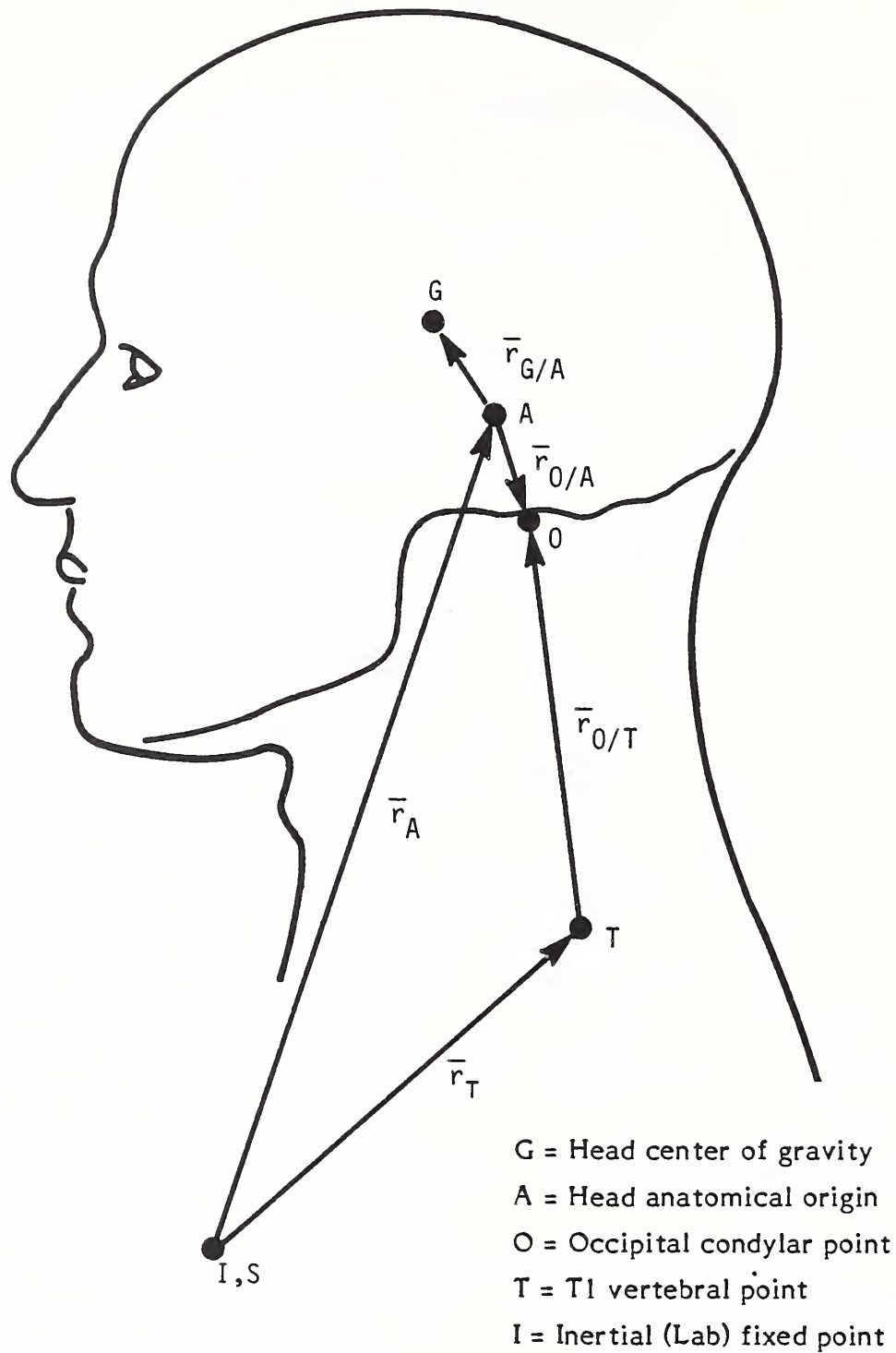
FIGURE 4-1. VECTOR POSITION OF SELECTED HEAD AND NECK LOCATIONS

2. The <u>sled reference coordinate system</u> (S) has its origin fixed to the sled chair target center with the axes parallel to the laboratory reference coordinate system.

3. The <u>head anatomical coordinate system</u> (H) (see Figure 4-2) is derived from an anatomical plane which is specified by the superior edge of each auditory meatus and by the infraorbital notches. The origin is at the midpoint of a line connecting the superior edges of the right and left auditory meati. The +x-axis is from the origin through the midpoint of a line connecting the infraorbital notches in the anatomical plane. The +z-axis is from the origin in the superior direction perpendicular to the anatomical plane.

4. The <u>spine anatomical coordinate system</u> (T) (see Figure 4-2) has its origin at the anterior superior corner of the first-thoracic vertebral body (the T1 vertebral point). The +x-axis is defined by a line connecting the midpoint of the superior corner and the inferior corner of the posterior spinous process of T1 to the anterior superior corner of T1. The +z-axis is perpendicular to the x-axis in the plane of the above three points and in the superior direction.

Angular position of the head anatomical coordinate system with respect to the laboratory coordinate system is defined by three sequential (Euler) angles:

1. Rotation, θ_{Hx}, about the x axis of the laboratory coordinate system.

2. Rotation, θ_{Hy}, about the carried y axis.

3. Rotation, θ_{Hz}, about the carried z-axis.
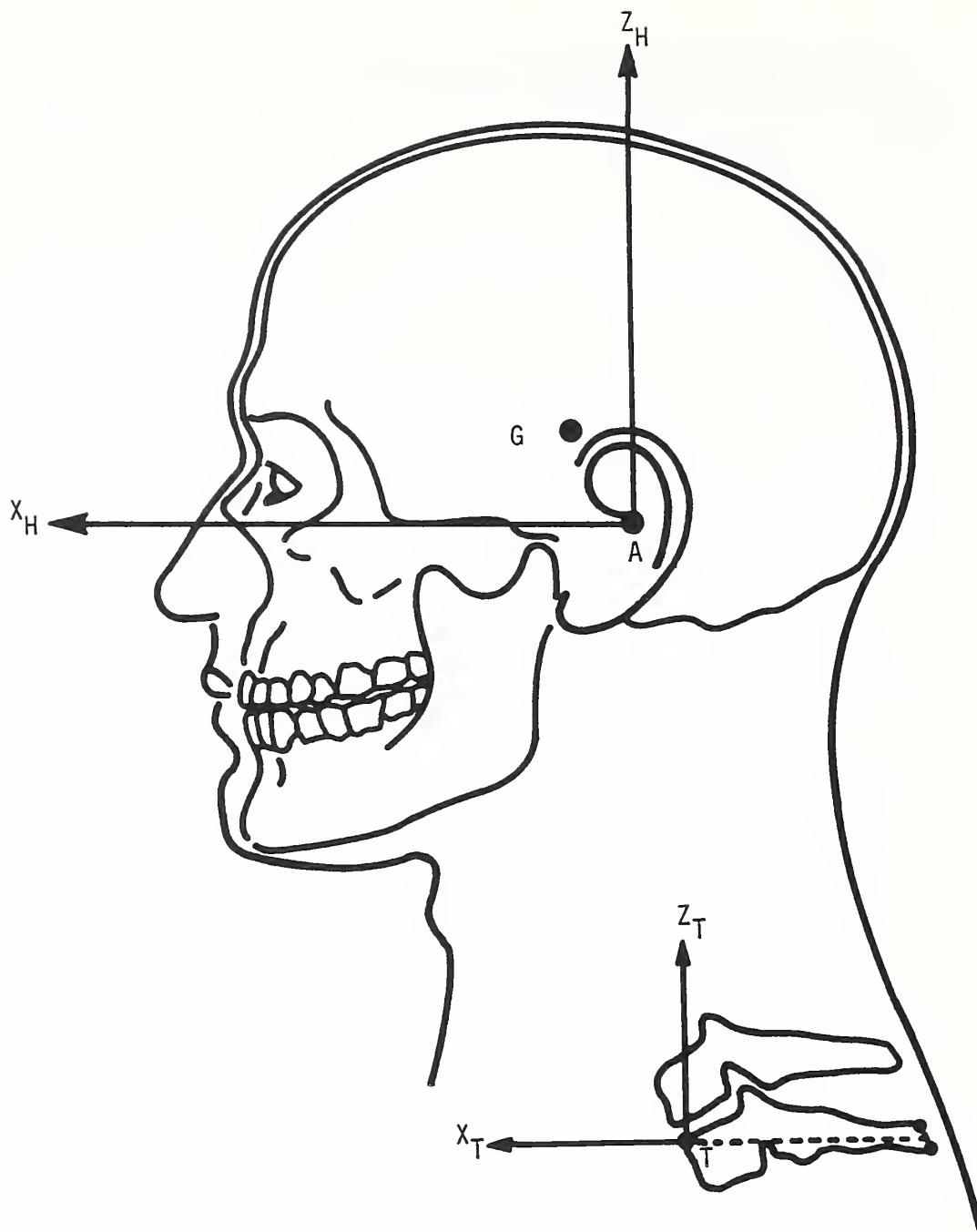
G = Head Center of gravity
A = Head anatomical origin
T = T1 Vertebral point

FIGURE 4-2. SKETCH OF THE ANATOMICAL COORDINATE SYSTEMS FOR THE
HEAD AND T1 VERTEBRAL BODY

The matrix transformation of laboratory components into head anatomical components is:

$$
R_H = \begin{bmatrix}
\cos\theta_{Hz} \cos\theta_{Hy} & \cos\theta_{Hx} \sin\theta_{Hz} + \cos\theta_{Hz} \sin\theta_{Hy} \sin\theta_{Hx} & \sin\theta_{Hz} \sin\theta_{Hx} - \cos\theta_{Hz} \sin\theta_{Hy} \cos\theta_{Hx} \\
-\sin\theta_{Hz} \cos\theta_{Hy} & \cos\theta_{Hz} \cos\theta_{Hx} - \sin\theta_{Hz} \sin\theta_{Hy} \sin\theta_{Hx} & \cos\theta_{Hz} \sin\theta_{Hx} + \sin\theta_{Hz} \sin\theta_{Hy} \cos\theta_{Hx} \\
\sin\theta_{Hy} & -\cos\theta_{Hy} \sin\theta_{Hx} & \cos\theta_{Hy} \cos\theta_{Hx}
\end{bmatrix}
\quad (2)
$$

Angular position of the spine anatomical coordinate system (T) with respect to the laboratory coordinate system is defined by three sequential (Euler) angles:

1. Rotation, θ_{Nx}, about the X axis of the laboratory coordinate system.

2. Rotation, θ_{Ny}, about the carried Y axis.

3. Rotation, θ_{Nz}, about the carried Z axis.

The matrix transformation of laboratory components into spine anatomical components is:

$$
R_N = \begin{bmatrix}
\cos\theta_{Nz} \cos\theta_{Ny} & \cos\theta_{Nx} \sin\theta_{Nz} + \cos\theta_{Nz} \sin\theta_{Ny} \sin\theta_{Nx} & \sin\theta_{Nz} \sin\theta_{Nx} - \cos\theta_{Nz} \sin\theta_{Ny} \cos\theta_{Nx} \\
-\sin\theta_{Nz} \cos\theta_{Ny} & \cos\theta_{Nz} \cos\theta_{Nx} - \sin\theta_{Nz} \sin\theta_{Ny} \sin\theta_{Nx} & \cos\theta_{Nz} \sin\theta_{Nx} + \sin\theta_{Nz} \sin\theta_{Ny} \cos\theta_{Nx} \\
\sin\theta_{Ny} & -\cos\theta_{Ny} \sin\theta_{Nx} & \cos\theta_{Ny} \cos\theta_{Nx}
\end{bmatrix}
\quad (3)
$$

An anatomical coordinate system, T_o is defined which has its origin at the T1 vertebral point and axes coincident with the laboratory axes at the start of each test. The orientation of the T_o coordinate system with respect to the T coordinate system is fixed for any test and is given by R_{No}^{-1} where the $^{-1}$ exponent indicates the matrix inverse and R_{No} are the elements of R_N evaluated at the start of each test. For angular motions expressed with respect to this torso fixed coordinate system, information on initial orientation in one test relative to another is lost. Since there is significant variation in orientation of the NBDL defined T coordinate system from test to test that is attributable to variation in sensor placement, the T_o coordinate system is a convenient alternative which eliminates this undesirable variation. It should be noted that <u>the T_o coordinate system is fixed in the torso in orientations that vary with the direction of the sled impact.</u> The y-axis is always perpendicular to the impact plane initially which implies that it may point out through the left shoulder, out through the chest, or out through a point midway between these. This "variable position" coordinate system proves useful in quantifying the head twist that is observed in lateral and oblique tests as described in the next section.

The Euler angles for equations (2) and (3) are test data provided by the NBDL.

4.1.3 Definition of Head and Neck Rotation Variables

The Euler angles of equation (2) define head orientation with respect to the laboratory coordinate system. It is desirable to express head orientation with respect to the torso using variables that are readily measured in a dummy.

Using matrix rotation, a unit vector, $\hat{l}$, along the head anatomical z-axis can be written in T_o coordinate system components:

$$\begin{Bmatrix} \hat{u}_x \\ \hat{u}_y \\ \hat{u}_z \end{Bmatrix} = \begin{bmatrix} R_{No} \end{bmatrix}^{-1} \begin{bmatrix} R_N \end{bmatrix} \begin{bmatrix} R_H \end{bmatrix}^{-1} \begin{Bmatrix} 0 \\ 0 \\ \hat{l} \end{Bmatrix} \qquad (4)$$

where the brackets $\{\ \}$ indicate 3 x 1 matrices, and $\hat{u}_x$, $\hat{u}_y$ and $\hat{u}_z$ are components along the x, y, and z axes of the T_o coordinate system. Head rotation with respect to the torso can then be expressed as

$$\phi_y = \tan^{-1}\left(\frac{u_x}{u_z}\right) \tag{5}$$

$$\phi_x = \sin^{-1}\left(\frac{u_y}{1}\right) \tag{6}$$

where

ϕ_y = the angle between the z-axis of the T_o coordinate system and the projection of the z-axis of the head anatomical coordinate system onto the x-z plane of the T_o coordinate system

ϕ_x = the angle between the head anatomical z-axis and the x-z plane of the T_o coordinate system.

Figure 4-3 shows the two angles. These angles uniquely define the angular orientation of the head z-axis relative to the torso. Angle ϕ_x measures out of impact plane motion and is always small. Angle ϕ_y can therefore be measured with sufficient accuracy in an ATD using a high speed camera that faces the impact plane to track head mounted targets. For a dummy with a segmented spine, instrumentation built into the joint at the occipital condylar point can be used to measure ϕ_y.

The angular orientation of the neck chord vector is defined in a manner similar to the head z-axis orientation. The components in laboratory coordinates, $\{r_{O/T}\}_t$ are transformed to T_o coordinate system components, $\{r_{O/T}\}_{T_o}$ by the relationship:
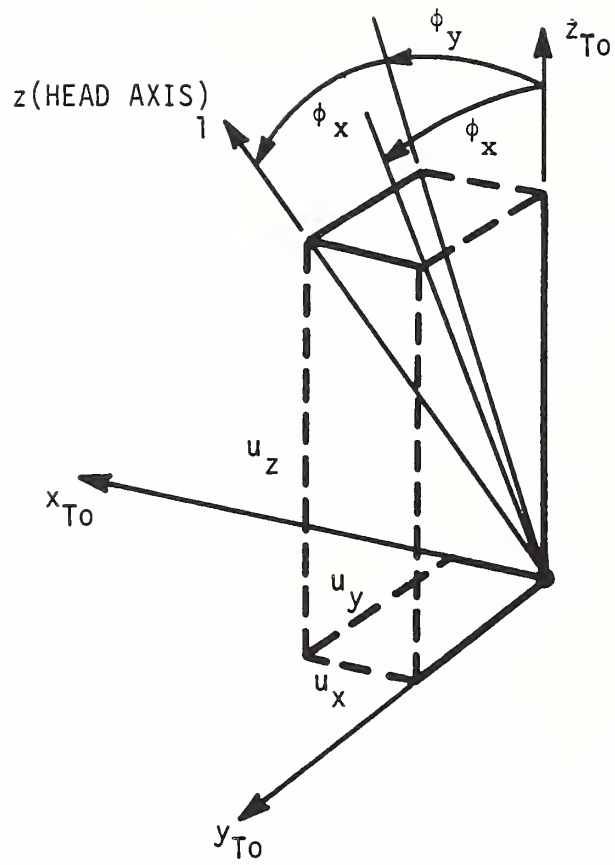
FIGURE 4-3. HEAD ROTATION ANGLES

$$\left\{ r_{O/T} \right\}_{T_O} = \left[R_{N_O} \right]^{-1} \left[R_N \right] \left\{ r_{O/T} \right\}_L \tag{7}$$

Then, neck chord vector orientation with respect to the torso becomes

$$\theta_y = \tan^{-1} \left(\frac{r_{O/Tx}}{r_{O/Ty}} \right) \tag{8}$$

$$\theta_x = \sin^{-1} \left(\frac{r_{O/Ty}}{r_{O/T}} \right) \tag{9}$$

where $r_{O/Tx}$, $r_{O/Ty}$ and $r_{O/Tz}$ are the scalar x, y and z components, respectively, of the neck chord vector in the T_O coordinate system, and

θ_y = the angle between the z-axis of the T_O coordinate system and the projection of the neck chord vector on the x-z plane of the T_O coordinate system.

θ_x = the angle between the neck chord vector and the x-z plane of the T_O coordinate system.

Figure 4-4 shows the two angles. As with the head rotation angles, only neck rotation, θ_y, is shown to be significant in the tests analyzed and, therefore, can be adequately measured in an ATD with a high speed camera that faces the impact plane or with internal sensors.

For lateral and oblique impacts the head also twists about a vertical axis in the head. The twist relative to the torso can be measured in an ATD with an overhead camera fixed to the sled or lab. The camera must observe an angle between a torso line that remains essentially horizontal throughout the impact e.g., a line in the x-y plane of the T_O coordinate system, and the projection of a head line, e.g. the x-axis of the H coordinate system, on the x-y plane of T_O. To obtain this angle from the NBDL test data, a unit vector, $\hat{i}$, along the head anatomical x-axis is converted to T_O components, analagous to equation (4).
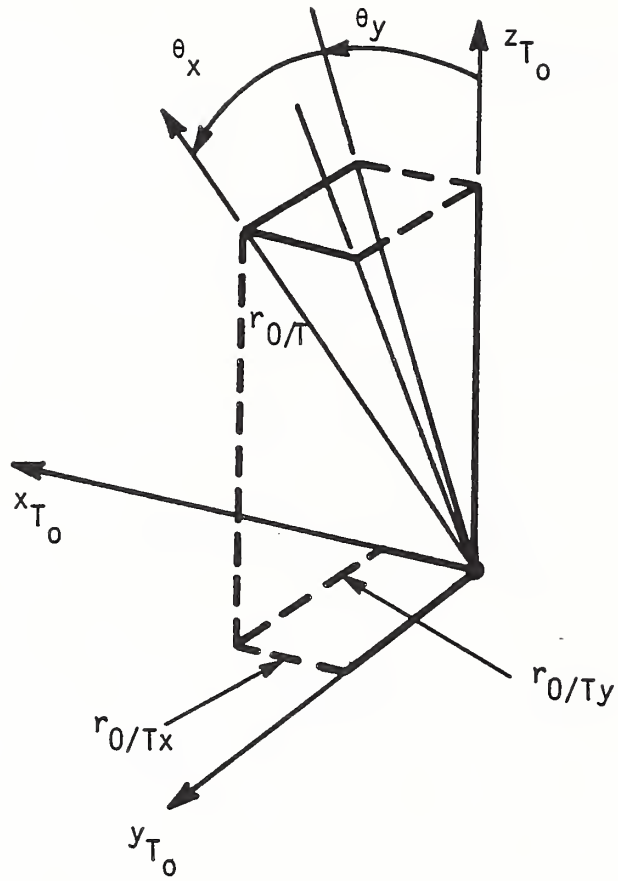
FIGURE 4-4. NECK ROTATION ANGLE

$$
\begin{Bmatrix} \hat{v}_x \\ \hat{v}_y \\ \hat{v}_z \end{Bmatrix} = [R_{No}]^{-1} \ [R_N] \ [R_H]^{-1} \begin{Bmatrix} \hat{1} \\ 0 \\ 0 \end{Bmatrix}
\qquad (10)
$$

and the twist angle, ψ_c, is given by:

$$
\psi_c = \tan^{-1} \left(\frac{v_y}{v_x} \right)
\qquad (11)
$$

Angle ψ_c is illustrated in Figure 4-5a for a frontal test.

When head twist is measured internally in an ATD, this generally implies that all of the twist is concentrated at one joint. The orientation of the twist joint changes the amount of relative motion required. The following equations define an alternate-twist angle, ψ_I, which is the amount of relative rotation required when the axis of twist is along the z-axis of the H coordinate system. Transformation from the T_O to H coordinate system is given by:

$$
\qquad (12)
$$

$$
[R_{TH}] = \left[[R_{No}]^{-1} \ [R_N] \ [R_H]^{-1} \right]^{-1}
$$

or defining three sequential Euler angles,

1. Rotation, θ_{Tx} about the x-axis of the T_O anatomical coordinate system.

2. Rotation, θ_{Ty}, about the carried y-axis.

3. Rotation, θ_{Tz}, about the carried z-axis.

4-11
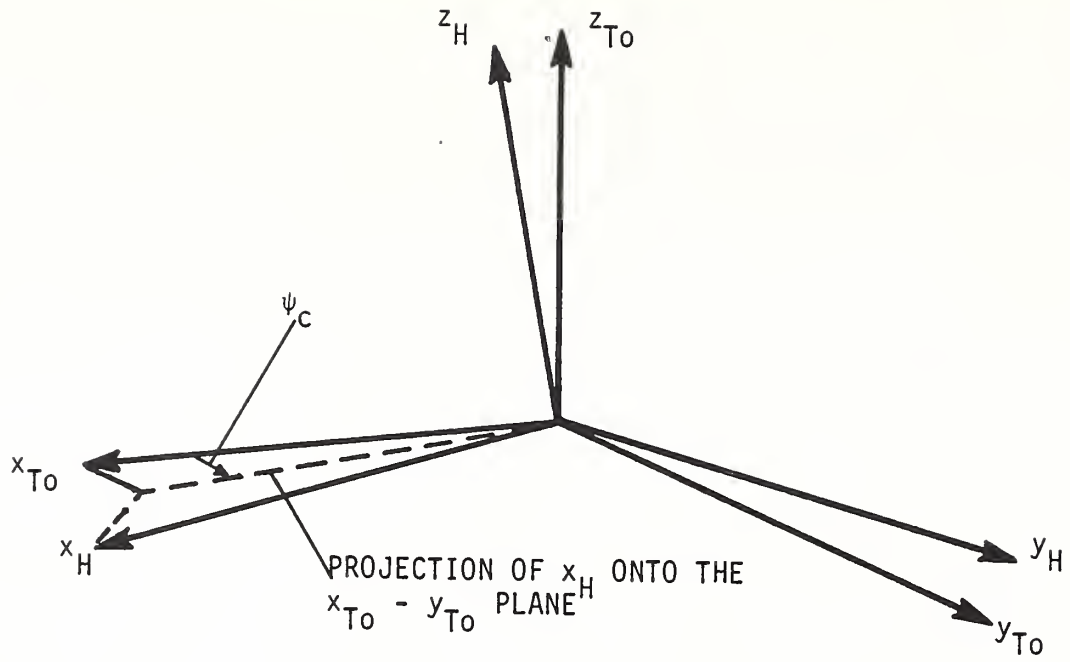
a) Angle ψ_C
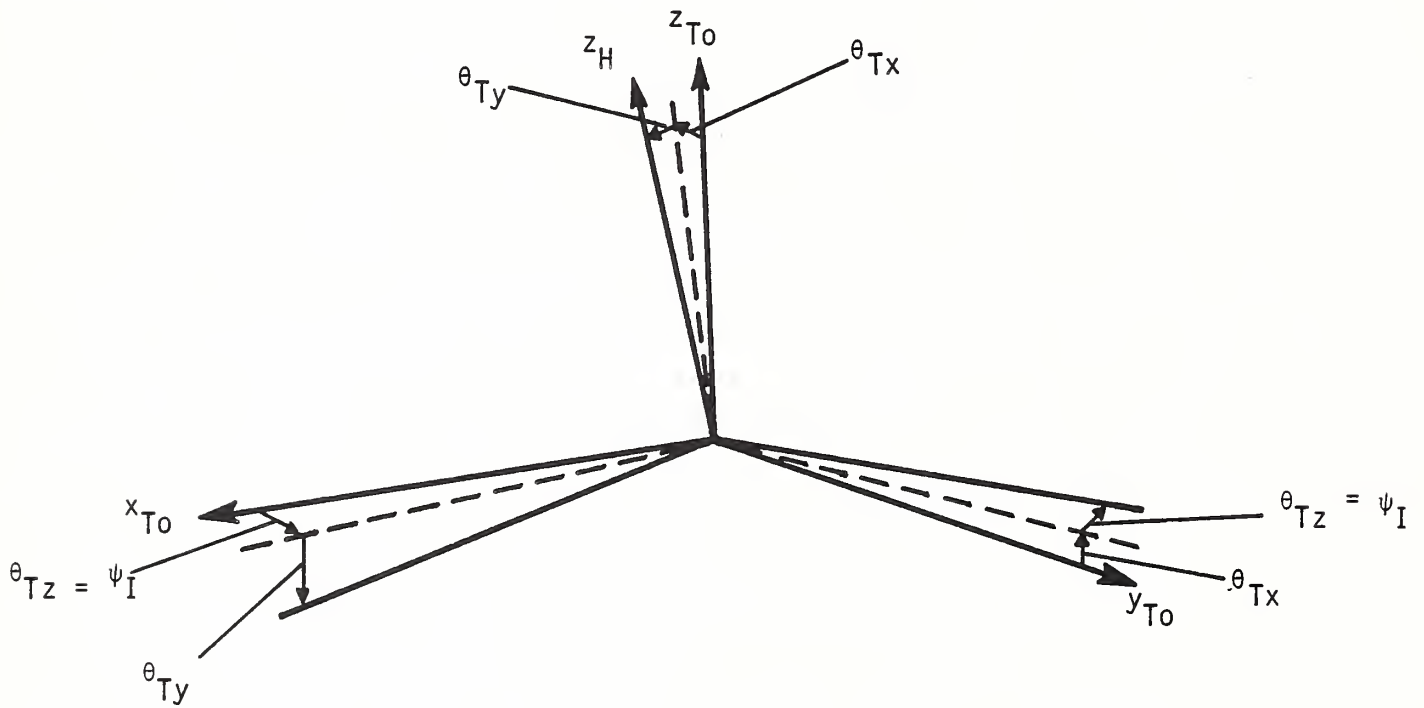
b) Angle ψ_I

FIGURE 4-5. HEAD TWIST ANGLES

the transformation can also be written:

$$[R_{TH}] = \begin{bmatrix} \cos\theta_{Tz} \cos\theta_{Ty} & \begin{array}{c} \cos\theta_{Tx} \sin\theta_{Tz} \\ + \cos\theta_{Tz} \sin\theta_{Ty} \sin\theta_{Tx} \end{array} & \begin{array}{c} \sin\theta_{Tz} \sin\theta_{Tx} \\ -\cos\theta_{Tz} \sin\theta_{Ty} \cos\theta_{Tx} \end{array} \\ -\sin\theta_{Tz} \cos\theta_{Ty} & \begin{array}{c} \cos\theta_{Tz} \cos\theta_{Tx} \\ -\sin\theta_{Tz} \sin\theta_{Ty} \sin\theta_{Tx} \end{array} & \begin{array}{c} \cos\theta_{Tz} \sin\theta_{Tx} \\ + \sin\theta_{Tz} \sin\theta_{Ty} \cos\theta_{Tx} \end{array} \\ \sin\theta_{Ty} & -\cos\theta_{Ty} \sin\theta_{Tx} & \cos\theta_{Ty} \cos\theta_{Tx} \end{bmatrix} \qquad (13)$$

Since the first Euler rotation, θ_{Tx} is always small, the third, θ_{Tz} is relatively independent of the first two. This makes θ_{Tz} a suitable definition for the rotation of a mechanical twist joint aligned to the head z-axis, i.e.;

$$\psi_I = \theta_{Tz} \qquad (14)$$

and is illustrated in Figure 4-5b.

The 3rd Euler angle is computed from equations (12) and (13) as follows:

$$\theta_{Ty} = \sin^{-1} (R_{TH31}) \qquad (15)$$

$$\theta_{Tz} = \sin^{-1} \frac{R_{TH21}}{\cos\theta_{Ty}} \qquad (16)$$

where R_{TH21} and R_{TH31} are the 2nd and 3rd direction cosine elements, respectively, in the first column of equation (12).

In Reference [9], head twist was defined to be the third Euler rotation, θ_{Hz} (See eq. (2)). This approximates θ_{Tz} (i.e. ψ_I) for the NBDL tests since the torso exhibits little rotation θ_{Nz} relative to the seat.

For a mechanical twist joint, aligned along another axis, as for example, alongs the neck chord line, establishing the equivalent relative rotation in the NBDL volunteers is more complicated and is not discussed in this report.

4.2   IMPACT LOAD ANALYSIS

In this analysis, the head/neck interface is defined to be a point: the intersection of the mid-sagittal plane with the line which joins the occipital condyles as defined by the NBDL [4]. The head is assumed to be a rigid body and loads are calculated at the interface by applying Newton's equations. While the head is not completely rigid, a significant portion of its mass is the skull bone and relatively tightly affixed tissue making the rigid body assumption reasonable.

The selection of the occipital condylar point as the head/neck interface was based on several considerations that would affect the utility and quality of the performance requirement being developed:

1.   The occipital condyles are the end point of the cervical spine. It is not unreasonable to expect to obtain some degree of correlation of neck injury with the loads applied at this point.

2.   Selection of an intermediate point on one of the cervical vertebra would compromise the analytical technique for calculating loads for the volunteer tests unless more detailed neck response data were obtained (namely response of individual cervical vertebra) in order to account for their inertia and relative motion.

3.   Internal neck loads measured in a dummy would not be meaningful, because its structure cannot be assured to be humanlike.

4.   The occipital condylar point can be located in human subjects using x-rays (although some degree of judgment is required).

5.   The occipital condyles is a significant skeletal pivot in flexion and extension that is frequently designed into mechanical models and instrumented to measure loads and deflections.

For design concepts for which there is no head/neck pivot or the pivot is located elsewhere, it is necessary to transform their response into equivalent response at the occipital condylar point in order to apply the performance requirements developed in this report and to evaluate neck injury using condylar loading.

Because the T1 vertebra is instrumented, its kinematics are known and it is possible to calculate the equivalent loading at this point if the inertia effects of the cervical neck structure are ignored. In Sections 4.2.1 and 4.2.2 which follow, the load analyses at the occipital condylar point and the T1 vertebral point, respectively, are developed.

4.2.1   Equations for Loading at the Occipital Condylar Point

The procedure for calculating the force and torque at the occipital condylar point for impact from any direction is described in this section.

Head response to lateral impact is three-dimensional. There is rotation of the midsagittal plane relative to the impact plane as well as motion of the head in the impact plane. The reactive torque is, therefore, of interest in the impact plane along the anatomical z-axis of the head as well as perpendicular to the impact plane. There is no significant motion of the head out of the impact plane, so the third torque component is of less interest.

The only significant head response to frontal impact is translation and rotation in the impact plane. Thus, the body's midsagittal plane and the impact plane remain essentially parallel and the reactive torque component at the occipital condylar point perpendicular to the midsagital and impact planes is the component of primary interest.

Figure 4-6 is a freebody diagram of the head. At the occipital point, a triad of force and torque components along the head anatomical axes are shown which represent the loads applied to the head by the neck. The only other external force acting is the force of gravity, provided the head makes no contact with other objects.

In vector notation, torque at the occipital condylar point is:

$$\bar{F}_O + \bar{W}_H = m_H \bar{a}_G \tag{17}$$

$$\bar{T}_O + \bar{r}_{G/O} \times \bar{W}_H = \dot{\bar{H}}_G + m_H \bar{r}_{G/O} \times \bar{a}_G \tag{18}$$

where:

$\bar{F}_O$ = Force applied to the head by the neck at the occipital condylar point

$\bar{W}_H$ = Weight of the Head.

m_H = Mass of the head

$\bar{a}_G$ = Acceleration of the head center of gravity

$\bar{T}_O$ = Torque applied to the head by the neck at the occipital condylar point

$\bar{r}_{G/O}$ = Position of head center of gravity with respect to the occipital condylar point

$\dot{\bar{H}}_G$ = Rate of change of the angular momentum of the head

Because the head response data is typically presented for some anatomical point that can be located in the test subject using x-rays, it is necessary to relate acceleration at the head center of gravity to acceleration at the anatomical origin:

$$\bar{a}_G = \bar{a}_A + \bar{a}_{G/A} = \bar{a}_A + \bar{\omega} \times (\bar{\omega} \times \bar{r}_{G/A}) + \bar{\alpha} \times \bar{r}_{G/A} \tag{19}$$

where:

$\bar{a}_A$ = acceleration of the head anatomical origin

$\bar{a}_{G/A}$ = acceleration of the head center of gravity with respect to the head anatomical origin

4-16
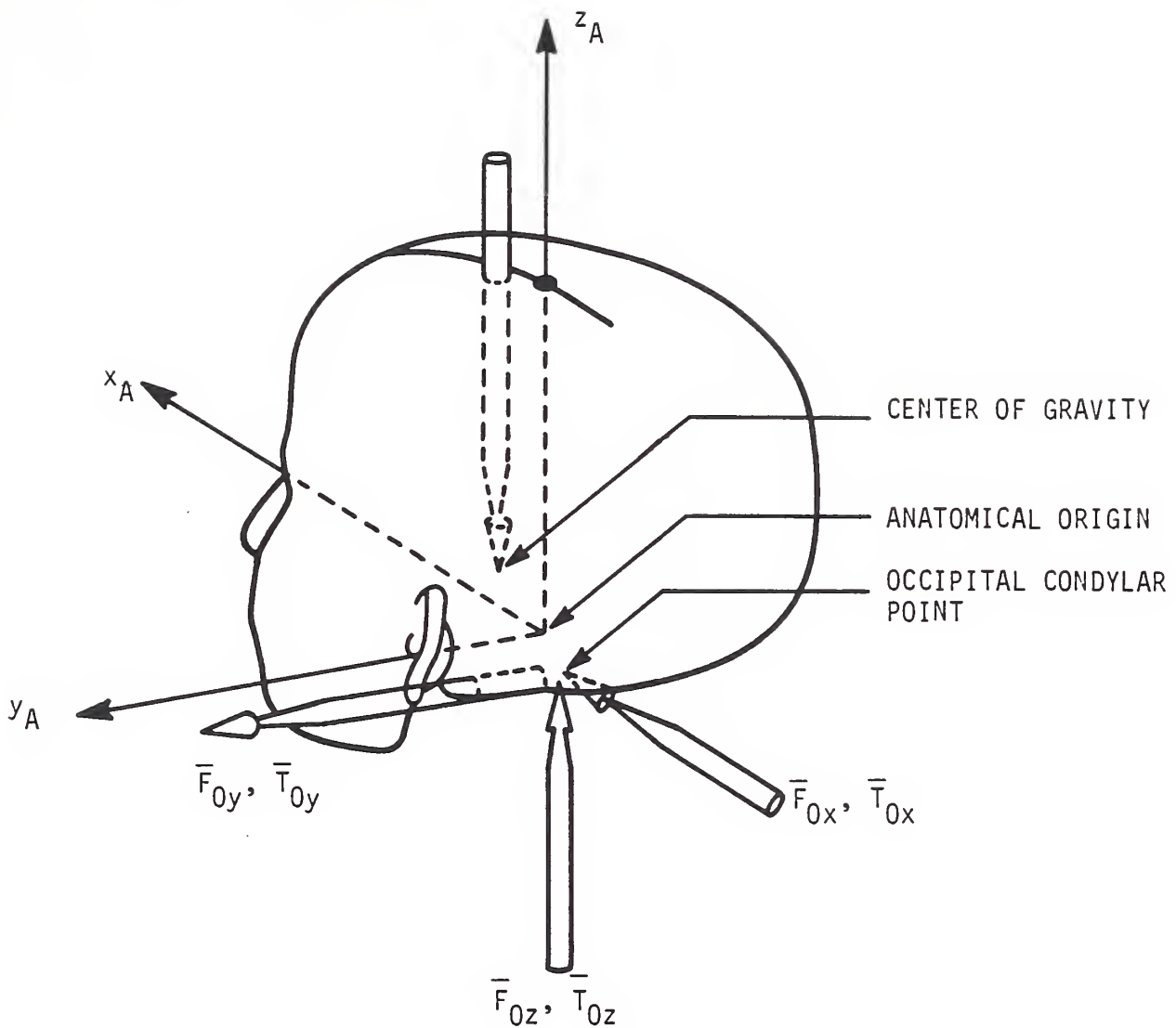
(x_A, y_A, z_A) HEAD ANATOMICAL COORDINATE AXES
(INITIALLY ALIGNED TO THE LABORATORY
FIXED COORDINATE SYSTEM)

FIGURE 4-6. FREEBODY DIAGRAM OF THE HEAD

$\overline{\alpha}$ = angular acceleration of the head with respect to an inertial coordinate system

$r_{G/A}$ = position of the head center of gravity with respect to the head anatomical origin. (See Figure 4-1)

$\overline{\omega}$ = Angular velocity of the head with respect to an inertial coordinate system.

The angular momentum can be expressed as the dot product of a body dependent parameter, the inertia tensor, I_G and the angular velocity vector,

$$\overline{H} = I_G \cdot \overline{\omega} \tag{20}$$

Equation (18) then becomes

$$\overline{T}_O + \overline{r}_{G/O} \times \overline{W}_H = d/dt\,(I_G \cdot \overline{\omega}) + m_H\,\overline{r}_{G/O} \times \overline{a}_G \tag{21}$$

4.2.2 Equations for Loading at the T1 Vertebral Point

(Note: This section is for information only and serves to define the procedure used in references [3] and [9] for calculating loads at the base of the neck. The loads are not part of the performance requirement developed in this report.)

The resistance applied by the torso to the neck can be represented by equivalent force and torque resultants at the T1 vertebral point using the test data provided the inertia effects of the neck are ignored. Figure 4-7 is a freebody diagram of the neck.

In vector notation, Newton's equations for equilibrium of the neck are:

$$\overline{F}_1 = \overline{F}_O \tag{22}$$

$$\overline{T}_1 = \overline{T}_O + \overline{r}_{O/T} \times \overline{F}_O = \overline{T}_O + (\overline{r}_A - \overline{r}_T + \overline{r}_{O/A}) \times \overline{F}_O \tag{23}$$

where

$\overline{F}_1$ = the force applied by the torso to the neck at the T1 vertebral point.

$\overline{T}_1$ = the torque applied by the torso to the neck at the T1 vertebral point.
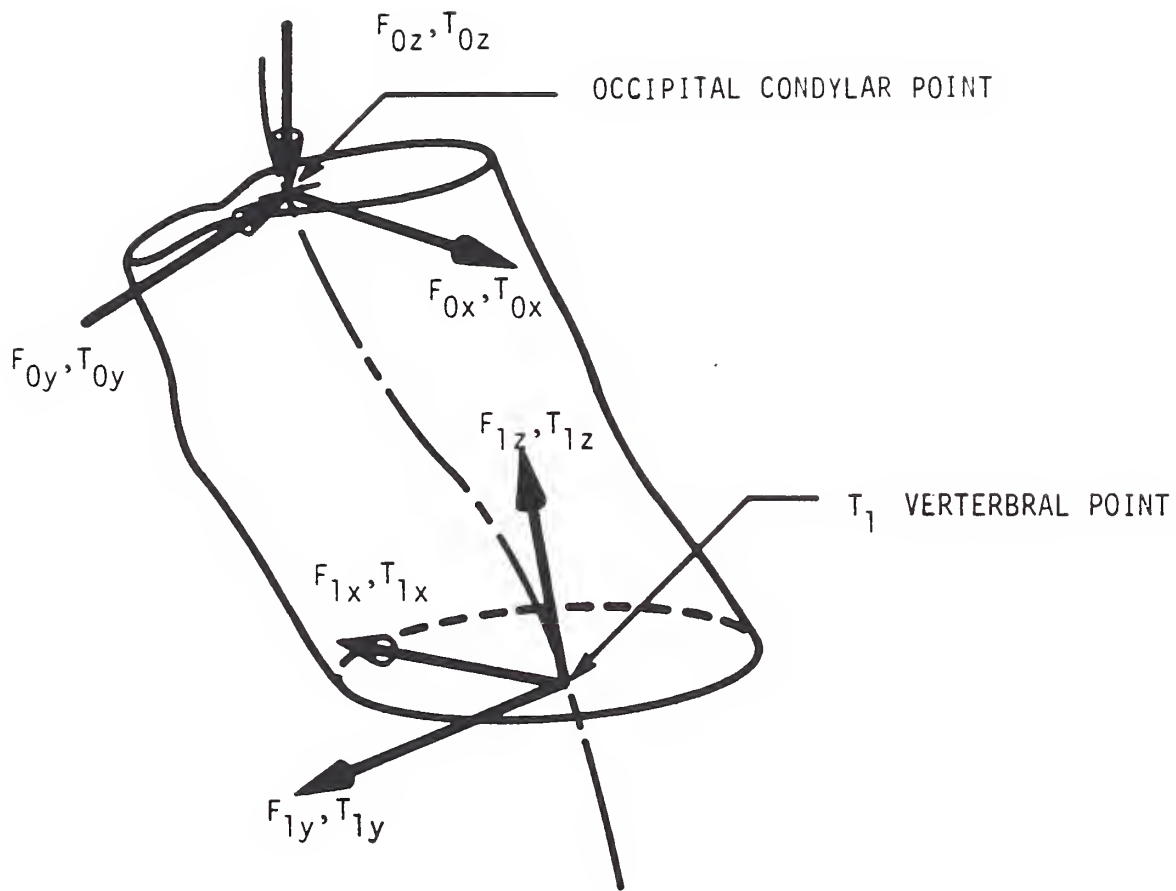
FIGURE 4-7. FREEBODY DIAGRAM OF THE NECK

and the position vectors, as shown in Figure 4-1, are:

$\bar{r}_{O/T}$ = position of the occipital condylar point relative to the T1 vertebral point ("neck chord length").

$\bar{r}_A$ = position of the head anatomical origin in the laboratory coordinate system

$\bar{r}_T$ = position of the T1 vertebral point in the laboratory coordinate system.

$\bar{r}_{O/A}$ = position of the occipital condylar point relative to the head anatomical origin.

4.2.3   Evaluation of Load Components

It is convenient to evaluate equations (17) and (21) in head anatomical components because test measurements for angular acceleration and angular velocity are provided in anatomical components and because inertia tensor, I_G, and vector magnitudes $r_{G/A}$ and $r_{G/O}$ do not vary with time in this frame. Linear acceleration and the acceleration of gravity in laboratory components are transformed using the Euler angles defined by equation (2).

Equations (17), (19) and (21) become in matrix form, respectively,

$$\begin{Bmatrix} F_{Ox} \\ F_{Oy} \\ F_{Oz} \end{Bmatrix} = \begin{Bmatrix} m_H \, (a_{Gx} - g_x) \\ m_H \, (a_{Gy} - g_y) \\ m_H \, (a_{Gz} - g_z) \end{Bmatrix} \qquad (24)$$

$$\begin{Bmatrix} a_{Gx} \\ a_{Gy} \\ a_{Gz} \end{Bmatrix} = \begin{Bmatrix} a_{Ax} \\ a_{Ay} \\ a_{Az} \end{Bmatrix} + \begin{Bmatrix} (\omega_z^2 - \omega_y^2) r_{G/Ax} + \omega_x \omega_z r_{G/Az} \\ \omega_x \omega_z R_{G/Ax} + \omega_y \omega_z \, r_{G/Az} \\ \omega_x \omega_z \, r_{G/Ax} + (-\omega_x^2 - \omega_y^2) r_{G/Az} \end{Bmatrix} + \begin{Bmatrix} r_{G/Az} \alpha_y \\ r_{G/Ax} \alpha_z - r_{G/Az} \alpha_x \\ -r_{G/Ax} \alpha_y . \end{Bmatrix} \quad (25)$$

$$\begin{Bmatrix} T_{Ox} \\ T_{Oy} \\ T_{Oz} \end{Bmatrix} = \begin{Bmatrix} I_{xx} \alpha_x \\ I_{yy} \alpha_y \\ I_{zz} \alpha_z \end{Bmatrix} + \begin{Bmatrix} m_H r_{G/Oz}(g_y - a_{Gy}) \\ -m_H r_{G/Oz}(g_x - a_{Gx}) + m_H r_{G/Ox}(g_z - a_{Gz}) \\ -m_H r_{G/Ox}(g_y - a_{Gy}) \end{Bmatrix}$$

$$+ \begin{Bmatrix} (I_{zz} - I_{yy})\omega_y \omega_z \\ (I_{xx} - I_{zz})\omega_x \omega_z \\ (I_{yy} - I_{xx})\omega_x \omega_y \end{Bmatrix} + \begin{Bmatrix} -I_{xy}\alpha_y - I_{xz}\alpha_z \\ -I_{yx}\alpha_x - I_{yz}\alpha_z \\ -I_{zx}\alpha_x - I_{zy}\alpha_y \end{Bmatrix} \quad (26)$$

$$+ \begin{Bmatrix} I_{yx}\omega_x\omega_z + I_{xz}\omega_z^2 - I_{zx}\omega_x\omega_y - I_{zy}\omega_y^2 \\ -I_{xy}\omega_y\omega_z - I_{xz}\omega_z^2 + I_{zx}\omega_x^2 + I_{zy}\omega_x\omega_y \\ I_{xy}\omega_y^2 + I_{xz}\omega_y\omega_z - I_{yx}\omega_x^2 - I_{yz}\omega_x\omega_z \end{Bmatrix}$$

where brackets $\left\{\begin{array}{c} \\ \\ \end{array}\right\}$ indicate 3x1 column matrices, subscripts x,y,z denote components of any variable along the x, y and z axes, respectively, of the head anatomical coordinate system, respectively, and g is the acceleration of gravity.

Terms in the equations which are significant for frontal and lateral impacts are identified in reference [17]. However, all terms are retained for computations presented herein.

Load components in other coordinate systems are readily obtained from equations (24) and (26) using transformation equations (2) and (3).

4.2.4   Subject Mass and Anthropometric Properties

Head mass and principal moments of inertia can be estimated for each subject from weight and size data using the recommendations of McConville [18]. The algorithm requires subject weight, height, seated height and head breadth, height and circumference. The mass and inertia properties for NBDL subjects H00044 through H00038 were calculated in references [3] and [9] using this procedure. For subjects H00118 through H00142 the anthropometric data was not provided (by the time of this study). Average mass and moment of inertia properties based on the initial subject characteristics was used, as indicated in Table 4-1.

The location of the principal axes is also based on McConville calculations. The principal y-axis is defined to be parallel to the head anatomical axis that is perpendicular to the sagittal plane. The principal axes in the sagittal plane are located with respect to the anatomical axes such that the angle is 36 degrees between one principal axis and the anatomical axis, x_a, defined by the superior edge of the auditory meati and the midpoint between the infraorbital notches. (See Figure 4-8)

TABLE 4-1. ESTIMATED MASS AND PRINCIPAL MOMENT OF INERTIA PROPERTIES

Subject	Without instrumentation				With Instrumentation			
	Head Mass (kg)	Moment of Inertia			Head Mass (kg)	Moment of Inertia		
		$I_{x'x'}$ (kgm^2)	$I_{y'y'}$ (kgm^2)	$I_{z'z'}$ (kgm^2)		$I_{x'x'}$ (kgm^2)	$I_{y'y'}$ (kgm^2)	$I_{z'z'}$ (kgm^2)
H00044	3.84	0.0164	0.0183	0.0122	4.37	0.0239	0.0258	0.0127
H00064	4.37	0.0203	0.0231	0.0151	4.90	0.0278	0.0306	0.0156
H00065	4.58	0.0219	0.0260	0.0162	5.11	0.0294	0.0335	0.0167
H00067	4.13	0.0187	0.0215	0.0137	4.66	0.0262	0.0290	0.0142
H00083	4.0	0.0176	0.0186	0.0129	4.53	0.0251	0.0261	0.0134
H00093	3.5	0.0134	0.0140	0.0105	4.03	0.0209	0.0215	0.0107
H00118	4.1	0.0158	0.0203	0.0134	4.6	0.0256	0.0278	0.0139
H00120	4.1	0.0158	0.0203	0.0134	4.6	0.0256	0.0278	0.0139
H00127	4.1	0.0158	0.0203	0.0134	4.6	0.0256	0.0278	0.0139
H00130	4.1	0.0158	0.0203	0.0134	4.6	0.0256	0.0278	0.0139
H00131	4.1	0.0158	0.0203	0.0134	4.6	0.0256	0.0278	0.0139
H00132	4.1	0.0158	0.0203	0.0134	4.6	0.0256	0.0278	0.0139
H00133	4.1	0.0158	0.0203	0.0134	4.6	0.0256	0.0278	0.0139
H00134	4.1	0.0158	0.0203	0.0134	4.6	0.0256	0.0278	0.0139
H00135	4.1	0.0158	0.0203	0.0134	4.6	0.0256	0.0278	0.0139
H00136	4.1	0.0158	0.0203	0.0134	4.6	0.0256	0.0278	0.0139
H00138	4.1	0.0158	0.0203	0.0134	4.6	0.0256	0.0278	0.0139
H00139	4.1	0.0158	0.0203	0.0134	4.6	0.0256	0.0278	0.0139
H00140	4.1	0.0158	0.0203	0.0134	4.6	0.0256	0.0278	0.0139
H00141	4.1	0.0158	0.0203	0.0134	4.6	0.0256	0.0278	0.0139
H00142	4.1	0.0158	0.0203	0.0134	4.6	0.0256	0.0278	0.0139

Transformation of the three principal moments of inertia to anatomical components results in three moments of inertia and three products of inertia, as follows [19] :

Moment of Inertia Coefficients:

$$I_{xx} = 1^2_{xx'}I_{x'x'} + 1^2_{xy'}I_{y'y'} + 1^2_{xz'}I_{z'z'} \qquad (27a)$$

$$I_{yy} = 1^2_{yx'}I_{x'x'} + 1^2_{yy'}I_{y'y'} + 1^2_{yz'}I_{z'z'} \qquad (27b)$$

$$I_{zz} = 1^2_{zx'}I_{x'x'} + 1^2_{zy'}I_{y'y'} + 1^2_{zz'}I_{z'z'} \qquad (27c)$$

Products of Inertia:

$$I_{xy} = -(1_{xx'}1_{yx'}I_{x'x'} + 1_{xy'}1_{yy'}I_{y'y'} + 1_{xz'}1_{yz'}I_{z'z'}) \qquad (28a)$$
$$I_{xz} = -(1_{zx'}1_{xx'}I_{x'x'} + 1_{zy'}1_{xy'}I_{y'y'} + 1_{zz'}1_{xz'}I_{z'z'}) \qquad (28b)$$
$$I_{yz} = -(1_{yx'}1_{zx'}I_{x'x'} + 1_{yy'}1_{zy'}I_{y'y'} + 1_{yz'}1_{zz'}I_{z'z'}) \qquad (28c)$$

where:

I_{xx}, I_{yy}, I_{zz} = moment of inertia coefficients about the x, y, z axes of the head anatomical coordinate system

$I_{x'x'}, I_{y'y'}, I_{z'z'}$ = principal moments of inertia

$1_{ij'}$ = direction cosine between ith axis of the head anatomical coordinate system and the j'th principal axis.

Table 4-2 summarizes the direction cosines for the orientation of principal coordinates described above.
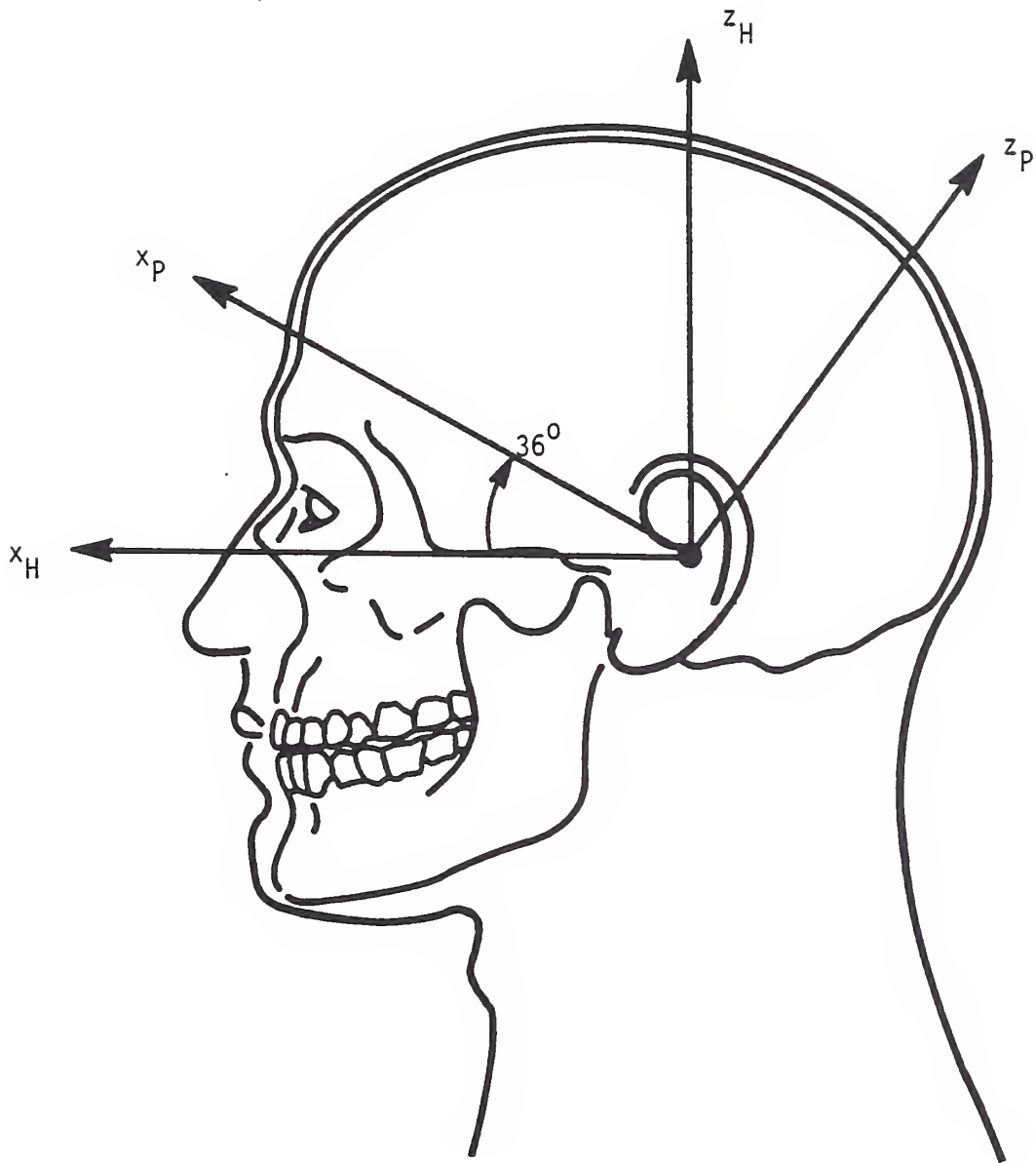
FIGURE 4-8. LOCATION OF THE HEAD PRINCIPAL AXES

TABLE 4-2. DIRECTION COSINES WHICH LOCATE THE PRINCIPAL
AXES RELATIVE TO THE HEAD AXES

Anatomical Coordinate Direction	Principal Coordinate Direction		
	x'	y'	z'
x	$\cos 36°$	0	$\cos 126°$
y	0	1	0
z	$\cos 54°$	0	$\cos 36°$

TABLE 4-3. MOMENT OF INERTIA PROPERTIES IN
HEAD ANATOMICAL COMPONENTS

Subject	Moment of Inertia Coefficients			Products of Inertia Dimensions		
	I_{xx}	I_{yy}	I_{zz}	I_{xy}	I_{xz}	I_{yx}
H00044	0.0233	0.0305	0.0196	0.0	-0.0059	0.0
H00064	0.0236	0.0315	0.0200	0.0	-0.0055	0.0
H00065	0.0227	0.0291	0.0192	0.0	-0.0054	0.0
H00067	0.0238	0.0311	0.0200	0.0	-0.0060	0.0
H00083	0.0211	0.0261	0.0174	0.0	-0.0056	0.0
H00118 to H00142	0.0215	0.0278	0.0179	0.0	-0.0057	0.0

Table 4-3 summarizes the moment of inertia properties in head anatomical coordinates for the subjects analyzed in this paper. The results include the instrumentation mass of 0.53 kg.

Average values are used for the location of head center of gravity and occipital condylar point relative to the head anatomical origin based on the results of Beier [20] and Ewing and Thomas [4], respectively. Table 4-4 summarizes the values used.

4.3   INTERPRETATION OF THE ANALYSIS PROCEDURES

No modelling assumptions were made in formulating the kinematic equations that would limit their applicability to a particular ATD design. Judgments were made as to which motions were significant and which were insignificant. The only modelling assumption made in developing the load equations was that the head was rigid. This could result in some error in predicting peak loads because the phase shift between the calculated loads and the accelerometer readings which produce these loads (resulting from dissipative forces in a nonrigid head) is ignored. This is thought to be a second order effect.

Thus, it can be stated that the computation of the kinematic and load variables is just mathematical manipulation of the test data and that the resulting information is applicable in assessing any ATD design.

Definition of neck chord length and neck rotation angle differ in this report from those of references [3] and [9]. In those papers, a constant neck length was assumed and a point in the torso was located about which a circular arc adequately approximated the trajectory of the occipital condylar point. The base point was shifted both vertically and horizontally in the impact plane relative to the T1 anatomical point, as required to achieve constant neck length. One average position was located for all subjects exposed to frontal impact and another for all subjects exposed to lateral impact.

TABLE 4-4. LOCATION OF THE HEAD CENTER OF GRAVITY AND OCCIPITAL CONDYLAR POINT RELATIVE TO THE HEAD ANATOMICAL ORIGIN

Dimension*	Distance(m)
$\bar{r}_{O/Ax}$	-0.011
$\bar{r}_{O/Ay}$	0.000
$\bar{r}_{O/Az}$	-0.026
$\bar{r}_{G/Ax}$	0.012
$\bar{r}_{G/Ay}$	0.000
$\bar{r}_{G/Az}$	0.029

*where $\bar{r}_{G/A} = \bar{r}_{O/A} + \bar{r}_{G/O}$ (refer to Figure 4-1) and the subscripts x,y and z refer to components along the head anatomical coordinate directions.

In this report, the base of the neck is the T1 anatomical point, as defined in section 4. This results in a <u>variable neck length</u> during impact as will be discussed in Section 5, that must be included in the performance requirement. For omni-directional ATD capability, the base of the neck will most likely be located on the spine. Performance requirements, based on the neck chord line definition of this report, are better suited to the evaluation of omni-directional capability than are those of references [3] and [9]. The two definitions of neck chord angle do not differ significantly because the distance between the base point and T1 is small compared to neck chord length.

5. RESULTS OF RESPONSE ANALYSIS

The qualitative assessment of response characteristics of the NBDL volunteers that was discussed in Section 2.3 is quantified in this section. The results are presented in graphical form using the variables defined in Section 4.

Sections 5.1, 5.2 and 5.3 contain response to frontal, lateral and oblique impact, respectively. Similarity of response between volunteers is demonstrated by superimposing like results on a single plot. This is the initial step in forming "performance corridors" commonly used in biomechanics. Results are also presented for a single subject selected to illustrate typical behavior for variation in peak sled impact level and impact direction. Oblique characteristics appear to be a logical combination of frontal and lateral characteristics, as illustrated in Section 5.3. In each section, the kinematic and kinetic characteristics are treated separately to maintain a distinction made in this study in the level of fidelity achieved by the performance requirements that are evolved from the two types of data.

No attempt is made in Sections 5.1-5.3 to correlate the time of response with the impact profile. In Section 5.4, the response of the T1 anatomical point is presented as a function of time and correlated with the head and neck response variables. In Section 5.5, performance requirements based on these multi-subject results are stated in the form of a prescribed response to a prescribed input, thereby providing a means for testing the fidelity of an ATD. In Section 5.6, the sensitivity of the requirements to variations in test conditions is described.

5.1   RESPONSE TO FRONTAL IMPACT

5.1.1   Frontal Kinematic Response

The major kinematic response of the head to frontal acceleration can be characterized by the three variables, $r_{O/T}$, ϕ_y and θ_y, which are illustrated in Figures 4-1, 4-3, and 4-4, respectively. Figures 5-1 and 5-2 are cross plots which describe the constraint between these variables during the response to rapid torso acceleration. In Figures 5-1a and 5-2a, the response is shown for one test and includes both the loading and unloading phases as indicated. In the multiple tests

of Figures 5-1b and c and 5-2b and c, only the loading phase is shown*. These plots are discussed in more detail in the paragraphs which follow.

Initially, the neck chord angle, θ_y, increases more rapidly than the head angle, ϕ_y as seen in Figure 5-1a (slope $>$ 1). This is typically followed by a phase in which head angle partially "catches up" to neck angle (slope $<$ 1). For the remainder of the loading phase and for the unloading phase, the head and neck move with essentially no relative motion (slope $\sim$ 1). An ATD with a rigid head/neck system would not exhibit the initial relative motion. A passive ATD which allows relative motion between the head and neck chord line would appear to require variable stiffness and/or a nonlinear kinematical (locking) mechanism to achieve the head lead observed in the volunteer response. The significance of including this characteristic in an ATD is discussed later in this section.

The relationship between angular response variables, ϕ_y and θ_y, for tests of nine different subjects at a 15 g peak sled impact level are shown in Figure 5-1c. The nine curves have the same general shape despite variations in initial head and neck angles of nearly 20°, leading to the conclusion that initial orientation does not result in significant variation in response. Similar results were observed in lateral and oblique response. This observation does not conflict with the effects of initial head position or response that were noted by others. [21]. The tests evaluated here have sufficiently small variation in initial orientation that they fall into a single orientation category of that study, namely the "neck up, chin up" category. (This category is designated NUCU in the initial condition column in the list of tests in Appendix A.)

---

*The loading phase terminates when head angle ϕ_y reaches peak value.
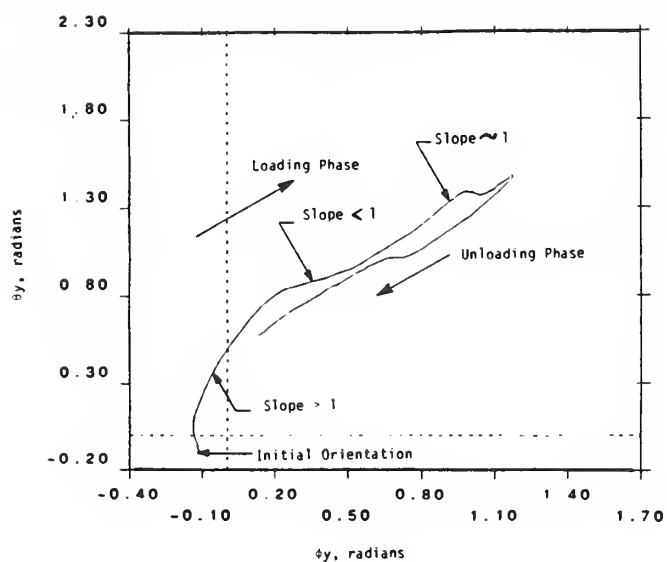
a) Subject H00134, 15-g Impact
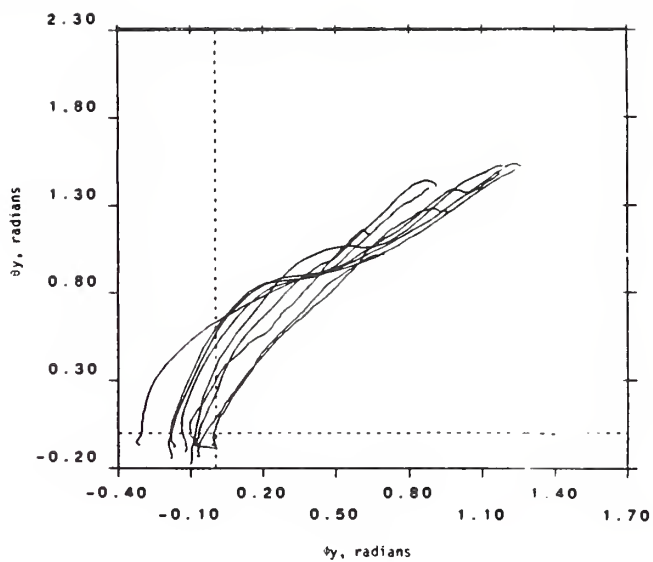
b) Subject H00134, Nine Tests (3-15g Impacts)
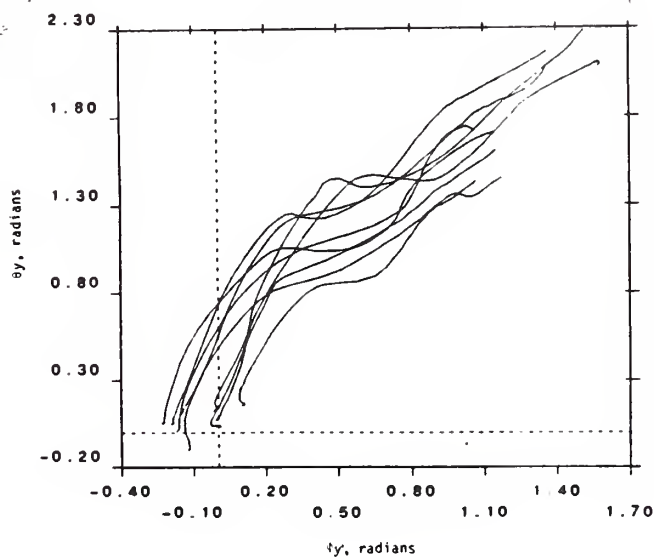
c) Nine Subjects, 15-g Impact

FIGURE 5-1. HEAD ANGLE, ϕy, VERSUS NECK CHORD LINE ANGLE, θy, FOR FRONTAL IMPACT
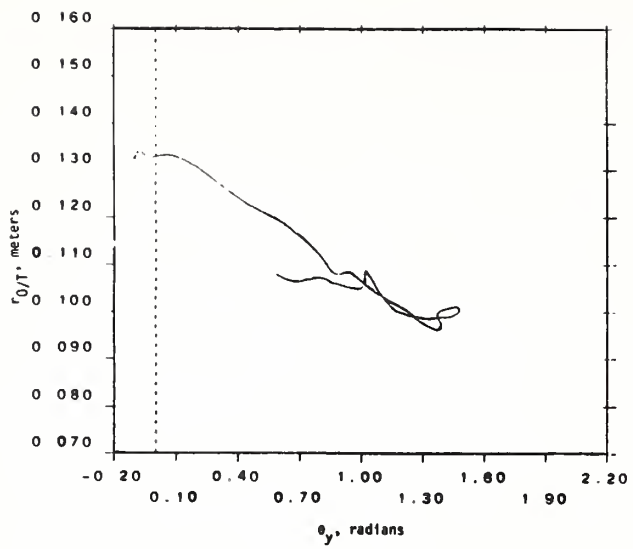
a) Subject H00134, 15-g Impact
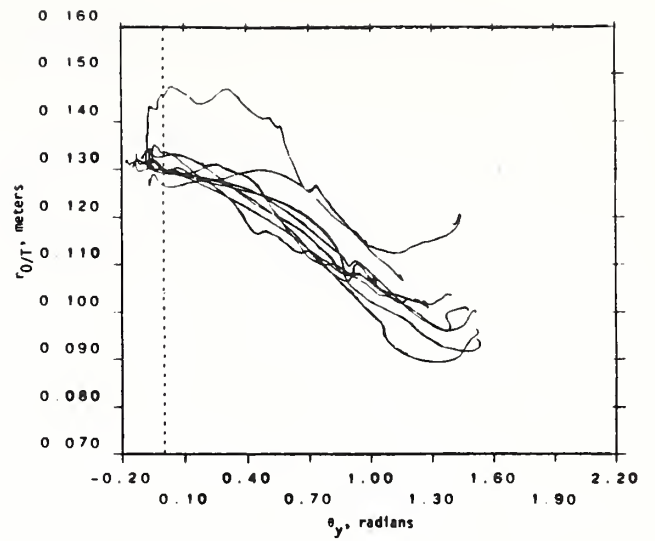
b) Subject H00134, Nine Tests (3-15g Impacts)
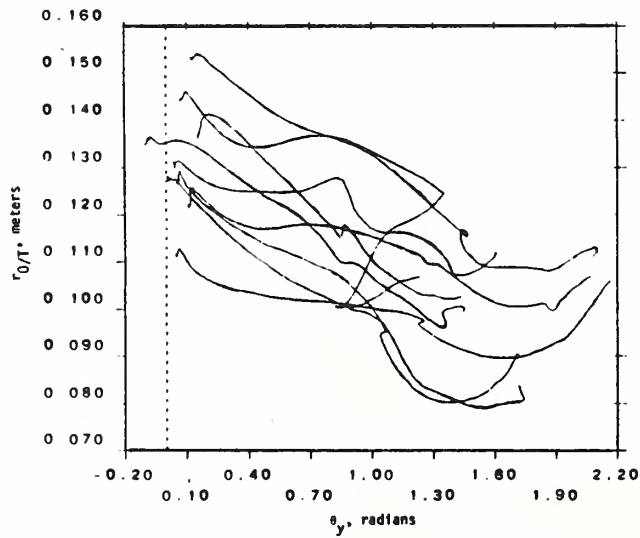
c) Nine Subjects, 15-g Impact

FIGURE 5-2.   NECK CHORD LENGTH, $r_{O/T}$, VERSUS NECK
CHORD LINE ANGLE, θ_y, FOR FRONTAL IMPACT

To illustrate other aspects of head and neck angular motion, variations in initial head or neck orientations are eliminated by plotting "excursion" angles, $\Delta\phi = \phi_y - \phi_{yo}$ versus $\Delta\theta = \theta_y - \theta_{yo}$ where the subscript o indicates the initial value of the variable. Figure 5-3 is Figure 5-1 replotted in this manner.

Peak head excursion for the nine 15 g tests of Figure 5-3c vary between 55° and 90° with eight of nine occurring within the 70°-90° range.

Variation in head angular excursion with variation in impact level is shown in Figure 5-3b. Sled impact levels vary from 3 g to 16 g peak. Peak head excursions increase more or less monotomically with impact level as indicated by Table 5-1. The peak head angles range from 0.62 radians for 4 g test LX3842 to 1.43 radians for 14 g test LX3968.

TABLE 5-1. COMPARISON OF PEAK HEAD EXCURSIONS FOR FRONTAL TESTS OF SUBJECT H00134

Test No.	G-Level	Peak Head Excursion
LX3807	3	1.03
LX3842	3	0.72
LX3822	4	0.62
LX3870	6	0.99
LX3890	8	1.20
LX3940	12	1.29
LX3961	13	1.43
LX3968	14	1.43
LX3983	15	1.30
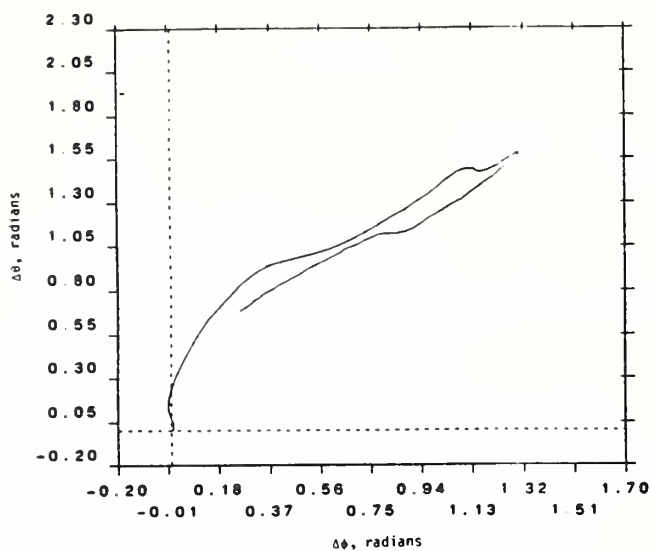
a) Subject H00134, 15-g Impact
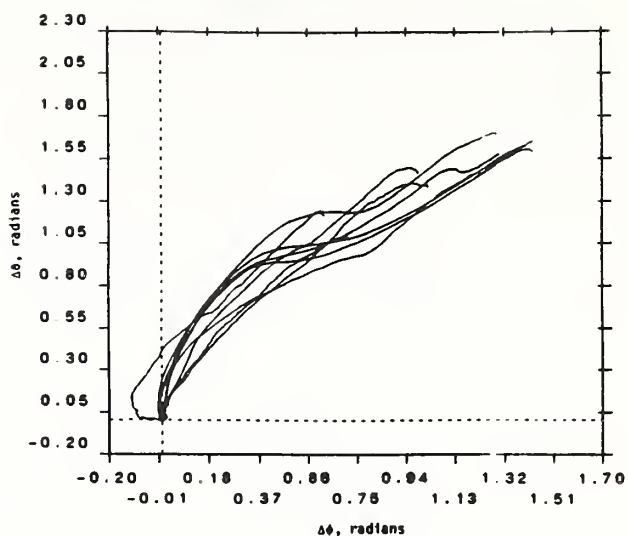
b) Subject H00134, Nine Tests
(3-15g Impacts)
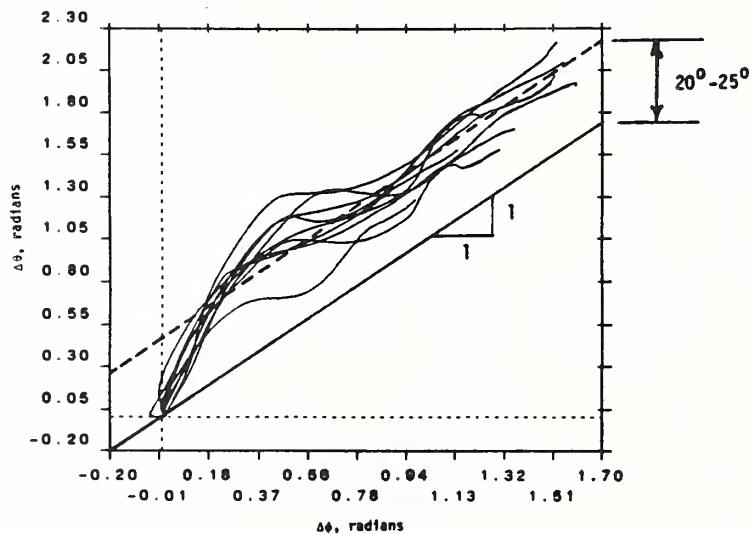
c) Nine Subjects, 15-g Impact

FIGURE 5-3. CHANGE IN HEAD ANGLE, ϕ_y, VERSUS CHANGE IN NECK
ANGLE, θ_y, FOR FRONTAL TESTS

The curves of Figure 5-3b form a relatively narrow corridor of response even though the individual curves correspond to tests at different impact levels. This occurs because the amount of initial neck rotation when there is no head rotation is relatively independent of impact level and because in the subsequent neck rotation, the head is essentially locked to the neck. The curves of Figure 5-3c form an equally narrow corridor which indicates that these corridors also have little subject dependence.

The peak flexion position of the head center of gravity is noteworthy. Figure 5-3c indicates that in the final phase the change in head angle lags the change in neck chord angle by approximately 20-25°. The data of Table 4-4 indicates that the line passing through the head center-of-gravity and the occipital condylar point forms an angle of approximately 23° with respect to the head z-axis. Thus, the position of the head as peak flexion approaches is such that the center of gravity lies essentially on the extension of the neck chord line. (Note in Figure 5-1 that the head z-axis and the neck chord line are initially nearly vertical.) This may well be a "protective position" that the volunteer seeks since it would minimize head acceleration. Once achieved, minimal muscular response is required to maintain this position.

The neck chord shortens during the loading phase and lengthens during the unloading phase. For the 15 g test of subject H00134 shown in Figure 5-2a, the chord length reduces from 13.5 cm to 9.5 cm during the loading phase. Shortening is more or less proportional to neck angle for subject H00134 as shown in Figure 5-2b. Note the T1 vertical position has been corrected in this figure as described in Appendix B, so that neck chord initially varies in length between runs by less than 0.5 cm. Figure 5-2c shows that there is significant variation in initial neck chord length between subjects. In order to make further comparisons between subjects, neck length was normalized as shown in Figure 5-4. Peak shortening for the nine subjects, on a normalized basis varies from approximately 0.62 to 0.88, as indicated in Figure 5-4b. This corridor broadens as neck angle increases. A possible explanation is that the degree of curvature at any instant is dependent on the amount of muscle reaction exerted by a subject, with different subjects exerting different amounts of control. Figure 5-5 depicts the variability possible in cervical spine curvature between two subjects at the time of peak head excursion. It is also possible that the T1 vertebra moves relative to the surface point at which
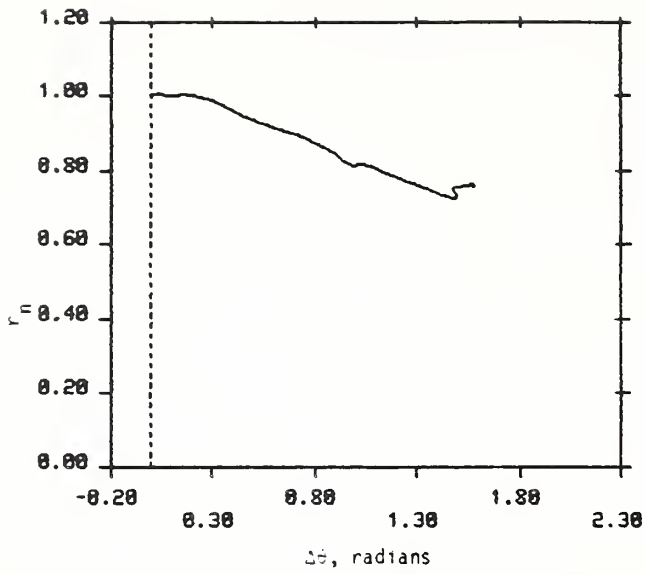
a) Subject H00134, 15-g Impact
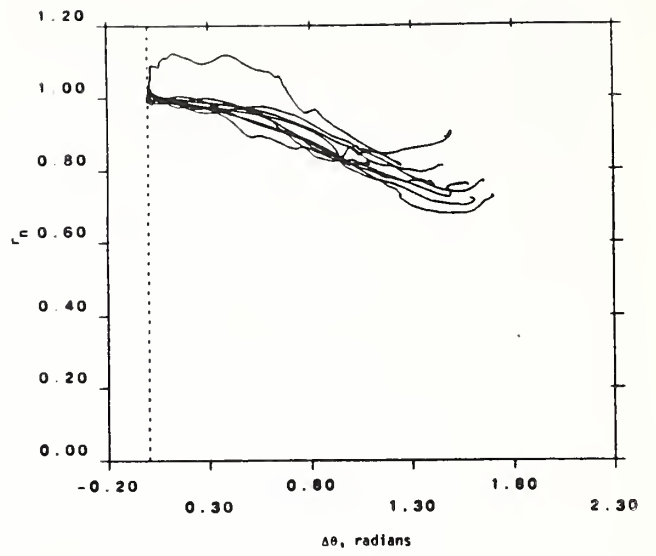
b) Subject H00134, Nine Tests
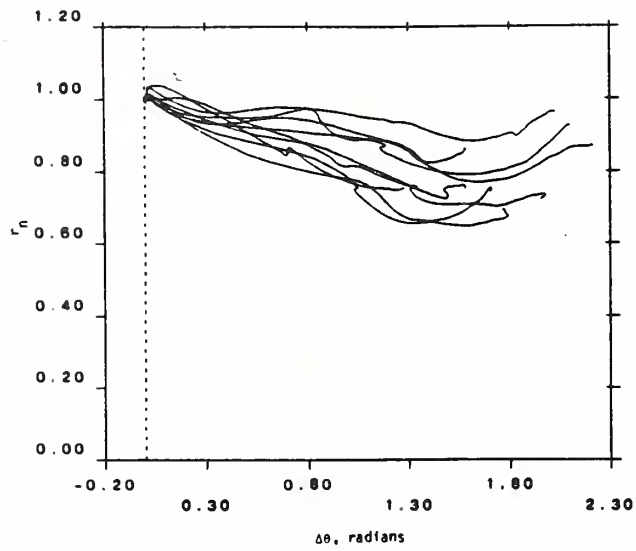
c) Nine Subjects, 15-g Impact (3-15g Impacts)

FIGURE 5-4.   NORMALIZED NECK CHORD LENGTH VERSUS
CHANGE IN HEAD ANGLE FOR FRONTAL TESTS
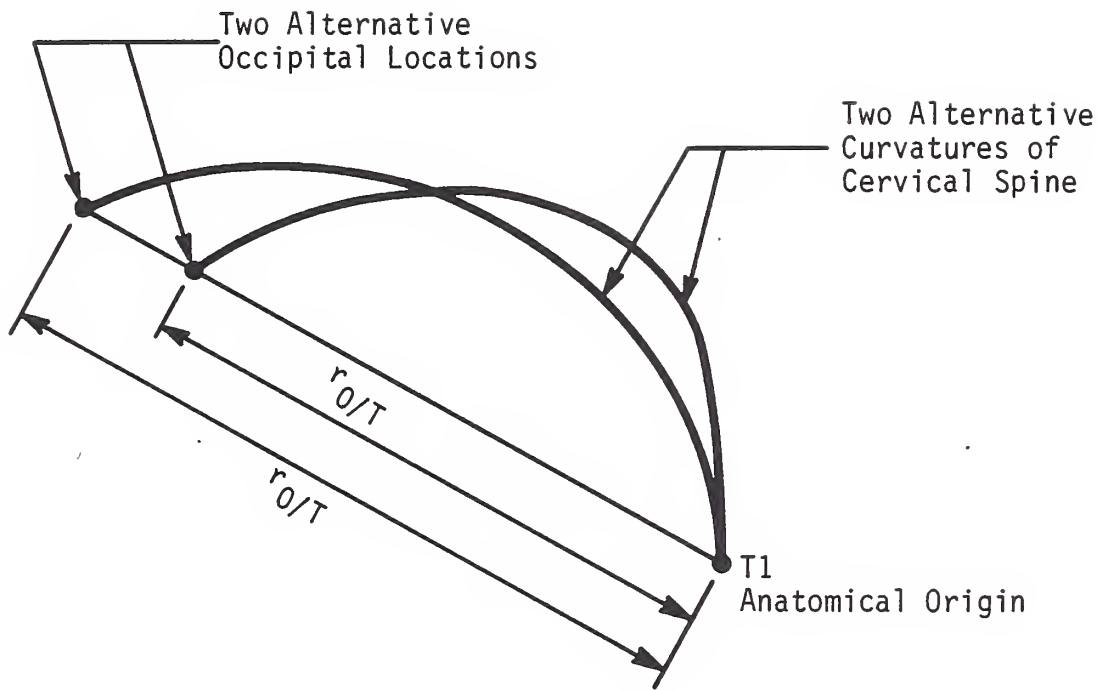
FIGURE 5-5. ILLUSTRATION OF ALTERNATIVE CONDYLAR POSITIONS
RELATIVE TO T1 AT PEAK HEAD EXCURSION

the T1 sensor is mounted. Such spinal motion, which has been recorded by Snyder, R.G., et al [22], includes T1 movement downward and rearward relative to the surface point when the head angular position relative to the torso increases in flexion. Since this phenomena is not accounted for in processing the test data, the shortening observed would be with respect to a surface landmark and should not necessarily be construed as shortening of the spine. Either of these hypotheses is further supported by the results of cadaver tests reported in Section 5.6. In those tests the T1 sensors are attached directly to the T1 vertebra, there is no muscle reaction and the neck chord is observed to be slightly longer at peak head excursion. Shortening of the neck chord with respect to the surface landmark posterior to T1 should be present whichever hypothesis is correct.

The consequence of not including the proper neck shortening and relative angular motion between the head and neck is illustrated by considering two alternative head/neck implementations:

1.   A rigid head/neck unit that pivots about T1 to achieve fidelity in head angular response relative to the torso.

2.   A two-link head/neck system that pivots about T1 and the occipital condylar points to achieve fidelity of both head and neck angular response.

Deviation of head center-of-gravity for each of these implementations relative to that of an average volunteer can be observed in Figure 5-6 for two instants of time within the loading phase where relative rotation of the head and neck has ceased. At the instant depicted in Figure 5-1a, the head center-of-gravity for the two-link design is within 2 centimeters of that observed for a typical volunteer. For the rigid head/neck design, the center-of-gravity is 4 cm above and 2 cm rearward. At the instant near to peak excursion depicted in Figure 5-6b, the center-of-gravity of the two-link design is 3 cm forward and 1 cm above and the rigid design is 5 cm above and 1-2 cm forward. The two-link design demonstrates better positional fidelity although it too may be unacceptable in an ATD intended to predict contact with a car interior.
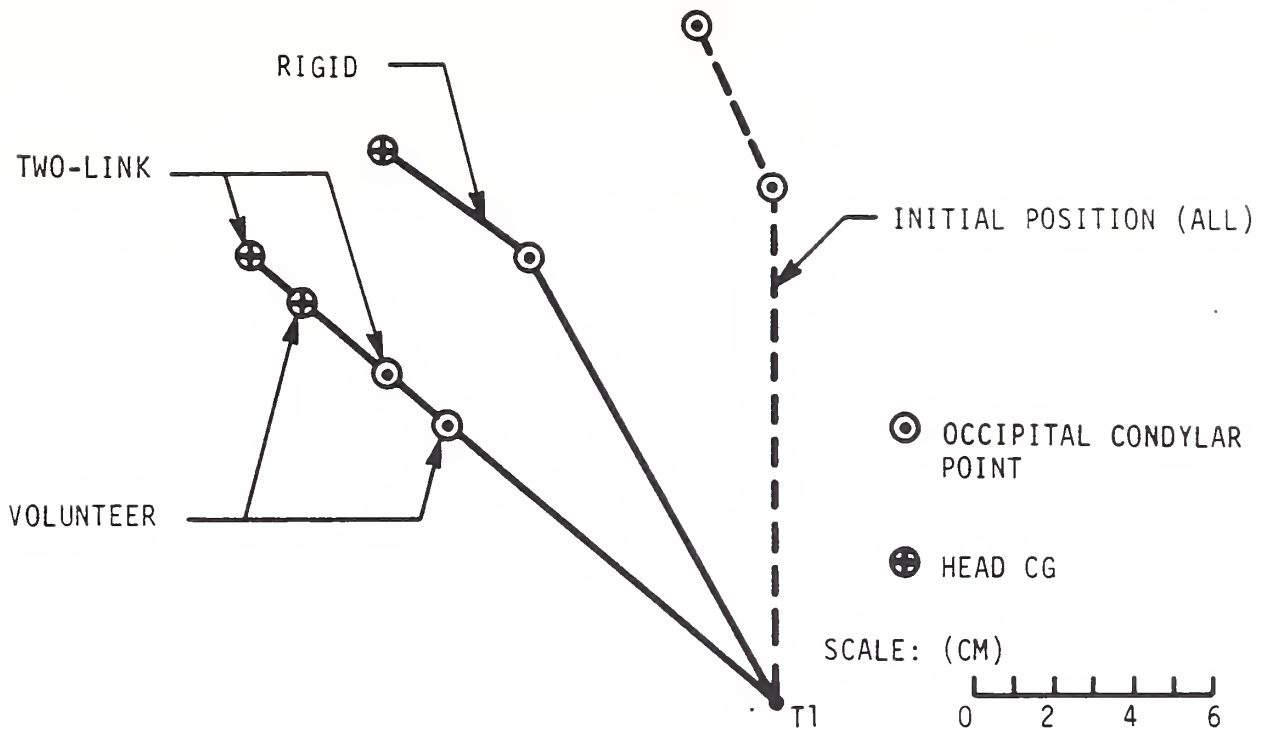
a) 125 Seconds After Impact
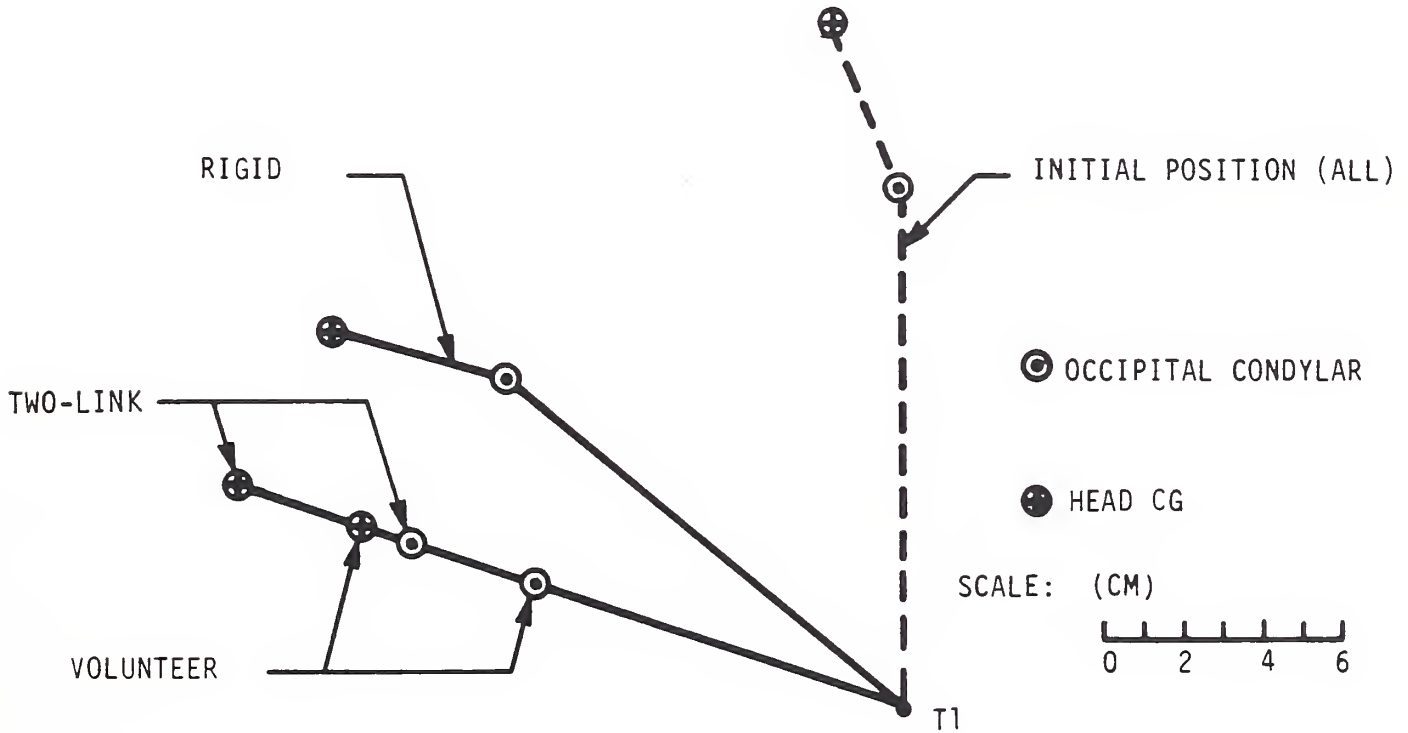
b) 150 Seconds After Impact

FIGURE 5-6. COMPARISON OF POSITION OF HEAD CG FOR RIGID AND TWO-LINK HEAD/NECK SYSTEMS

Out-of-plane rotations, ϕ_x and θ_x, defined by equations (6) and (9) do not change significantly during the impact. Figure 5-7a shows the peak out of plane rotation of the head and neck to be less than 0.1 radians for test LX3983 or less than 10 percent of the peak in-plane motion (of Figure 5-3a). Figure 5-7b shows the out-of-impact plane displacement of the head and T1 anatomical origins to deviate by less than 1.5 cm from the initial position for test LX3983. Displacement of T1 in the direction of impact for this test is 7 cm. For the performance requirement developed in this study, these out-of-plane motions are disregarded in light of the more significant in-plane response characterized by $r_{O/T}$, ϕ_y and θ_y.

5.1.2   Frontal Kinetic Response

The forces and moments at the occipital condylar point are calculated in head anatomical components using equations (24) and (26), respectively. Laboratory components are then calculated using the inverse of the transformation of equation (2). Figure 5-8 shows both sets of components for test LX3983. There is little detectable difference between the laboratory and anatomical components of moment for frontal tests since the response is nearly planar.

The force component in the y-direction and the moment components about the x and z axes are small as expected. The non-negligible loads which include moment T_{Oy} about the head y-axis and forces F_{Ox} and F_{Oz} along the head x and z axes, will, therefore, form the kinetic performance requirement. Moment is cross plotted versus change in head angle in Figure 5-9 and the two anatomical forces F_{Ox} and F_{Oz} are cross plotted versus neck chord angle in Figure 5-10 and 5-11, respectively. These anatomical components of force provide a measure of shear and tension in the neck which are likely to be useful in conjunction with moment in predicting neck injury.

The moment versus head angle plots of Figure 5-9 are similar to those used by Mertz in formulating a necessary condition for head response [1]. In Figures 5-9b and c the Mertz loading corridors, which represent bounds on acceptable dummy response, have been superimposed. The horizontal axis has been shifted in accordance with the offset (13 degrees) of the Mertz corridor with respect to the average initial value of the head angle for the test data [23]. The corridor created by the NBDL volunteer data is quite similar to that of Mertz even though
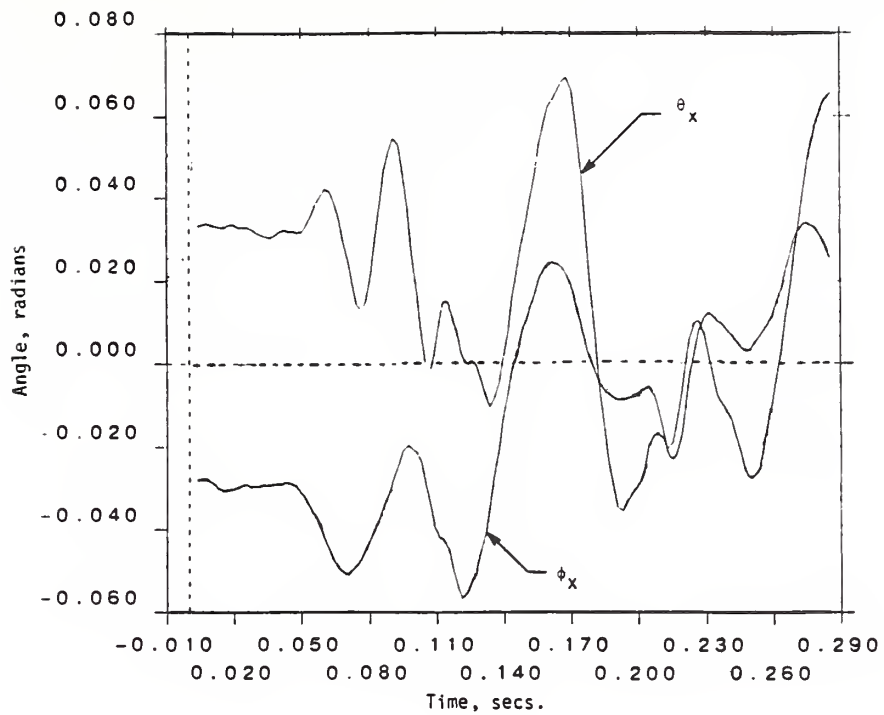
a) Angular Response
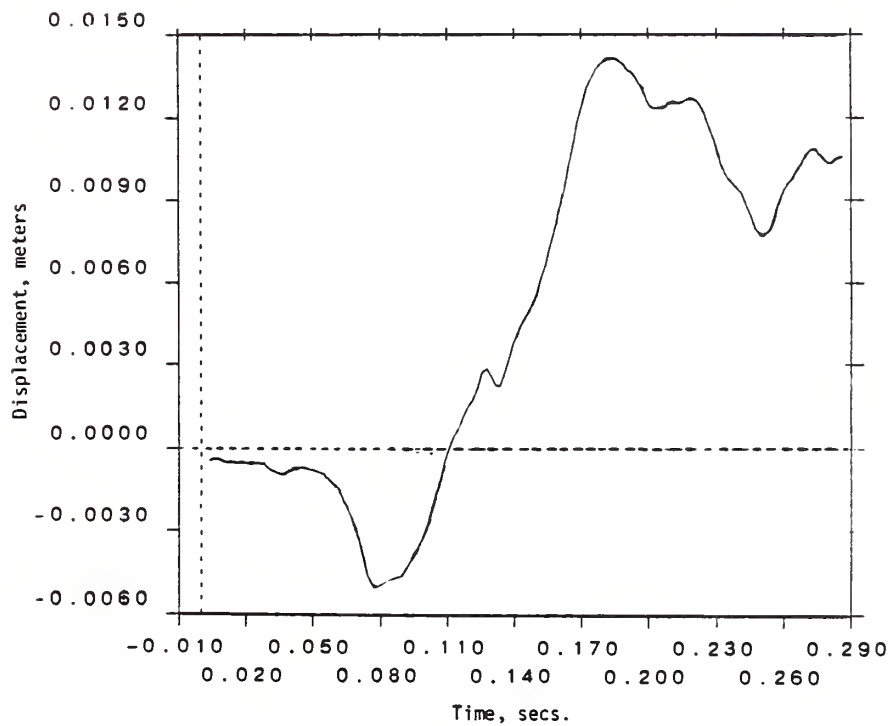
b) Linear Displacement of Head Anatomical Origin Out of Impact Plane

FIGURE 5-7. OUT-OF-IMPACT PLANE MOTIONS FOR TEST LX3983 (SUBJECT H00134, 15-G IMPACT)

5-13
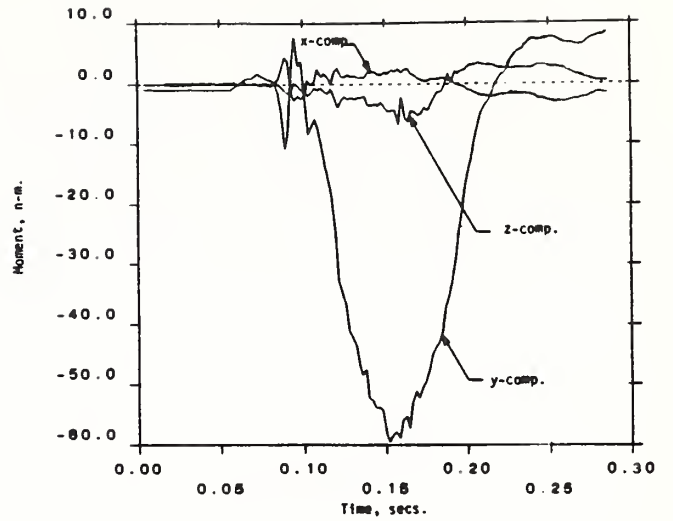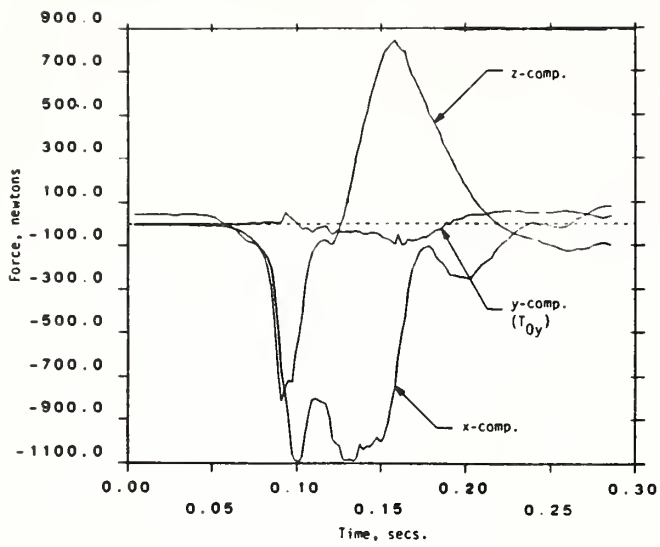
a) Laboratory Components
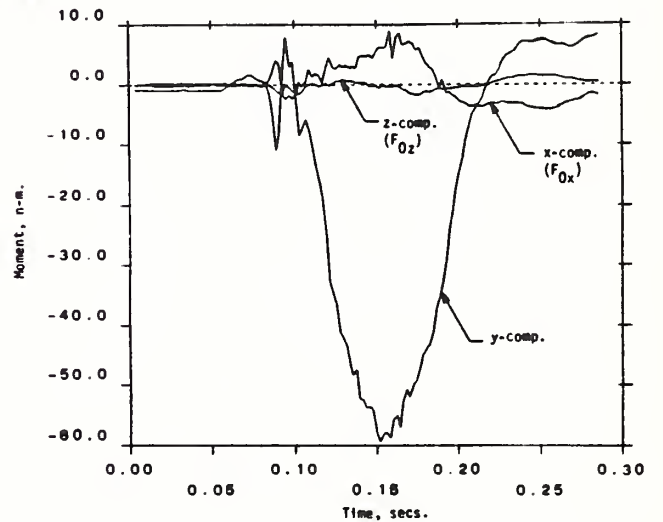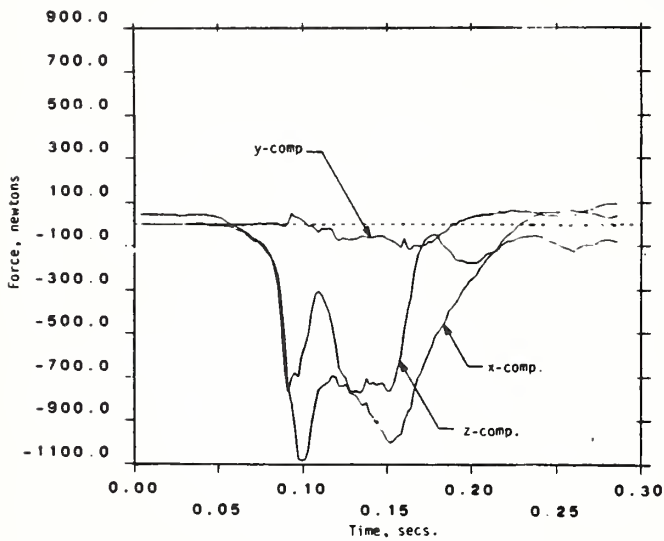
b) Anatomical Components

FIGURE 5-8. HEAD ANATOMICAL AND LABORATORY COMPONENTS OF LOAD AT
THE OCCIPITAL CONDYLAR POINT FOR FRONTAL TEST LX3983
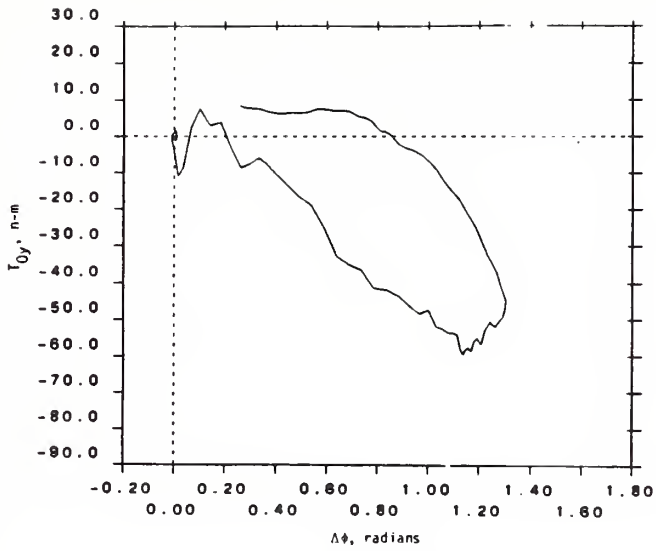
5-14

a) Subject H00134, 15-g Impact
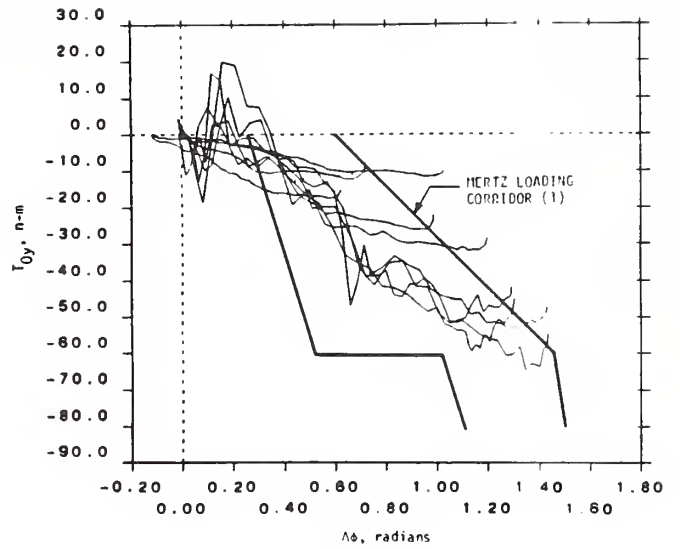
b) Subject H00134, Nine Tests
(3-15g Impacts)
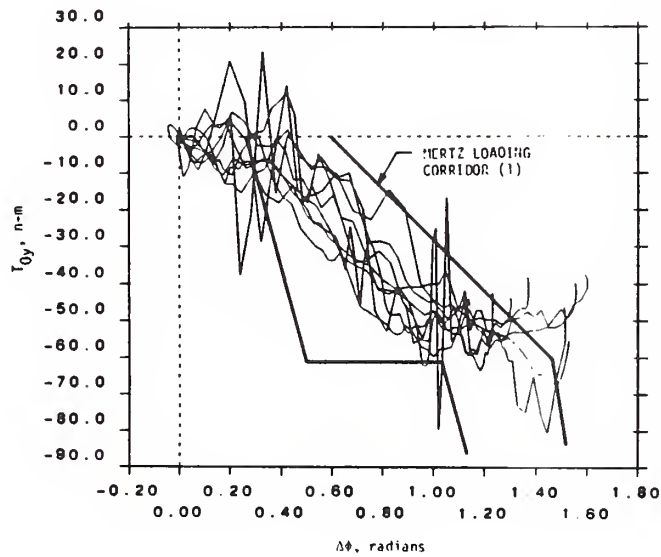
c) Nine Subjects, 15-g Impact

FIGURE 5-9. MOMENT, T_{Oy}, PERPENDICULAR TO THE MID-
SAGITTAL PLANE AT THE OCCIPITAL CONDYLAR POINT
VERSUS CHANGE IN HEAD ROTATION, $\Delta\phi$, FOR FRONTAL
IMPACT
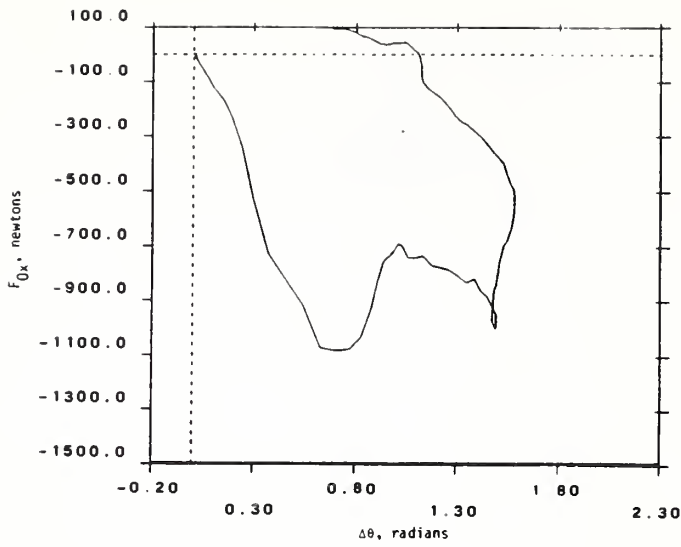
a) Subject H00134, 15-g Impact
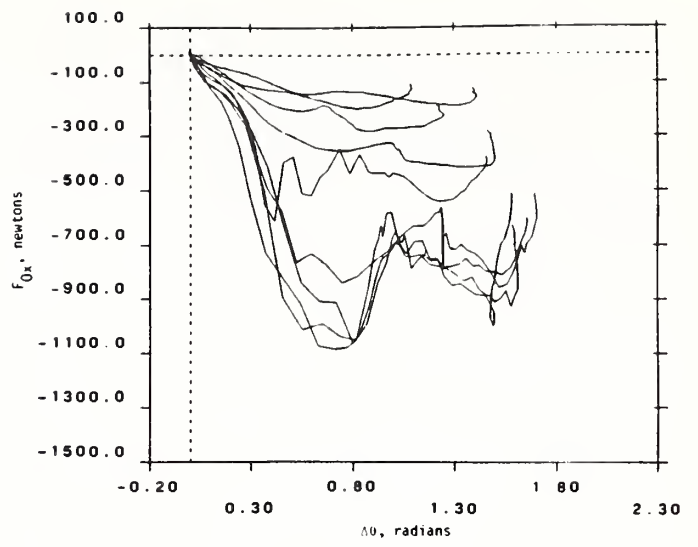
b) Subject H00134, Nine Tests
    (3-15g Impacts)
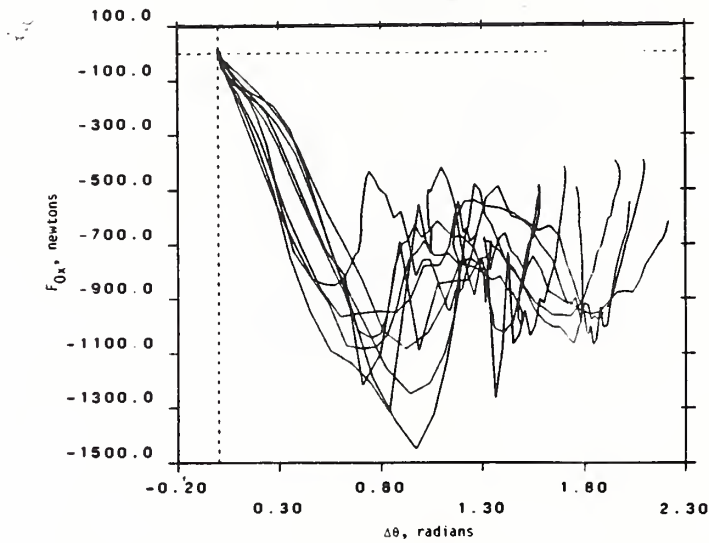
c) Nine Subjects, 15-g Impact

FIGURE 5-10. FORCE COMPONENT, F_{Ox}, OF THE HEAD
              ANATOMICAL COORDINATE SYSTEM VERSUS CHANGE IN
              NECK CHORD LINE ANGLE, $\Delta\phi$, FOR FRONTAL IMPACT
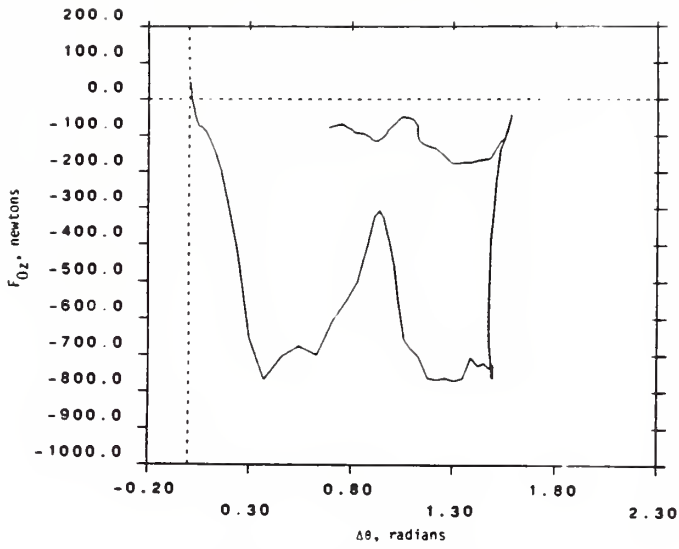
a) Subject H00134, 15-g Impact
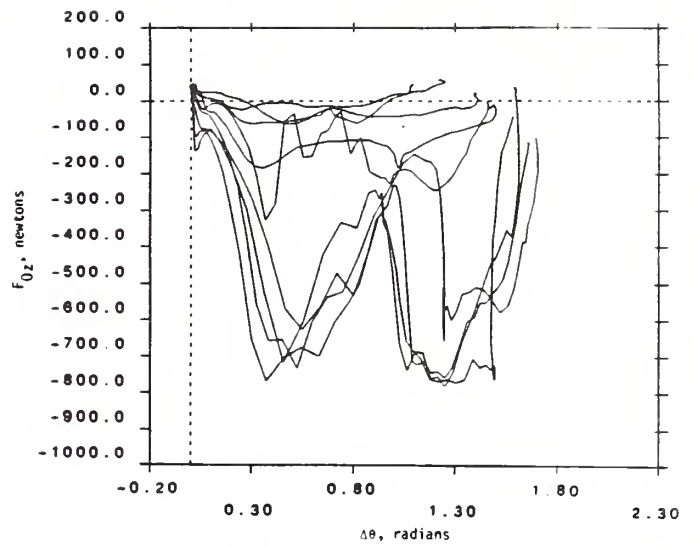
b) Subject H00134, Nine Tests
   (3-15g Impacts)
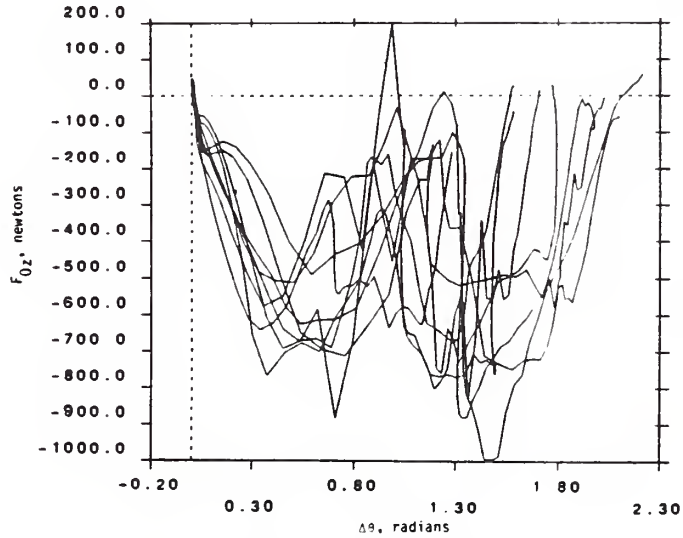
c) Nine Subjects, 15-g Impact

FIGURE 5-11. FORCE COMPONENT, F_{Oz}, OF THE HEAD
ANATOMICAL COORDINATE SYSTEM VERSUS CHANGE IN
NECK CHORD LINE ANGLE, $\Delta\theta$, FOR FRONTAL IMPACT

the latter was created by a different range of impact levels and varying amounts of weight added to the head. Note in Figure 5-9b that the response to lower level impacts do not terminate within the corridor created by the higher level impacts as was the case for the kinematic variables in the previous section. This suggests that the Mertz performance corridor would be more constraining if it were partitioned into subcorridors corresponding to different impact levels. In Figure 5-12, the Mertz corridor is overlayed on mean response curves corresponding to four sled impact levels. The mean responses were generated from tests of all subjects exposed to the particular impact level. Comparable force corridors could be produced that would exhibit the same dependence on impact level.

The deviation in load response when different volunteers are subjected to the same impact condition is greater than the deviation in kinematic response for the same tests (e.g., compare Figures 5-10c and 5-11c with Figure 5-3c). This is further discussed in Section 5.4.

5.2   RESPONSE TO LATERAL IMPACT

5.2.1   Lateral Kinematic Response

In general, lateral response in the impact plane is similar to that of frontal response and can be characterized using the same three variables, r_n, $\Delta\phi$, and $\Delta\theta$ that were used for frontal response. Out-of-impact plane motion is also present and is characterized by the single variable $\Delta\psi = \psi_c - \psi_{co}$ where ψ_c is illustrated in Figure 4-5. Figures 5-13, 5-14 and 5-15 are cross plots which describe the constraint between excursions of these four variables during response to rapid torso acceleration. The response characteristics are discussed in detail in the paragraphs which follow by noting the similarities and differences between lateral and frontal response.

As indicated in the test summary of Appendix A, the most severe lateral test level produced a factor of two less velocity change and peak acceleration for the sled when compared to the most severe frontal test level. The most severe lateral tests were conducted at a 7-g peak sled impact level with a velocity change of 7 m/s. The most severe frontal tests were conducted at 15-g with a velocity change in excess of 17 m/s. Thus, the peak lateral excursions observed are

IMPACT LEVEL CHARACTERISTICS		
LEVEL CURVE	PEAK SLED ACC. (m/s^2)	CHANGE IN, T1 VEL. m/s
LI	4	7
LII	8	12
LIII	12	15
LIV	15	17
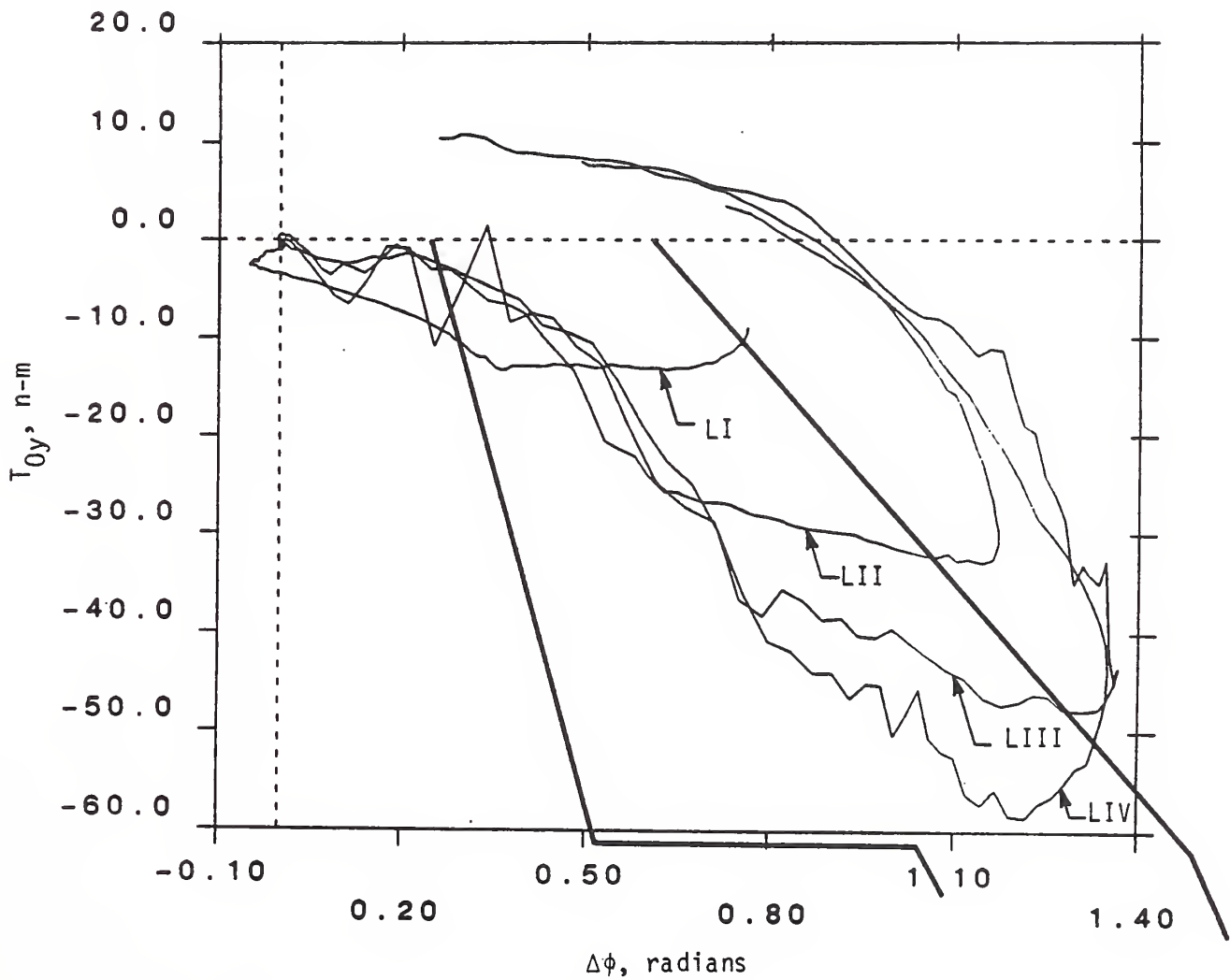
FIGURE 5-12. OVERLAY OF MEAN RESPONSE CURVES FOR FOUR SLED IMPACT LEVELS ON THE MERTZ PERFORMANCE CORRIDOR
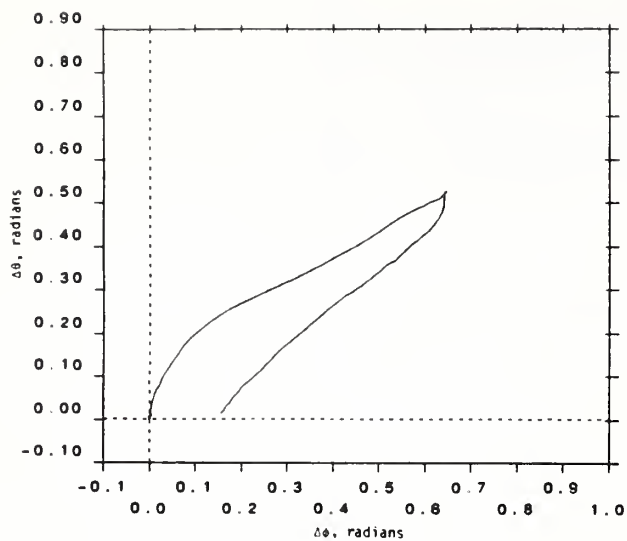
a) Subject H00134, 7-g Impact
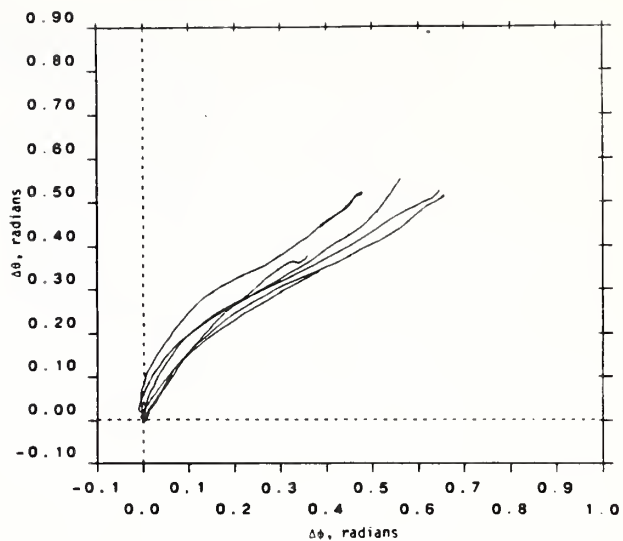
b) Subject H00134, Six Tests
(3.7 g Impacts)
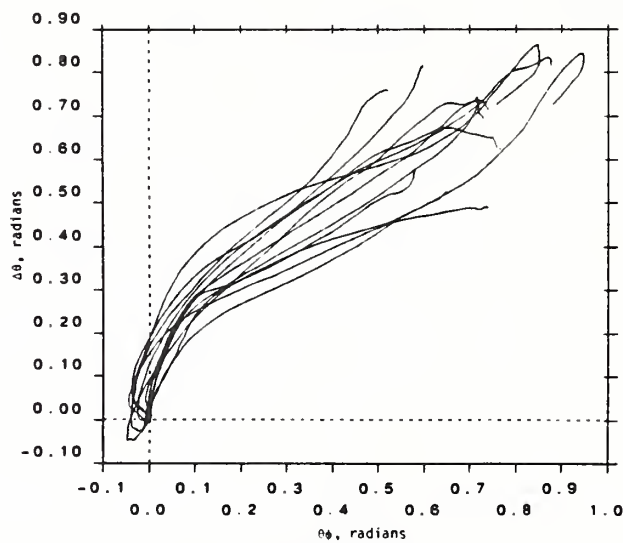
c) Twelve Subjects, 7-g Impact

FIGURE 5-13. CHANGE IN HEAD ANGLE, $\Delta\phi$, VERSUS CHANGE
IN NECK CHORD LINE ANGLE, $\Delta\theta$, FOR LATERAL IMPACT
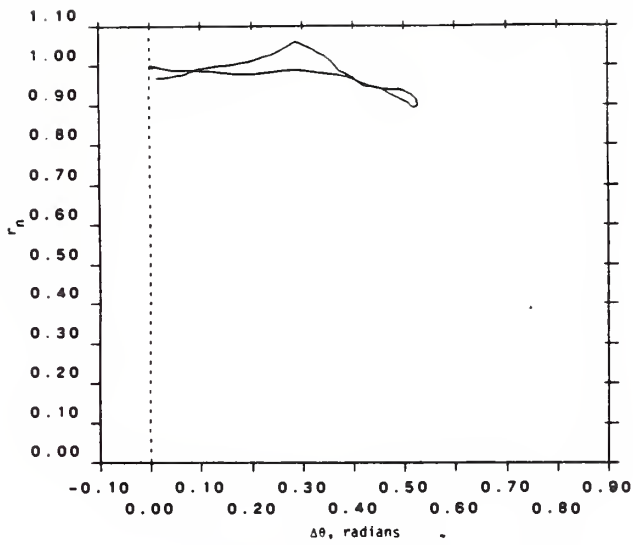
a) Subject H00134, 7-g Impact
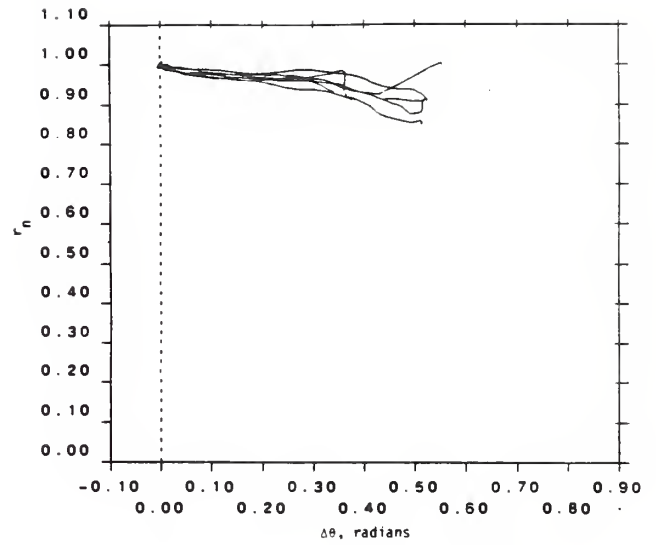
b) Subject H00134, Six Tests
(3-7g Impacts)
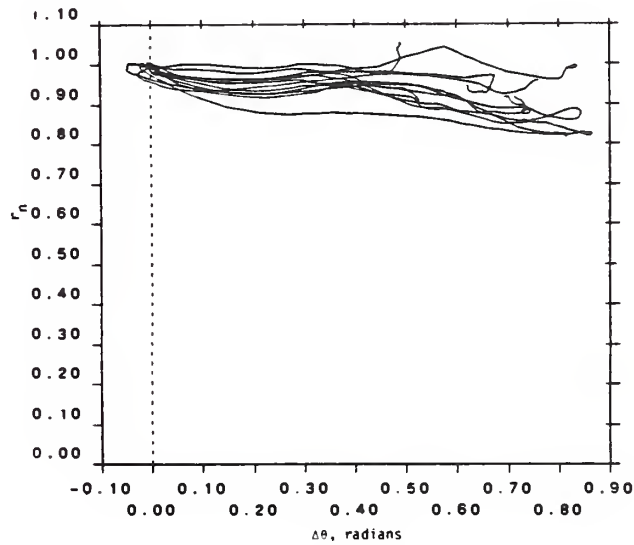
c) Twelve Subjects, 7-g Impact

FIGURE 5-14. NORMALIZED NECK CHORD LENGTH, r_n, VERSUS
CHANGE IN NECK CHORD LINE ANGLE, $\Delta\theta$, FOR
LATERAL IMPACT
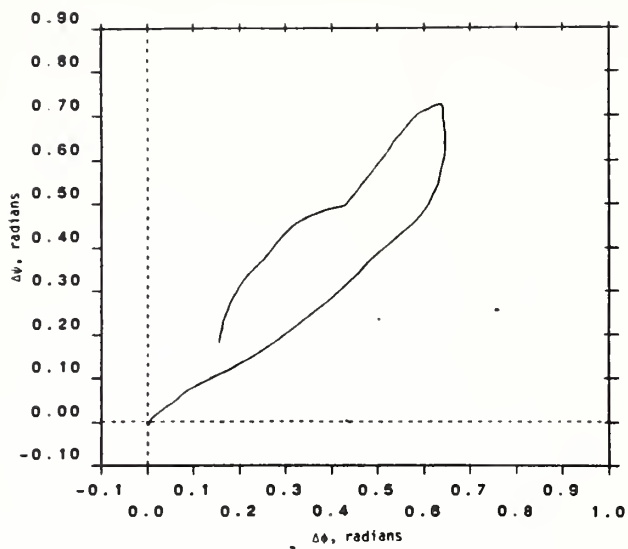
a) Subject H00134, 7-g Impact
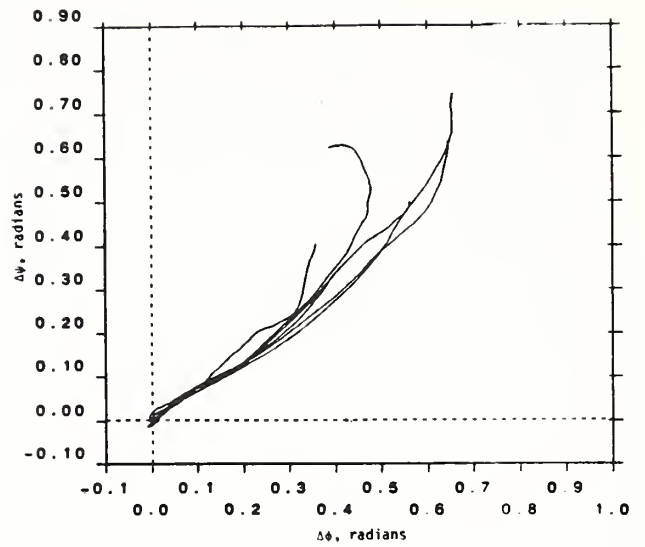
b) Subject H00134, Six Tests
(3-7g Impacts)
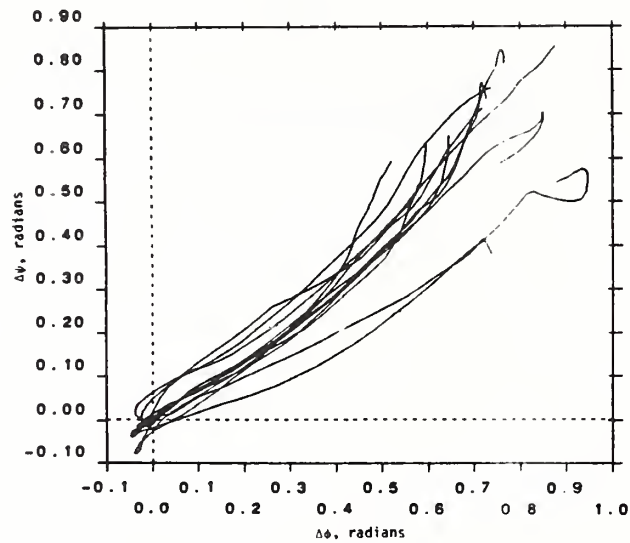
c) Twelve Subjects, 7-g Impact

FIGURE 5-15. CHANGE IN HEAD TWIST ANGLE, $\Delta\psi$, VERSUS
CHANGE IN HEAD ANGLE, $\Delta\phi$, FOR LATERAL IMPACT

correspondingly less, as can be noted by comparing Figures 5-13c and 5-14c with Figures 5-3c and 5-4c. The only tests conducted in both directions that have comparable input conditions are the 4-g tests. Change in sled velocity in these tests is within the range 7.0 to 7.3 m/s for all tests of all subjects. Peak impact level is within the range 4.0 to 4.2 g's for all of these tests.

Figure 5-16 compares 4-g frontal and lateral tests of subject H00134. Peak head excursion is somewhat less for the lateral test and peak neck angle is a factor of three less. For other subjects tested at 4-g, the lateral response is even smaller. This suggests variation in stiffness characteristics in the two directions, although variation in inertia characteristics and variations in torso restraint may also influence the peak excursion.

There is an initial hesitation in head rotational response, followed by a phase in which the head rotates faster than the neck chord. The latter is indicated in Figure 5-16 by the straight line portion of the curve that has a slope less than unity. There is only a short segment of the lateral response near peak excursion where the slope is unity representing no relative motion between the head and neck. In many of the other lateral tests this "protective position" is never reached as can be seen in multi-subject plots of Figures 5-13b and 5-13c. Note in the lateral case of Figure 5-16 that the protective position lies close to the dotted straight line through the origin with unity slope and is not offset as it was in the frontal response. This result is consistent with the protective position hypothesis, i.e., the sagittal plane of the head, which contains the head center-of-gravity, contains the neck chord only when there is no lateral rotation of the head relative to the neck.

The neck chord shortens due to lateral impact, as indicated in Figures 5-14a, b, and c. On a normalized basis, the range is 0.80 to 1.05 for the twelve 7-g tests of Figure 5-14c with ten of the twelve in the range 0.82 to 0.96. This corresponds approximately to the degree of shortening noted in the frontal tests for comparable head excursion angles. The corridor created by the multi-subject tests of Figure 5-14c is broadest near peak excursion, as was the case for frontal impact. For any one subject the amount of shortening is more consistent and forms a relatively narrow corridor as indicated by Figure 5-14b.
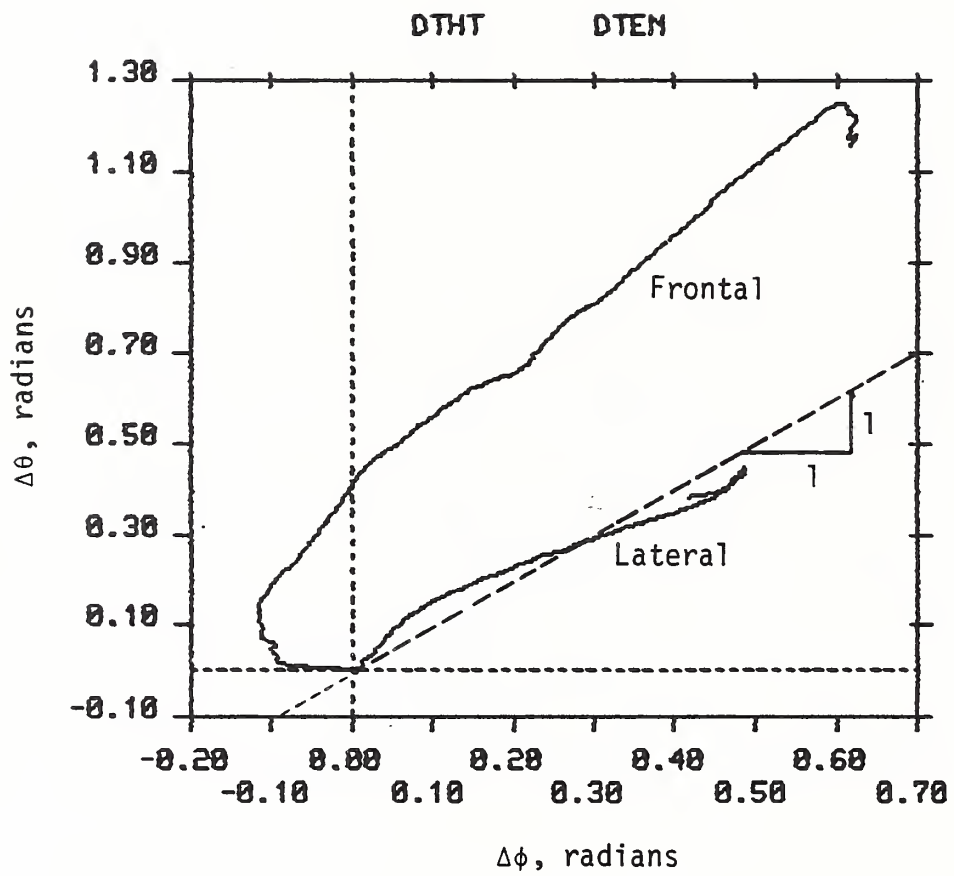
FIGURE 5-16. COMPARISON OF ANGULAR RESPONSE OF THE HEAD AND NECK
FOR 4-G FRONTAL AND LATERAL IMPACTS (SUBJECT H00134)

There is significant change in head twist, $\Delta\psi$, as indicated in Figure 5-15. This results from the head center-of-gravity being slightly forward relative to the neck chord line. The twist is nearly linearly related to the head angle, $\Delta\phi$. In Figure 5-17, the alternate twist angle, $\Delta\psi_i$, is compared to $\Delta\psi$. It is also linearly related to head angle , $\Delta\phi$, but reaches a somewhat larger peak value (ψ_c is the rotation of the head relative to the torso as observed from an overhead camera; ψ_i is the rotation of the head about the head anatomical z-axis relative to the torso).

Out-of-impact plane angles, ϕ_x and θ_x, do not change significantly during the loading phase of the tests but are more significant than for frontal impact. The deviation during the loading phase (the first 0.2 seconds) for the 7-g test of subject H00134 in Figure 5-18a is less than 0.2 radians which is 25-30 percent of the peak excursion in the impact plane (Figure 5-13a). Deviation of the head displacement is less than 3 cm.

5.2.2   Lateral Kinetic Response

Figure 5-19 shows both the laboratory and head anatomical components of force and moment at the condylar point for lateral test LX4126. The laboratory force y component perpendicular to the impact plane remains small throughout the impact as do the moment x and z components in the impact plane. The remaining three laboratory components characterize the significant load response.

Laboratory moment component T_{Oy} measures the moment at the top of the neck perpendicular to the impact plane and is a variable which is likely to be useful in predicting neck injury. Generally, a load cell in an ATD will measure anatomical components of moment so calculation of T_{Oy} requires knowledge of head orientation in the laboratory during the test. Moment is plotted versus change in head angle in Figure 5-20.

Anatomical components of force are characterized in lieu of laboratory components. The head z-component of force F_{Oz} is plotted in Figure 5-21 versus neck angle. In Figure 5-22, the vector sum of the head x and y components of force F_{xy} are plotted versus neck angle. These components provide a measure of tension and shear in the neck and are likely to show correlation with neck injury.
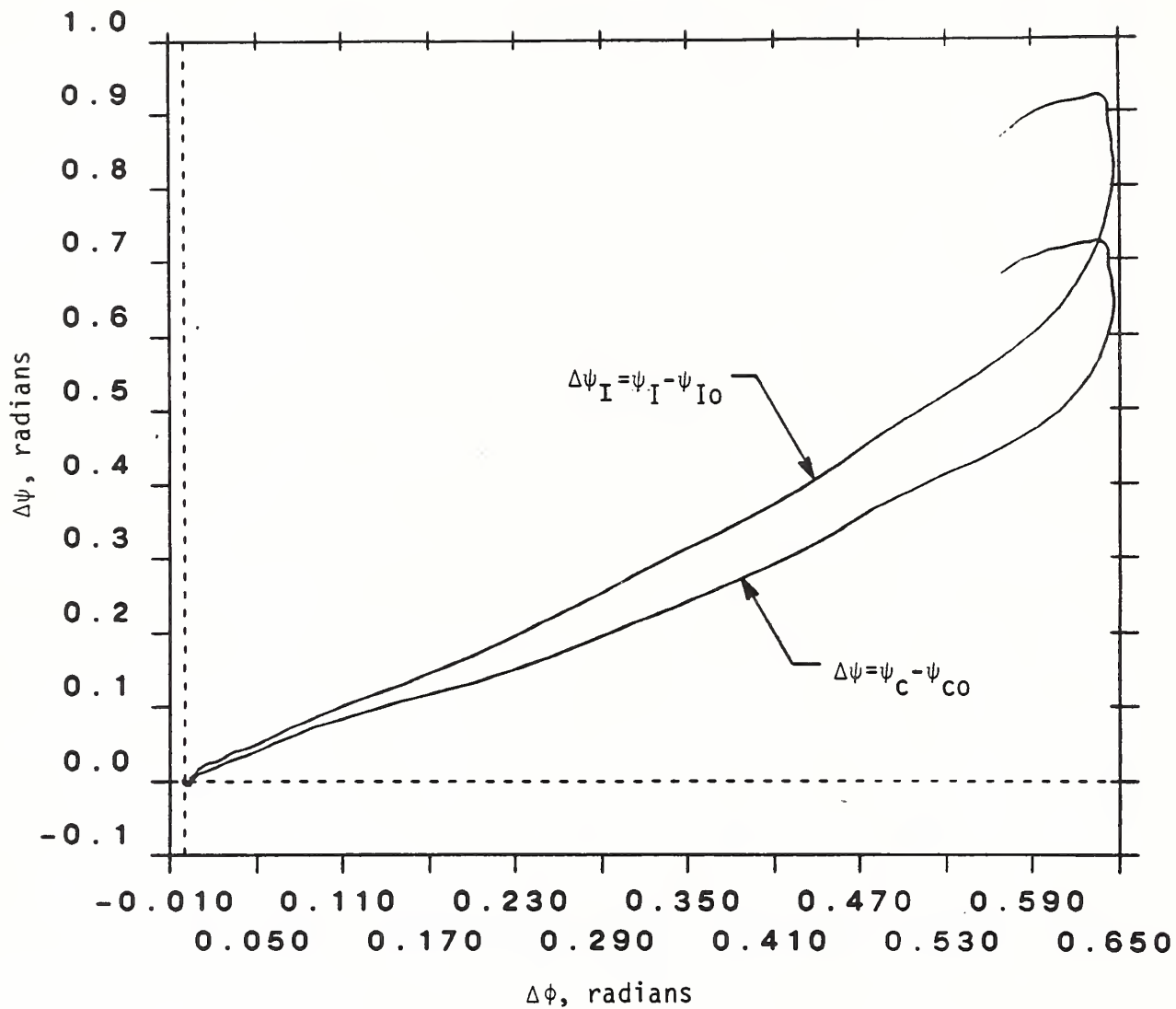
FIGURE 5-17. COMPARISON OF HEAD TWIST ANGLES, $\Delta\psi_c$ AND $\Delta\psi_I$, FOR LATERAL IMPACT

5-26
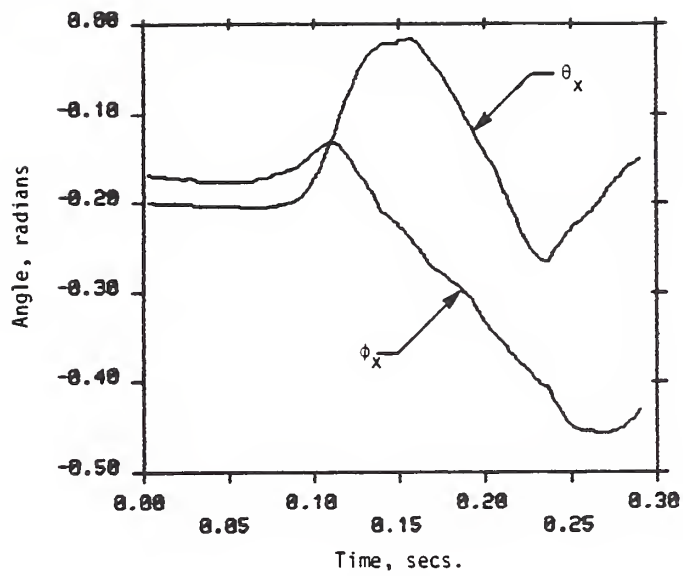
a) Angular Response
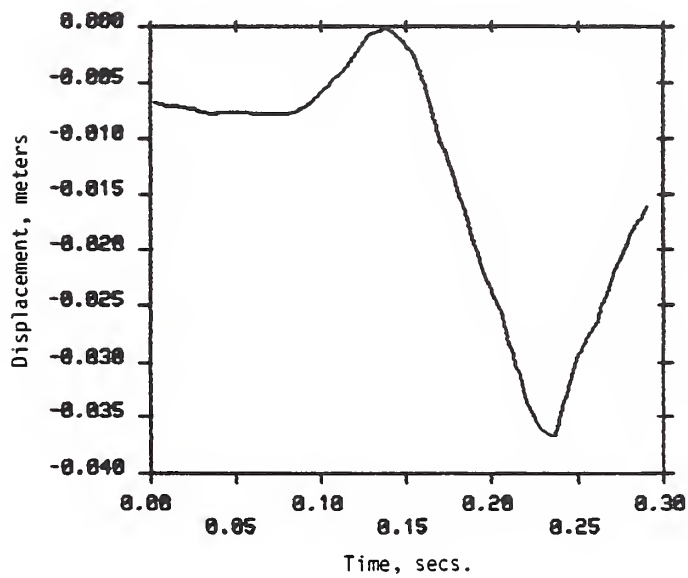
b) Linear Displacement of Head Anatomical Origin

FIGURE 5-18. OUT-OF-PLANE MOTIONS FOR LATERAL TEST LX4126
(Subject H00134, 7-G Impact)

5-27
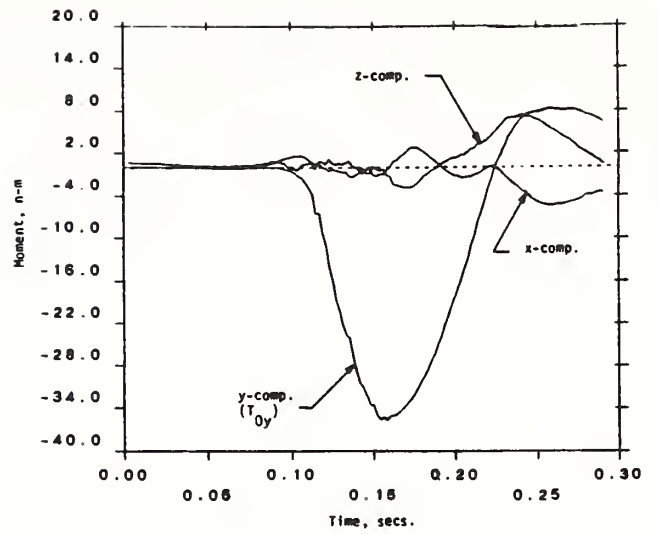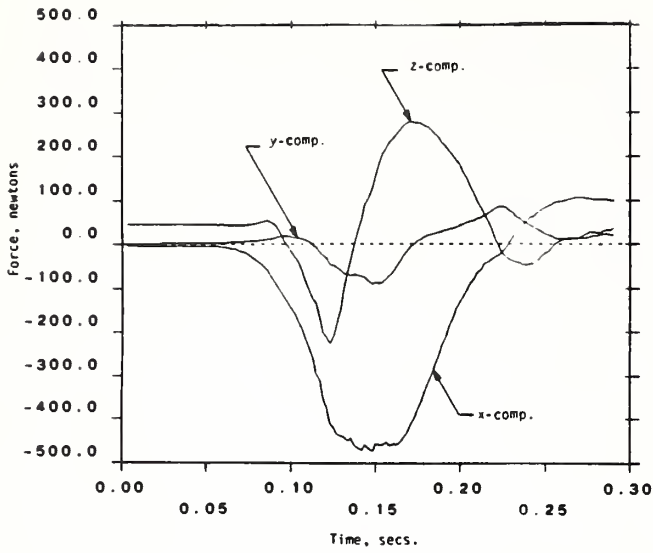
a) Laboratory Components
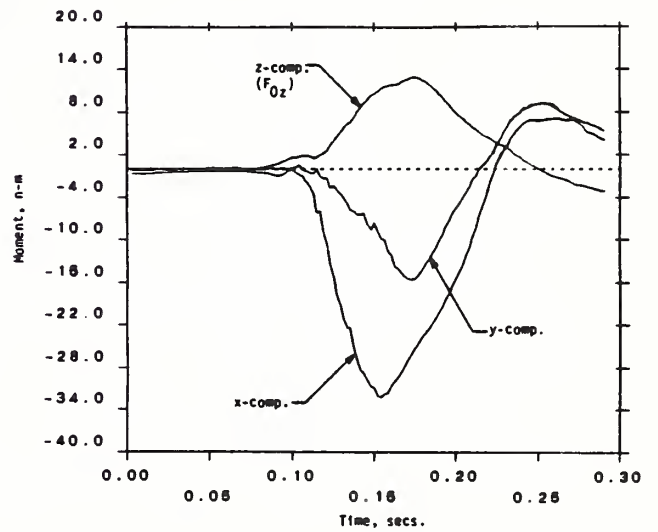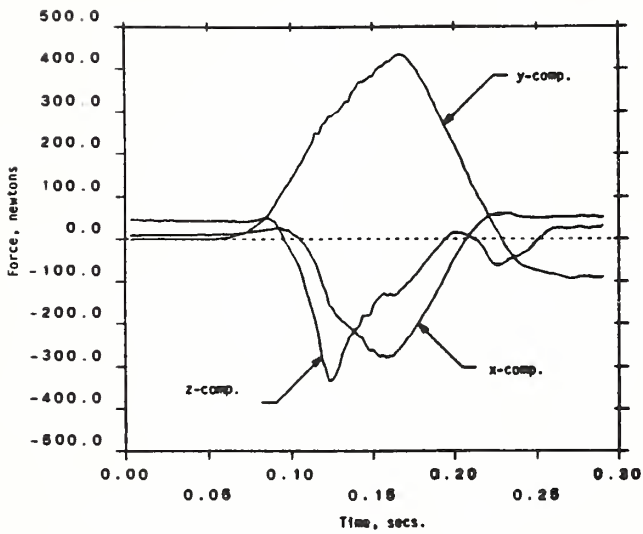
b) Anatomical Components

FIGURE 5-19. HEAD ANATOMICAL AND LABORATORY COMPONENTS OF LOAD AT
THE OCCIPITAL CONDYLAR POINT FOR LATERAL TEST LX4126
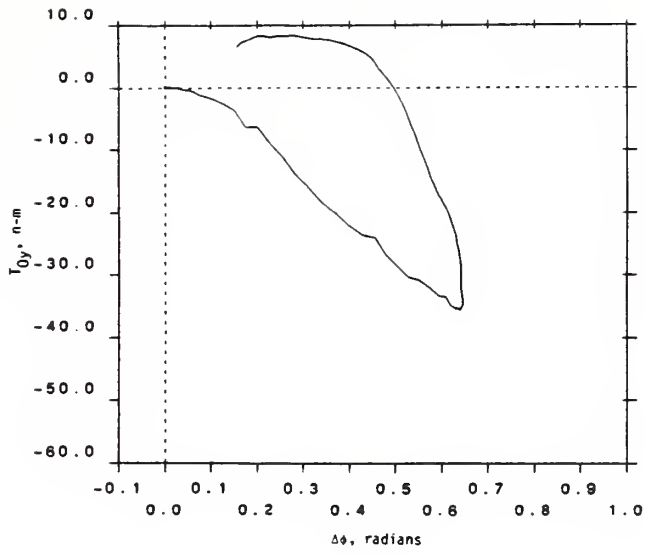
a) Subject H00134, 7-g Impact
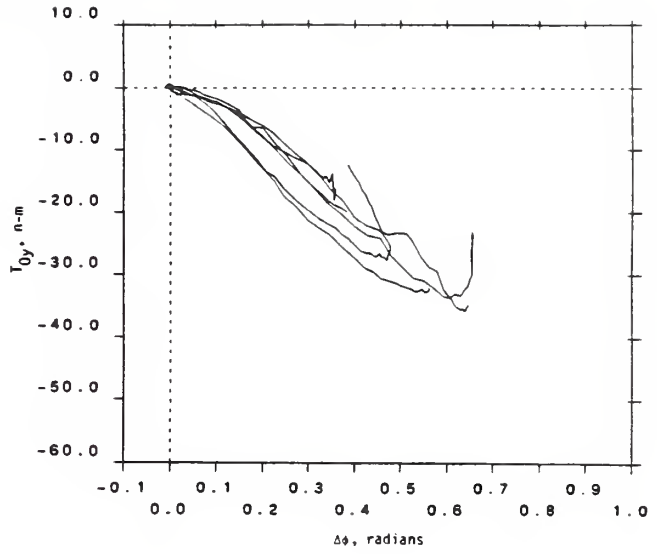
b) Subject H00134, Six Tests
(3-7g Impacts)
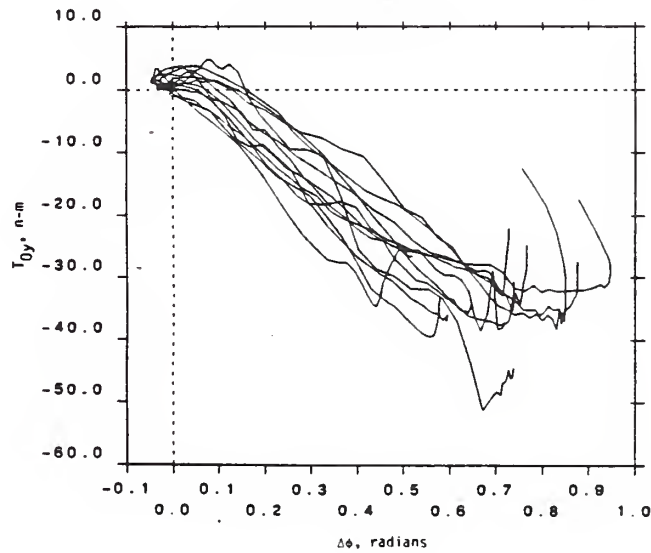
c) Twelve Subjects, 7-g Impact

FIGURE 5-20. MOMENT PERPENDICULAR TO THE IMPACT PLANE
APPLIED AT THE OCCIPITAL CONDYLAR POINT VERSUS
CHANGE IN HEAD ROTATION, $\Delta\phi$, FOR LATERAL IMPACT
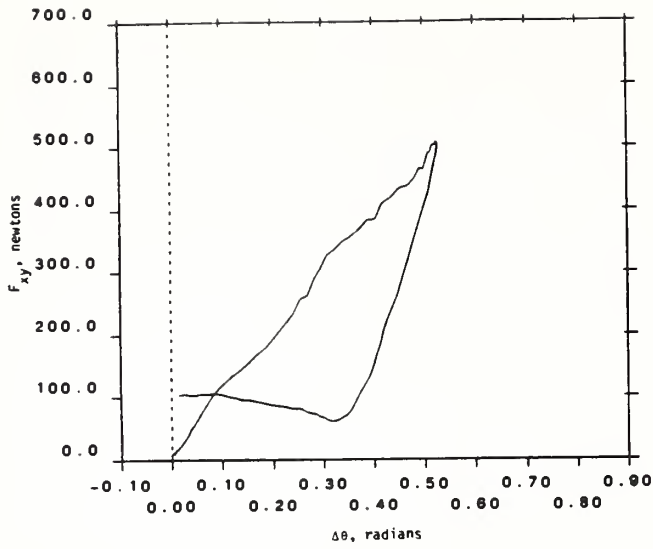
a) Subject H00134, 7-g Impact
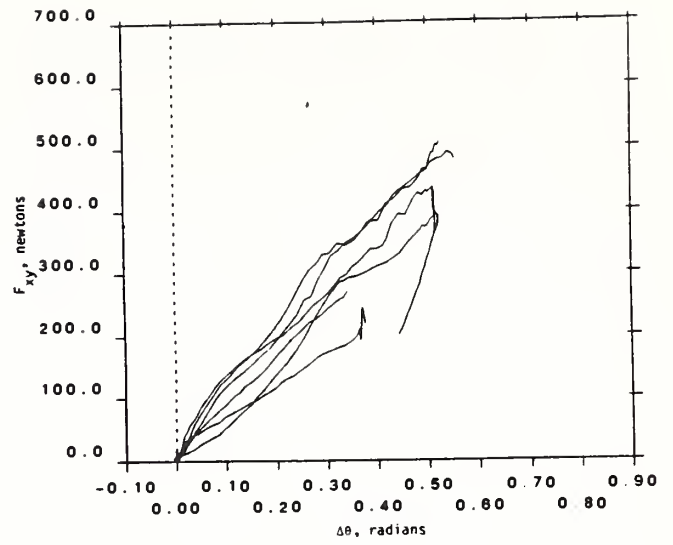
b) Subject H00134, Six Tests (3-7g Impacts)
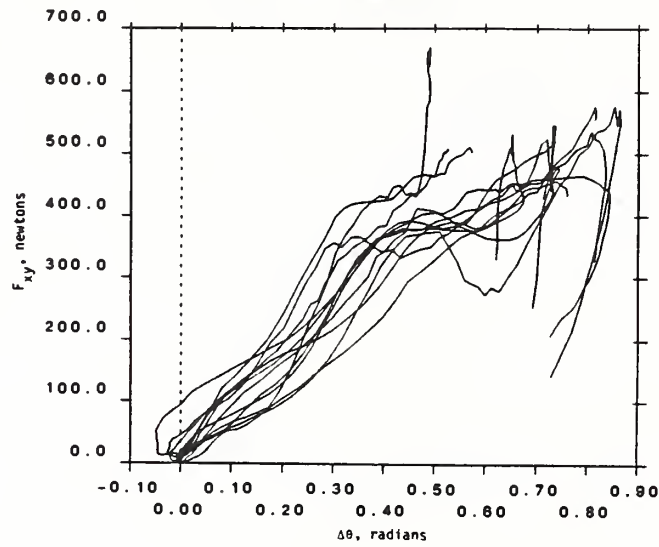
c) Twelve Subjects, 7-g Impact

FIGURE 5-21. RESULTANT FORCE AT THE OCCIPITAL CONDYLAR POINT IN THE HEAD X-Y PLANE VERSUS CHANGE IN NECK ANGLE, $\Delta\theta$, FOR LATERAL IMPACT
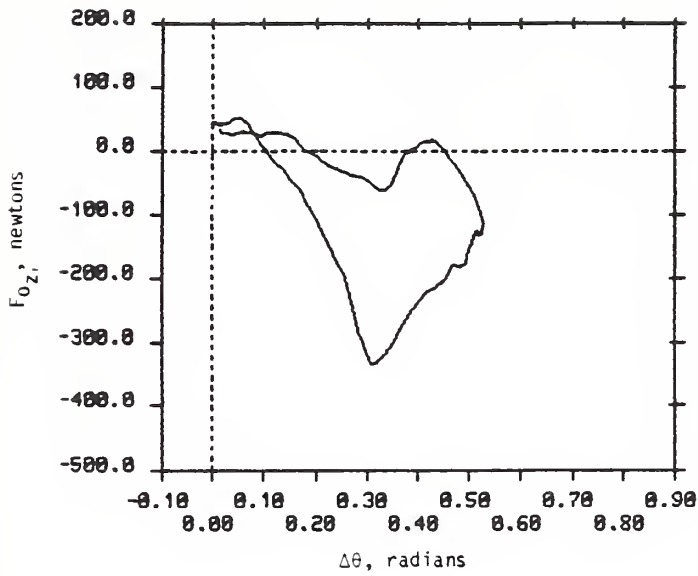
a) Subject H00134, 7-g Impact
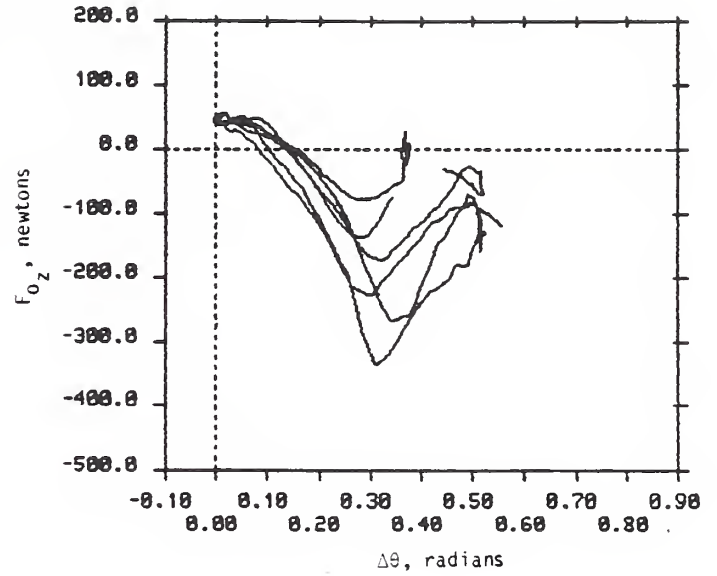
b) Subject H00134, Six Tests
(3-7g Impacts)
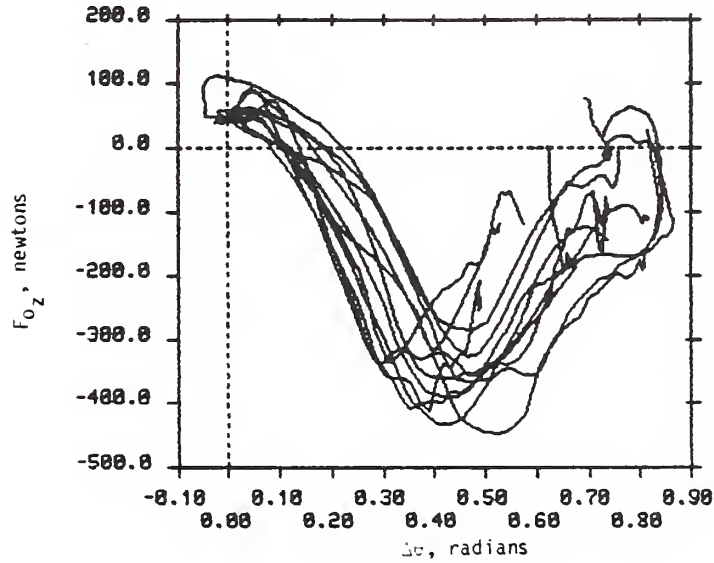
c) Twelve Subjects, 7-g Impact

FIGURE 5-22. FORCE AT THE OCCIPITAL CONDYLAR POINT
ALONG THE HEAD Z-AXIS VERSUS CHANGE IN NECK
ANGLE, $\Delta\theta$, FOR LATERAL IMPACT

Condylar moment about the head z-axis is also included as part of the load characterization. Figure 5-23 is a plot of head z-axis moment T_{Oz} versus head twist angle, $\Delta\psi$, which portrays the torsional (dynamical) stiffness about that axis.

As in the case of frontal impact, the kinetic variables exhibit more dependence on impact level and show more subject-to-subject variation than do the kinematic variables.

5.3   RESPONSE TO OBLIQUE IMPACT

Whether the characteristics of human response to impacts in the oblique direction bear any resemblance to frontal or lateral characteristics is dependent on the structure of the neck. A different degree of restriction on inter-vertebral motion in the oblique direction or use of ligamentous and muscular tissue in a different way could result in oblique response that differs significantly from either frontal or lateral response. Such is not the case as will be seen in this section. To the contrary, oblique response appears to be a predictable combination of frontal and lateral response in all aspects except one which is noted.

Whether the characteristics of an ATD's response to impacts in the oblique direction bears any resemblance to frontal and lateral characteristics is dependent on the structure of its neck. They should bear some resemblance since human oblique characteristics do. However, this must be verified for each neck design. Thus, the characteristics of oblique response are presented here not only as evidence of predictability of (human) oblique response but more importantly because performance requirements must be evolved to verify ATD response.

Oblique response is characterized by the same kinematic and kinetic variables used in Section 5.2 for lateral response.

5.3.1   Oblique Kinematic Response

Figures 5-24, 5-25, and 5-26 are cross plots which describe the constraint between significant kinematic response variables. The general shape of the curves for each plot is quite similar to the corresponding lateral plots. Peak head and
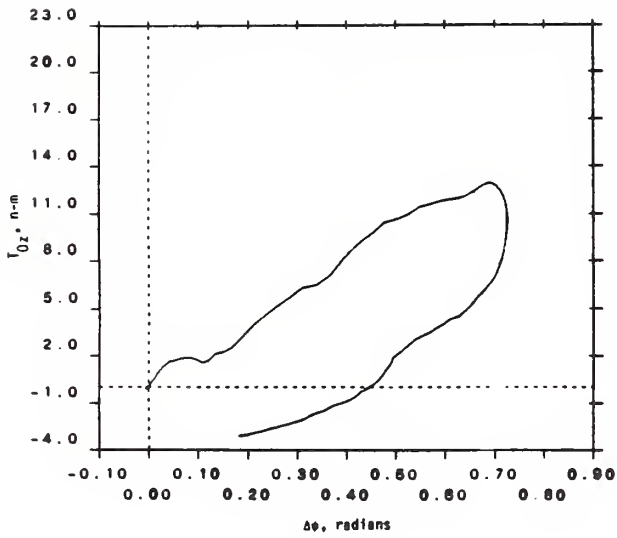
a) Subject H00134, 7-g Impact
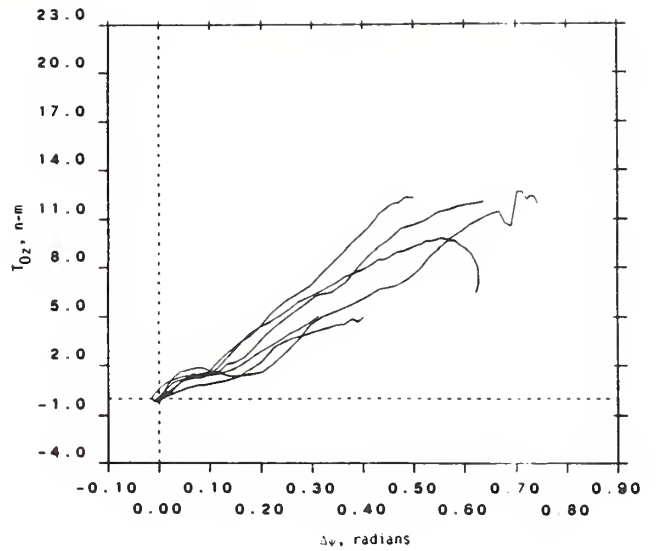
b) Subject H00134, Six Tests
(3-7g Impacts)
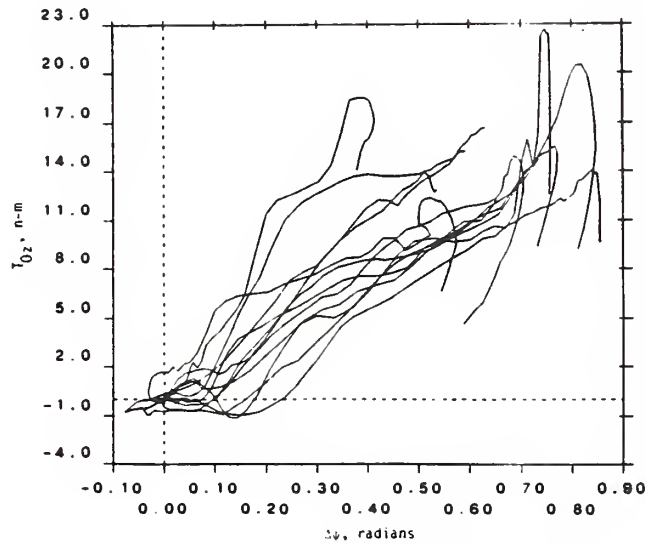
c) Twelve Subjects, 7-g Impact

FIGURE 5-23. MOMENT ABOUT THE HEAD Z-AXIS APPLIED AT
THE OCCIPITAL CONDYLAR POINT VERSUS CHANGE IN
HEAD TWIST, $\Delta\psi$, FOR LATERAL IMPACT
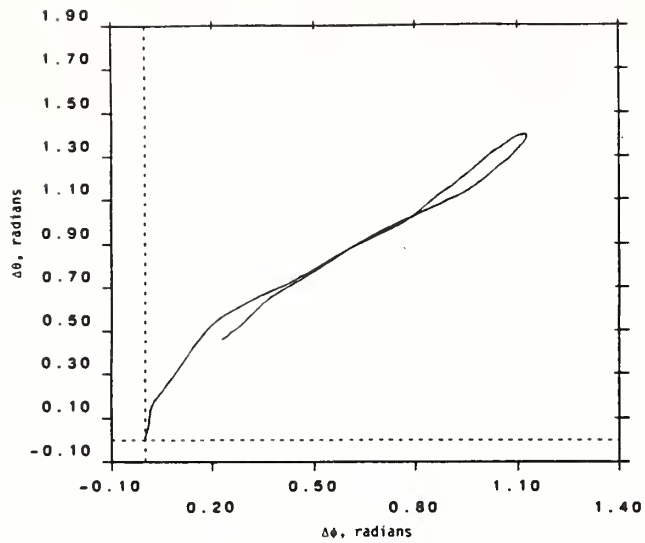
a) Subject H00134, 11-g Impact
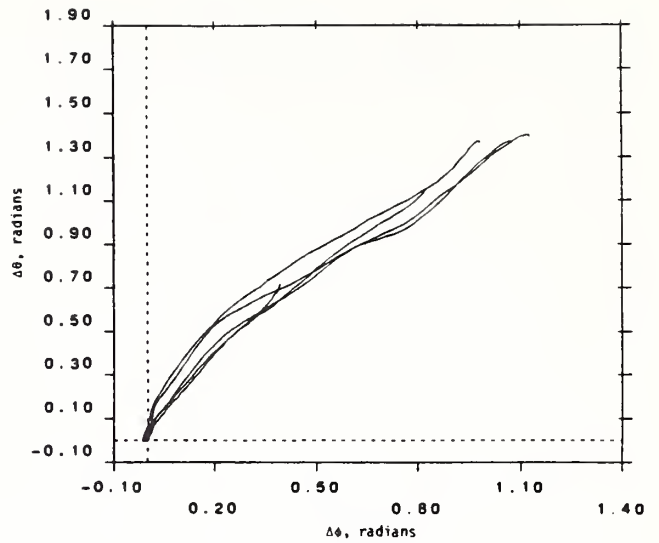
b) Subject H00134, Five Tests
   (4-10g Impacts)
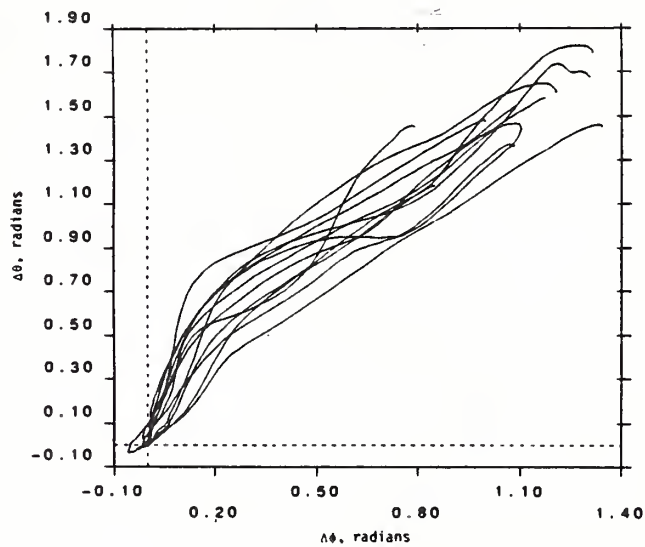
c) Twelve Subjects, 10-g Impact

FIGURE 5-24. CHANGE HEAD ANGLE, $\Delta\phi_y$, VERSUS CHANGE IN NECK
ANGLE, $\Delta\theta$, FOR OBLIQUE IMPACT
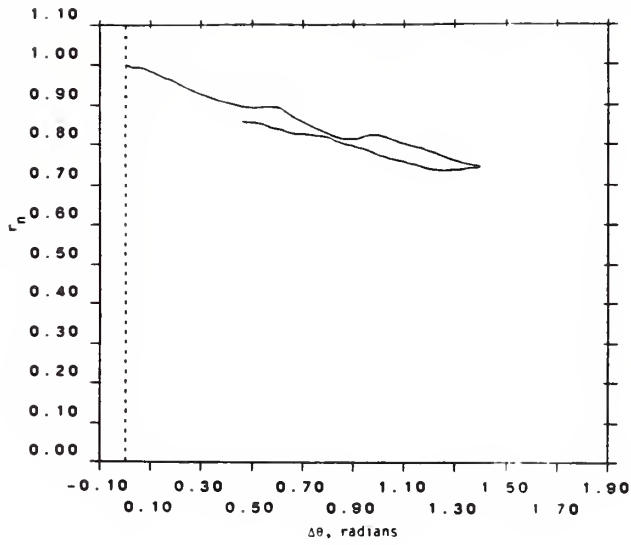
a) Subject H00134, 11-g Impact
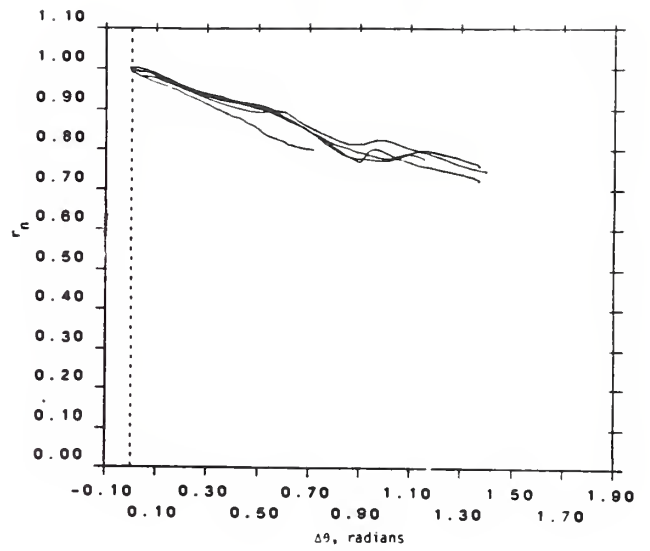
b) Subject H00134, Five Tests (4-10g Impacts)
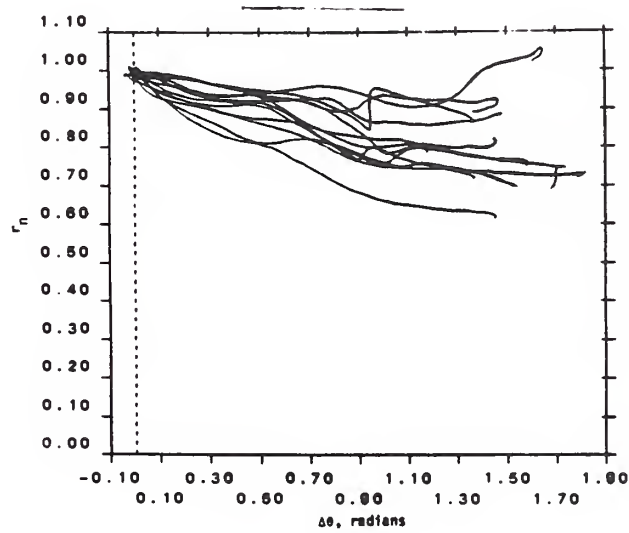
c) Twelve Subjects, 10-g Impact

FIGURE 5-25. NECK CHORD LENGTH, r_n, VERSUS CHANGE IN NECK ANGLE, $\Delta\theta$, FOR OBLIQUE IMPACT
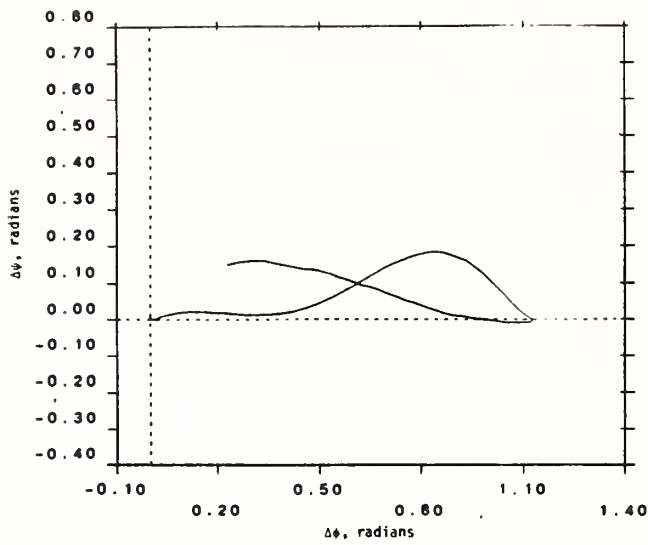
a) Subject H00134, 11-g Impact
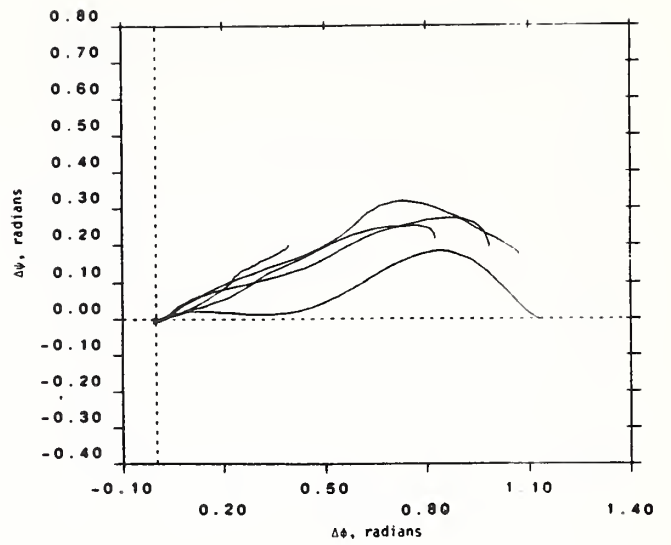
b) Subject H00134, Five Tests
    (4-10g Impacts)
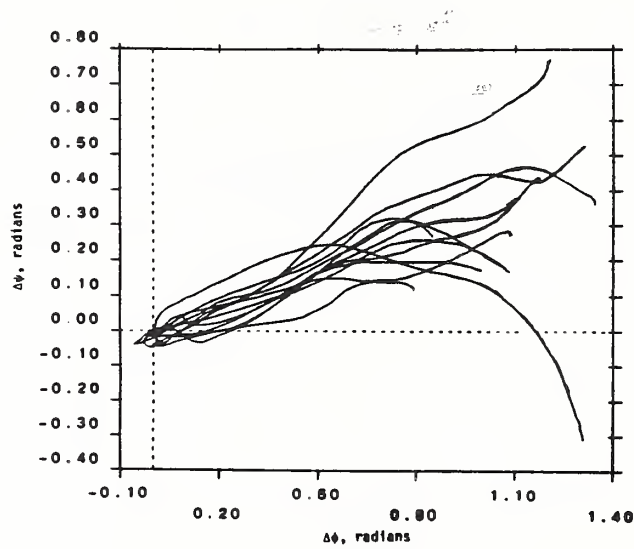
c) Twelve Subjects, 10-g Impact

FIGURE 5-26. CHANGE IN HEAD TWIST ANGLE, $\Delta\psi$, VERSUS
              CHANGE IN HEAD ANGLE, $\Delta\phi$, FOR OBLIQUE IMPACT

neck angular excursions for the most severe oblique tests are intermediate in level between excursions of the lateral and frontal tests, the result of conducting oblique tests up to impact levels that are intermediate between those of the lateral and frontal tests. The peak sled impact level of lateral tests was 11 g's with a velocity change of 15 m/s.

Response when the impact levels are comparable are shown in Figure 5-27a. Change in sled velocity in these tests is within the range 7.0 to 7.3 m/s for all tests of all subjects, and peak impact level is within the range 4.0 to 4.2 g's for all tests. Peak neck angular response for oblique impact is intermediate in magnitude while peak head angular response for oblique impact is less than for either lateral or frontal impact. The latter observation suggests that head articulation of an ATD in the oblique direction needs to be restricted. This conclusion appears to be valid at all impact levels. Figure 5-27b compares frontal and oblique response of 10 g, 14 m/s. Tests at other impact levels need to be conducted to verify this conclusion and tests at other impact directions should be conducted to adequately characterize omni-directional response.

The neck shortens due to oblique impact as indicated in Figure 5-25. On a normalized basis, the range is 0.68 to 0.88 for 10 of 12 subjects tested at 10g's. This corresponds approximately to the degree of shortening noted in the frontal tests for comparable head excursion angles. The corridor created by the multi-subject tests of Figure 5-25c is broadest near peak excursion, as was the case for frontal and lateral impact. Likewise, for any one subject the amount of shortening is more uniform, as indicated by Figure 5-25b.

Note in Figure 5-26c that the head twist increases in a relatively linear way over most of the loading phase. The slope of these curves is approximately 0.3 as compared to approximately 1.0 for lateral response (Figure 5-15c). For a few of the subjects, the linear relationship is not maintained to peak head excursion (peak head angle in the impact plane). Rather there appears to be muscular or inertial response that reduces the twist angle. In Figure 5-28 the alternate head twist variable definitions, ψ_c and ψ_I, are compared. As in the case of lateral response, the ψ_I measure of twist has a slightly greater slope. Both exhibit the reduction prior to peak excursion in the impact plane.
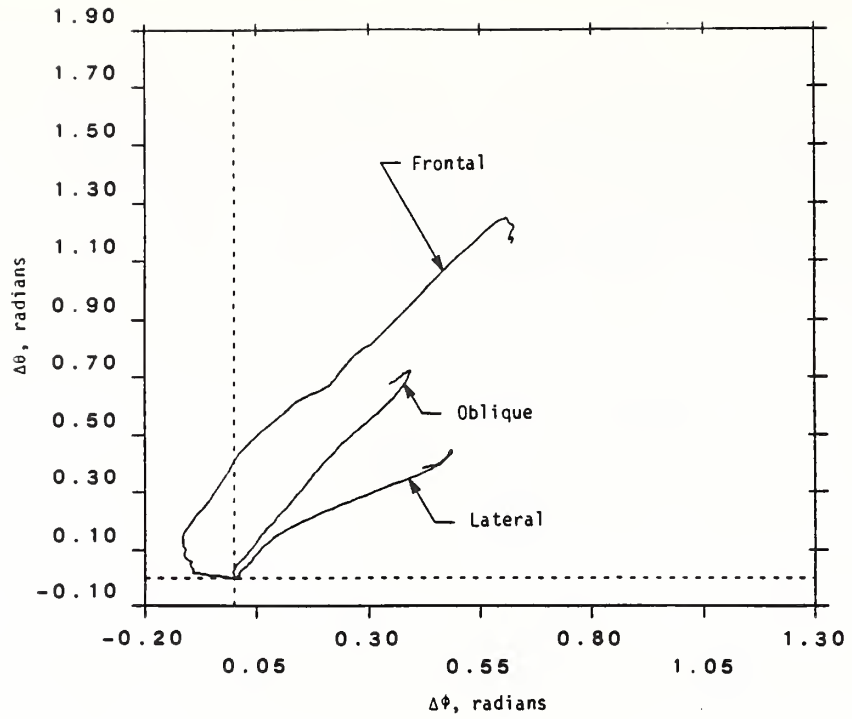
a) Subject H00134, 4-g, 7 m/s Impact Level
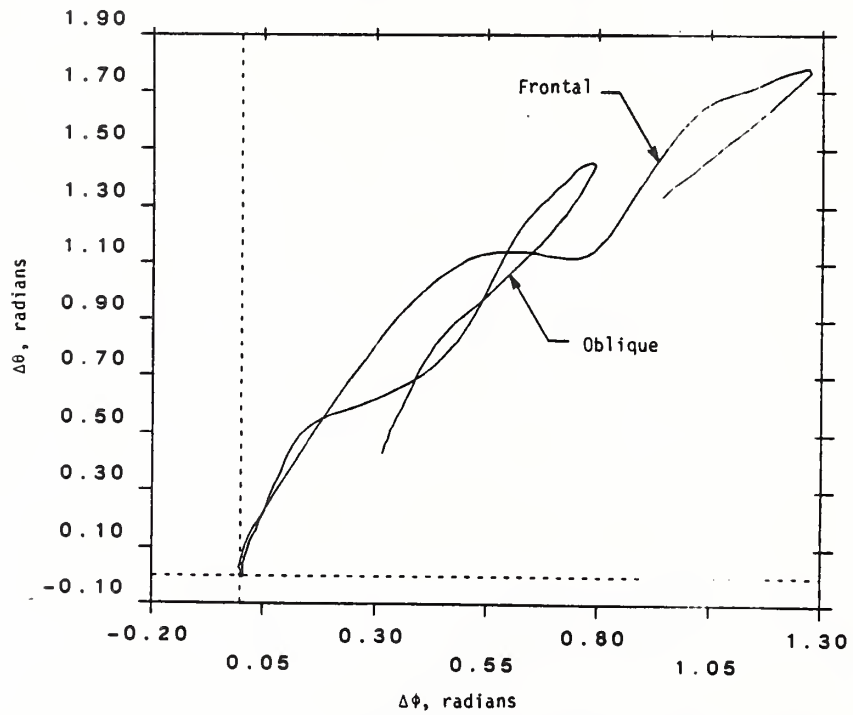
b) Subject H00135, 10-g, 14 m/s Impact Level

FIGURE 5-27. COMPARISON OF ANGULAR RESPONSE OF THE HEAD AND NECK
FOR OBLIQUE, LATERAL AND FRONTAL IMPACT
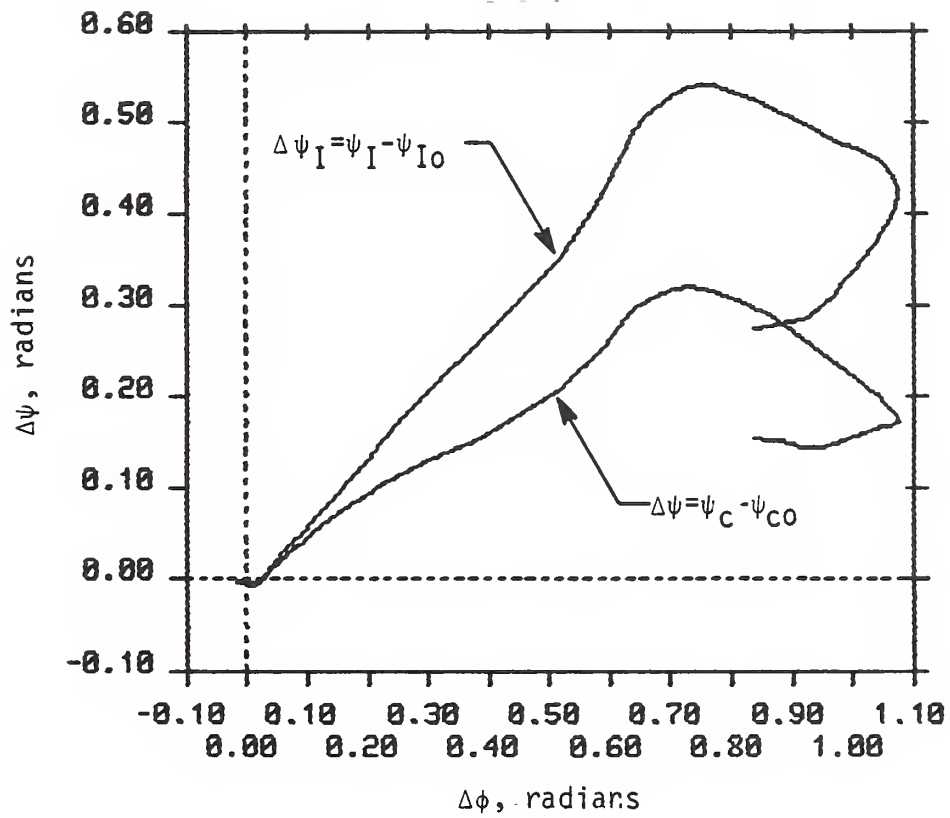
FIGURE 5-28. COMPARISON OF HEAD TWIST ANGLES, $\Delta\psi_c$ AND $\Delta\psi_I$, FOR OBLIQUE IMPACT

There is more out-of-impact plane motion than was observed in either the frontal or lateral tests. Figure 5-29 compares the in- and out-of-plane components of head and neck angle and head displacement. In the case of the head, the out-of-plane rotation is 30-40 percent of the change in in-plane rotation and the out-of-plane displacement is less than one-third of the in-plane displacement. The out-of-plane peaks occur subsequent to peak excursion in the impact plane.

5.3.2 Oblique Kinetic Response

Figure 5-30 shows both the laboratory and head anatomical components of force and moment at the condylar point for oblique test LX4307. The laboratory force y component, perpendicular to the impact plane remains small relative to the remaining force components as do the laboratory moment x and y components in the impact plane. The remaining three laboratory load components are used to characterize the significant load response even though the neglected variables are more significant than was the case for lateral impact (compare Figures 5-19 and 5-30).

Laboratory moment component T_{Oy} is plotted versus head angle in Figure 5-31. As in the lateral case, anatomical components of force are characterized in lieu of laboratory components. The head z-component of force F_{Oz} is plotted in Figure 5-32 versus neck angle. In Figure 5-33, the vector sum of the head x and y components of force F_{xy} is plotted versus neck angle.

Condylar moment about the head z-axis is also included as part of the load characterization. Figure 5-34 is a plot of head z-axis moment T_{Oz} versus change in head twist angle, $\Delta\psi_c$. The peak moment is comparable in magnitude to that for lateral response as seen by comparing Figures 5-23 and 5-34. The twist response $\Delta\psi$ is less for oblique impact resulting in a greater slope for the moment-angle plot.

As in the cases of frontal and lateral impact, the kinetic variables exhibit more dependence on impact level and show more subject-to-subject variation than do the kinematic variables.
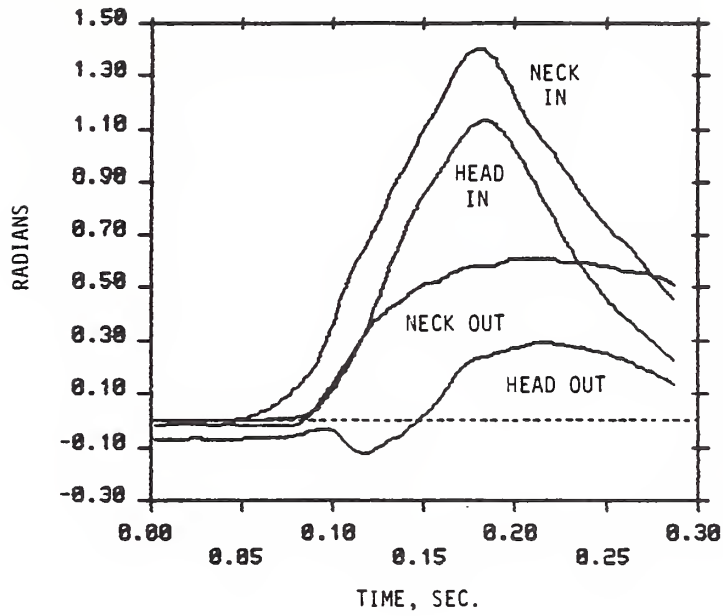
a) Angular Response
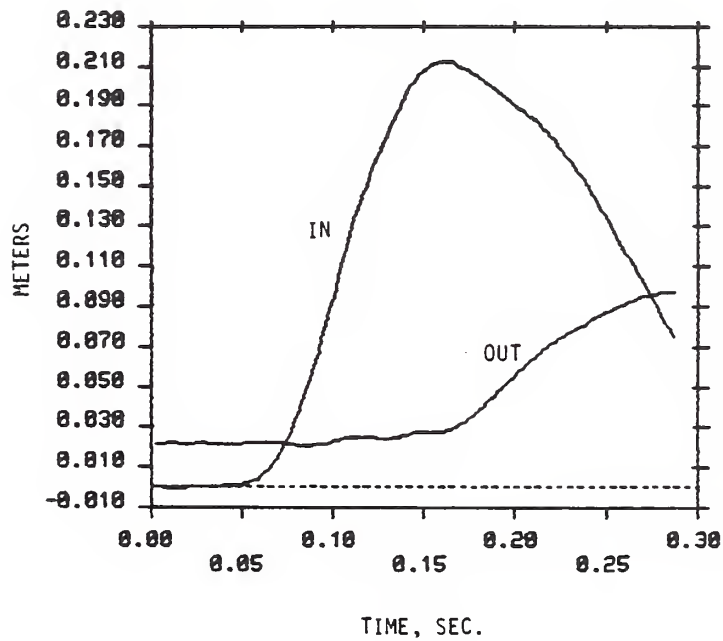
b) Linear Displacement of Head Anatomical Origin

FIGURE 5-29. COMPARISON OF IN- AND OUT-OF-IMPACT PLANE MOTIONS FOR OBLIQUE TEST LX4307 (SUBJECT H00134, 11-G IMPACT)
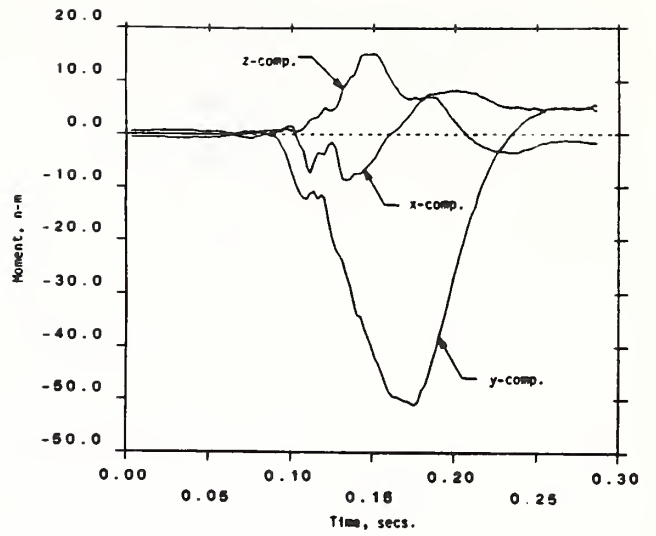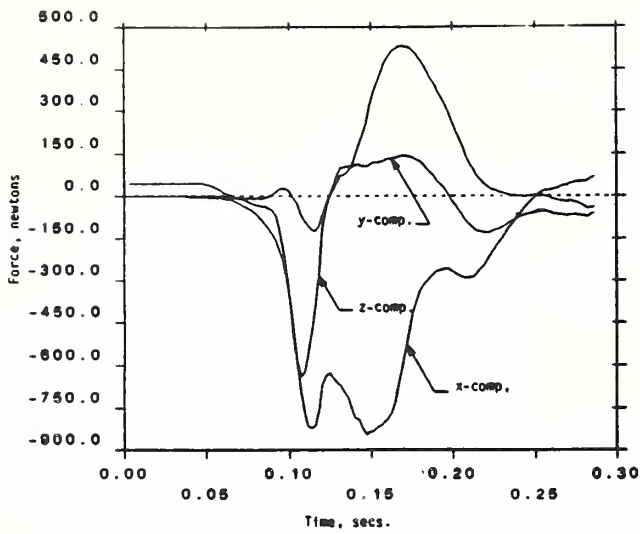
a) Laboratory Components
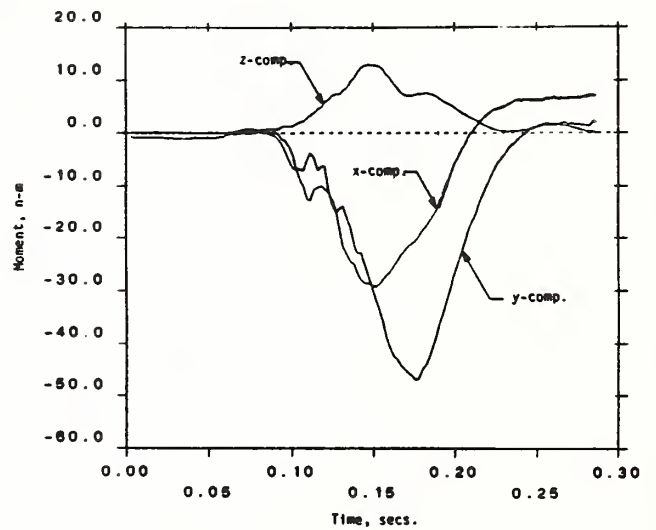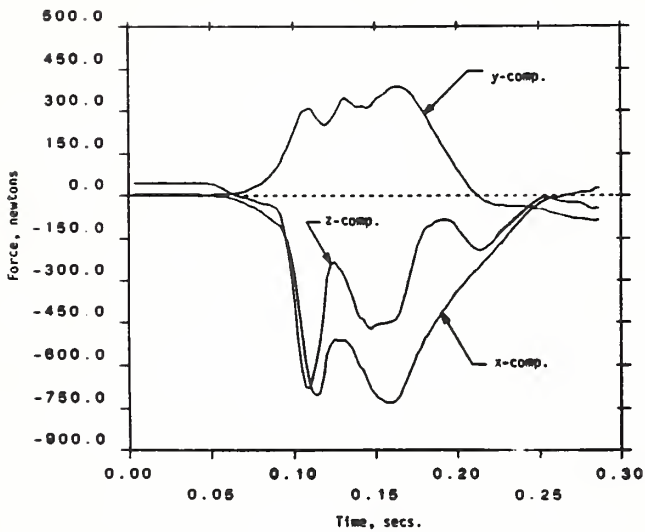
b) Anatomical Components

FIGURE 5-30. HEAD ANATOMICAL AND LABORATORY COMPONENTS OF LOAD AT
THE OCCIPITAL CONDYLAR POINT FOR OBLIQUE TEST LX4307
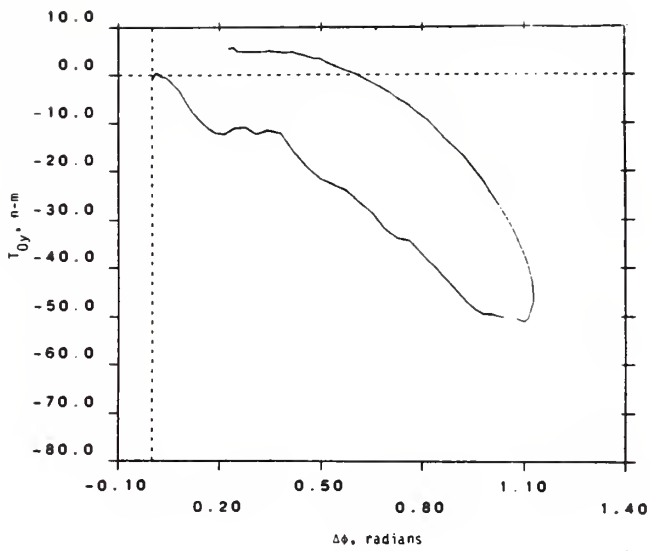
a) Subject H00134, 11-g Impact
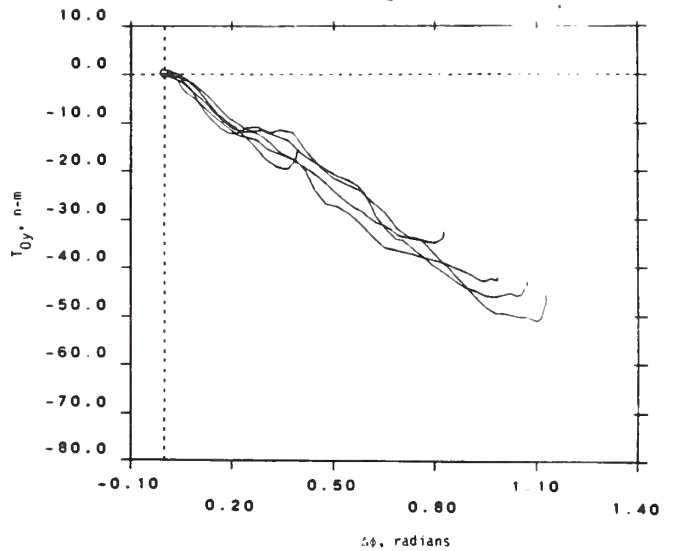
b) Subject H00134, Five Tests (4-10g Impacts)
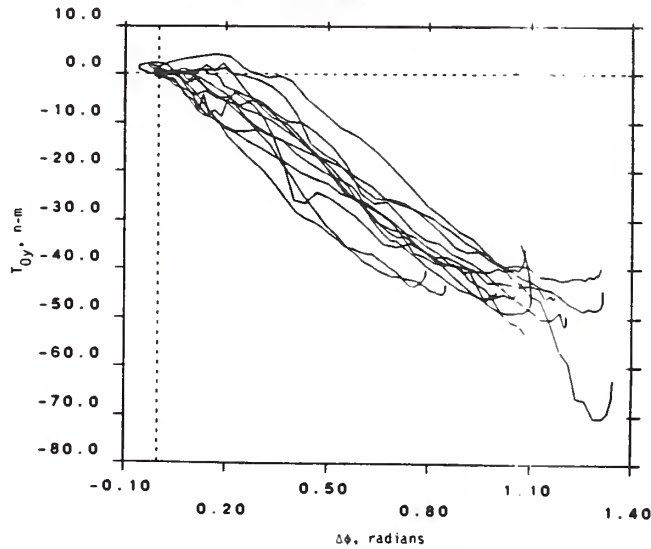
c) Twelve Subjects, 10-g Impact

FIGURE 5-31. MOMENT PERPENDICULAR TO THE IMPACT
PLANE AT THE OCCIPITAL CONDYLAR POINT VERSUS
CHANGE IN HEAD ROTATION, $\Delta\phi$, FOR OBLIQUE IMPACT
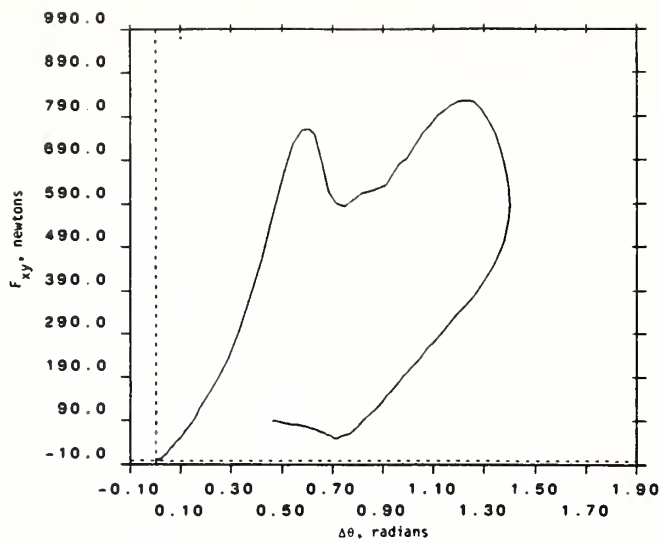
a) Subject H00134, 11-g Impact
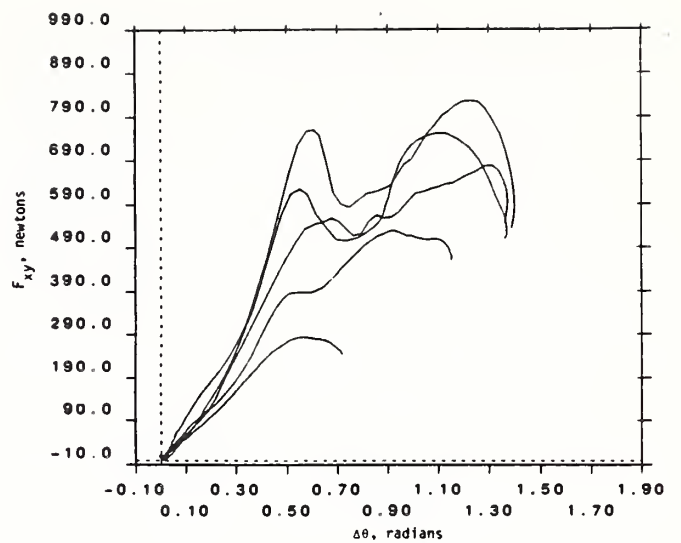
b) Subject H00134, Five Tests
(4-10g Impacts)
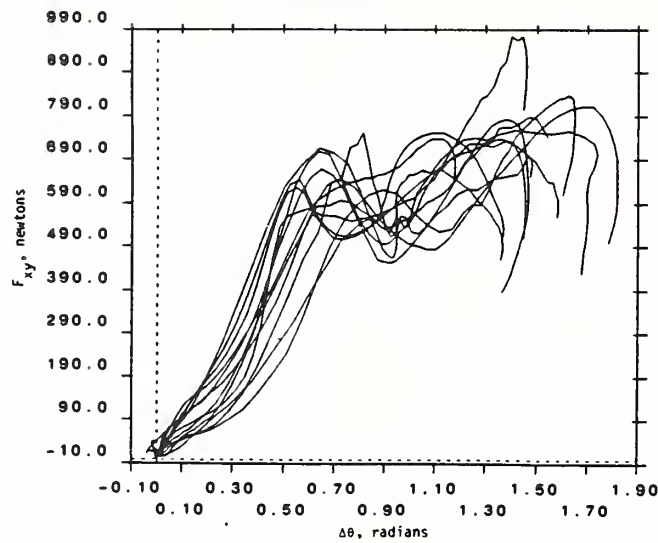
c) Twelve Subjects, 10-g Impact

FIGURE 5-32. RESULTANT FORCE AT THE OCCIPITAL
CONDYLAR POINT PARALLEL TO THE HEAD X-Y PLANE
VERSUS CHANGE IN NECK ANGLE, Δθ, FOR OBLIQUE
IMPACT
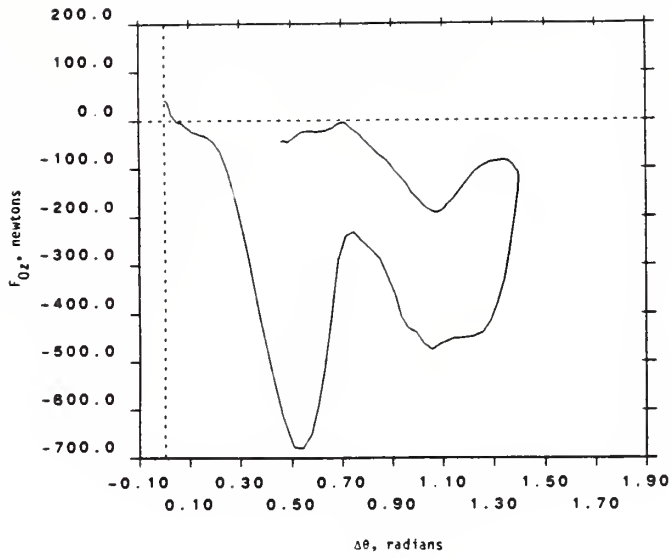
a) Subject H00134, 11-g Impact
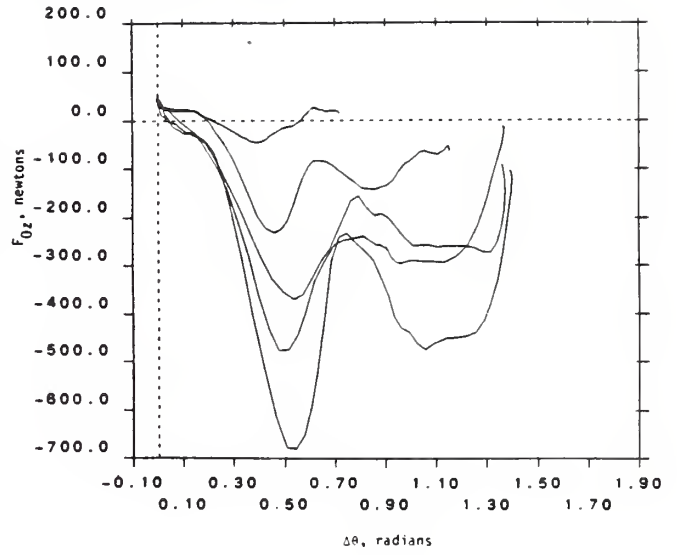
b) Subject H00134, Five Tests
(4-10g Impacts)
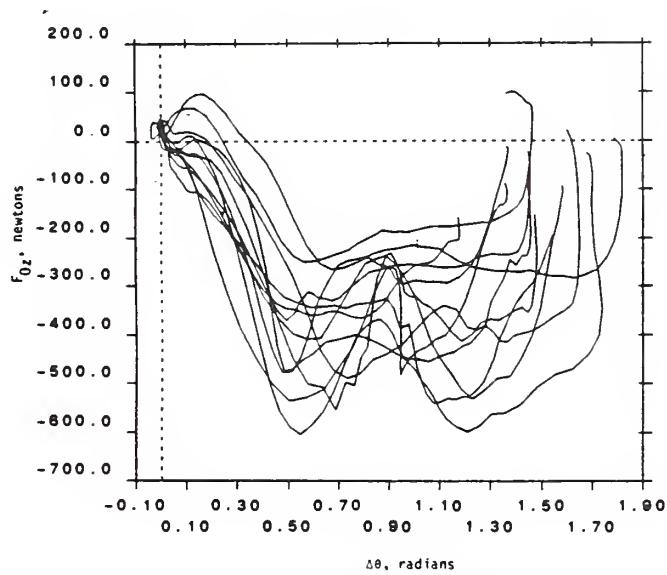
c) Twelve Subjects, 10-g Impact

FIGURE 5-33. FORCE AT THE OCCIPITAL CONDYLAR POINT
ALONG THE HEAD Z-AXIS VERSUS CHANGE IN NECK
ANGLE, $\Delta\theta$, FOR OBLIQUE IMPACT
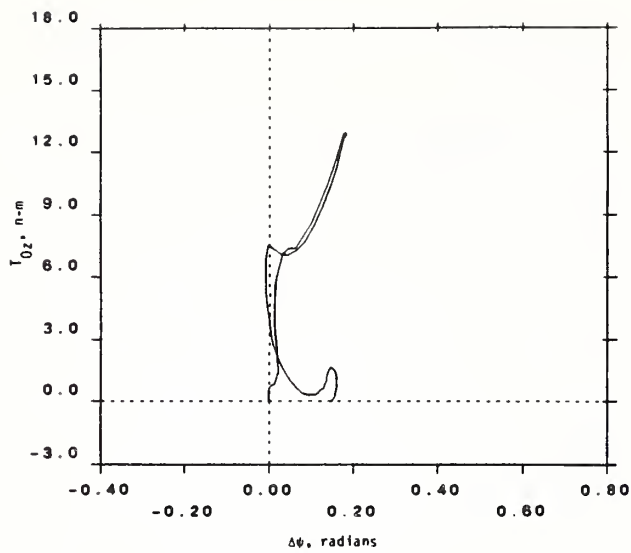
a) Subject H00134, 11-g Impact
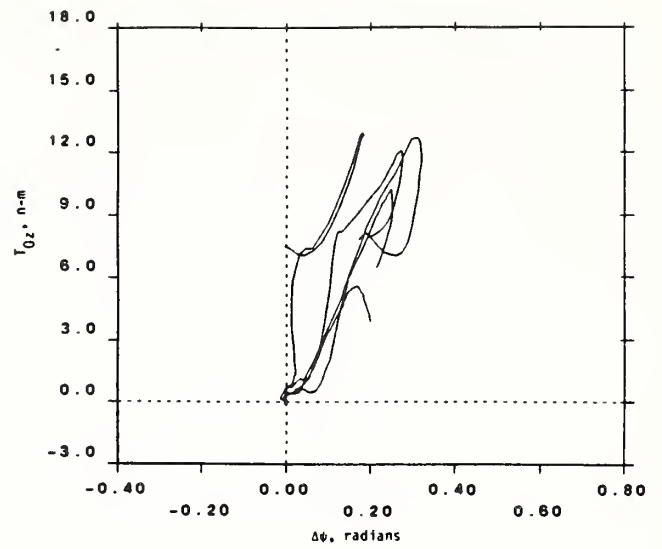
b) Subject H00134, Five Tests
   (4-10g Impacts)
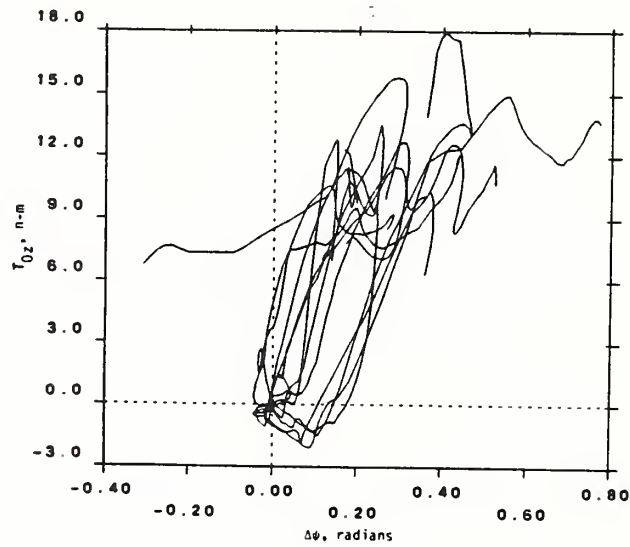
c) Twelve Subjects, 10-g Impact

FIGURE 5-34.   MOMENT ABOUT THE HEAD Z-AXIS APPLIED AT
                THE OCCIPITAL CONDYLAR POINT VERSUS CHANGE IN
                HEAD TWIST, $\Delta\psi$, FOR OBLIQUE IMPACT

5.4   CORRELATION OF HEAD RESPONSE WITH IMPACT CHARACTERISTICS

The performance requirements developed in this study are intended to serve as a standard, based on average human response, for measuring the fidelity of the kinematic and kinetic response of the head of an ATD. To achieve a high degree of fidelity, the output magnitude(s) should be related to the input magnitude at every instant. There are two questions to be resolved with regard to the input which best accomplishes this objective:

1. At what location should the input be prescribed?
2. What variable(s) should be used to characterize the input?

For a pendulum test of the detached head/neck system, the input must be prescribed for the base of the neck. For a sled test in which the ATD is seated, the input could be prescribed for either the sled or the base of the neck. As will be shown below, the restraint system may affect head response and should, therefore, be controlled. Indirect control of the restraint system affects can be accomplished by stipulating that the restraint system type and sled motion in an ATD test match that of the volunteer tests from which the performance requirements are formulated. More positive control is achieved by stipulating that the T1 motion of an ATD match that of the volunteers thereby eliminating restraint effects. The latter option is followed in formulating performance requirements in this study.

The most significant motion of the T1 vertebral point is translation in the direction of sled deceleration. Figure 5-35 shows (change in) the three laboratory components of linear displacement of T1 for tests of subject H00134 in each of the three impact directions. The forward motion of T1 is between 5 and 8 centimeters for each of these tests before belt and/or shoulder restraint stops further motion. Vertical displacements (z) are approximately one quarter of forward displacement and out-of-impact plane displacements (y) are even less, as indicated in the plots. Figure 5-36 shows that there is no Euler angle rotation of T1 which exceeds 0.35 radians.*

---

* Since the equations used in this study (Section 4.1) calculate head and neck chord line rotations relative to the torso, it is not necessary that T1 rotations be small. This makes possible analysis of the lap and three-point restraint data from Wayne State University where torso motions are large.
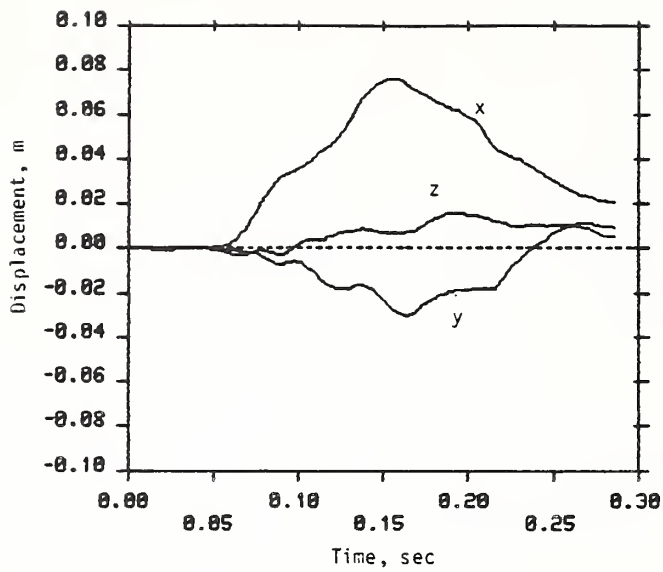
a) Frontal Test LX 3983
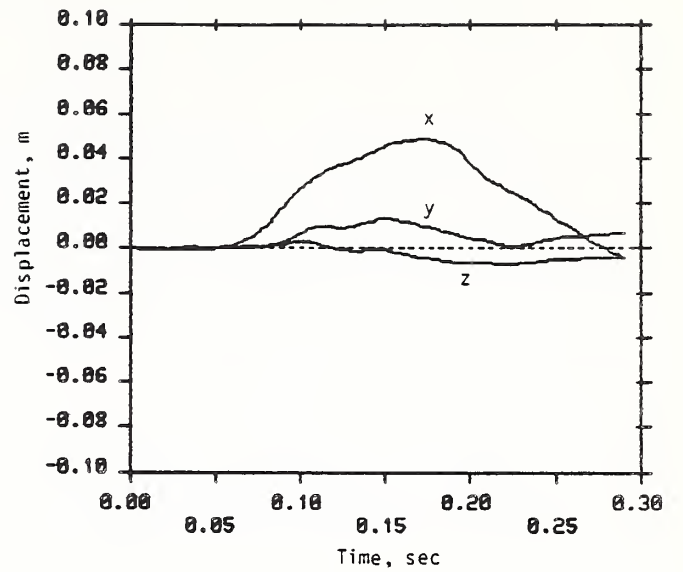
b) Oblique Test LX 4126
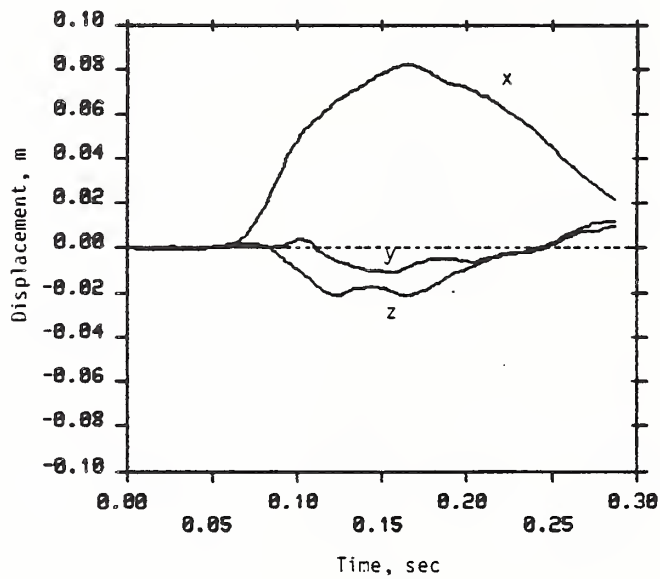
c) Lateral Test LX 4307

FIGURE 5-35. LABORATORY COMPONENTS OF DISPLACEMENT OF THE T1
ANATOMICAL ORIGIN FOR THREE TESTS OF SUBJECT H00134

a) Frontal Test LX <u>3983</u>
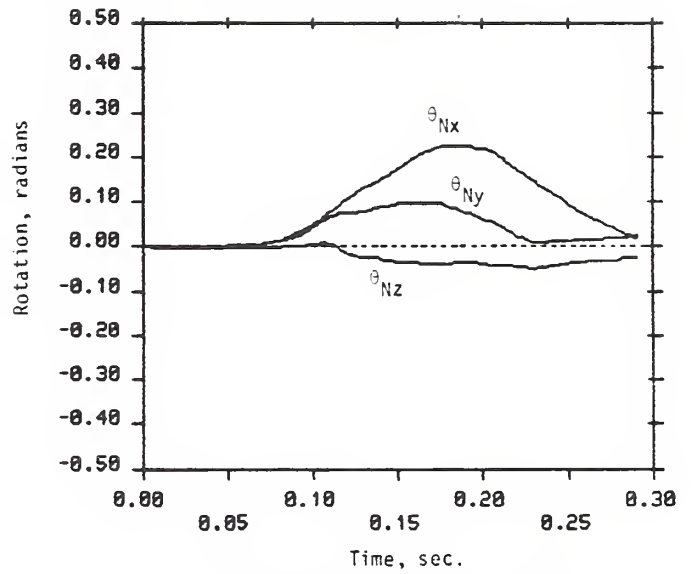
b) Obilque Test LX <u>4307</u>
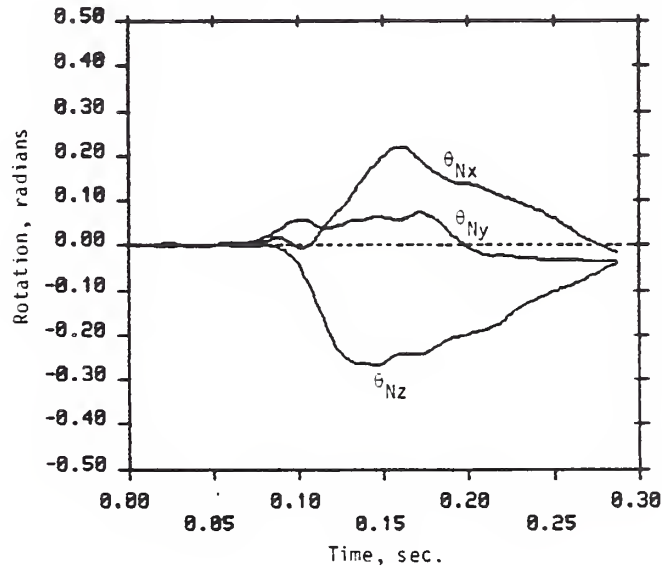
c) Lateral Test LX <u>4126</u>

FIGURE 5-36. EULER ANGLE ROTATIONS OF THE T1
VERTEBRAL BODY FOR THREE TESTS OF
SUBJECT H00134

Likewise, linear components of velocity and acceleration of T1 in the direction of sled deceleration predominate. Thus, prescription of the time history of a T1 kinematic variable in that direction assures that the significant aspects of volunteer input are duplicated.

The prescribed input for the volunteer tests was acceleration of the sled. In Figure 5-37 the acceleration of the sled and T1 are compared for tests in each of the three impact orientations. For the frontal and oblique tests, the T1 acceleration has a peak that is nearly twice the sled peak followed by a series of smaller peaks, none of which are present in the sled acceleration. The initial peak is less predominant in the lateral test but does exist. These may be high frequency spikes transmitted through the neck to the head. In Figure 5-38, head acceleration along the X-axis of the head anatomical coordinate system is compared to T1 acceleration in the sled impact direction for test LX3958. Note they have a similar frequency content. The variation between the sled and T1 acceleration profiles can be attributed to the nonrigid restraint system interacting with the nonrigid torso. Or it may be the result of feedback of head/neck response. Or it may be the result of nonrigid sensor mounting or local skin resonance at the head and T1 mounting locations. The actual source is unknown.* Comparing Figures 5-35 and 5-38 indicates that the spikes occur over the time period that T1 is in motion relative to the seat, thereby making any of the above possible explanations for their occurrence. If they are related to gross head response, they should be input to an ATD intended to have load fidelity, since peak accelerations correspond to peak loads which are typically used in injury analysis. If they are the result of nonrigid sensor mounting or local skin resonance, they should not be produced by an ATD.

---

*T1 and the head are separately instrumented with accelerometers so the spikes are not likely to be accelerometer noise or ringing.
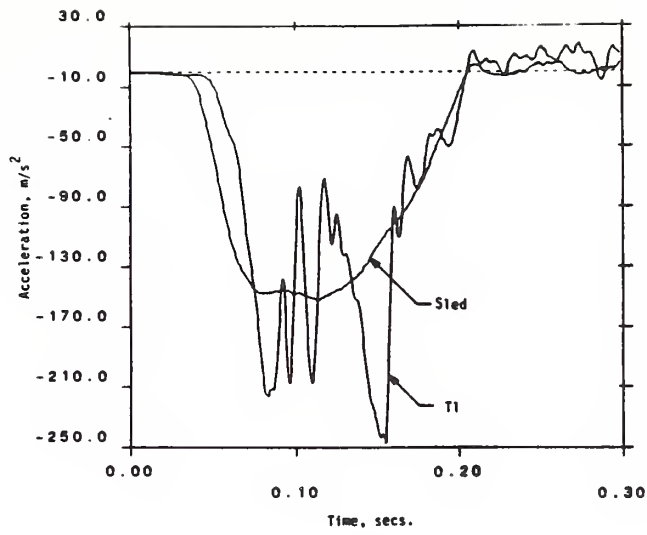
a) Frontal Test LX3983
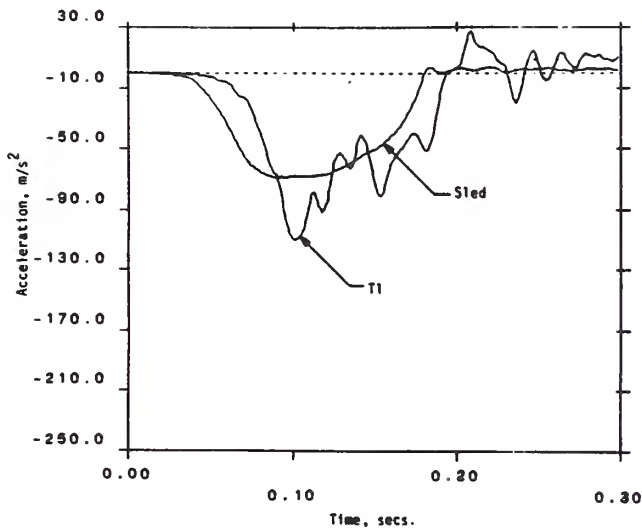
b) Lateral Test LX4126
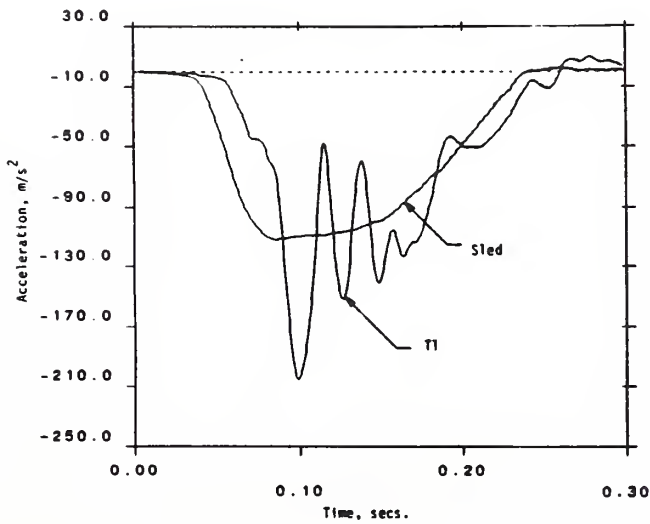
c) Oblique Test LX4307

FIGURE 5-37. COMPARISON OF SLED AND T1 ACCELERATIONS IN THE IMPACT DIRECTION FOR THREE TESTS OF SUBJECT H00134
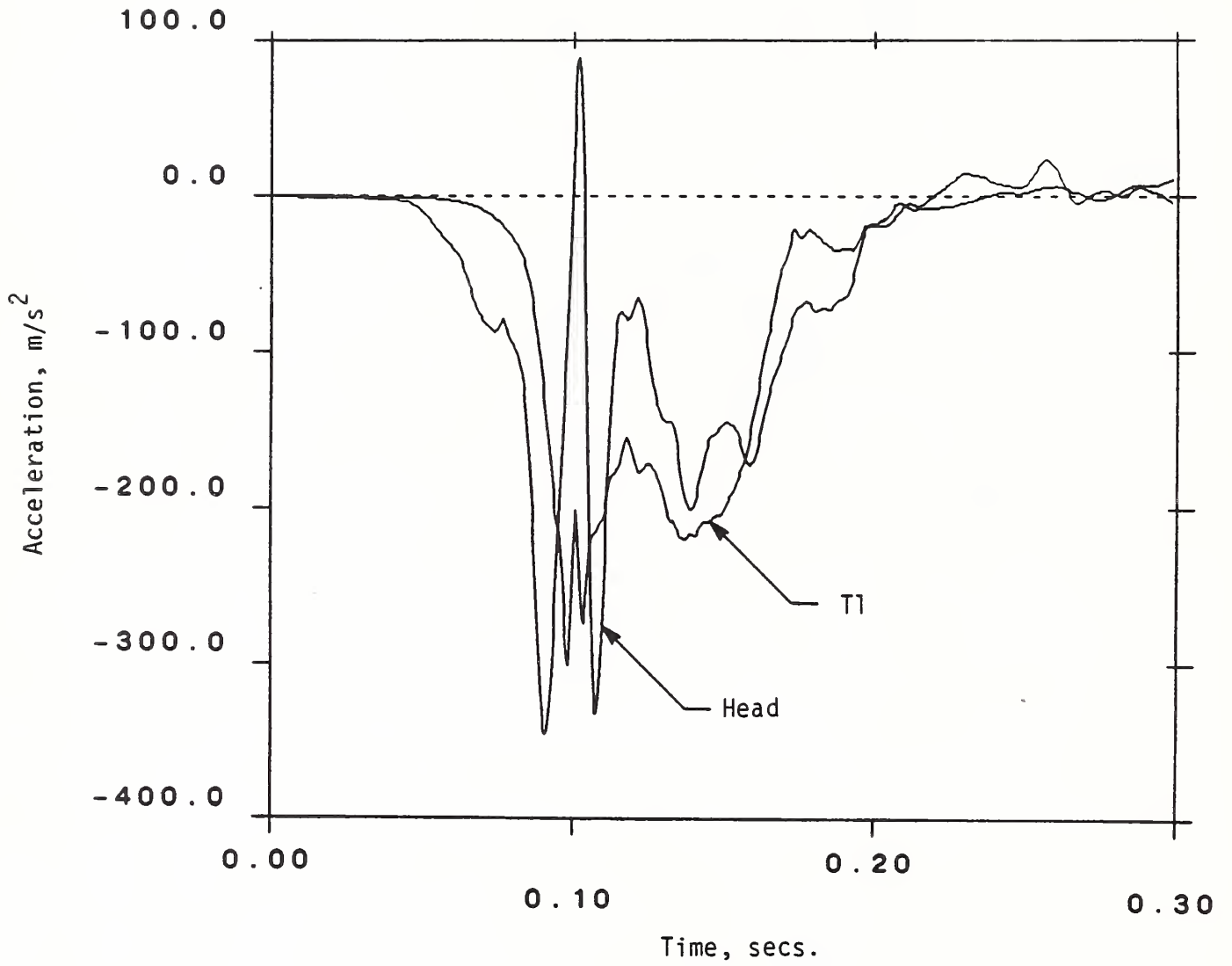
FIGURE 5-38. COMPARISON OF LINEAR ACCELERATION OF T1 AND THE HEAD
ANATOMICAL ORIGINS FOR A 15-G TEST OF SUBJECT H00118

T1 acceleration in the impact direction exhibits significant variation from subject to subject in the volunteer tests, apparently the result of differences in torso or head/neck system response. The variation is in both amplitude and phase, as illustrated for two subjects in Figure 5-39a. With this degree of variation response of the head/neck system in a volunteer will, likewise, show considerable variation. Thus, a performance requirement formulated from the NBDL volunteer data that attempts to relate average head acceleration to average T1 acceleration on an instantaneous basis (average for all volunteers at one test condition) will have the load peaks smoothed and possess a rather broad statistical deviation about the mean. A dummy which matches such a requirement will not necessarily be accurate at peak load prediction (during unobstructed head motion) but will possess basic kinetic fidelity.*

Average T1 acceleration could be calculated for the volunteer tests and defined as the standard input for ATD tests. A more convenient input is average T1 velocity. The acceleration spikes are sufficiently smoothed by integration to make variation in velocity between volunteers relatively small as indicated by the T1 velocity plots of Figure 5-39b. Figure 5-40 shows the velocity of T1 for frontal tests at four discrete sled impact levels. The numbers of the tests included at each impact level is indicated. The sled impact acceleration that produced each of these profiles is recorded in parentheses next to the designated T1 impact level. Similar velocity profiles exist for lateral and oblique tests, as indicated in Figures 5-41 and 5-42, respectively.

The test procedure described above produces acceleration, and, hence, load fidelity, albeit only average load fidelity. A less demanding type of fidelity is duplication of volunteer head position as a function of time. To assure position fidelity in an ATD, average head position, computed from the volunteer tests, must be related to an average T1 input variable. Velocity can also be used for this input.

---

*It would be preferrable to formulate the performance requirement from a set of volunteer tests in which the T1 acceleration profile was controlled to reduce the variation in condyle response.
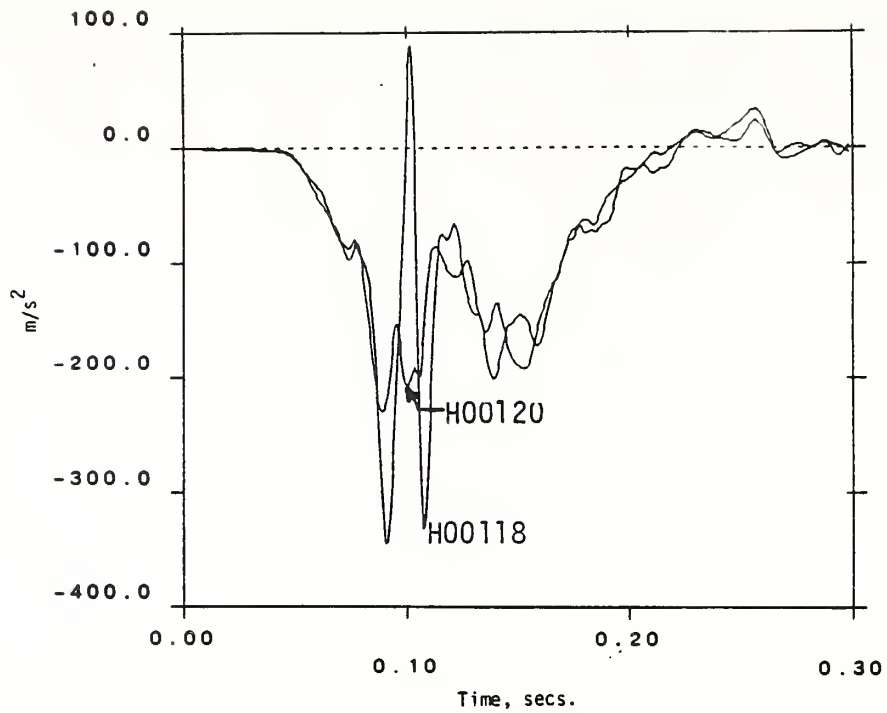
a) Acceleration
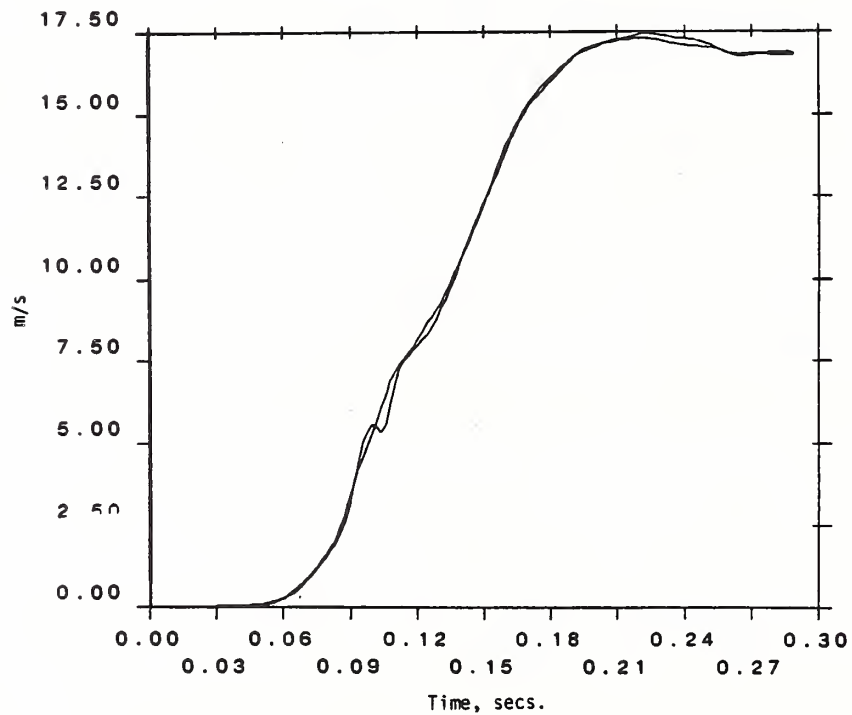
b) Velocity

FIGURE 5-39. COMPARISON OF ACCELERATION AND VELOCITY OF T1 FOR TWO FRONTAL TESTS CONDUCTED AT A SLED IMPACT LEVEL OF 15 G's
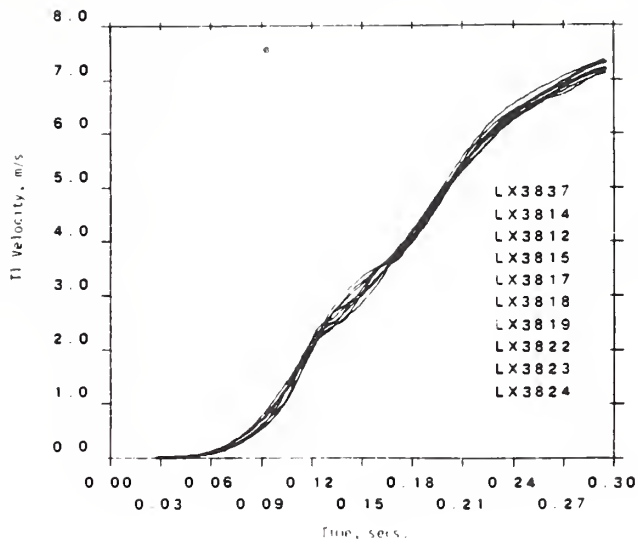
a) Level F1 (4-g Sled, Impact)
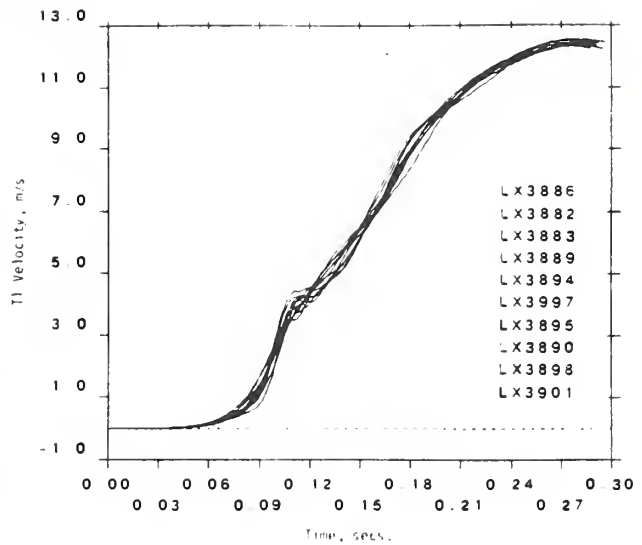
b) Level F2 (8-g Sled Impact)
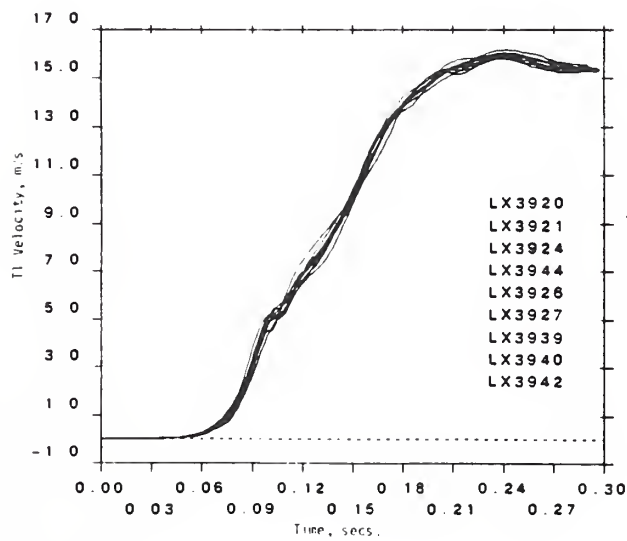
c) Level F3 (12-g Sled Impact)
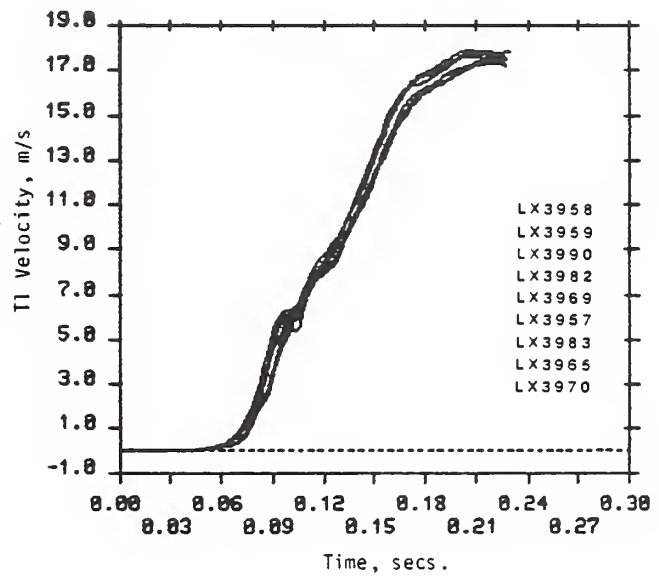
d) Level F4 (15-g Sled Impact)

FIGURE 5-40. T1 VELOCITY CORRIDORS FOR FOUR DISCRETE LEVELS OF FRONTAL SLED IMPACT
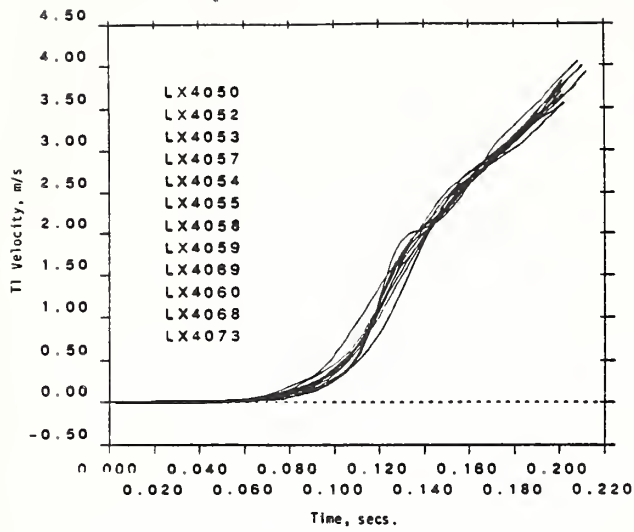
a) Level L1 (3-g Sled Impact)
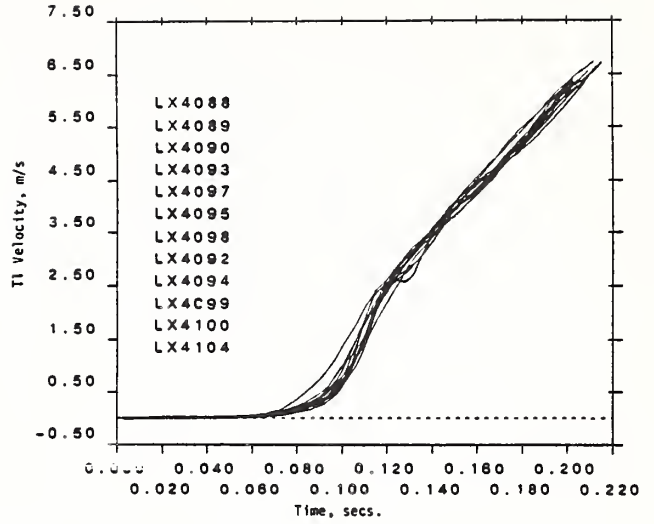
b) Level L2 (5-g Sled Impact)
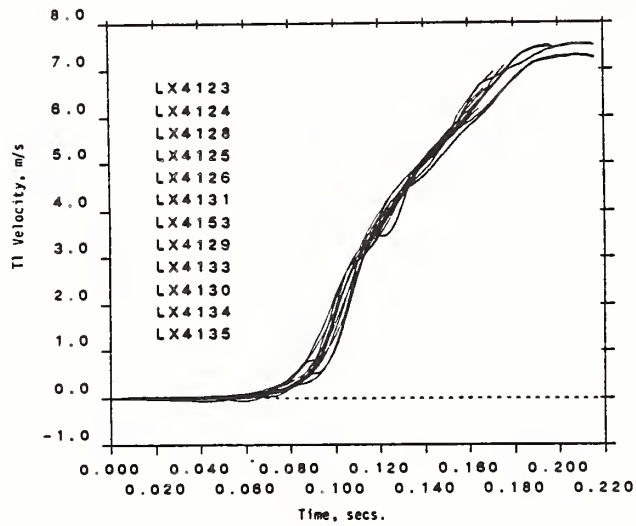
c) Level L3 (7-g Sled Impact)

FIGURE 5-41. T1 VELOCITY CORRIDORS FOR THREE DISCRETE LEVELS OF LATERAL SLED IMPACT
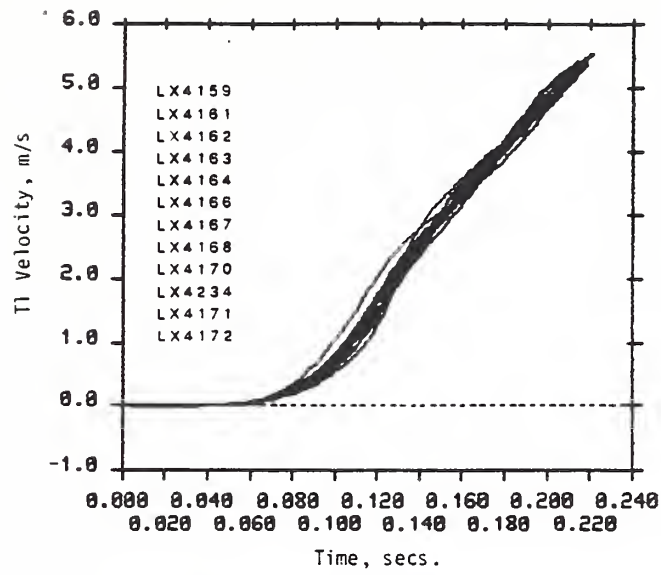
a) Level 01 (4-g Sled Impact)
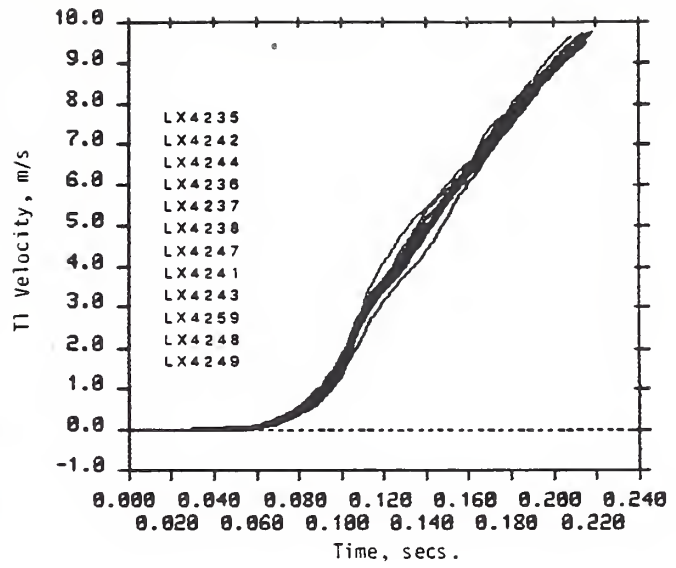
b) Level 02 (7-g Sled Impact)
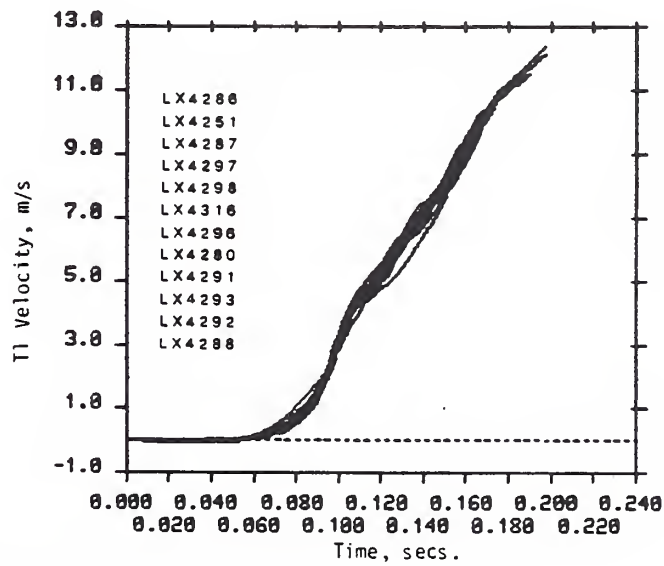
c) Level 03 (10-g Sled Impact)

FIGURE 5-42. T1 VELOCITY CORRIDORS FOR THREE DISCRETE LEVELS OF OBLIQUE SLED IMPACT

5-57

The relationship between T1 velocity and head angle during the loading phase is shown in Figure 5-43 for frontal tests. Relatively narrow response corridors are created by the nine subjects, as indicated in Figures 5-43c. The response to different impact levels do not overlay, as indicated in Figure 5-43b. For lateral and oblique impact, similar relationships exist between T1 velocity and head angle, as indicated by Figures 5-44 and 5-45.

5.5 PERFORMANCE REQUIREMENTS

The degree of fidelity designed into an ATD should be dependent upon the intended use. It is possible to specify three levels of fidelity for the head/neck system during the loading phase using volunteer test data:

1. Position fidelity - head displacement relative to the torso is sufficiently humanlike so that secondary head contact can be adequately predicted.

2. Velocity fidelity - momentum is sufficiently humanlike so that secondary head impact injury can be adequately predicted [24].

3. Load fidelity - peak loads are sufficiently humanlike to permit neck injury prediction during unobstructed head motion.

Complexity of design and costs to manufacture and maintain an ATD would increase with each level of fidelity. Performance requirements are described in this study for position and velocity fidelity.

The type of performance requirements proposed in this study require that the magnitude of the response variables be within a specified range at any instant of time following initiation of a prescribed rapid acceleration of T1. This is more stringent than a requirement which only specifies peak excursions in response to a
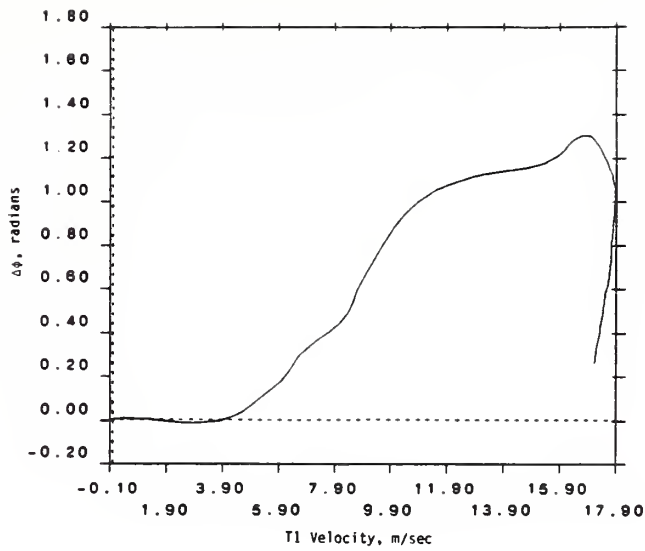
a) Subject H00134, 15-g Impact
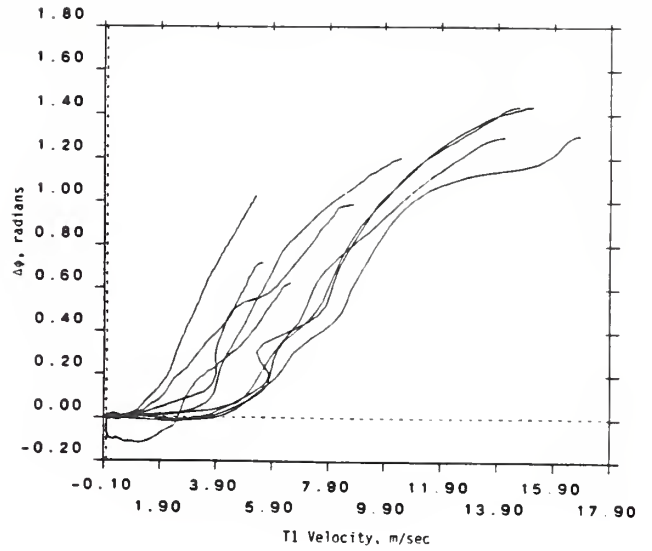
b) Subject H00134, Nine Tests (3-15g Impacts)
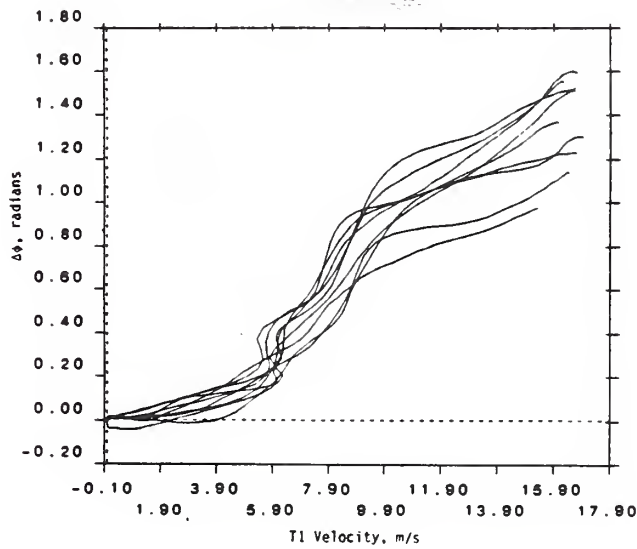
c) Nine Subjects, 15-g Impact

FIGURE 5-43. T1 VELOCITY VERSUS CHANGE IN HEAD ANGLE, $\Delta\phi$, FOR FRONTAL IMPACT
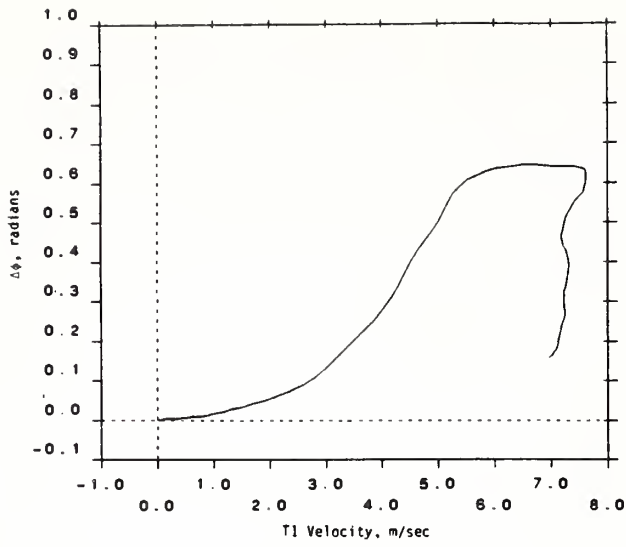
a) Subject H00134, 7-g Impact
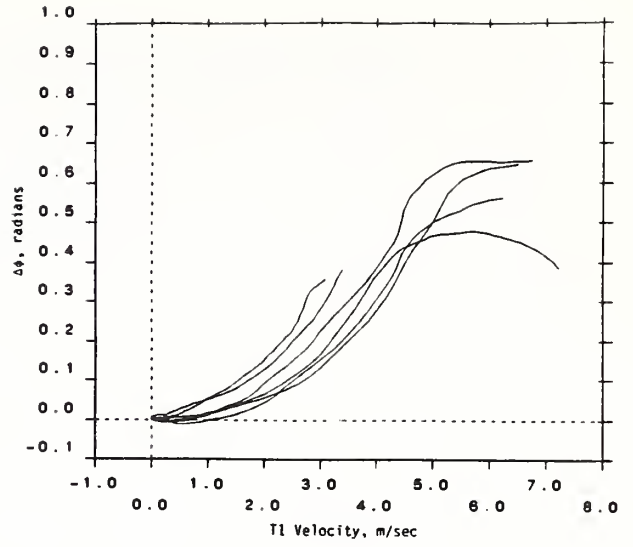
b) Subject H00134, Six Tests
(3-7g Impacts)
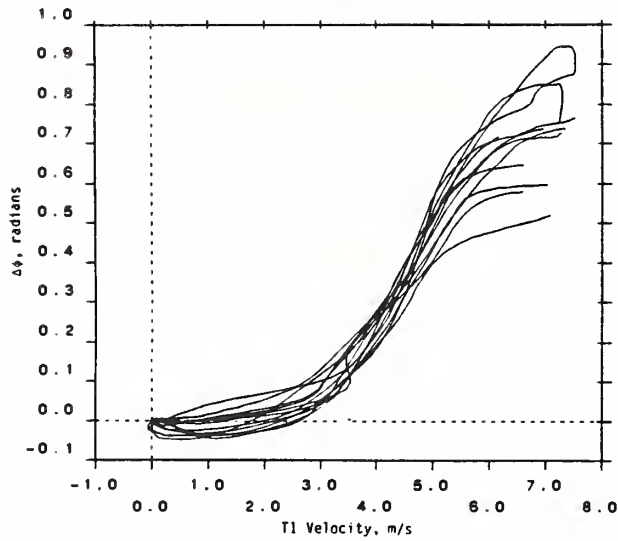
c) Twelve Subjects, 7-g Impact

FIGURE 5-44. T1 VELOCITY VERSUS CHANGE IN HEAD ANGLE, $\Delta\phi$, FOR LATERAL IMPACT
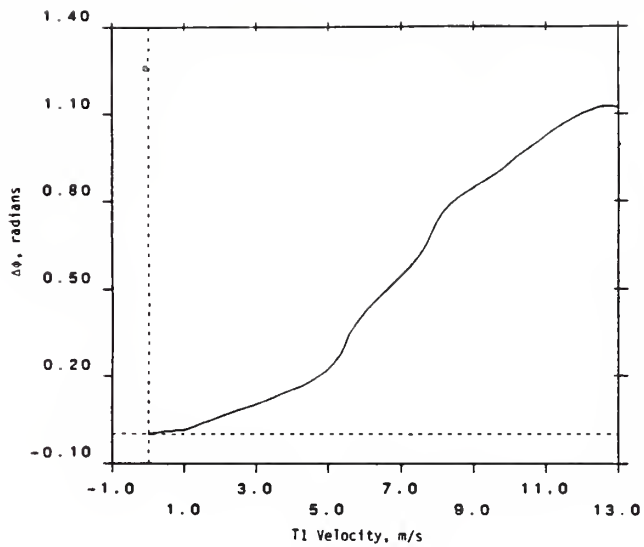
a) Subject H00134, 11-g Impact
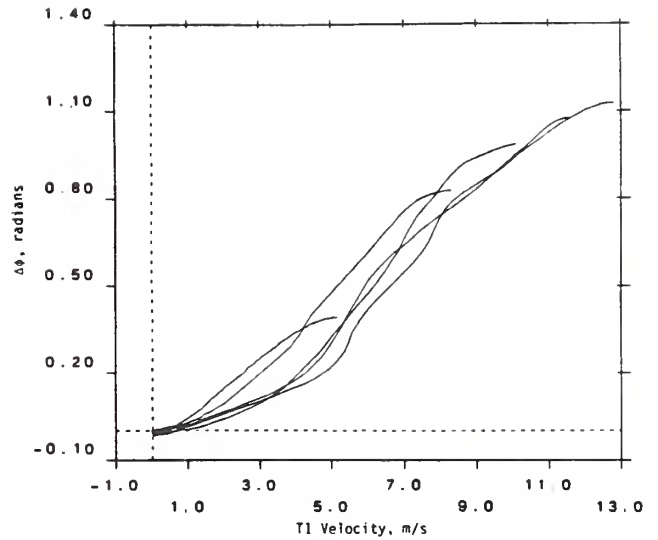
b) Subject H00134, Five Tests
(4-10g Impacts)
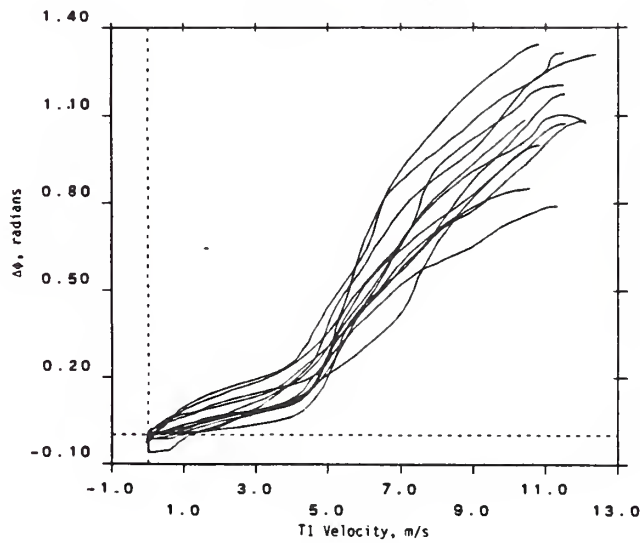
c) Twelve Subjects, 10-g Impact

FIGURE 5-45. T1 VELOCITY VERSUS CHANGE IN HEAD ANGLE, $\Delta\phi$, FOR OBLIQUE IMPACT

specified input or peak excursions at a specified time. It is also more stringent than one which expresses the continuous relationship between response variables but only relates them to peak input levels. Both of these less stringent forms are contained in the "instantaneous" requirement developed in this study.

In formulating a performance requirement, it is generally desirable to use the results of multiple tests of multiple subjects in order to eliminate random measurement error and in order to obtain "average" subject data. Response corridors are created by the family of curves when one test variable is plotted versus another for multiple tests.* One approach in attempting to prescribe the instantaneous relationship in an ATD test between input and output variables is to require that all input and output data fall within the corridors created from the volunteer test data. The logic of imposing such a requirement is that if the time history of the impact variable(s) is nearly repeatable for many test subjects and the response variables are nearly repeatable for those same subjects, (i.e., response corridors are narrow) then any input waveform within the bounds of all subjects should produce response within the bounds of all observed response.

Three comments should be made regarding usefulness of this type of performance requirement. First, since there are an infinite number of untested input profiles that fall within the bounds of the finite set tested, there is no assurance that the output corridors are fully formed. Practically, performance corridors formulated from a finite set of volunteer tests can be expected to assure fidelity of response if the compliance test input profile is controlled to have a shape (frequency content) similar to that of the volunteer tests.

Second, a performance corridor does not adequately limit the range of the variables from which it is constructed. This is particularly evident when the corridor is parallel to one of the variable axes. In this case, the corridor places constraint only on the variable whose value is constant.

---

*Mathematically, the response corridor is defined as the locus of all points in the two-variable space between the lowest and highest measured values of the first variable when the second is held fixed at any measured value, provided that each of these points is also between the lowest and highest measured values of the second variable.

The third comment to be made with regard to imposition of a corridor based performance requirement is that it attempts to guarantee an ATD response that is within the bounds of observed subject variation. It may be desirable to have more or less fidelity than this. That is a program decision based on considerations such as intended use of the ATD, cost of development and maintenance and the state-of-the art limitations.

The performance requirement formulated in this study consists only of mean volunteer response, thereby allowing the designer the freedom to choose the degree of fidelity. Statistical variation from the mean for each variable is provided as an indication of the degree of consistency observed between volunteers and, as such, identifies any points in the response where an ATD might be expected to exhibit the largest deviation from the mean.

5.5.1   Position Fidelity

The proposed performance requirement for verifying position fidelity of an ATD consists of one input variable, T1 velocity in the direction of the impact, which is given as a function of time, and four response variables, head angle, $\Delta\phi$, neck chord line angle, $\Delta\theta$, head twist angle, $\Delta\psi$, and neck chord length, r_n. Figures 5-46, 5-47, and 5-48 each contain a set of plots which constitute the position performance requirement for frontal, lateral and oblique impacts, respectively. In the case of frontal impact, there are only three response variables since head twist is negligible.

Four T1 velocity curves (solid lines) appear in Figures 5-46a and b corresponding to four different frontal impact levels, F1 to F4, for which responses are characterized. For lateral or oblique testing, response is characterized for three impact levels as indicated in Figures 5-47a and b and 5-48a and b, respectively. The solid lines of the remaining plots of Figures 5-46 to 5-48 provide head and neck response. A single mean line adequately displays a response variable for any impact level and sled orientation.
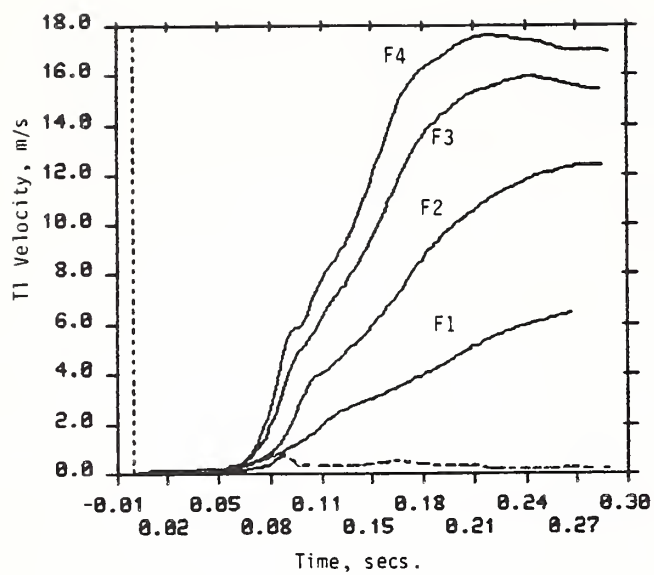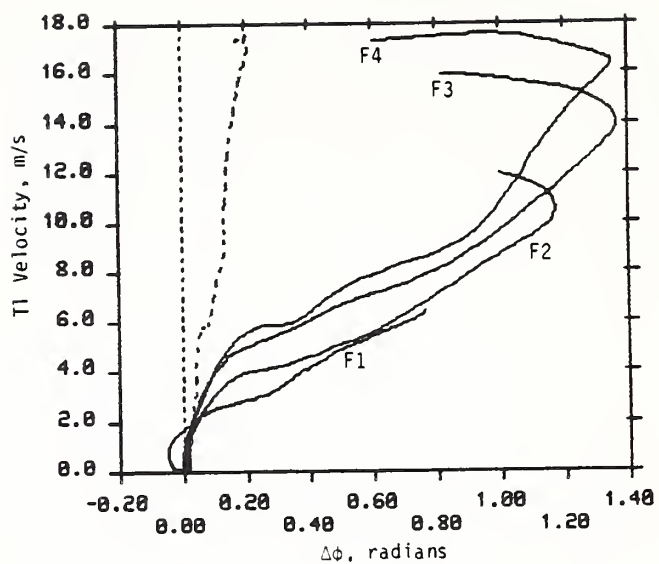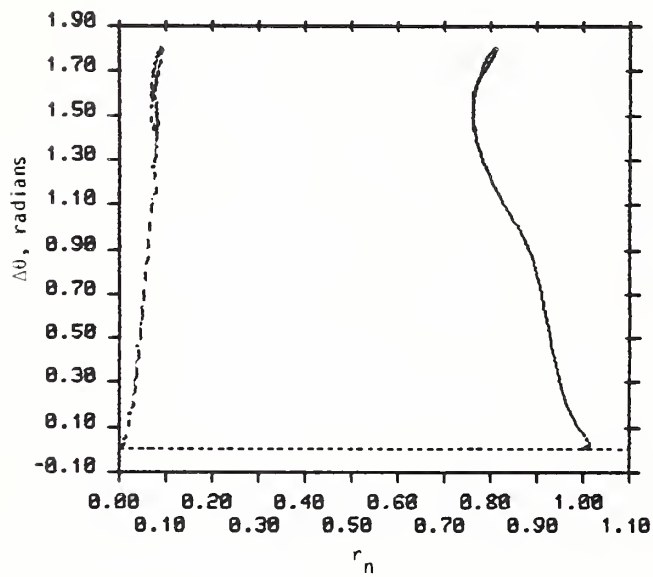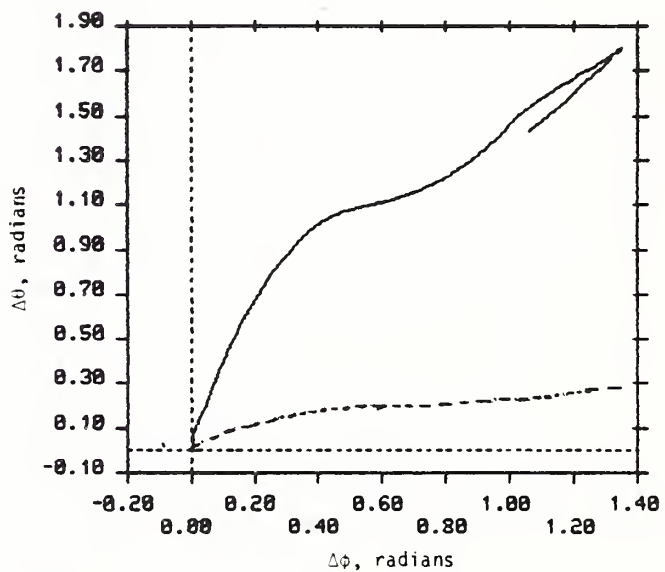
FIGURE 5-46. PERFORMANCE REQUIREMENT FOR POSITION FIDELITY IN
FRONTAL IMPACT RESPONSE
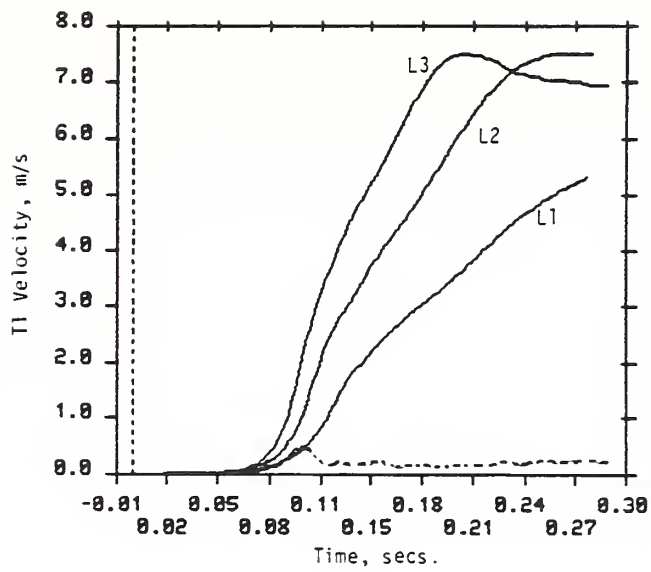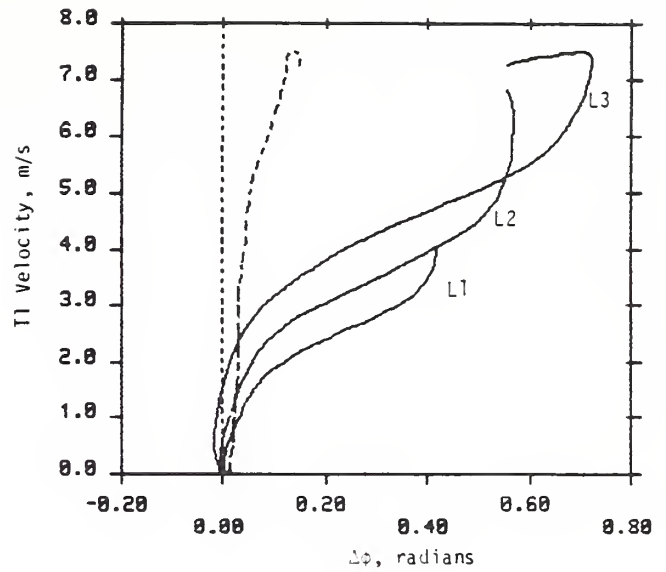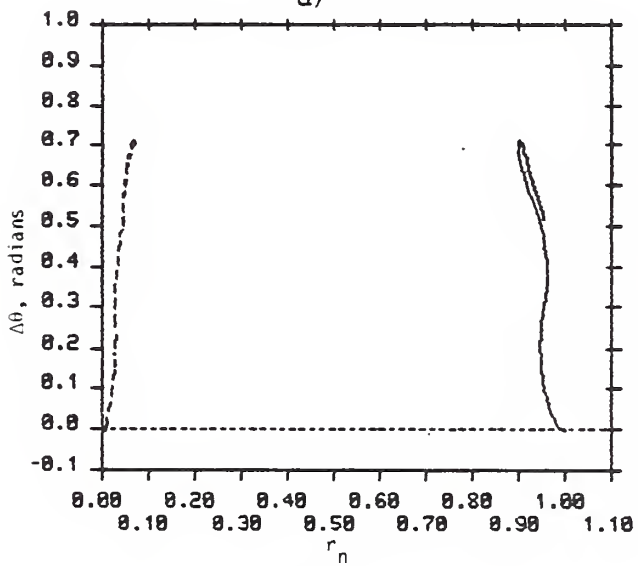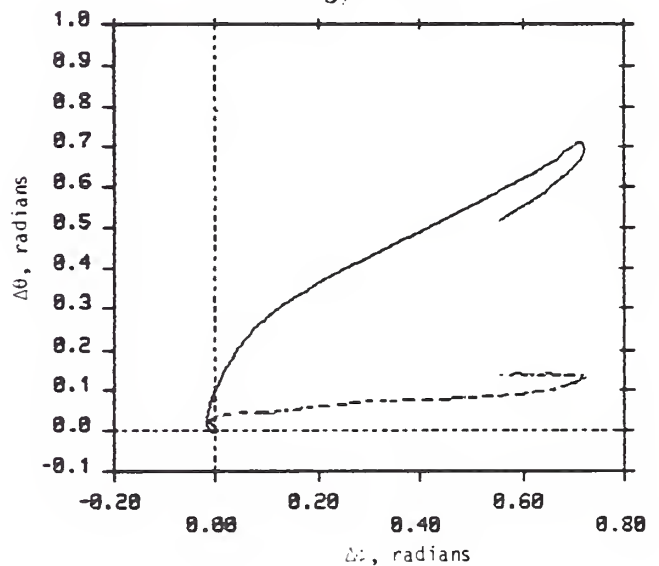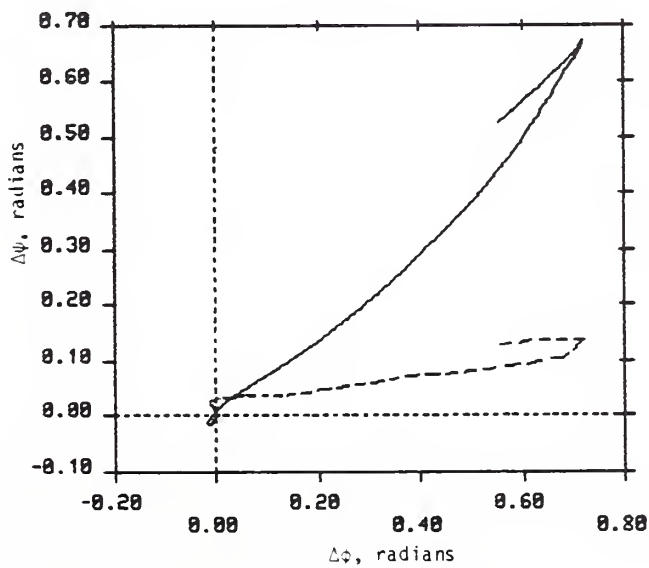
FIGURE 5-47. PERFORMANCE REQUIREMENT FOR POSITION FIDELITY IN
LATERAL IMPACT RESPONSE
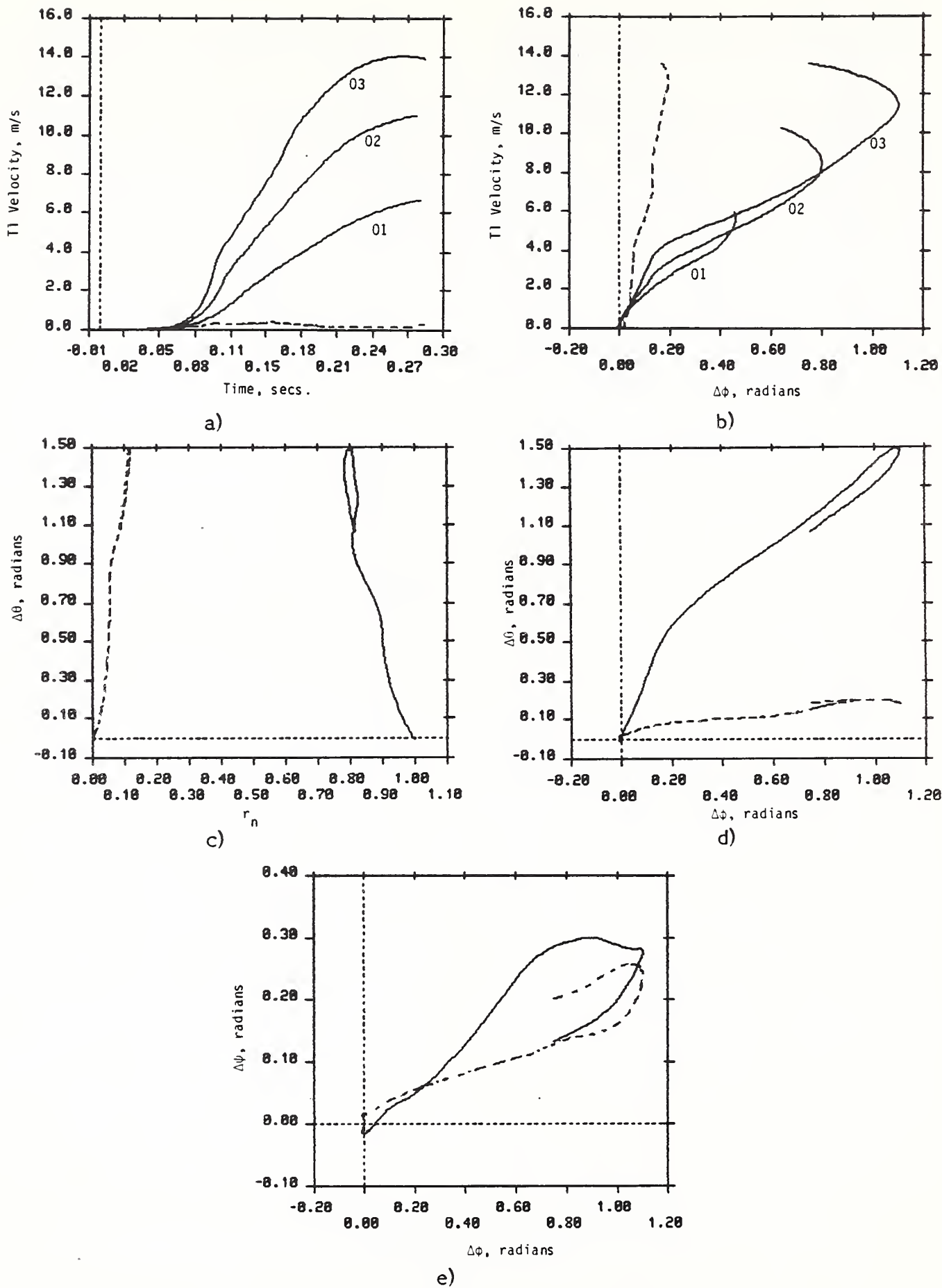
FIGURE 5-48. PERFORMANCE REQUIREMENT FOR POSITION FIDELITY IN
OBLIQUE IMPACT RESPONSE

The mean response curves were generated from all subjects exposed to the highest impact level test for that sled orientation*. Figures 5-40d, 5-41c and 5-42c list the tests used for mean response data for frontal, lateral and oblique tests, respectively. The mean T1 velocity curves were obtained from the tests of all subjects exposed to the respective impact levels also as indicated in Figures 5-40, 5-41 and 5-42. The dotted lines are the standard deviations of the variables as indicated. The standard deviation plotted for T1 velocity is for the largest impact level. They provide a measure of the consistency of the response relationships between subjects.

To obtain a set of instantaneous response values from Figure 5-46, velocity at the selected time is read from plot a for a particular impact level. Change in head angle, $\Delta\phi$, can then be read from plot b, followed by neck chord line angle, $\Delta\theta$, from plot d, followed by normalized neck length from plot c. Figures 5-47 and 5-48 are read in a similar manner, with head twist angle as the last to be read. In an ATD compliance test, each of the response variables would be recorded on a continuous basis and compared with these plots.

For an ATD designed to have omni-directional capability all of the constraints of Figures 5-46, 5-47, and 5-48 must be satisfied. If all of these constraints are satisfied it will probably have omni-directional capability. When only unidirectional fidelity is required of an ATD, the constraints for the other two directions can be ignored.

Imposition of these requirements assures fidelity in an ATD for what has been judged to be significant motion observed in the volunteers. Should a higher degree of fidelity be required for some application, it may be necessary to include motions that have been judged insignificant in this study. The requirements as stated here remain valid and any additional requirements would supplement these.

---

*In Appendix D, mean response to lower impact levels is compared to that presented here in order to justify the use of single mean line representation of response variables.

5.5.2 Load Based Fidelity

Anatomical components of condylar load are calculated using equations (24) and (26). These equations map six acceleration variables (a_{Ax}, a_{Ay}, a_{Az}, α_x, α_y, and α_z) and three angular velocity variables (w_x, w_y, and w_z) into six anatomical load variables (F_{Ox}, F_{Oy}, F_{Oz}, T_{Ox}, T_{Oy} and T_{Oz}). The significant load variables, identified in Sections 5.1.2, 5.2.2 and 5.3.2, are two head anatomical force components, F_{Oz} and the vector sum of components F_{Ox} and F_{Oy}, moment about an axis perpendicular to the impact plane and, in the case of lateral and oblique motion, moment about the head anatomical z-axis T_{Oz}. Moment perpendicular to the impact plane T_{Oy} is derived from the anatomical components T_{Ox}, T_{Oy}, and T_{Oz} via transformation equation (2).

It is possible to express a constraining relationship between each of the significant variables and T1 input in a manner similar to that for which position fidelity is expressed. However, all of the acceleration and velocity variables are derived from the head mounted linear accelerometers. As noted in Section 5.4, there is a large statistical variation in acceleration levels at the head anatomical origin for the volunteers tested. This results in a large variation in the load response of the head. This is illustrated for the frontal tests by Figures 5-9c, 5-10c, and 5-11c, which show subject to subject variation in the magnitude of the condyle load components that at some points exceed the average load levels. Performance corridors developed from such plots would be quite broad compared to those of the position constraints.

Figures 5-49, 5-50, and 5-51 each contain a set of plots which constitute the mean load performance requirements for frontal, lateral and oblique impact, respectively. For example, in Figure 5-49 the curves labelled F4 in plots a, b and c are the mean of the plots of Figures 5-9c, 5-10c, and 5-11c, respectively. Mean loads are plotted versus head or neck angles, which are, in turn, related to the T1 velocity on an instantaneous basis through the position fidelity plots defined in the previous section.
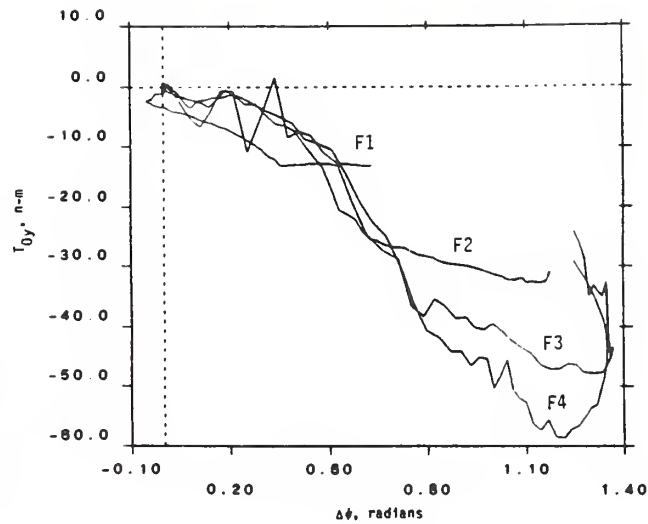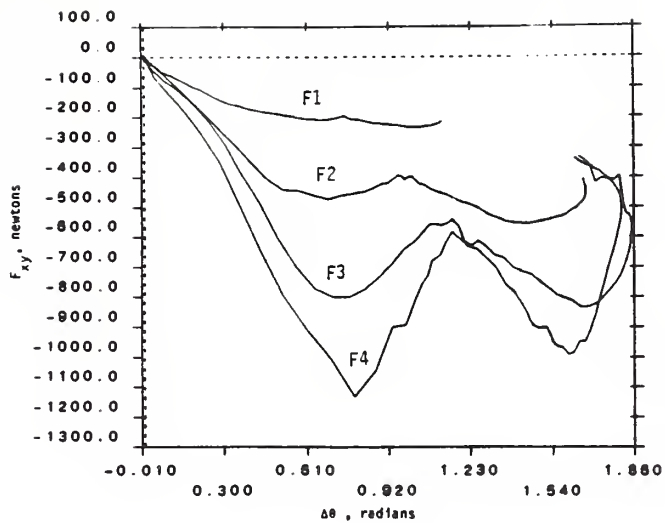
a) Resultant Force F_{xy} in the Head x-y Plane

b) Moment T_{Oy} Perpendicular to the Impact Plane
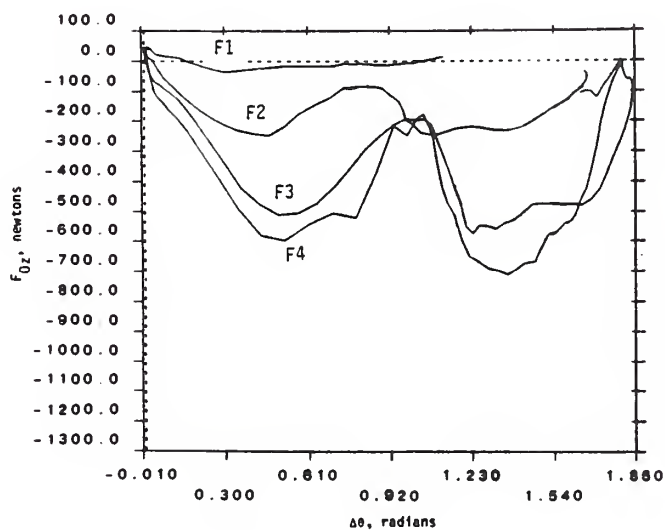
c) Force F_{Oz} Parallel to the Head z-Axis

FIGURE 5-49. PERFORMANCE REQUIREMENT FOR LOAD FIDELITY AT THE OCCIPITAL CONDYLAR POINT IN RESPONSE TO FRONTAL IMPACT
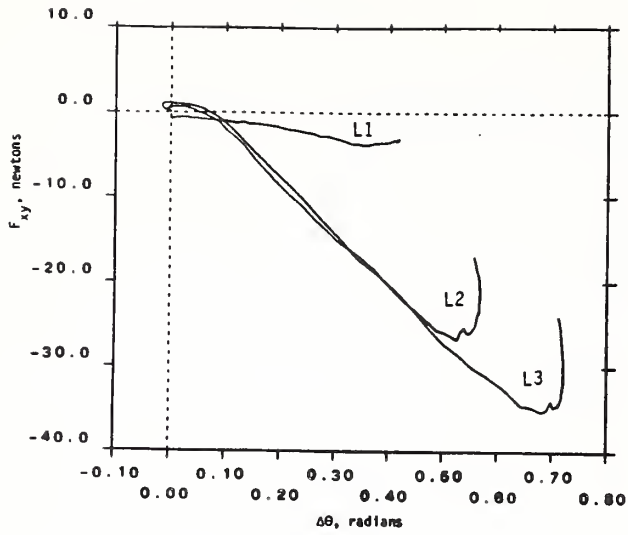
a) Resultant Force F_{xy} in the Head x-y Plane
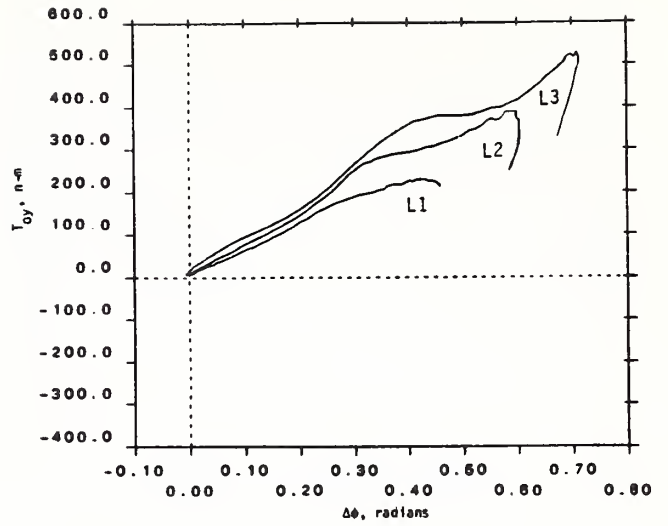
b) Moment T_{Oy} Perpendicular to the Impact Plane
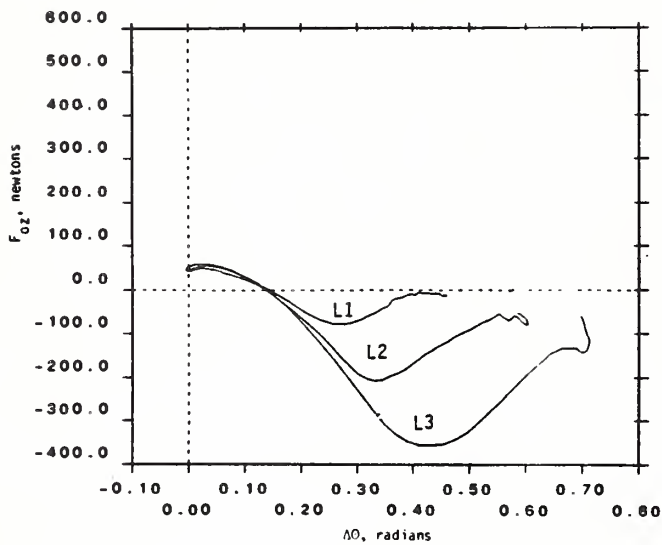
c) Resultant Force F_{Oz} Parallel to the Head z-Axis
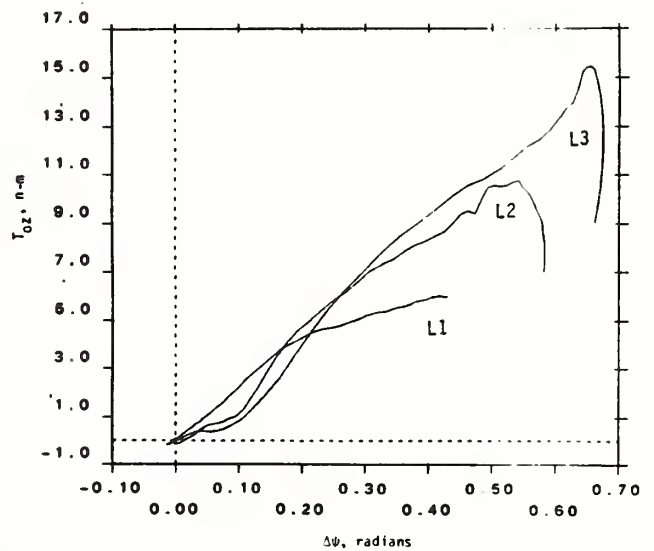
d) Moment T_{Oz} Parallel to the Head z-Axis

FIGURE 5-50. PERFORMANCE REQUIREMENT FOR LOAD FIDELITY AT THE OCCIPITAL CONDYLAR POINT IN RESPONSE TO LATERAL IMPACT
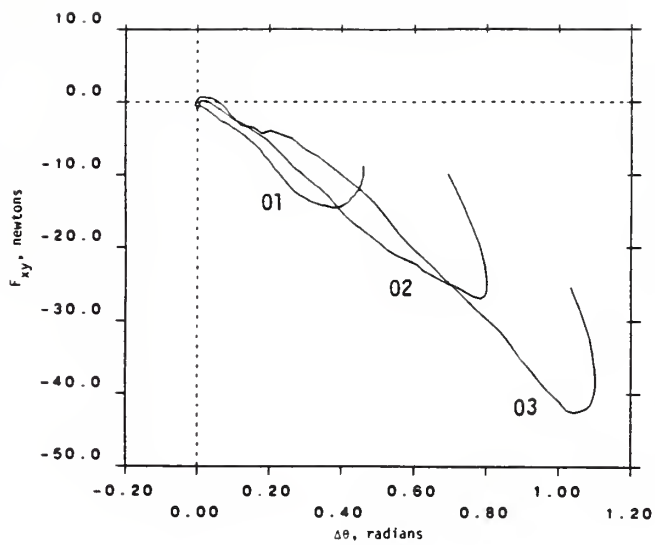
a) Resultant Force F_{xy} in the Head x-y Plane
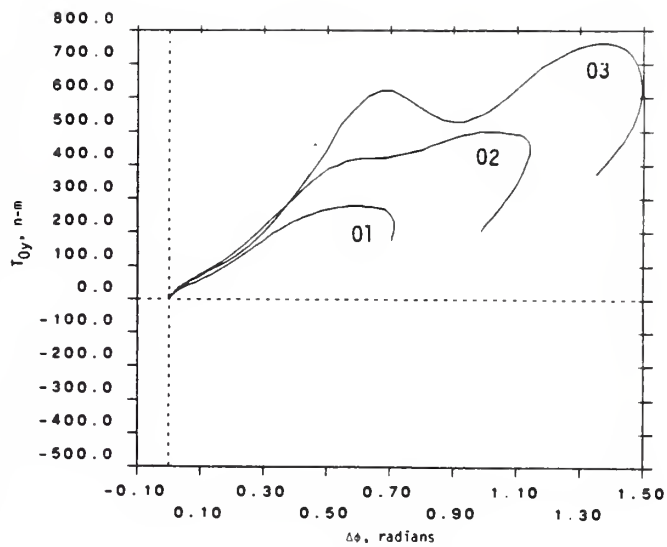
b) Moment T_{Oy} Perpendicular to the Impact Plane
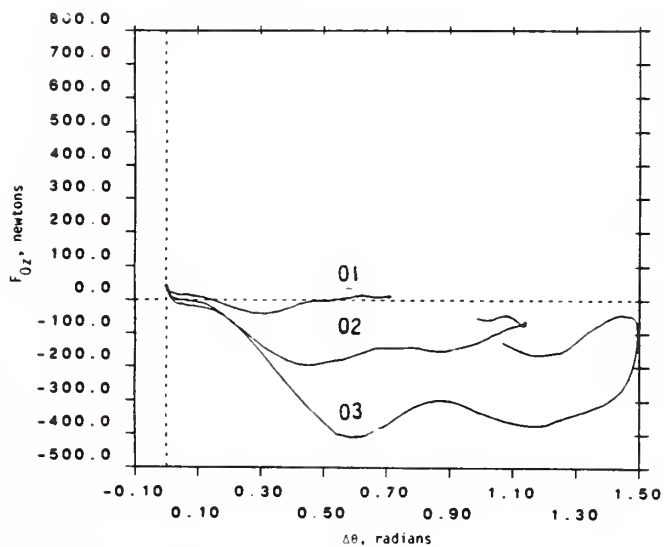
c) Resultant Force F_{Oz} Parallel to the Head z-Axis
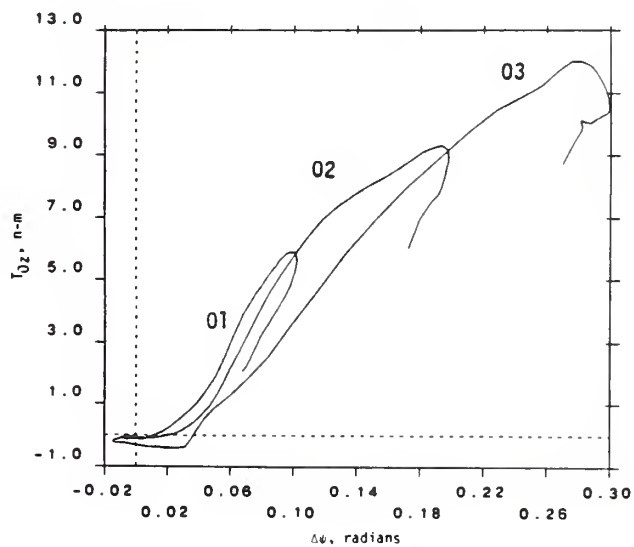
d) Moment T_{Oz} Parallel to the Head z-Axis

FIGURE 5-51. PERFORMANCE REQUIREMENT FOR LOAD FIDELITY AT THE OCCIPITAL CONDYLAR POINT IN RESPONSE TO OBLIQUE IMPACT

Imposition of this performance requirement must be interpreted in light of the uncertainty with regard to the peak accelerations measured in the volunteer tests. If the peaks are the result of nonrigid sensor mounting or local skin resonance and not desired in the ATD response, this performance requirement assures instantaneous fidelity including reasonable peak load response of an ATD during unobstructed head motion. Since the load equations can be inverted to establish the significant accelerations from loads, the ATD would also exhibit both position and velocity (momentum) fidelity. It would not be necessary to separately impose the performance requirement for position fidelity. Conversely, if the acceleration peaks are integral to gross head response, the load based performance requirement as formulated does not evaluate peak loading capability of an ATD. It only assures average load fidelity along with velocity and position fidelity at any instant. Since, in this study, the source of the acceleration peaks was not established, the load (injury) predicting capability of an ATD cannot be evaluated. The load based performance requirement does assure an ATD with position (contact predicting) and velocity (momentum) fidelity. Further analysis is required before load fidelity can be assured.

5.6 SENSITIVITY OF THE PERFORMANCE REQUIREMENTS TO VARIATION IN TEST CONDITIONS

Some of the factors on which head and neck motion may be functionally dependent are: 1) deceleration level, 2) initial position of the head, 3) variation in human physiques, 4) deceleration pulse shapes, 5) type of restraint, and 6) state of muscle contraction.

The first three factors have been discussed above with regard to the NBDL volunteers. Larger deceleration levels result in larger excursions. This variation is incorporated into the proposed performance requirement. Variation in human physiques causes some variation in response and is thought to be the principal contributor to corridor width. This variation, however, is small enough so that the corridors provide a good indication of average human response to an impact. Initial angular position of the head, varies by up to 1/4 radian, for this set of NBDL volunteers, who were all part of a "neck up, chin up" set of tests as denoted by the NBDL [20]. This level of variation in initial head orientation has no significant effect on the shape of the performing corridors. The last three factors of the list,

which have not been discussed previously in this report, are discussed in the remainder of this section.

Deceleration Pulse Shape - The effect of the deceleration pulse shape can be illustrated with two tests of subject H00083, tests LX2124 and LX2302. Test LX2124 is referred to by the NBDL as a high rate of onset, short duration (HOSD) test. Test LX2302 is referred to by the NBDL as a low rate of onset, long duration (LOLD) test. The test characteristics for these tests are shown in Table 5-2. The shorter duration of the peak acceleration for LX2124 results in less sled velocity change and hence less T1 velocity change as illustrated in Figure 5-52a and b, even though the peak acceleration is somewhat greater than for LX2302. The resulting head and neck angles are attenuated somewhat, as illustrated in Figure 5-52c and the relationship between head and neck response is altered somewhat. This data suggests that matching the velocity profile at T1 is extremely important when performing a compliance test to check conformity of an ATD with the (proposed) performance requirement.

Type of Restraint - When the subject is less restrained in the seat, he exhibits initial head and neck extension that is not present in the NBDL tests with four-point restraint. Figure 5-53 shows the head versus neck response of the three tests of WSU volunteer 0252 who was lap belt restrained. Note both angles initially decrease in contrast with typical NBDL response in which there is only an initial pause in head angle while the neck chord lines moves in flexion. In the final portion of the loading phase of WSU volunteer response both the head and neck angles are increasing in the positive direction (flexion). At peak head excursion, the neck angular position relative to the torso is less than its initial value. This

TABLE 5-2. SLED ACCELERATION CHARACTERISTICS FOR NBDL
TESTS LX2124 AND LX 2302

SUBJECT	RUN NO.	SLED VELOCITY CHANGE (m/s)	PEAK SLED ACC.(m/s^2)	RATE OF ONSET (m/s^3)
H00083	2124	3.1	89	9435
H00083	2302	6.4	69	1497
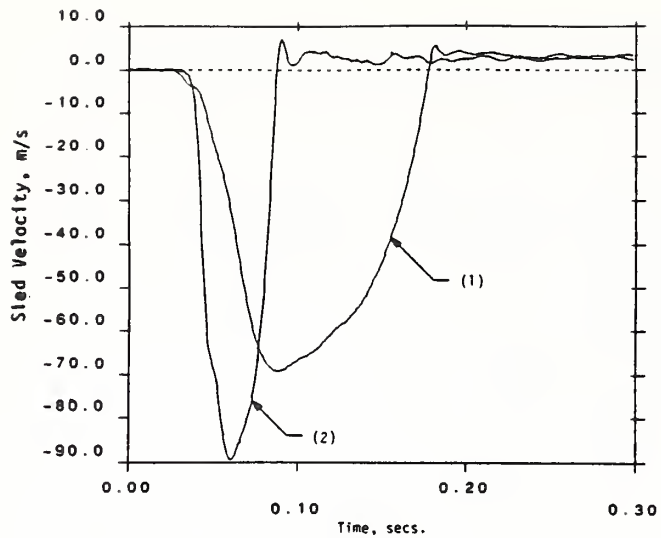
a.) Input Profile
(1) Test LX2302 (7-g, 1500_n)
(2) Test LX2124 (9-g, 9400_n)
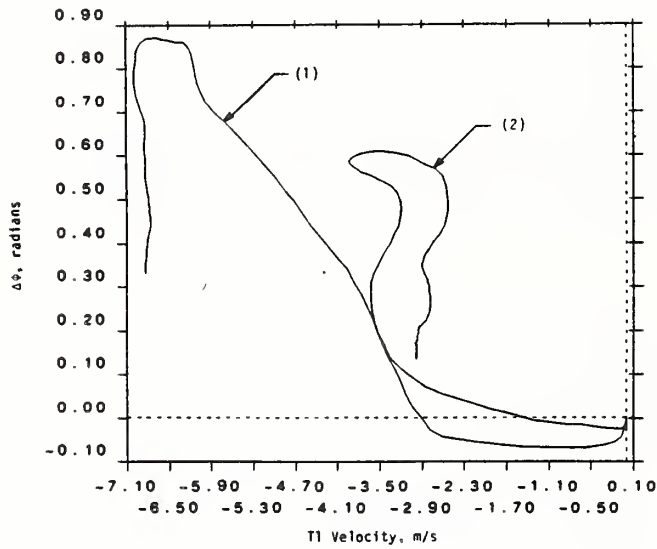
b.) T1 Response
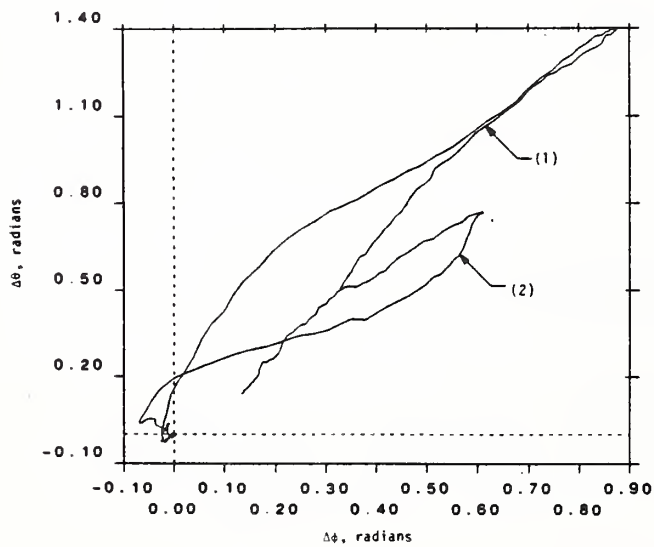
c.) Head and Neck Angular
    Response

FIGURE 5-52. ILLUSTRATION OF VELOCITY DEPENDENCE OF HEAD AND NECK
RESPONSE
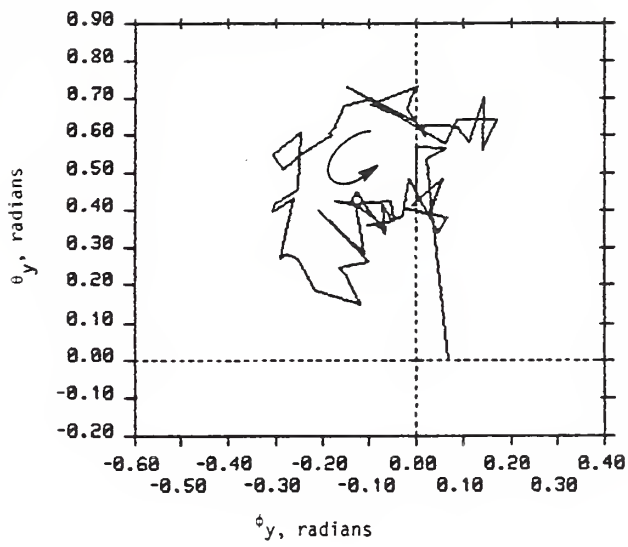
a) DOT 453
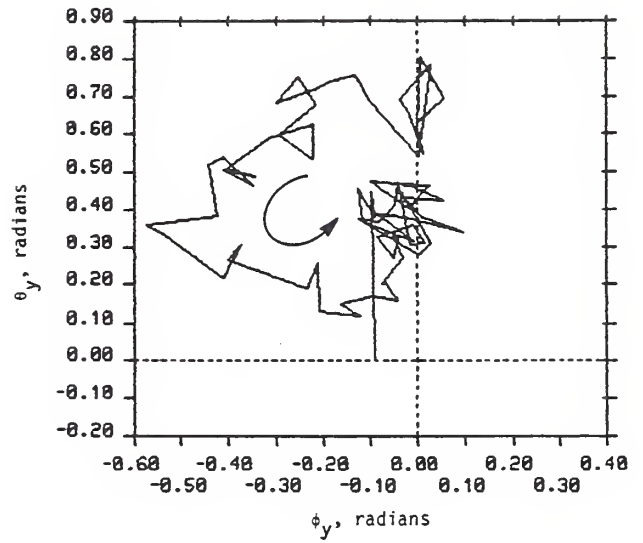
b) DOT 454
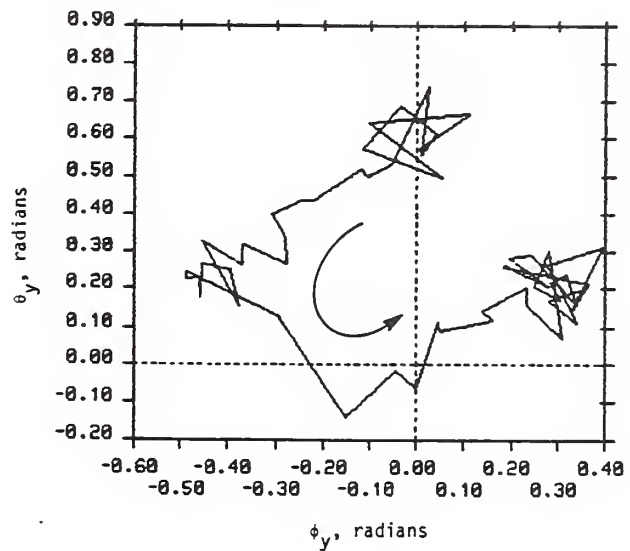
c) DOT 455

FIGURE 5-53. COMPARISON OF HEAD AND NECK ANGULAR RESPONSE IN THREE
TESTS OF WSU VOLUNTEER 0252 AT A 6-G SLED IMPACT LEVEL

behavior is quite different from that of the NBDL volunteers, apparently the result of the large angular torso excursion that delays the onset of head and neck flexion.

The peak sled acceleration is the same for test DOT455 and test LX3870 of Figure 5-54. However, the magnitude of the head rotation relative to the torso is seen to be significantly less in the lap belt restrained test, as would be expected when the torso is free to pivot about the hips. The net increase in head angle relative to the torso over the loading phase is approximately 0.5 radians for the WSU test. The angle of the neck chord line relative to the torso decreases by approximately 0.4 radians over the loading phase.

Each of the lap belt restrained cadaver tests of WSU exhibit head and neck extension initially that is similar to those for the WSU volunteer exhibiting both extension and flexion during buildup of the impact response. Three-point restrained cadavers exhibited less torso rotation and, therefore, have a head versus neck response that more closely resembles that in four-point restrained NBDL volunteers. Typical cadaver responses are shown in Figure 5-55.

The variations in form and magnitude of the head response when the type of restraint is different suggests that duplicating the restraint of the four-point system is extremely important when performing a compliance test to check conformity of an ATD with the proposed performance requirement.

The slope of the plot of head angle versus neck chord line angle provides a measure of the relative stiffness at the condyles and T1. Note the slope of the curves is nearly the same in Figure 5-53 for both extension and flexion. This implies that the relative amounts of stiffness at the condyles and T1 are the same during extension and flexion. As indicated in Figure 5-54, the slope is approximately the same for the WSU and NBDL volunteers.

State of Muscle Contraction - The neck chord distance in the cadavers maximum head excursion is greater than the initial length. This is shown in Figure 5-56 for two of the tests in which the cadaver is three-point restrained. This is a different characteristic than was observed in the volunteer tests, where neck length generally is shortened by 10-40 percent at the point of maximum excursion.
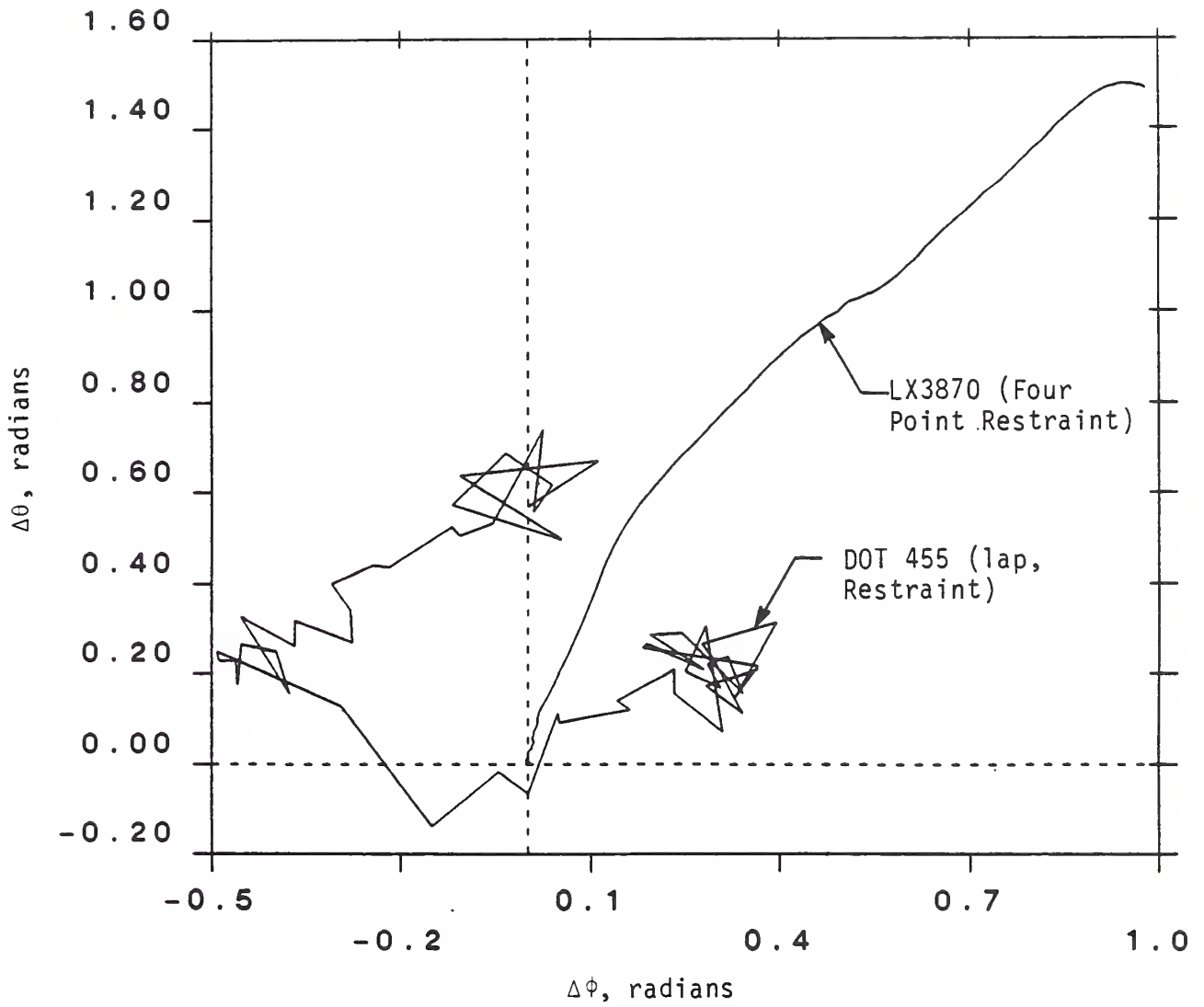
FIGURE 5-54. COMPARISON OF VOLUNTEER RESPONSE WITH LAP BELT VERSUS
FOUR-POINT RESTRAINT

5-77
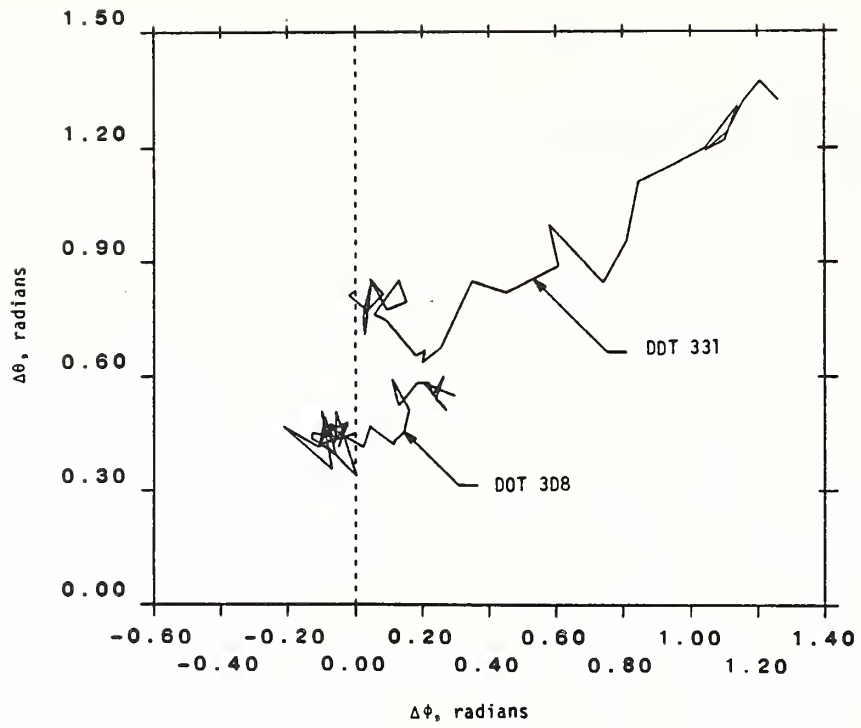
a) Three-point Restraint
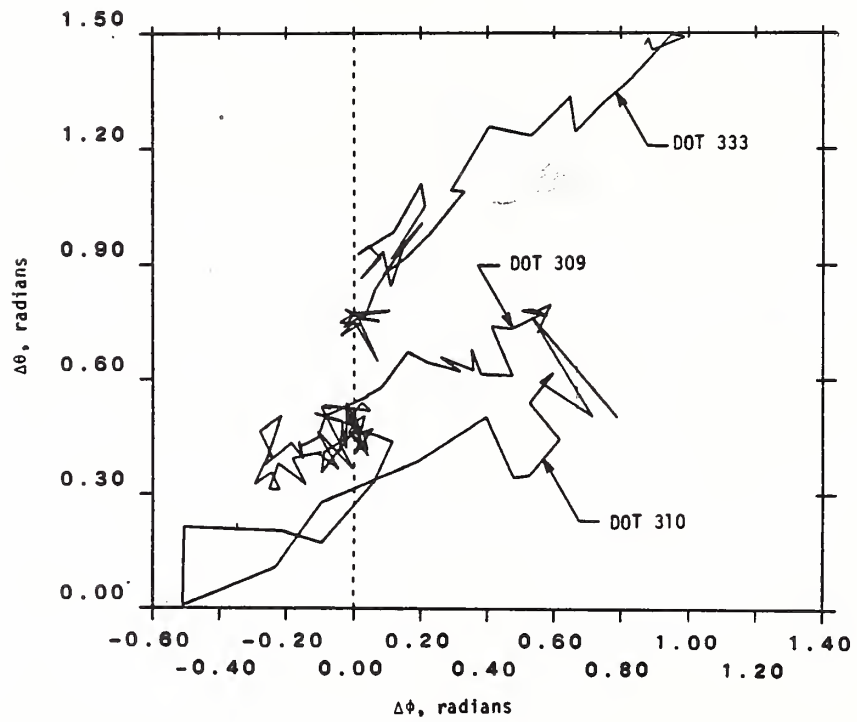
b) Lap Belt Restraint

FIGURE 5-55. TYPICAL HEAD VERSUS NECK ANGULAR RESPONSE FOR CADAVERS RESTRAINED BY A LAP BELT AND BY A THREE-POINT RESTRAINT SYSTEM

5-73
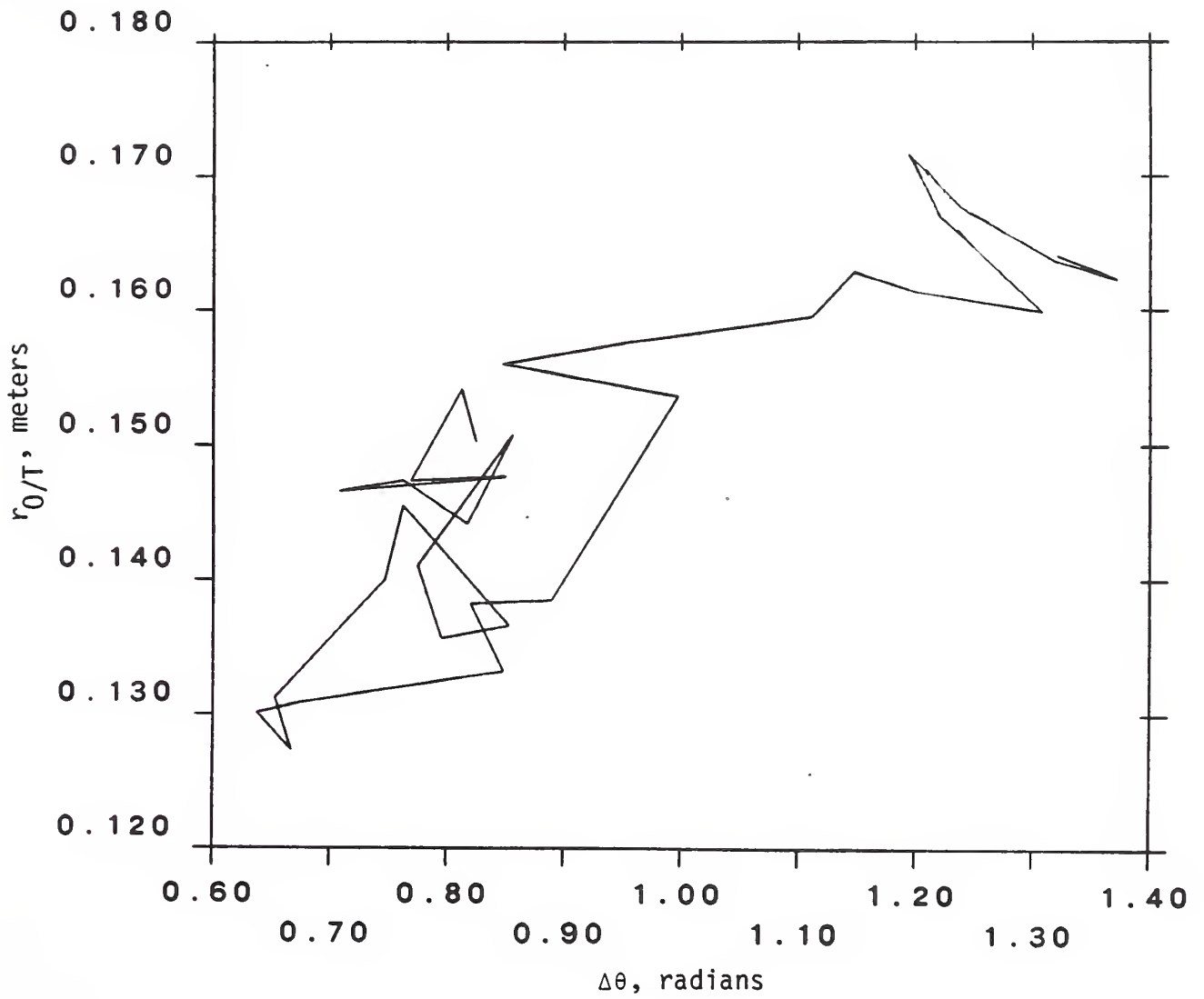
FIGURE 5-56. NECK CHORD, $r_{O/T}$, VERSUS NECK ANGLE, $\Delta\theta$, FOR THREE-POINT RESTRAINED CADAVER TEST DOT331

As discussed in Section 5.1.1, the lack of muscle activity to control the degree of curve in the cervical spine would explain stretching observed in the cadavers.

The number of WSU tests examined, and the detail and level of accuracy to which they were examined, is insufficient to make the results useful for extending the performance requirements as formulated from the NBDL volunteer tests. They serve only to place interpretations and limitations on the applicability of the requirements, as noted above in this section. Some assurance is required that an ATD designed to the volunteer based performance requirements and cadaver based limitations, will exhibit fidelity under a different restraint system. Ideally, the performance requirements should be based on tests which employed the restraint system for which the ATD will most typically be used. In the case of an ATD for automotive safety, this would be either a lap or three-point restraint system. Mathematical modelling was performed to provide some assurance that an ATD designed to meet the proposed, four-point based performance requirements, would then perform with sufficient fidelity in two- and three-point restraint systems. [25] This was accomplished by demonstrating that the math model would adequately predict the response for both restrained and unrestrained subjects without altering modelling parameters of the subject.

_____

*While the relative stiffnesses are nearly identical, the actual stiffness at the condyles or T1 may vary between embalmed and unembalmed cadavers. There was insufficient data to provide conclusive evidence of such.

6. SUMMARY AND RECOMMENDATIONS

Performance requirements are developed which define the significant kinematic and kinetic response of the head for a seated subject exposed to frontal, lateral or oblique impact. Response is expressed in terms of variables which can be measured in the laboratory, thereby making the performance requirements useful for evaluating the fidelity of an anthropomorphic test device (dummy).

The performance requirements are defined for two levels of fidelity: (1) position fidelity in which head displacement relative to the torso is sufficiently humanlike to permit prediction of secondary head contact, and (2) velocity fidelity in which momentum at any time is sufficiently humanlike to predict secondary head impact force levels.

The performance requirements are based solely upon subinjury level volunteer tests in which the torso is tightly restrained by a four-point belt system. Examination of tests in which lap belt and three-point restraint systems were employed indicate that the characteristics of the head and neck response are critically dependent on the degree of torso restraint. Thus, ATD conformance tests must be conducted with a torso restraint similar to that of the four-point system in order to apply the performance requirements. Mathematical modelling has shown that an ATD which demonstrates fidelity with a four-point restraint can also be expected to have fidelity when used with a lap belt or three-point restraint system.

Variations are noted between volunteer and cadaver response in the change in neck chord length during the impact. This variation is attributed to different levels of muscle activity present. The requirements in this study are based on the response of volunteers with muscle activity present, since there ·was insufficient cadaver data to establish a typical response with no muscle activity and, more importantly, because no data exists to indicate what level of muscle activity would be exhibited by a live human at higher impact levels where reaction times are shorter.

Neck rotation in response to oblique impact is somewhat less than the response to either frontal or lateral impact when equivalent input levels are compared. It is conjectured that there is less neck articulation in this direction, thereby limiting rotation. If this is the case, an ATD with frontal and lateral fidelity would have omni-directional fidelity only if the limitation on articulation is incorporated into the design for intermediate angles.

Recommendations for further work include:

1. Extension of the analysis of the cadaver tests of this study to include load analysis using the acceleration data that exists but has not been processed.

2. Additional sled testing with two- and three-point restraint in order to shift the basis for the performance requirements to the more nominal automotive restraint systems.

3. Development of the performance requirements for load fidelity, necessary for evaluation of an ATD with the capability to predict injury during unobstructed head motion.

Other recommendations of a more general nature include extension of the performance requirements to include three-axis response and to include response during the unloading phase (post secondary impact), both of which are important in examining rollover accidents.

7. REFERENCES

1. Mertz, H.J., Neathery, R.F. and Culver, C.C., "Performance Requirements and Characteristics of Mechanical/Necks," Human Impact Response Measurement and Simulation, Plenum Press, N.Y., pp 263-289, 1973.

2. Foster, J., King, P.P., Kortge, J.O. and Wolanim, M.J., "Hybrid III-A Biomechanically-Based Crash Test Dummy," Proc. of the 21st STAPP Car Crash Conference, 1977, 770938, pp 975-1014.

3. Wismans, J. and Spenny, C.H., "Head-Neck Response in Frontal Flexion," Proc. of the 28th STAPP Car Crash Conference, 1984, 841666, pp 161-172.

4. Ewing, C.L. and Thomas, D.J., "Human Head and Neck Response to Impact Acceleration," NARML Monograph 21, Naval Aerospace Medical Research Laboratory, Pensacola, Florida 32512, 1973.

5. Becker, E.B., "A Photographic Data System for Determination of Three-Dimensional Effects of Multiaxis Impact Acceleration on Living Humans," Proc. of the Society of Photo-Optical Instrumentation Engineers, Vol. 57, SPIE, Box 1146, Palos Verdas Estates, CA 90274, 1975.

6. Becker, E.B. and Willems, G.C., "An Experimentally Validated Three-Dimensional Inertial Tracking Package for Application in Biodynamics Research," Proc. of the 19th STAPP Car Crash Conference, (SAE Paper 751173), 1975.

7. Ewing, C.L., Thomas, D.J., Lustick, L., Willems, G.C., Muzzy III, W.H., Becker, E.B. and Jessop, M.E., "Dynamic Response of Human and Primate Head and Neck to + Gy Impact Acceleration," Report DOT HS-803 058, 1978.

8. Letter Correspondence, Naval Biodynamics Laboratory to the U.S. Department of Transportation/TSC, April 30, 1985.

9. Wismans, J. and Spenny, C.H., "Performance Requirements for Mechanical Necks in Lateral Flexion," Proc. of the 27th STAPP Car Crash Conference 831613, 1983.

10. Seemann, M.R., Lustick, L.S. and Frisch, G.D., "Mechanism for Control of Head and Neck Dynamic Response," Proc. of the 28th STAPP Car Crash Conference, 1984, 841669, PP 207-222.

11. "Preliminary Development, Head/Neck Simulator," Third Progress Report, SRL-59, NHTSA Vehicle Research and Test Center, E. Liberty, OH, February 1983.

12. Seeman, M.R. and Lustick, L., "Combination of Accelerometer and Photographic-derived Kinematic Variables Defining Three-Dimensional Rigid Body Motion," Proc. of the 2nd International Symposium of Biomechanics Cinematography and High Speed Photography, Society of Photo-Optical Instrumention Engineers, Box 1146, Palos Verdes Estates, CA 90274, 1981.

13. Mital, N.K., Cheng, R., Levine, R. and King, A., "Dynamic Characteristics of the Human Spine During $-G_x$ Acceleration," Proc. of the 22nd STAPP Car Crash Conference, 1978, 780889, pp 141-165.

14. Cheng, R., Mital, N.K., Levine, R. and King, A., "Biodynamics of the Living Human Spine During $-G_x$ Impact Acceleration," Proc. of the 23rd STAPP Car Crash Conference, 1979, 791027, pp 723-763.

15. Alem, N. and Sanford, T.Z., "Motion Analysis Package User's Manual," Concurrent Processing, Inc., Ann Arbor, MI, May, 1985.

16. Becker, E.B., "Stereoradiographic Measurements for Anatomical Mounted Instruments," Proc. of the 21st STAPP Car Crash Conference, 1977, 770926, pp 475-504. .

17. Spenny, C.H. and Wismans, J., "Dynamic Analysis of Head Motion," MECHANISMS OF HEAD AND SPINE TRAUMA, eds. Sances Jr., A., Thomas, D.J., Ewing, C.L., Larson, S.J. and Unterharnscheidt, F., Aloray Publisher, NY, 1986.

18. McConville, J.T., Churchill, T.D., Kaleps, I., Clauser, C.E. and Cuzzi, J., "Anthropometric Relationships of Body and Body Segment Moments of Inertia," Report AFAMRL-TR-80-119, Air Force Aerospace Medical Research Laboratory, Wright Patterson Airforce Base, Ohio 45433.

19. Housner, George W., and Hudson, D.E., DYNAMICS, Van Norstrand, 1959, page 197.

20. Beier, G.E., Schuller, E., Schuck, M., Ewing, C.L., Becker, E.B. and Thomas, D.J., "Center of Gravity and Moments of Inertia of Human Heads," Proc. of the 6th Conference of the International Research Committee on the Biokinetics of Impact, Birmingham, England, 1980, pp 218-228.

21. Ewing, C.L., Thomas, D.J., Lustick, L.S., Becker, E., Willems, G.C. and Muzzy III, W.H., "The Effect of Initial Position of the Head and Neck on the Dynamic Response of the Human Head and Neck to $-G_x$ Impact Acceleration," Proc. of the 19th STAPP Car Crash Conference, 1975, 751157, pp 487-512.

22. Snyder, R.G., Chafin, D.B., and Schulz, R.K., "Link System of the Human Torso," AMRL Wright-Patterson Air Force Base Contract F336K-70-C-1777 (NTIS AD-754924), 1971.

23. Mertz, H.J. and Patrick, L.M., "Strength and Response of the Human Neck," Proc. of the 15th STAPP Car Crash Conference, 1971.

24. Mucciardi, A.N., Sanders, J.D. and Eppinger, R.H., "Prediction of Brain Injury Measures from Head Motion Parameters," Proc. of the 21st STAPP Car Crash Conference, 1977, 770923, pp 367-416.

25. "Analysis of Head and Neck Dynamic Response of Human Volunteer and Cadaver Test Subjects," Report by the University of Michigan's Transportation Research Institute to the U.S. DOT/Transportation Systems Center under contract DTRS 57-83-C-00055, March, 1985.

26. Davenport Jr., W.B. and Root, W.L., RANDOM SIGNALS AND NOISE, McGraw-Hill, 1958, pp 55-56.

APPENDIX A

SUMMARY OF VOLUNTEER IMPACT TESTS

NBDL VOLUNTEERS:

RUN NUMBER	SUBJECT NUMBER	PEAK SLED ACCEL	RATE OF ONSET G/S	DURATION OF PEAK MSEC	END STROKE VELOCITY M/S	INITIAL CONDITION	SLED PROFILE CHARACTER	VECTOR DIRECTION	DATE OF TEST DAY YEAR
LX1441	H00044	2						+y	
LX1452	H00044	3						+y	
LX1458	H00044	4						+y	
LX1504	H00044	6						+y	
LX1512	H00044	7						+y	
LX1528	H00044	7.5						+y	
LZ1443	H00049	2						+y	
LX1470	H00049	3						+y	
LX1474	H00049	4						+y	
LX1442	H00060	2						+y	
LX1468	H00060	3						+y	
LX1475	H00060	4						+y	
LX1445	H00064	2						+y	
LX1449	H00064	3						+y	
LX1456	H00064	4						+y	
LX1471	H00064	5						+y	
LX1501	H00064	5						+y	
LX1507	H00064	6						+y	
LX1513	H00064	7						+y	
LX1524	H00064	7.5						+y	
LX1446	H00065	2						+y	
LX1448	H00065	3						+y	
LX1454	H00065	4						+y	

A-3

RUN NUMBER	SUBJECT NUMBER	PEAK SLED ACCEL	RATE OF ONSET G/S	DURATION OF PEAK MSEC	END STROKE VELOCITY M/S	INITIAL CONDITION	SLED PROFILE CHARACTER	VECTOR DIRECTION	DAY	YEAR
NBDL VOLUNTEERS:										
LX1487	H00065	5						+y		
LX1505	H00065	6						+y		
LX1510	H00065	7						+y		
LX1526	H00065	7.5						+y		
LX1450	H00067	2						+y		
LX1453	H00067	3						+y		
LX1457	H00067	4						+y		
LX1484	H00067	5						+y		
LX1503	H00067	6						+y		
LX1509	H00067	7						+y		
LX1525	H00067	7.5						+y		
LX3524	H00083	3			7.5		LOLD	-x		
LX3530	H00083	5			10.5		LOLD	-x		
LX3536	H00083	7			12.4		LOLD	-x		
LX3544	H00083	9					LOLD	-x		
LX2763	H00083	3					HOLD	-x+y		
LX2772	H00083	4					HOLD	-x+y		
LX2776	H00083	5					HOLD	-x+y		
LX2801	H00083	6					HOSD	-x+y		
LX2815	H00083	7					HOSD	-x+y		
LX2829	H00083	8					HOSD	-x+y		
LX2872	H00083	6					HOLD	-x+y		
LX2973	H00083	12					HOSD	-x+y		
LX2979	H00083	13					HOSD	-x+y		
LX2982	H00083	11					HOSD	-x+y		
LX2985	H00083	7					HOLD	-x+y		
LX3053	H00083	3					LOLD	-x+y		
LX3065	H00083	4					LOLD	-x+y		
LX3077	H00083	5					LOLD	-x+y		

|---|---|---|---|---|---|---|---|---|---|
NBDL VOLUNTEERS:									
LX3085	H00083	6					LOLD	-x+y	
LX3093	H00083	7					LOLD	-x+y	
LX3100	H00083	6					LOLD	-x+y	
LX3102	H00083	7					LOLD	-x+y	
LX3133	H00083	8					LOLD	-x+y	
LX3145	H00083	9					LOLD	-x+y	
LX3153	H00083	8					HOLD	-x+y	
LX1785	H00083	3					HOLD	+y	
LX1793	H00083	4					HOLD	+y	
LX1831	H00083	5			6.5		HOLD	+y	
LX1860	H00083	6					HOLD	+y	
LX1960	H00083	3					LOLD	+y	
LX1998	H00083	4					LOLD	+y	
LX2013	H00083	5			6.3		LOLD	+y	
LX2027	H00083	6					LOLD	+y	
LX2060	H00083	5					HOSD	+y	
LX2090	H00083	7					HOSD	+y	
LX2102	H00083	8					HOSD	+y	
LX2124	H00083	9			3.1		HOSD	+y	
LX2137	H00083	10					HOSD	+y	
LX2148	H00083	11					HOSD	+y	
LX2302	H00083	7			6.4		LOLD	+y	
LX2341	H00083	5					HOLD	+y	
LX3525	H00093	3			7.6		LOLD	-x	
LX3531	H00093	5			10.1		LOLD	-x	
LX3537	H00093	7			12.2		LOLD	-x	
LX3548	H00093	9			13.3		LOLD	-x	
LX3550	H00093	10			14.3		LOLD	-x	
LX3558	H00093	11					LOLD	-x	
LX3573	H00093	12			16.0		LOLD	-x	
LX3578	H00093	13			16.7		LOLD	-x	
LX3583	H00093	14			17.2		LOLD	-x	
LX3616	H00093	15					LOLD	-x	
LX2770	H00093	4					HOLD	-x+y	

NBDL VOLUNTEERS:

RUN NUMBER	SUBJECT NUMBER	PEAK SLED ACCEL	RATE OF ONSET G/S	DURATION OF PEAK MSEC	END STROKE VELOCITY M/S	INITIAL CONDITION	SLED PROFILE CHARACTER	VECTOR DIRECTION	DATE OF TEST DAY YEAR
LX2784	H00093	5					HOLD	-x+y	
LX2799	H00093	6			2.4		HOSD	-x+y	
LX2813	H00093	7			2.6		HOSD	-x+y	
LX2827	H00093	8					HOSD	-x+y	
LX2843	H00093	9			3.0		HOSD	-x+y	
LX2876	H00093	6					HOLD	-x+y	
LX2916	H00093	13			3.8		HOSD	-x+y	
LX2955	H00093	11			3.4		HOSD	-x+y	
LX2988	H00093	7					HOLD	-x+y	
LX3049	H00093	3					LOLD	-x+y	
LX3061	H00093	4					LOLD	-x+y	
LX3089	H00093	5					LOLD	-x+y	
LX3097	H00093	7					LOLD	-x+y	
LX3106	H00093	6					LOLD	-x+y	
LX3122	H00093	8					LOLD	-x+y	
LX3129	H00093	9					LOLD	-x+y	
LX3148	H00093	10					LOLD	-x+y	
LX3158	H00093	8					HOLD	-x+y	
LX3417	H00093	6					HOLD	-x+y	
LX1874	H00093	3					HOLD	+y	
LX1916	H00093	4					HOLD	+y	
LX2010	H00093	5			6.5		LOLD	+y	
LX2032	H00093	6			6.5		LOLD	+y	
LX2056	H00093	5					HOSD	+y	
LX2072	H00093	6					HOSD	+y	
LX2151	H00093	10			3.3		HOSD	+y	
LX2182	H00093	11					HOSD	+y	
LX2282	H00093	7					LOLD	+y	
LX2294	H00093	5					LOLD	+y	
LX2313	H00093	5					HOLD	+y	
LX2326	H00093	6			6.5		HOLD	+y	
LX2338	H00093	7					HOLD	+y	
LX2355	H00093	5			6.5		HOLD	+y	

A-6

RUN NUMBER	SUBJECT NUMBER	PEAK SLED ACCEL	RATE OF ONSET G/S	DURATION OF PEAK MSEC	END STROKE VELOCITY M/S	INITIAL CONDITION	SLED PROFILE CHARACTER	VECTOR DIRECTION	DATE OF TEST DAY	YEAR
NBDL VOLUNTEERS:										
LX4007	H00118	0	0	0	.00	NUCU	VOLM	VOLM	63	82
LX4011	H00118	0	0	0	.00	NUCU	VOLM	VOLM	63	82
LX4009	H00118	0	0	0	.00	NUCU	VOLM	VOLM	63	82
LX3782	H00118	2.1	49	135.6	3.82	NUCU	LOLD	x	278	81
LX3833	H00118	3.1	68	129.4	5.59	NUCU	LOLD	-x	307	81
LX3796	H00118	3.1	70	130.0	5.55	NUCU	LOLD	-x	287	81
LX3837	H00118	4.1	94	124.5	7.09	NUCU	LOLD	-x	309	81
LX3856	H00118	6.1	139	121.0	9.90	NUCU	LOLD	-x	328	81
LX3875	H00118	6.2	136	118.5	9.87	NUCU	LOLD	-x	336	81
LX3880	H00118	8.2	136	118.7	9.98	NUCU	LOLD	-x	341	81
LX3886	H00118	10.2	203	114.6	12.02	NUCU	LOLD	-x	343	81
LX3903	H00118	10.3	284	106.7	13.72	NUCU	LOLD	-x	6	82
LX3985	H00118	10.3	292	106.4	13.82	NUCU	LOLD	-x	56	82
LX3920	H00118	12.3	392	101.7	15.39	NUCU	LOLD	-x	21	82
LX3945	H00118	13.4	437	92.6	15.97	NUCU	LOLD	-x	34	82
LX3958	H00118	14.6	495	91.0	16.85	NUCU	LOLD	-x	40	82
LX3969	H00118	15.4	547	88.1	17.21	NUCU	LOLD	-x	47	82
LX3785	H00119	2.1	48	133.5	3.86	NUCU	LOLD	x	279	81
LX3821	H00119	3.1	68	129.5	5.52	NUCU	LOLD	x	301	81
LX3797	H00119	3.1	68	130.0	5.56	NUCU	LOLD	x	287	81
LX4005	H00120	.0	0	.0	.00	NUCU	VOLM	VOLM	63	82
LX4001	H00120	.0	0	.0	.00	NUCU	VOLM	VOLM	63	82
LX4003	H00120	.0	0	.0	.00	NUCU	VOLM	VOLM	63	82
LX3779	H00120	2.1	49	134.6	3.94	NUCU	LOLD	-x	274	81
LX3793	H00120	3.1	70	131.7	5.53	NUCU	LOLD	-x	286	81
LX3814	H00120	4.1	90	122.6	7.14	NUCU	LOLD	-x	299	81
LX3851	H00120	6.2	137	117.5	9.80	NUCU	LOLD	-x	327	81
LX3878	H00120	6.3	142	118.6	9.97	NUCU	LOLD	-x	337	81
LX3882	H00120	8.2	206	113.5	11.93	NUCU	LOLD	-x	342	81
LX3906	H00120	10.2	281	107.6	13.69	NUCU	LOLD	-x	7	82
LX3995	H00120	10.2	281	106.4	13.84	NUCU	LOLD	-x	61	82
LX3921	H00120	12.1	382	100.8	15.14	NUCU	LOLD	-x	21	82
LX3946	H00120	13.6	435	93.5	16.16	NUCU	LOLD	-x	34	82

A-7

RUN NUMBER	SUBJECT NUMBER	PEAK SLED ACCEL	RATE OF ONSET G/S	DURATION OF PEAK MSEC	END STROKE VELOCITY M/S	INITIAL CONDITION	SLED PROFILE CHARACTER	VECTOR DIRECTION	DATE OF TEST DAY	YEAR
NBDL VOLUNTEERS:										
LX3954	H00120	14.1	479	92.9	16.50	NUCU	LOLD	-x	39	82
LX3972	H00120	15.4	554	88.9	17.29	NUCU	LOLD	-x	48	82
LX4013	H00127	.0	0	.0	.00	NUCU	VOLM	VOLM	63	82
LX4062	H00127	.0	0	.0	.00	NUCU	VOLM	VOLM	85	82
LX4016	H00127	.0	0	.0	.00	NUCU	VOLM	VOLM	63	82
LX4066	H00127	.0	0	.0	.00	NUCU	VOLM	VOLM	85	82
LX4064	H00127	.0	0	.0	.00	NUCU	VOLM	VOLM	85	82
LX4017	H00127	.0	0	.0	.00	NUCU	VOLM	VOLM	63	82
LX3780	H00127	2.1	51	133.4	3.94	NUCU	LOLD	-x	274	81
LX3794	H00127	3.1	71	128.6	5.66	NUCU	LOLD	-x	286	81
LX3812	H00127	4.2	98	120.4	7.18	NUCU	LOLD	-x	295	81
LX3893	H00127	6.2	140	117.9	10.00	NUCU	LOLD	-x	349	81
LX3852	H00127	6.4	141	119.9	10.16	NUCU	LOLD	-x	327	81
LX3883	H00127	8.2	206	113.0	11.99	NUCU	LOLD	-x	342	81
LX3904	H00127	10.3	277	106.2	13.76	NUCU	LOLD	-x	6	82
LX3924	H00127	12.4	387	98.5	15.43	NUCU	LOLD	-x	27	82
LX3949	H00127	13.6	445	92.8	16.09	NUCU	LOLD	-x	35	82
LX3959	H00127	14.8	467	88.9	16.84	NUCU	LOLD	-x	40	82
LX4041	H00130	.0	0	.0	.00	NUCU	VOLM	VOLM	67	82
LX4190	H00130	.0	0	.0	.00	NUCU	VOLM	VOLM	137	82
LX4186	H00130	.0	0	.0	.00	NUCU	VOLM	VOLM	137	82
LX4037	H00130	.0	0	.0	.00	NUCU	VOLM	VOLM	67	82
LX4039	H00130	.0	0	.0	.00	NUCU	VOLM	VOLM	67	82
LX4188	H00130	.0	0	.0	.00	NUCU	VOLM	VOLM	137	82
LX3789	H00130	2.1	51	135.6	3.85	NUCU	LOLD	-x	280	81
LX3803	H00130	3.1	71	131.4	5.52	NUCU	LOLD	-x	293	81
LX3839	H00130	3.2	73	123.2	5.61	NUCU	LOLD	-x	314	81
LX3815	H00130	4.1	89	121.4	7.12	NUCU	LOLD	-x	299	81
LX3876	H00130	6.0	135	119.8	9.82	NUCU	LOLD	-x	336	81
LX3854	H00130	6.1	137	121.0	9.85	NUCU	LOLD	-x	328	81
LX3889	H00130	8.2	200	114.1	12.02	NUCU	LOLD	-x	344	81
LX3991	H00130	10.3	293	107.4	13.93	NUCU	LOLD	-x	60	82

NBDL VOLUNTEERS:

RUN NUMBER	SUBJECT NUMBER	PEAK SLED ACCEL	RATE OF ONSET G/S	DURATION OF PEAK MSEC	END STROKE VELOCITY M/S	INITIAL CONDITION	SLED PROFILE CHARACTER	VECTOR DIRECTION	DATE OF TEST DAY	DATE OF TEST YEAR
LX3928	H00130	10.3	278	105.5	13.81	NUCU	LOLD	-x	28	82
LX3944	H00130	12.3	393	100.2	15.47	NUCU	LOLD	-x	34	82
LX4159	H00130	4.1	84	125.1	7.16	NUCU	LOLD	-x+y	123	82
LX4235	H00130	7.0	159	116.3	10.89	NUCU	LOLD	-x+y	140	82
LX4260	H00130	9.1	242	105.8	12.79	NUCU	LOLD	-x+y	152	82
LX4301	H00130	9.3	252	105.6	13.12	NUCU	LOLD	-x+y	166	82
LX4286	H00130	10.1	281	105.5	13.64	NUCU	LOLD	-x+y	160	82
LX4276	H00130	10.1	283	104.9	13.70	NUCU	LOLD	-x+y	158	82
LX4309	H00130	11.3	334	100.8	14.64	NUCU	LOLD	-x+y	168	82
LX4050	H00130	3.0	63	130.0	5.53	NUCU	LOLD	+y	81	82
LX4070	H00130	4.2	81	118.7	7.14	NUCU	LOLD	+y	88	82
LX4088	H00130	5.2	108	102.5	7.11	NUCU	LOLD	+y	95	82
LX4107	H00130	6.0	133	90.2	7.03	NUCU	LOLD	+y	98	82
LX4137	H00130	6.1	131	89.7	7.19	NUCU	LOLD	+y	111	82
LX4123	H00130	7.2	170	75.9	6.98	NUCU	LOLD	+y	105	82
LX4043	H00131	.0	0	.0	.00	NUCU	VOLM	VOLM	67	82
LX4047	H00131	.0	0	.0	.00	NUCU	VOLM	VOLM	67	82
LX4045	H00131	.0	0	.0	.00	NUCU	VOLM	VOLM	67	82
LX4257	H00131	.0	0	.0	.00	NUCU	VOLM	VOLM	146	82
LX4255	H00131	.0	0	.0	.00	NUCU	VOLM	VOLM	146	82
LX4253	H00131	.0	0	.0	.00	NUCU	VOLM	VOLM	146	82
LX3783	H00131	2.1	48	139.8	3.94	MUCU	LOLD	-x	278	81
LX3840	H00131	3.1	68	129.5	5.62	NUCU	LOLD	-x	314	81
LX3804	H00131	3.1	66	129.9	5.61	NUCU	LOLD	-x	293	81
LX3817	H00131	4.1	96	123.6	7.15	NUCU	LOLD	-x	300	81
LX3885	H00131	6.1	135	119.6	9.84	NUCU	LOLD	-x	343	81
LX3857	H00131	6.2	135	120.6	10.06	NUCU	LOLD	-x	328	81
LX3894	H00131	8.4	205	111.0	12.07	NUCU	LOLD	-x	349	81
LX3908	H00131	10.2	275	105.9	13.71	NUCU	LOLD	-x	13	82
LX3999	H00131	10.3	287	105.6	13.93	NUCU	LOLD	-x	62	82
LX3926	H00131	12.1	380	100.8	15.03	NUCU	LOLD	-x	28	82
LX3948	H00131	13.7	451	91.0	16.06	NUCU	LOLD	-x	35	82
LX3987	H00131	14.5	480	91.7	16.76	NUCU	LOLD	-x	56	82
LX3990	H00131	15.4	527	88.9	17.26	NUCU	LOLD	-x	60	82

RUN NUMBER	SUBJECT NUMBER	PEAK SLED ACCEL	RATE OF ONSET G/S	DURATION OF PEAK MSEC	END STROKE VELOCITY M/S	INITIAL CONDITION	SLED PROFILE CHARACTER	VECTOR DIRECTION	DATE OF TEST DAY	YEAR
NBDL VOLUNTEERS:										
LX4161	H00131	4.1	81	126.0	7.19	NUCU	LOLD	-x+y	124	82
LX4242	H00131	7.3	170	115.3	11.41	NUCU	LOLD	-x+y	144	82
LX4246	H00131	9.1	238	107.0	12.92	NUCU	LOLD	-x+y	145	82
LX4251	H00131	10.2	281	105.2	13.83	NUCU	LOLD	-x+y	146	82
LX4052	H00131	3.0	62	126.3	5.49	NUCU	LOLD	+y	83	82
LX4071	H00131	4.1	81	120.2	7.14	NUCU	LOLD	+y	88	82
LX4089	H00131	5.1	105	101.8	7.07	NUCU	LOLD	+y	95	82
LX4109	H00131	6.2	133	89.6	7.21	NUCU	LOLD	+y	102	82
LX4138	H00131	6.2	133	89.0	7.22	NUCU	LOLD	+y	111	82
LX4124	H00131	7.2	169	74.9	6.94	NUCU	LOLD	+y	105	82
LX4029	H00132	.0	0	.0	.00	NUCU	VOLM	VOLM	64	82
LX4025	H00132	.0	0	.0	.00	NUCU	VOLM	VOLM	64	82
LX4027	H00132	.0	0	.0	.00	NUCU	VOLM	VOLM	64	82
LX3788	H00132	2.0	48	130.4	3.71	NUCU	LOLD	x	200	81
LX3805	H00132	3.0	66	129.7	5.43	NUCU	LOLD	-x	293	81
LX3818	H00132	4.1	88	124.3	7.08	NUCU	LOLD	-x	300	81
LX3887	H00132	6.0	134	120.2	9.83	NUCU	LOLD	-x	343	81
LX3858	H00132	6.2	140	118.5	9.96	NUCU	LOLD	-x	328	81
LX3900	H00132	8.1	202	112.6	12.00	NUCU	LOLD	-x	5	82
LX3997	H00132	8.1	203	114.5	12.12	NUCU	LOLD	-x	62	82
LX3989	H00132	10.2	290	106.5	13.78	NUCU	LOLD	-x	60	82
LX3909	H00132	10.3	279	106.0	13.91	NUCU	LOLD	-x	13	82
LX3927	H00132	12.2	377	101.2	15.34	NUCU	LOLD	-x	28	82
LX3950	H00132	13.6	441	94.1	16.14	NUCU	LOLD	-x	35	82
LX3957	H00132	14.6	509	90.9	16.75	NUCU	LOLD	-x	40	82
LX3982	H00132	15.6	542	88.4	17.47	NUCU	LOLD	-x	49	82
LX4162	H00132	4.0	80	125.6	7.00	NUCU	LOLD	-x+y	124	82
LX4244	H00132	7.3	175	116.7	11.40	NUCU	LOLD	-x+y	144	82
LX4261	H00132	9.0	240	106.4	12.72	NUCU	LOLD	-x+y	152	82
LX4297	H00132	10.0	282	105.8	13.78	NUCU	LOLD	-x+y	165	82
LX4287	H00132	10.2	288	105.6	13.83	NUCU	LOLD	-x+y	160	82
LX4306	H00132	11.1	335	101.5	14.54	NUCU	LOLD	-x+y	167	82
LX4053	H00132	3.1	62	127.8	5.61	NUCU	LOLD	+y	83	82
LX4155	H00132	4.1	81	124.3	7.09	NUCU	LOLD	+y	117	82

NBDL VOLUNTEERS:

RUN NUMBER	SUBJECT NUMBER	PEAK SLED ACCEL	RATE OF ONSET G/S	DURATION OF PEAK MSEC	END STROKE VELOCITY M/S	INITIAL CONDITION	SLED PROFILE CHARACTER	VECTOR DIRECTION	DATE OF TEST DAY	YEAR
LX4074	H00132	4.1	81	120.6	7.16	NUCU	LOLD	+y	89	82
LX4090	H00132	5.1	105	102.0	7.09	NUCU	LOLD	+y	95	82
LX4143	H00132	6.1	130	91.4	7.17	NUCU	LOLD	+y	112	82
LX4110	H00132	6.1	130	90.9	7.14	NUCU	LOLD	+y	102	82
LX4128	H00132	7.1	165	76.5	6.91	NUCU	LOLD	+y	109	82
LX4334	H00132	2.1	170	136.4	3.74	NUCU	HOLD	+z	271	82
LX4337	H00132	3.1	217	131.0	5.23	NUCU	HOLD	+z	272	82
LX4023	H00133	.0	0	.0	.00	NUCU	VOLM	VOLM	64	82
LX4019	H00133	.0	0	.0	.00	NUCU	VOLM	VOLM	64	82
LX4021	H00133	.0	0	.0	.00	NUCU	VOLM	VOLM	64	82
LX4230	H00133	.0	0	.0	.00	NUCU	VOLM	VOLM	130	82
LX4228	H00133	.0	0	.0	.00	NUCU	VOLM	VOLM	130	82
LX4292	H00133	.0	0	.0	.00	NUCU	VOLM	VOLM	130	82
LX3701	H00133	2.1	47	131.8	3.90	NUCU	LOLD	-x	281	81
LX3841	H00133	3.1	71	133.4	5.66	NUCU	LOLD	-x	314	81
LX3798	H00133	3.1	67	129.6	5.63	NUCU	LOLD	-x	287	81
LX3819	H00133	4.1	87	125.9	7.20	NUCU	LOLD	-x	300	81
LX3869	H00133	6.2	141	121.4	10.01	NUCU	LOLD	-x	334	81
LX3895	H00133	8.2	206	112.2	12.00	NUCU	LOLD	-x	349	81
LX3998	H00133	10.2	285	106.2	13.71	NUCU	LOLD	-x	62	82
LX3913	H00133	10.3	274	105.9	13.87	NUCU	LOLD	-x	18	82
LX3939	H00133	12.4	382	99.7	15.36	NUCU	LOLD	-x	33	82
LX3951	H00133	13.4	431	92.1	15.96	NUCU	LOLD	-x	35	82
LX3963	H00133	14.5	476	91.1	16.69	NUCU	LOLD	-x	41	82
LX3986	H00133	15.6	538	87.1	17.31	NUCU	LOLD	-x	56	82
LX4163	H00133	4.0	82	124.9	7.04	NUCU	LOLD	-x+y	124	82
LX4236	H00133	7.3	171	115.8	11.36	NUCU	LOLD	-x+y	140	82
LX4240	H00133	9.1	236	107.9	12.95	NUCU	LOLD	-x+y	144	82
LX4057	H00133	3.0	62	127.0	5.48	NUCU	LOLD	+y	84	82
LX4075	H00133	4.1	80	122.4	7.20	NUCU	LOLD	+y	89	82
LX4093	H00133	5.1	105	102.3	7.11	NUCU	LOLD	+y	96	82
LX4151	H00133	6.1	130	90.7	7.17	NUCU	LOLD	+y	117	82
LX4111	H00133	6.1	132	90.5	7.25	NUCU	LOLD	+y	102	82
LX4125	H00133	7.2	164	75.8	7.02	NUCU	LOLD	+y	105	82

A-11

NBDL VOLUNTEERS:

RUN NUMBER	SUBJECT NUMBER	PEAK SLED ACCEL	RATE OF ONSET G/S	DURATION OF PEAK MSEC	END STROKE VELOCITY M/S	INITIAL CONDITION	SLED PROFILE CHARACTER	VECTOR DIRECTION	DATE OF TEST DAY	DATE OF TEST YEAR
LX4184	HOO134	.0	0	.0	.00	NUCU	VOLM	VOLM	107	82
LX4182	HOO134	.0	0	.0	.00	NUCU	VOLM	VOLM	107	82
LX4180	HOO134	.0	0	.0	.00	NUCU	VOLM	VOLM	107	82
LX3786	HOO134	2.1	53	137.9	3.91	NUCU	LOLD	-x	279	81
LX3807	HOO134	3.0	69	128.2	5.31	NUCU	LOLD	-x	294	81
LX3842	HOO134	3.1	66	132.5	5.62	NUCU	LOLD	-x	314	81
LX3822	HOO134	4.1	92	119.4	7.16	NUCU	LOLD	-x	301	81
LX3870	HOO134	6.2	138	119.4	9.96	NUCU	LOLD	-x	334	81
LX3890	HOO134	8.2	205	113.2	11.97	NUCU	LOLD	-x	344	81
LX3940	HOO134	12.3	379	101.2	15.42	NUCU	LOLD	-x	33	82
LX3961	HOO134	13.4	437	96.7	16.07	NUCU	LOLD	-x	41	82
LX3968	HOO134	14.3	489	92.1	16.54	NUCU	LOLD	-x	47	82
LX3983	HOO134	15.6	539	89.1	17.55	NUCU	LOLD	-x	49	82
LX4164	HOO134	4.0	80	124.8	7.03	NUCU	LOLD	-x+y	124	82
LX4237	HOO134	7.2	170	116.4	11.26	NUCU	LOLD	-x+y	140	82
LX4264	HOO134	9.3	248	106.9	13.03	NUCU	LOLD	-x+y	153	82
LX4290	HOO134	10.1	288	107.4	13.77	NUCU	LOLD	-x+y	161	82
LX4298	HOO134	10.1	285	105.3	13.78	NUCU	LOLD	-x+y	165	82
LX4307	HOO134	11.4	337	101.3	14.89	NUCU	LOLD	-x=Y	167	82
LX4054	HOO134	3.1	61	128.6	5.59	NUCU	LOLD	+y	83	82
LX4076	HOO134	4.2	82	124.0	7.29	NUCU	LOLD	+y	89	82
LX4097	HOO134	5.0	104	104.1	7.06	NUCU	LOLD	+y	97	82
LX4139	Hoo134	6.1	128	91.1	7.16	NUCU	LOLD	+y	111	82
LX4112	HOO134	6.1	128	88.4	7.13	NUCU	LOLD	+y	102	82
LX4126	HOO134	7.1	167	74.7	6.90	NUCU	LOLD	+y	105	82
LX4208	HOO135	.0	0	.0	.00	NUCU	VOLM	VOLM	138	82
LX4206	HOO135	.0	0	.0	.00	NUCU	VOLM	VOLM	138	82
LX4204	HOO135	.0	0	.0	.00	NUCU	VOLM	VOLM	138	82
LX3800	HOO135	2.1	50	122.0	3.88	NUCU	LOLD	-x	292	81
LX3808	HOO135	3.1	67	127.0	5.50	NUCU	LOLD	-x	294	81
LX3823	HOO135	4.1	87	121.3	7.15	NUCU	LOLD	-x	301	81
LX3871	HOO135	6.2	140	119.2	9.96	NUCU	LOLD	-x	334	81
LX3898	HOO135	8.3	207	114.4	12.15	NUCU	LOLD	-x	350	81
LX3916	HOO135	10.3	276	104.9	13.83	NUCU	LOLD	-x	19	82

A-12

RUN NUMBER	SUBJECT NUMBER	PEAK SLED ACCEL	RATE OF ONSET G/S	DURATION OF PEAK MSEC	END STROKE VELOCITY M/S	INITIAL CONDITION	SLED PROFILE CHARACTER	VECTOR DIRECTION	DATE OF TEST DAY	DATE OF TEST YEAR
NBDL VOLUNTEERS:										
LX3994	H00135	10.3	286	106.4	13.92	NUCU	LOLD	-x	61	82
LX3941	H00135	12.5	382	97.7	15.52	NUCU	LOLD	-x	33	82
LX3955	H00135	13.6	444	93.7	16.18	NUCU	LOLD	-x	39	82
LX3965	H00135	14.6	493	89.9	16.67	NUCU	LOLD	-x	42	82
LX3970	H00135	15.6	534	87.6	17.26	NUCU	LOLD	-x	47	82
LX4166	H00135	4.1	80	124.3	7.06	NUCU	LOLD	-x+y	125	82
LX4238	H00135	7.3	169	117.0	11.44	NUCU	LOLD	-x+y	140	82
LX4314	H00135	9.1	244	106.9	12.90	NUCU	LOLD	-x+y	180	82
LX4266	H00135	9.3	249	106.1	13.10	NUCU	LOLD	-x+y	153	82
LX4316	H00135	10.1	290	105.7	13.62	NUCU	LOLD	-x+y	182	82
LX4277	H00135	10.2	283	105.8	13.75	NUCU	LOLD	-x+y	158	82
LX4055	H00135	3.1	65	125.8	5.62	NUCU	LOLD	+y	83	82
LX4078	H00135	4.1	81	121.2	7.14	NUCU	LOLD	+y	90	82
LX4095	H00135	5.2	105	103.3	7.14	NUCU	LOLD	+y	96	82
LX4114	H00135	6.1	132	90.0	7.19	NUCU	LOLD	+y	103	82
LX4140	H00135	6.1	127	88.8	7.16	NUCU	LOLD	+y	111	82
LX4131	H00135	7.3	164	72.8	6.94	NUCU	LOLD	+y	109	82
LX4033	H00136	.0	0	.0	.00	NUCU	VOLM	VOLM	67	82
LX4031	H00136	.0	0	.0	.00	NUCU	VOLM	VOLM	67	82
LX4035	H00136	.0	0	.0	.00	NUCU	VOLM	VOLM	67	82
LX4174	H00136	.0	0	.0	.00	NUCU	VOLM	VOLM	137	82
LX4178	H00136	.0	0	.0	.00	NUCU	VOLM	VOLM	137	82
LX4176	H00136	.0	0	.0	.00	NUCU	VOLM	VOLM	137	82
LX3801	H00136	2.1	54	136.3	3.93	NUCU	LOLD	-x	292	81
LX3809	H00136	3.0	66	126.3	5.49	NUCU	LOLD	-x	294	81
LX3824	H00136	4.1	88	123.0	7.19	NUCU	LOLD	-x	301	81
LX3872	H00136	6.1	137	121.5	9.92	NUCU	LOLD	-x	334	81
LX3901	H00136	7.9	200	116.5	11.88	NUCU	LOLD	-x	5	82
LX3918	H00136	10.2	293	109.3	14.03	NUCU	LOLD	-x	20	82
LX3942	H00136	12.0	382	102.2	15.26	NUCU	LOLD	-x	33	82
LX3953	H00136	13.3	443	97.2	16.03	NUCU	LOLD	-x	39	82
LX3962	H00136	14.1	474	93.9	16.59	NUCU	LOLD	-x	41	82
LX4167	H00136	4.1	81	124.6	7.03	NUCU	LOLD	-x+y	125	82
LX4247	H00136	7.1	166	117.4	11.11	NUCU	LOLD	-x+y	145	82

NBDL VOLUNTEERS:

RUN NUMBER	SUBJECT NUMBER	PEAK SLED ACCEL	RATE OF ONSET G/S	DURATION OF PEAK MSEC	END STROKE VELOCITY M/S	INITIAL CONDITION	SLED PROFILE CHARACTER	VECTOR DIRECTION	DATE OF TEST DAY	YEAR
LX4263	HOO136	9.2	247	107.7	12.98	NUCU	LOLD	-x+y	153	82
LX4058	HOO136	3.0	63	129.8	5.47	NUCU	LOLD	+y	84	82
LX4079	HOO136	4.1	80	123.6	7.11	NUCU	LOLD	+y	90	82
LX4098	HOO136	5.1	106	102.8	7.03	NUCU	LOLD	+y	97	82
LX4142	HOO136	6.0	131	91.0	7.07	NUCU	LOLD	+y	112	82
LX4153	HOO136	7.1	157	75.1	6.86	NUCU	LOLD	+y	117	82
LX4202	HOO138	.0	0	.0	.00	NUCU	VOLM	VOLM	138	82
LX4198	HOO138	.0	0	.0	.00	NUCU	VOLM	VOLM	138	82
LX4200	HOO138	.0	0	.0	.00	NUCU	VOLM	VOLM	138	82
LX4158	HOO138	4.1	80	123.7	7.12	NUCU	LOLD	-x+y	125	82
LX4241	HOO138	7.2	167	116.1	11.17	NUCU	LOLD	-x+y	144	82
LX4265	HOO183	9.2	245	106.7	12.98	NUCU	LOLD	-x+y	153	82
LX4284	HOO138	9.9	280	106.2	13.49	NUCU	LOLD	-x+y	160	82
LX4296	HOO138	10.1	286	106.5	13.77	NUCU	LOLD	-x+y	165	82
LX4305	HOO138	11.4	342	101.2	14.81	NUCU	LOLD	-x+y	167	82
LX4059	HOO138	3.1	63	124.3	5.49	NUCU	LOLD	+y	84	82
LX4080	HOO138	4.1	79	120.0	7.11	NUCU	LOLD	+y	90	82
LX4092	HOO138	5.1	106	101.7	7.05	NUCU	LOLD	+y	96	82
LX4147	HOO138	6.0	126	89.2	7.06	NUCU	LOLD	+y	116	82
LX4115	HOO138	6.0	127	89.7	7.11	NUCU	LOLD	+y	103	82
LX4129	HOO138	7.2	162	75.3	6.92	NUCU	LOLD	+y	109	82
LX4192	HOO139	.0	0	.0	.00	NUCU	VOLM	VOLM	138	82
LX4194	HOO139	.0	0	.0	.00	NUCU	VOLM	VOLM	138	82
LX4196	HOO139	.0	0	.0	.00	NUCU	VOLM	VOLM	138	82
LX4170	HOO139	4.1	80	123.0	7.06	NUCU	LOLD	-x+y	126	82
LX4243	HOO139	7.3	170	115.8	11.31	NUCU	LOLD	-x+y	144	82
LX4313	HOO139	9.1	252	106.7	12.81	NUCU	LOLD	-x+y	180	82
LX4268	HOO139	9.2	246	106.9	12.96	NUCU	LOLD	-x+y	154	82
LX4280	HOO139	10.2	290	105.4	13.76	NUCU	LOLD	-x+y	159	82
LX4291	HOO139	10.3	290	106.7	13.01	NUCU	LOLD	-x+y	161	82
LX4292	HOO139	11.3	339	101.2	14.77	NUCU	LOLD	-x+y	166	82
LX4069	HOO139	3.1	62	124.8	5.67	NUCU	LOLD	+y	88	82
LX4085	HOO139	4.1	78	121.1	7.16	NUCU	LOLD	+y	91	82

RUN NUMBER	SUBJECT NUMBER	PEAK SLED ACCEL	RATE OF ONSET G/S	DURATION OF PEAK MSEC	END STROKE VELOCITY M/S	INITIAL CONDITION	SLED PROFILE CHARACTER	VECTOR DIRECTION	DATE OF TEST DAY	YEAR
NBDL VOLUNTEERS:										
LX4100	H00139	5.1	107	101.2	7.08	NUCU	LOLD	+y	97	82
LX4118	H00139	6.1	128	89.0	7.13	NUCU	LOLD	+y	104	82
LX4144	H00139	6.1	130	89.8	7.25	NUCU	LOLD	+y	112	82
LX4133	H00139	7.2	165	75.0	6.91	NUCU	LOLD	+y	110	82
LX4210	H00140	.0	0	.0	.00	NUCU	VOLM	VOLM	138	82
LX4212	H00140	.0	0	.0	.00	NUCU	VOLM	VOLM	138	82
LX4214	H00140	.0	0	.0	.00	NUCU	VOLM	VOLM	138	82
LX4234	H00140	4.1	81	122.3	6.99	NUCU	LOLD	-x+y	140	82
LX4259	H00140	7.2	172	115.5	11.18	NUCU	LOLD	-x+y	152	82
LX4269	H00140	9.1	241	106.5	12.83	NUCU	LOLD	-x+y	154	82
LX4302	H00140	9.1	248	107.7	12.96	NUCU	LOLD	-x+y	166	82
LX4293	H00140	10.1	286	107.4	13.76	NUCU	LOLD	-x+y	161	82
LX4281	H00140	10.2	287	104.8	13.83	NUCU	LOLD	-x+y	159	82
LX4310	H00140	11.2	334	100.8	14.69	NUCU	LOLD	-x+y	168	82
LX4060	H00140	3.1	61	126.4	5.56	NUCU	LOLD	+y	84	82
LX4081	H00140	4.1	77	117.9	7.05	NUCU	LOLD	+y	90	82
LX4099	H00140	5.1	108	102.6	7.11	NUCU	LOLD	+y	97	82
LX4145	H00140	6.1	127	91.0	7.20	NUCU	LOLD	+y	112	82
LX4116	H00140	6.1	128	89.3	7.20	NUCU	LOLD	+y	103	82
LX4130	H00140	7.1	161	75.1	6.89	NUCU	LOLD	+y	109	82
LX4218	H00141	.0	0	.0	.00	NUCU	VOLM	VOLM	139	82
LX4220	H00141	.0	0	.0	.00	NUCU	VOLM	VOLM	139	82
LX4216	H00141	.0	0	.0	.00	NUCU	VOLM	VOLM	139	82
LX4171	H00141	4.0	79	122.2	7.03	NUCU	LOLD	-x+y	126	82
LX4248	H00141	7.1	166	115.9	11.11	NUCU	LOLD	-x+y	145	82
LX4270	H00141	9.2	247	106.8	12.90	NUCU	LOLD	-x+y	154	82
LX4292	H00141	10.1	285	107.3	13.86	NUCU	LOLD	-x+y	161	82
LX4282	H00141	10.2	286	105.7	13.80	NUCU	LOLD	-x+y	159	82
LX4068	H00141	3.1	63	127.8	5.55	NUCU	LOLD	+y	88	82
LX4083	H00141	4.1	78	123.9	7.13	NUCU	LOLD	+y	91	82
LX4094	H00141	5.1	106	101.3	7.12	NUCU	LOLD	+y	96	82
LX4119	H00141	5.9	128	93.3	7.06	NUCU	LOLD	+y	104	82
LX4148	H00141	6.0	124	90.9	7.10	NUCU	LOLD	+y	116	82
LX4134	H00141	7.1	161	75.2	6.85	NUCU	LOLD	+y	110	82

RUN NUMBER	SUBJECT NUMBER	PEAK SLED ACCEL	RATE OF ONSET G/S	DURATION OF PEAK MSEC	END STROKE VELOCITY M/S	INITIAL CONDITION	SLED PROFILE CHARACTER	VECTOR DIRECTION	DATE OF TEST DAY	YEAR
NBDL VOLUNTEERS:										
LX4224	H00142	.0	0	.0	.00	NUCU	VOLM	VOLM	139	82
LX4222	H00142	.0	0	.0	.00	NUCU	VOLM	VOLM	139	82
LX4226	H00142	.0	0	.0	.00	NUCU	VOLM	VOLM	139	82
LX4172	H00142	4.1	80	123.0	7.01	NUCU	LOLD	-x+y	126	82
LX4249	H00142	7.4	174	116.2	11.45	NUCU	LOLD	-x+y	145	82
LX4271	H00142	9.1	242	106.9	12.93	NUCU	LOLD	-x+y	154	82
LX4295	H00142	9.2	249	108.4	13.06	NUCU	LOLD	-x+y	165	82
LX4288	H00142	10.1	288	106.9	13.76	NUCU	LOLD	-x+y	160	82
LX4073	H00142	3.1	63	125.0	5.61	NUCU	LOLD	+y	89	82
LX4064	H00142	4.1	79	123.4	7.12	NUCU	LOLD	+y	91	82
LX4104	H00142	5.1	108	102.3	6.99	NUCU	LOLD	+y	98	82
LX4120	H00142	6.1	131	89.9	7.06	NUCU	LOLD	+y	104	82
LX4149	H00142	6.1	128	90.2	7.13	NUCU	LOLD	+y	116	82
LX4135	H00142	7.2	161	75.3	6.87	NUCU	LOLD	+y	110	82

APPENDIX B

CORRECTION OF MEASURED VERTICAL POSITION OF THE T1 VERTEBRAL POINT

Considerable variation exists in a subjects initial neck chord length from test to test. For example, variation for the 20 tests of subject H00134 is nearly 4 cm as indicated in Figure B-1.

Variations in initial length between subjects is expected. However, variations of this magnitude between tests of the same subject suggest a possible inconsistency in the data. Accuracy in the computation of neck chord length is critically dependent on placement of the photo target/sensor packages on the head and T1 vertebral body. Some difficulty in repeatedly placing the T1 package at the same location and in the same orientation has been acknowledged by the NBDL.

Correlation has been obseved by Wismans[11] for subjects H00083 and H00093 of the initial distance from the T1 vertebral point to the head anatomical origin with the initial vertical position of T1 relative to the seat. A similar correlation is observed for subjects in the more recent tests. Figure B-2 shows the correlation for subject H00134. Deviation from the least squares line fit to the data is rather small.

The vertical position of T1 can be corrected based on this correlation. Figure B-3 illustrates the procedure used in this study. For a selected test of a subject, his computed neck length (note neck length in Figures B-2 and B-3 differs from that used elsewhere in the report) is used in the regression equation to compute the corresponding T1 vertical position. The difference, Δ , between this computed T1 position and the mean T1 position (from all tests of that subject)
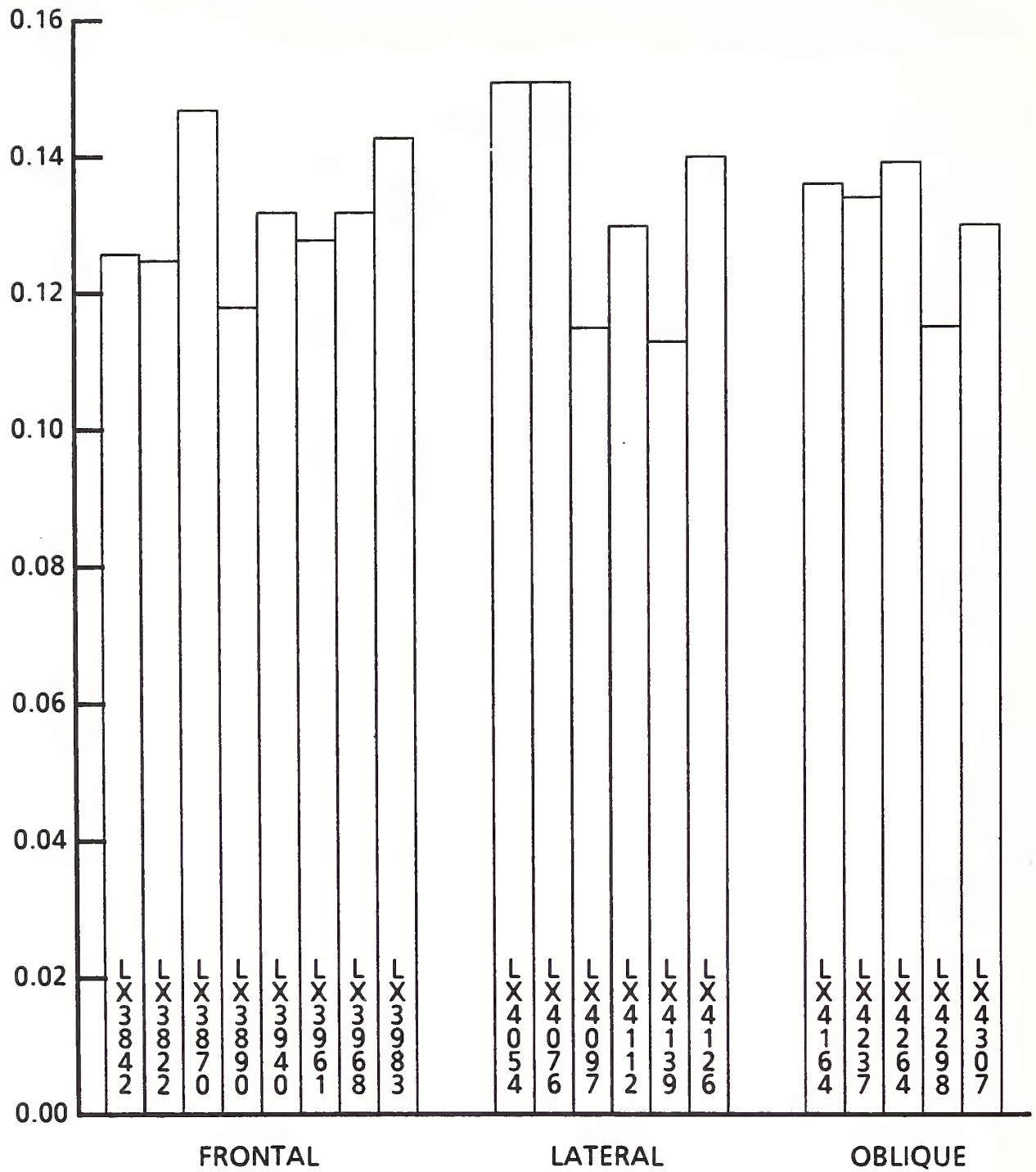
FIGURE B-1. INITIAL UNCORRECTED NECK CHORD LENGTH r_{Oy} FOR 20 TESTS OF SUBJECT H00134
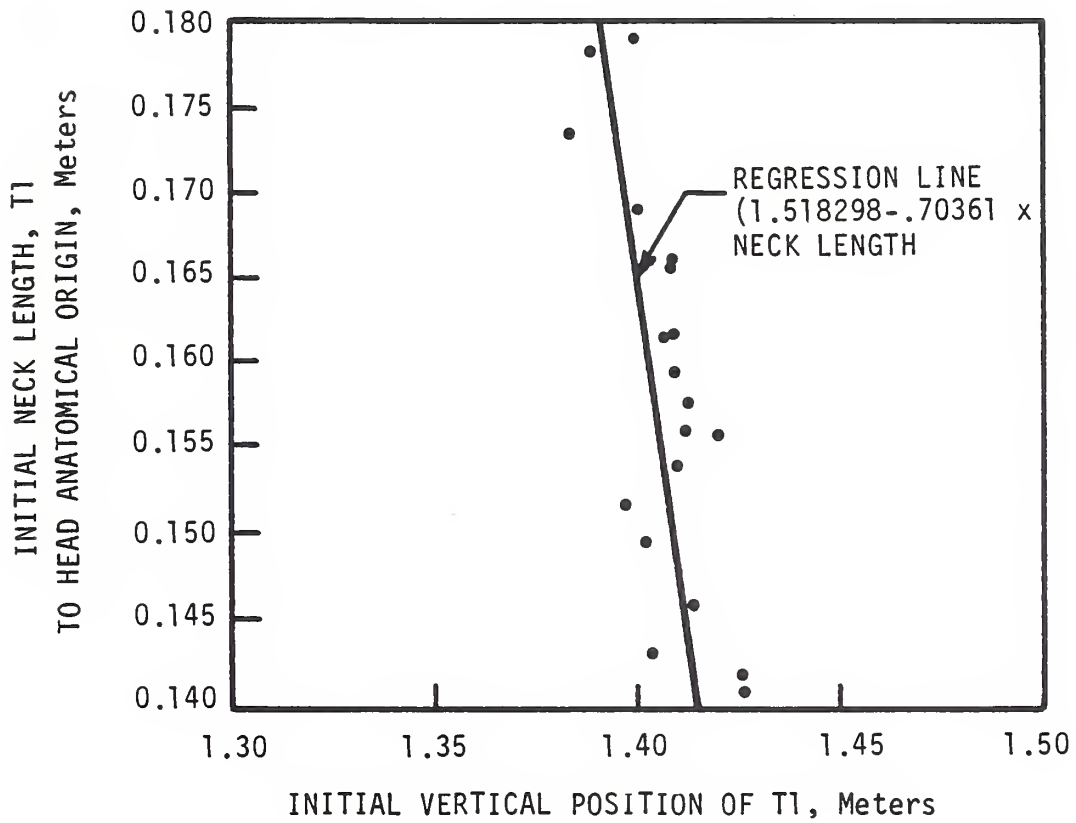
FIGURE B-2. INITIAL DISTANCE FROM T1 TO THE HEAD ANATOMICAL
ORIGIN VERSUS VERTICAL POSITION OF T1 RELATIVE TO
THE SEAT FOR 20 TESTS OF SUBJECT H00134

B-5
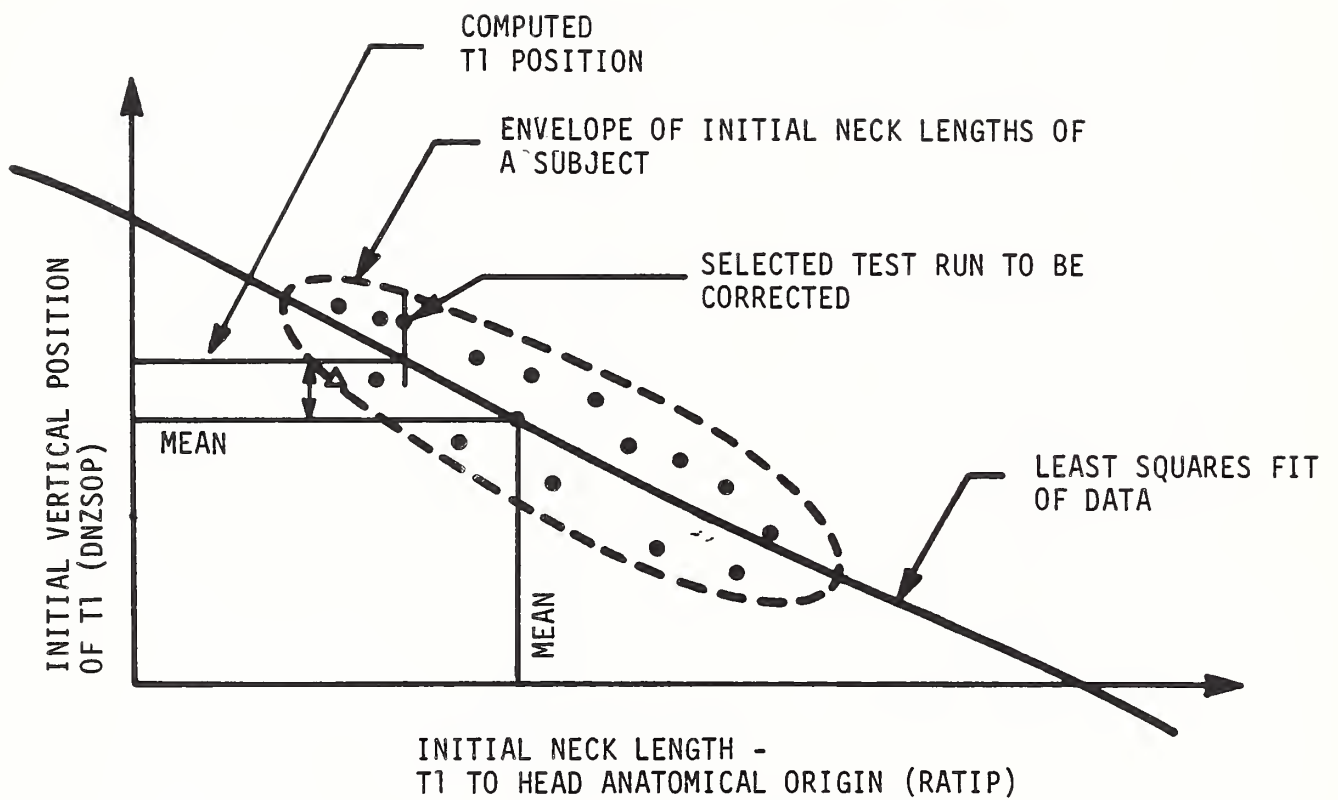
FIGURE B-3. ILLUSTRATION OF THE PROCEDURE FOR CORRECTING THE MEASUREMENT OF INITIAL VERTICAL POSITION OF T1

is subtracted from the measured vertical position.

The linear regression equation is given by [26]

$$(DNZSOP)_P = (DNZSOP)_M + \frac{\mu_{11}}{\sigma_R^2} \left[(RATIP) - (RATIP)_M \right] \qquad (B1)$$

$$= (DNZSOP)_M + \Delta$$

where subscript P denotes a least squares predicted value, subscript M denotes a mean value for all tests of a subject and

σ_R = standard deviation of variable RATIP

μ_{11} = covariance of the variables RATIP and DNZSOP

and the corrected value of vertical position of the T1 vertebral point by

$$(DNZSOP)_C = DNZSOP - \Delta \qquad (B2)$$

The correction is made at each timestep under the premise that the deviation in initial neck length is a bias present throughout the test resulting from vertical misalignment of the sensor relative to T1.*

Table B-1 indicates how correction of the initial T1 position in the runs of subject H00134 reduces the statistical variance by nearly a factor of two in the neck length. The remaining variation results from other measurement and transformation error and possible variation in neck chord length from test to test.

All data presented in this report has this correction applied. The primary purpose of the correction is to gain more consistency between runs in neck chord angle, θ_y. Neck length of a subject also becomes more uniform but this variation would be eliminated anyway because neck length is normalized to eliminate subject to subject variations in neck length.

_____

*This correction can be a simple addition or subtraction to the laboratory z-component of T1 position because the rotational response of the vertebral body to impact is negligible with the four-point restraint.

TABLE B-1. COMPARISON OF INITIAL NECK LENGTH BEFORE AND AFTER CORRECTING VERTICAL LOCATION OF T1

(Subject H00134)

RUN NO.	INITIAL DISTANCE T1 TO HEAD ANATOMICAL ORIGIN (cm)		INITIAL DISTANCE T1 TO OCCIPITAL CONDYLAR POINT (cm)	
	UNCORRECTED	CORRECTED	UNCORRECTED	CORRECTED
3807	16.8	16.2	14.3	13.6
3842	15.2	15.8	12.6	13.2
3822	15.0	17.5	12.5	14.7
3870	17.4	16.5	14.7	13.9
3890	14.6	15.6	11.8	12.8
3940	15.8	15.9	13.2	13.3
3961	15.4	15.9	12.8	13.2
3968	16.0	16.3	13.2	13.5
3983	16.9	16.4	14.3	13.7
4054	17.8	16.5	15.0	13.8
4076	17.9	16.5	15.1	13.7
4097	14.3	15.4	11.5	12.6
4112	15.6	15.8	13.0	13.2
4139	14.1	15.4	11.3	12.6
4126	16.6	17.9	14.0	15.1
4164	16.2	16.0	13.6	13.4
4237	16.2	16.0	13.4	13.3
4264	16.6	16.1	13.9	13.4
4298	14.2	15.4	11.5	12.7
4307	15.6	15.8	13.0	13.1
MEAN	15.9	16.1	13.2	13.3
STD.DEV.	1.1	0.6	1.1	0.6

APPENDIX C

CONVERSION OF THE WAYNE STATE DATA TO THE NBDL FORMAT

Orientation of the head is given by:

$$\phi' = \tan^{-1} \left(\frac{y_3 - y_1}{x_1 - x_3} \right) \qquad \text{(C1)}$$

and orientation of the neck is given by:

$$\theta' = \tan^{-1} \left(\frac{y_4 - y_6}{x_6 - x_4} \right) \qquad \text{(C2)}$$

where x_i and y_i are the horizontal and vertical digitizer components, respectively, of the ith numbered point of Figure 3-1. The digitizer x and y components are assumed to be aligned with the laboratory x and z coordinates, respectively, the latter defined in Section 4.1.2.

When the initial values of head and neck orientation, ϕ_o' and θ_o' respectively, are subtracted from the instantaneous values, the result is the change in orientations and is identical to the definitions used in Section 5.

$$\Delta\phi = \phi' - \phi_o' \qquad \text{(C3)}$$

$$\delta\theta = \theta' - \theta_o'$$

The laboratory x and z components of displacement of the head anatomical origin (see Figure 4-1) are given, respectively, by :

$$r_{Ax} = (x_7 - x_2) + \ell_H \cos(\phi' + \gamma_H) \qquad \text{(C4)}$$

and

$$r_{Az} = (y_2 - y_7) - \ell_H \sin(\phi' + \gamma_H) \qquad \text{(C5)}$$

C-3

where ℓ_H and γ_H are defined in Figure 3-1, and were estimated for each test subject based on measurements from a frame of each test of that subject. The purpose of subtracting sled position, (x_7, y_7) in these equations is to eliminate flexural motions between the camera and sled which were observed in the films.

The laboratory x and z components of T1 anatomical origin are given, respectively, by:

$$r_{Tx} = x_7 - x_5 + \ell_N \cos (\theta' - \gamma_N) \qquad (C6)$$

and

$$r_{Tz} = y_5 - y_7 - \ell_N \sin (\theta' - \gamma_N) \qquad (C7)$$

where ℓ_H and γ_H are also defined in Figure 3-1 and estimated as described above.

Sled motion is given by:

$$DCXSOP = X_8 \qquad (C8)$$

APPENDIX D

COMPARISON OF MEAN RESPONSE OF PERFORMANCE REQUIREMENT
VARIABLES FOR DIFFERENT IMPACT LEVELS
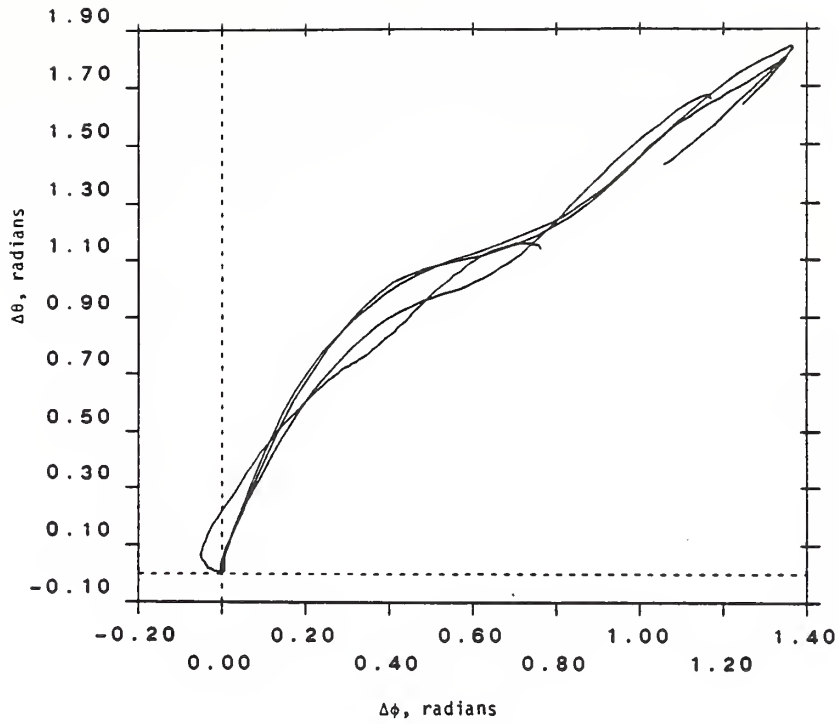
a)
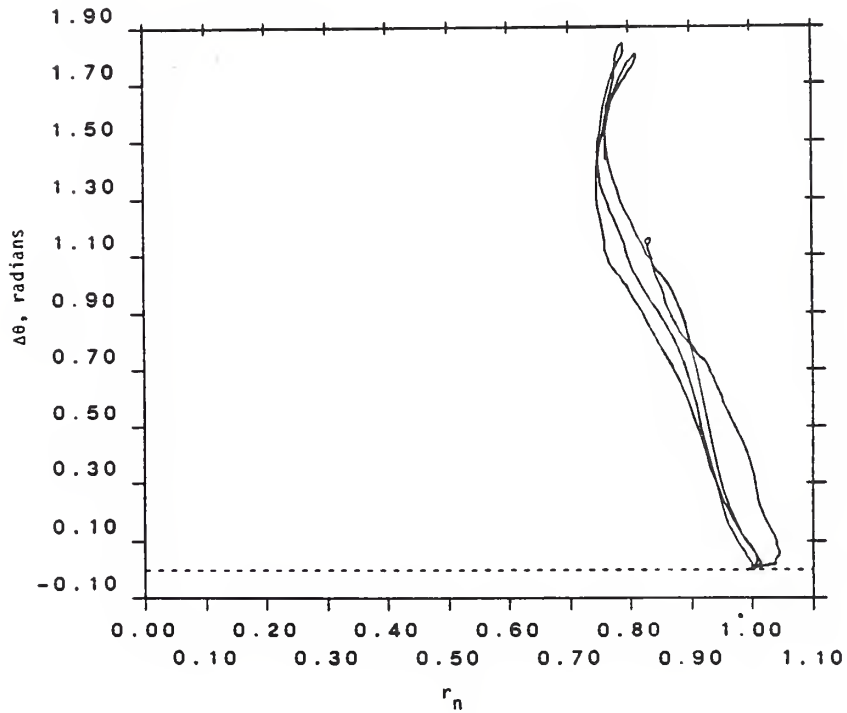
b)

FIGURE D-1. MEAN RESPONSE OF THE PERFORMANCE REQUIREMENT
VARIABLES FOR FRONTAL IMPACT AT FOUR LEVELS
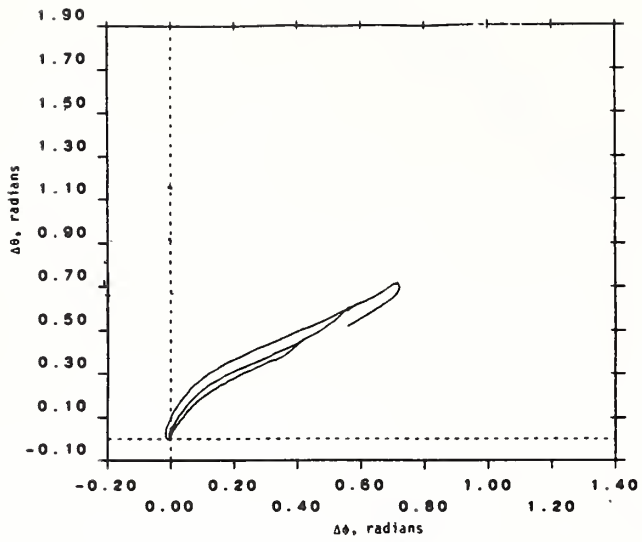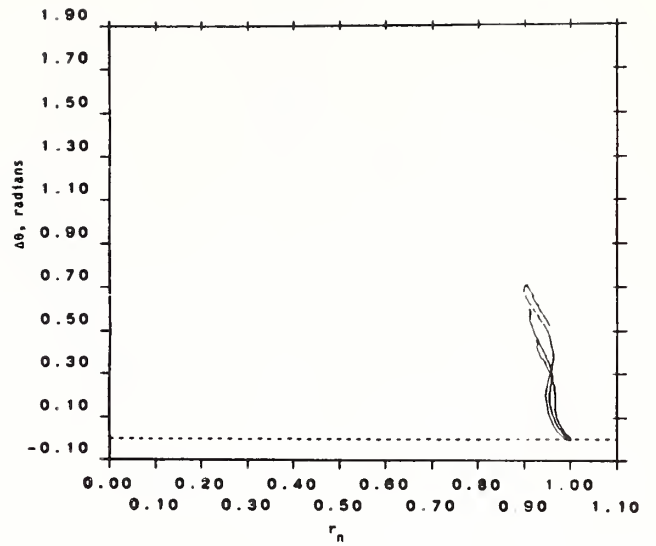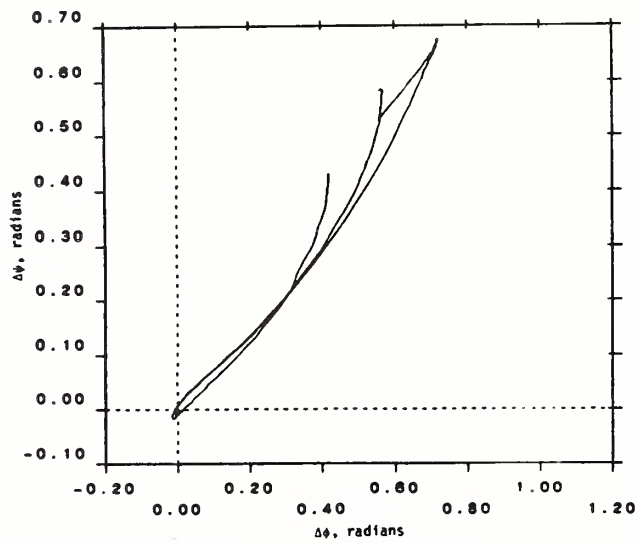
FIGURE D-2. MEAN RESPONSE OF THE PERFORMANCE REQUIREMENT
VARIABLES FOR LATERAL IMPACT AT THREE LEVELS
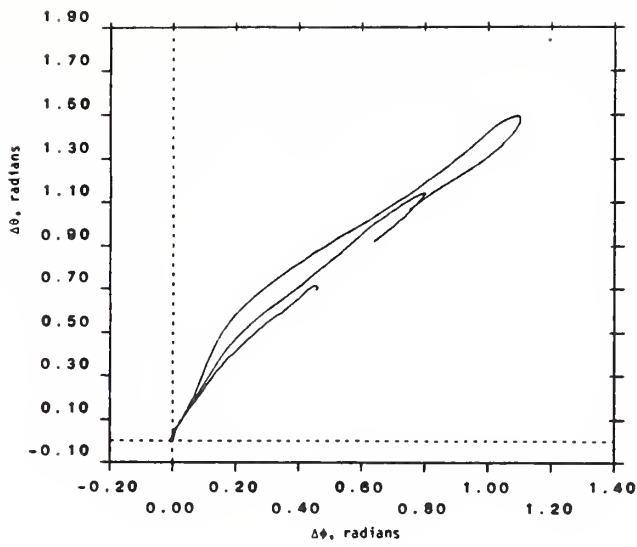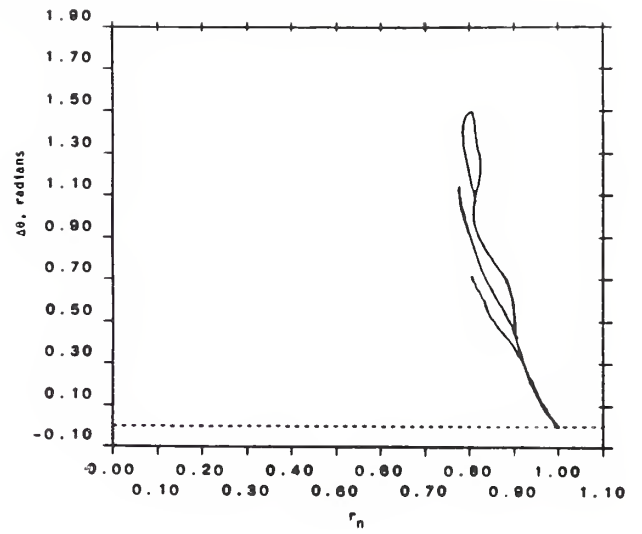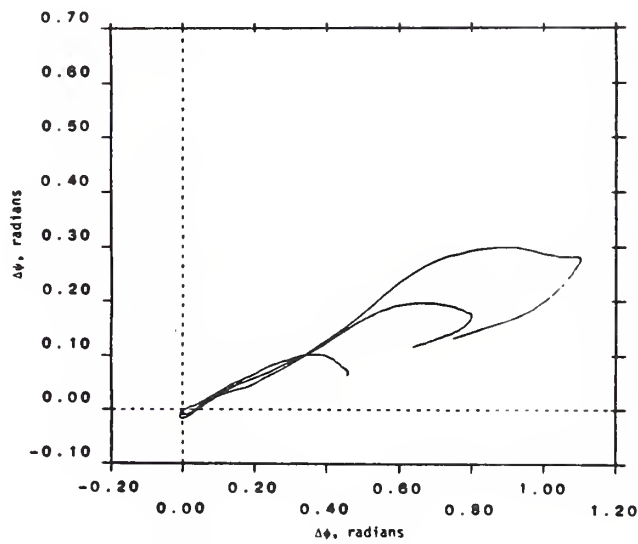
FIGURE D-3. MEAN RESPONSE OF THE PERFORMANCE REQUIREMENT
VARIABLES FOR OBLIQUE IMPACT AT THREE LEVELS

Form DOT F 1720

FORMERLY FORM DOT

lassachusetts 02142

||||||||||||||||||||||||||||
00348009

U.S.MAIL